

SKELETAL MUSCLE ION REGULATION AND METABOLISM
AT REST AND DURING INTENSE EXERCISE

By

© MICHAEL IVAN LINDINGER, B.SC., M.SC.

A Thesis

Submitted to the School of Graduate Studies
in Partial Fulfillment of the Requirements
for the Degree
Doctor of Philosophy

McMaster University

February, 1987

MUSCLE ION REGULATION AND METABOLISM IN INTENSE EXERCISE

DOCTOR OF PHILOSOPHY (1987)
(Medical Science)

McMASTER UNIVERSITY
Hamilton, Ontario

TITLE: Skeletal Muscle Ion Regulation and Metabolism at Rest
and During Intense Exercise

AUTHOR: Michael Ivan Lindinger, B.Sc. (University of Victoria)
M.Sc. (McMaster University)

8 SUPERVISOR: -Dr. George J.F. Heigenhauser

NUMBER OF PAGES: xvii, 311

ABSTRACT

In intense exercise the maintenance of muscle contraction and metabolism is critically dependent on the regulation of intracellular homeostasis. The present studies have examined the physiological and biochemical effects of three factors which influence this regulation at rest and in exercise; these factors are the strong ions, the weak ions (weak acid and base electrolytes), and carbon dioxide (CO_2).

This thesis describes three series of experiments which were designed to demonstrate the importance of ion regulation in the maintenance of muscle performance and metabolism in intense exercise. The purposes of these studies were three-fold: (1) to quantify the intracellular composition of strong ions of fast- and slow-twitch skeletal muscles at rest and at the end of intense exercise; (2) to determine the relative contributions of strong ions, weak acids and bases, and CO_2 to the total intracellular ionic composition of muscle at rest and in exercise; and (3) to demonstrate the inter-relationships between intracellular ion regulation, muscle metabolism and muscle performance during intense exercise.

The first series of experiments examined the ionic and metabolic composition rat hindlimb muscles (white gastrocnemius, WG; plantaris, PL; red gastrocnemius, RG; soleus, SL) sampled at rest and following 4.5 min of intense swimming exercise. Intracellular ionic status is dependent upon the PCO_2 , strong ion difference ($[\text{SID}]$), and the total concentration of weak acids and bases ($[\text{A}_{\text{TOT}}]$) of the intracellular fluids. PCO_2 was held constant at various levels and

intracellular strong ion concentrations were measured using instrumental neutron activation analysis. $[A_{TOT}]$ is a pooled term representing all of the intracellular weak electrolytes and cannot be directly measured. A method for determining $[A_{TOT}]$ indirectly from measurements of pH, $[SID]$ and PCO_2 muscle homogenates was formulated and is described. Intracellular $[SID]$ was found to be significantly higher in fast twitch WG (161 mEq/l) than in slow twitch SL (137 mEq/l); this was primarily due to a higher $[K^+]$ in resting WG. Muscle $[A_{TOT}]$ averaged 190 mEq/l at rest, and there was little difference between muscles. Intramuscular pH was determined using three methods: the distribution of the weak acid DMO, from pH measurements of muscle homogenates, and was calculated from the independent variables $[SID]$, $[A_{TOT}]$, and PCO_2 . Corresponding to its higher $[SID]$, the WG had a significantly higher intracellular pH at rest (6.94) than SL (6.72).

The second series of experiments examined changes in extra- and intra-cellular ion and metabolite concentrations, and quantified the ion and metabolite fluxes between muscle and blood at rest and during intense electrical stimulation using an isolated perfused rat hindlimb preparation. These studies confirmed that K^+ and La^- leave the muscle cells during contraction and that Na^+ and Cl^- enter, and that these ionic disturbances cause the increase in intracellular $[H^+]$ associated with the decrease in muscle performance. With stimulation, the major changes affecting intracellular ion status and metabolism were large increases in intracellular lactate concentration ($[La^-]_i$) and $[Na^+]_i$, and a marked reduction in $[K^+]_i$.

These changes were greatest in WG, a highly glycolytic muscle, and

least in SL, a predominantly oxidative muscle; the rise in $[La^-]_i$ accounted for 67% and 50% of the fall in $[SID]_i$ in WG and SL, respectively. Correspondingly, the largest changes in ion status occurred in WG. The high initial $[SID]_i$ in resting WG prevented excessive increases in $[H^+]$ and protein ionization state during muscle contraction.

The third series of experiments examined the effects of extracellular metabolic and respiratory alkalosis on muscle performance, metabolism and ion regulation, and provided an opportunity to test the hypothesis that changes in intracellular ionic status will affect the regulation of metabolism. With alkalosis, compared to controls, there were no differences with respect to performance and metabolism, however, the rate of La^- efflux from muscle was significantly increased and $[La^-]_i$ was significantly reduced. Extracellular alkalosis was also associated with increased fluxes of Na^+ from perfusate into muscles, resulting in large increases in $[Na^+]$ at rest and during stimulation; K^+ efflux in alkalotic hindlimbs was significantly reduced, compared to controls, during stimulation. A theory is proposed whereby exercise-induced changes in intracellular $[La^-]$, $[K^+]$ and $[Na^+]$ exert direct effects on the ionized state of intracellular proteins and on metabolic regulation during exercise.

ACKNOWLEDGEMENTS

Firstly, I am deeply indebted to my supervisor and friend George Heigenhauser for fully supporting in thought and action these lines of investigation, and for the many opportunities for presenting the results at international meetings. I am very grateful for the excellent technical assistance and friendship provided by M. Ganagarsjah, Sandra Peters, Joceline Otis, George Obminski and Tanys Chypchar, without whose help much of this work would not have been possible. Special thanks to Sandy for proof-reading the manuscript.

I am thankful to my supervisory committee, Drs. G. Heigenhauser, Norman L. Jones, Chris M. Wood and C.J. Toews, and also to Alan J. McComas for their support and guidance through the quantlet of comprehensive exams, presentations, manuscript and thesis writing, and the final defense.

I would also like to thank Dr. Lawrence Spriet for helping me get started in the 'rat race' and for his continued friendship and support. In his brief stay at McMaster, Dr. Peter Stewart was instrumental in the consolidation of my vague and muddled impresssions of physical chemistry; I thank him for his time and constructive criticisms of many aspects of this work.

Finally, but most importantly, I thank Mary for her love and enduring support through the years of a graduate student's life; may we both reap the benefits in the years to come.

This work was supported by the Medical Research Council of Canada, the Ontario Heart and Stroke Foundation, and the Ontario Graduate Scholarship program.

"Increase in our understanding of the buffering reactions has proceeded as it should over the last 67 years, expanding toward the more comprehensive — from the part to the whole. On the other hand, analysis in terms of the roles played by the individual electrolytes has shown a trend in the reverse direction, focusing down upon a single ion (H^+) and thus giving diminished emphasis to all others."

James L. Gamble, Jr., 1984

The Physiologist, 27: 375-379

TABLE OF CONTENTS

<u>Chapter</u>		<u>Page</u>
	Title Page	i
	Descriptive Note	ii
	Abstract	iii
	Acknowledgements	vi
	Table of Contents	viii
	List of Figures	xiii
	List of Tables	xv
1	INTRODUCTION	1
1.1	<u>Theme and Purpose</u>	1
1.2	<u>Biological and Physical Chemistry of Skeletal Muscle</u>	2
1.2.1	Preface	2
1.2.2	Physico-chemical Relationships in Physiological Solutions	3
1.2.3	Biochemical Basis of Muscle Fatigue	13
1.2.3.1	Historical Perspective	13
1.2.3.2	Metabolism and Energy Supply	16
1.2.3.3	Events Related to Excitation-Contraction Coupling	19
1.3	<u>Historical Development of Muscle Ion Regulation</u>	23
1.3.1	Muscle Fiber Composition and General Properties	23
1.3.2	Intramuscular Compartmentation of Ions	29
1.3.3	Trans-Sarcolemmal Ion Movements and Membrane Potential	35
1.3.4	Hydrogen Ion and pH in Skeletal Muscle	41
1.3.5	Activity Induced Changes in Muscle and Blood	47
1.3.6	Dependence of Metabolism on Strong Ions	52

<u>Chapter</u>	<u>Page</u>
2 METHODS	59
2.1 Introduction	59
2.2 Animals	59
2.3 New Techniques	59
2.4 Experimental Design	61
2.4.1 The Isolated Rat Hindlimb	61
2.4.2 Intense Swimming Exercise	62
2.5 Statistics	64
3 PHYSICO-CHEMICAL PROPERTIES OF SKELETAL MUSCLE AT REST AND AFTER INTENSE EXERCISE	65
3.1 Introduction	65
3.2 Methods	68
3.2.1 Animals	68
3.2.2 Protocol	68
3.2.3 Analyses	70
3.2.4 Muscle Homogenate Titrations	71
3.2.5 Calculations	73
3.3 Results	78
3.3.1 Performance	78
3.3.2 Muscle Fluid and Ions	81
3.3.3 Effect of K_A	81
3.3.4 Muscle pH	82
3.3.5 Physico-chemical Relationships in Muscle	86
3.4 Discussion	93
3.4.1 Theoretical considerations	94

<u>Chapter</u>	<u>Page</u>
3.4.2 Comparison of Methods for Muscle pH	99
3.4.3 Effects of Changing the Independent Variables	102
3.4.4 Significance	103
3.4.5 Summary and Conclusions	106
 4 SKELETAL MUSCLE METABOLISM AND ION FLUXES IN THE STIMULATED PERFUSED RAT HINDLIMB	 107
4.1 Introduction	107
4.2 Methods	108
4.2.1 Experimental Protocol	109
4.2.2 Analytical Procedures	109
4.3 Results	112
4.3.1 Performance	112
4.3.2 Perfusate Ion Fluxes	113
4.3.3 Muscle Ions	122
4.3.4 Muscle [SID] and $[H^+]$	127
4.3.5 Membrane Potential	128
4.4 Discussion	128
4.4.1 Fluid Balance	129
4.4.2 Ion Balance	130
4.4.3 [SID] and $[H^+]$	133
4.4.4 Significance	135
4.4.5 Summary and Conclusions	138

<u>Chapter</u>	<u>Page</u>
5 MODULATION OF SKELETAL MUSCLE METABOLISM AND ION FLUXES BY ALKALOSIS	139
5.1 Introduction	139
5.2 Methods	141
5.3 Results	146
5.3.1 Performance and Metabolism	146
5.3.2 Venous Perfusate	147
5.3.3 Ion Fluxes	153
5.3.4 Relationship Between Lactate and NVA Fluxes	154
5.3.5 Muscle Fluid and Ion Fluxes	158
5.4 Discussion	162
5.4.1 Ion Fluxes in Resting Muscle	162
5.4.2 Ionic Changes in Stimulated Muscle	163
5.4.3 Mechanism for Trans-Sarcolemmal Lactate Efflux	164
5.4.4 NVA Flux from Muscle	168
5.4.5 Intracellular Ion Regulation During Exercise	169
5.4.6 Muscle Performance and Metabolism	170
5.4.7 Summary and Conclusions	176

<u>Chapter</u>		<u>Page</u>
6	GENERAL DISCUSSION	177
6.1	Introduction	177
6.2	Inter-relationships Between Ion Balance and Regulation of Skeletal Muscle Metabolism During Exercise	178
6.3	Conclusions	183
6.4	Future Directions	184

APPENDIX

A	Acid-base and Respiratory Properties of a Buffered Bovine Erythrocyte Perfusion Medium	187
B	Intracellular Ion Content of Skeletal Muscle Measured by Instrumental Neutron Activation Analysis	208
C	Comparison of Intense Swimming Exercise and Tetanic Electrical Stimulation on Skeletal Muscle Ions and Metabolites	234
D	Role of the Red Blood Cell in Maximal Exercise	261
	BIBLIOGRAPHY	262

LIST OF FIGURES

<u>Figure</u>		<u>Page</u>
1	The glycolytic pathway	18
2	Schematic of the rat hindlimb preparation	63
3	Intracellular changes in dependent physico-chemical variables with changes in PCO_2 , $[A_{TOT}]_i$ and $[SID]_i$	88
4	no figure	
5	Changes in $[SID]_i$ and $[H^+]_i$ in white gastrocnemius during high intensity exercise	89
6	Effects of changing K_A on the dependent variables	90
7	no figure	
8	Hindlimb isometric tension generation in controls	114
9	Venous plasma pH, PCO_2 , $[SID]$, and fluid shifts in controls	115
10	Total changes in muscle fluid volumes during stimulation in controls	116
11	Venous plasma $[NVA]$, $[La^-]$, $[K^+]$ and $[Cl^-]$ in controls	119
12	Perfusate ion fluxes during hindlimb stimulation in controls	120
13	Total perfusate ion fluxes in controls	121
14	Total changes in intracellular strong ion concentrations during stimulation in controls	124

<u>Figure</u>		<u>Page</u>
15	Hindlimb tension generation in alkalosis	144
16	Hindlimb oxygen uptake in alkalosis	145
17	Muscle CP and ATP contents	149
18	Muscle glycogen and lactate contents	150
19	Changes in venous plasma pH, PCO_2 and [NVA] in alkalosis	151
20	Perfusate ion fluxes during hindlimb stimulation in alkalosis	152
21	Total perfusate ion fluxes in alkalosis	155
22	Lactate flux as a function of NVA flux in controls, in acidosis, and in alkalosis	156
23	Relationships between La^- and NVA fluxes as a function of arterial composition in perfused hindlimb in controls, in acidosis, and in alkalosis	157
24	Total changes in intracellular strong ion contents during stimulation in alkalosis	161
A-1	Perfusate oxygen dissociation curve	197
A-2	Perfusate carbon dioxide dissociation curve	198
A-3	Perfusate acid-base alignment diagram	199
B-1	Instrumental neutron activation analysis energy spectrum of rat plantaris muscle	220
C-1	Isometric tetanic tension generated by the hindlimb	244
C-2	Mean changes in intracellular ion contents with exercise	253

LIST OF TABLES

<u>Table</u>		<u>Page</u>
1	Discoveries of factors associated with muscle fatigue	14
2	Skeletal muscle composition at rest. I. Metabolites, fluid volumes, ion concentrations, membrane potentials, contractile properties and blood flows in rats, cats and humans	25
3	Skeletal muscle composition at rest. II. Myoglobin contents, organelle volume densities and enzyme activities in rats and humans	27
4	Intracellular compartmentation of ions in vertebrate skeletal muscle at rest, membrane potentials and ion activities	31
5	Effects of temperature in tissue pH	43
6	Resting muscle pH of various animals at 37°C	44
7	Physico-chemical constants in skeletal muscle	79
8	Composition of arterial blood in rats at rest and after exhaustive swimming exercise	80
9	Muscle fluid volumes, ion concentrations, and CP contents in hindlimb muscles at rest and after swimming exercise	83
10	Comparison of muscle pH methods in resting muscle	84
11	Comparison of muscle pH methods in hindlimb muscles at rest and after swimming exercise	85

<u>Table</u>	<u>Page</u>
12 Physico-chemical properties of hindlimb muscles at rest and after swimming exercise	92
13 How the homogenate technique estimates muscle pH	96
14 Acidic dissociation constants (K_a 's) of major intracellular constituents in skeletal muscle	100
15 Characteristics of the arterial perfusate in controls	110
16 Muscle fluid volumes and intracellular ion concentrations at rest and after 5 min stimulation in controls	123
17 Comparison of intracellular and perfusate ion fluxes during stimulation in controls	125
18 Muscle [SID] _i , dependent variables and K^+ equilibrium potential in control, rest perfused, and stimulated perfused muscles in controls	126
19 Perfusate composition in alkalosis	143
20 Plantaris muscle fuel and metabolite concentrations	148
21 Fluid volumes, and intracellular ion contents in resting control, and in alkalotic rest perfused and stimulated perfused muscles	160
22 Total lactate produced and released in control and alkalotic hindlimb muscles during stimulation	165
23 Total energy released in control and alkalotic hindlimb muscles during stimulation	171

<u>Table</u>	<u>Page</u>
A-1 Chemical composition of the perfusion medium	195
A-2 <u>In vitro</u> respiratory characteristics of bovine and rat bloods, and of the perfusion medium	196.
A-3 Relations between $[\text{HCO}_3^-]$ and pH in the perfusate	201
B-1 Intracellular ion contents in rat hindlimb muscles determined by INAA and AAS	223
B-2 Comparison of rat muscle total tissue water, extra- cellular fluid volume, and intracellular fluid volume	224
B-3 Hindlimb muscle fluid volumes and intracellular ion concentrations	225
C-1 Characteristics of the perfusion medium	239
C-2 Relative contributions of soleus, plantaris, red and white gastrocnemius muscles to perfused and stimulated hindlimb muscle masses	245
C-3 Muscle metabolite contents after intense electrical stimulation and exhaustive swimming	246
C-4 Muscle fluid volumes	250
C-5 Intracellular ion contents of hindlimb muscles	251
C-6 Intracellular ion concentrations of hindlimb muscles in control limbs, during rest perfusion, after intense electrical stimulation, and after exhaustive swimming	252

1 INTRODUCTION

1.1 THEME and PURPOSE

The physiological and biochemical characteristics of resting and fatigued skeletal muscle, such as metabolism, contractile and membrane properties, are highly dependent upon the ionic composition of the extra- and intra-cellular fluids. The underlying theme of the present studies is the importance of the ionic changes which occur within muscle intracellular fluid (ICF) on intracellular homeostasis and metabolism during intense muscular contraction. Special consideration is given to those changes which are proposed to exert direct effects on physiological and biochemical regulatory mechanisms of muscle during exercise.

The purposes of these studies were three-fold: (1) to characterize the physico-chemical properties (PCO_2 , concentrations of strong and weak ions) of skeletal muscle at rest and at the end of high intensity exercise; (2) to develop a working model of trans-sarcolemmal ion movements between extra- and intracellular fluids which could be explained within the physico-chemical constraints imposed on the system; and (3) to examine the inter-relationships between ion regulation and metabolism in skeletal muscle.

The following section briefly describes the known physico-chemical and biochemical factors associated with muscle fatigue, and serves to provide a framework for the remainder of the dissertation. The remainder of the Introduction describes the

1

historical events associated with the study of skeletal muscle ion regulation and its integration with muscle metabolism and contraction.

1.2 BIOLOGICAL AND PHYSICAL CHEMISTRY OF SKELETAL MUSCLE

1.2.1 Preface

Skeletal muscle fatigue has been defined by the Fifth International Symposium on Biochemistry of Exercise (1982) as "the inability of a physiological process to continue functioning at a particular level and/or the inability of the total organism to maintain a predetermined exercise intensity". Edwards (1981) has simply defined fatigue as the "failure to maintain the required or expected force and power output". The proximate cause of muscle fatigue, or decrease in force, has thus been attributed to a reduction in the number of simultaneously attached actin-myosin cross-bridges in the force generating state (Donaldson, 1983; Hultman & Sjoholm, 1986).

At the present time it is difficult to state with any degree of certainty that specific changes observed in skeletal muscle, or in the blood perfusing the muscle, during exercise and fatigue are the causative factors responsible for the decrement in force. Therefore care must be taken in the interpretation of reported results to avoid the constraints of unknown cause/effect relationships.

The biochemical factors associated with skeletal muscle fatigue may be divided into three fundamental events: (1) impairment of metabolism and reduction of energy supply; (2) alteration of sarcolemmal or transverse tubular membrane properties; and (3) impaired function of contractile proteins. The latter two events are dependent

on muscle metabolism and extra- and intracellular fluid physico-chemical (and particularly ionic) properties. The physico-chemical properties in turn determine the biochemical and physiological characteristics of skeletal muscle at rest and fatigue.

In the following order, the proceeding sections will briefly describe: (a) the physico-chemical properties of physiological solutions; (b) the metabolic, and (c) the ionic, events which affect the physical chemistry of muscle; and (d) excitation-contraction coupling.

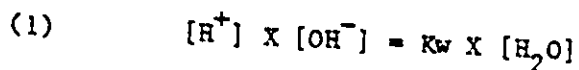
1.2.2 Physico-chemical Relationships in Physiological Solutions

The analysis of variables susceptible to change within any system must take into consideration the physico-chemical constraints imposed on the system by physical and chemical laws. The body's extra- and intracellular fluids are solutions consisting of water, strong ions, weak ions and proteins, and dissolved gases -- primarily oxygen and carbon dioxide. Stewart (1978, 1981, 1983) has outlined the fundamental physico-chemical relationships governing ionic equilibria in physiological fluid systems. In his monograph, Stewart (1981) shows the development of these relationships from a simple water solution to those solutions containing CO_2 , strong ions and weak acids and bases.

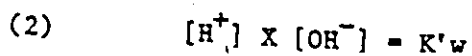
The terminology and definitions used in the dissertation are essentially those used by Stewart. Quantitative analysis of the variables in any system requires the distinction between independent variables and dependent variable. The independent variables are those variables which can be altered only by external manipulation; a change

in any other independent or dependent variable will exert no influence on an independent variable in an open system. A dependent variable is therefore one which is internal to the system and which is susceptible to changes imposed by the independent variables. Within the system there is an equation which describes the equilibrium relationship for each dependent variable, and the dependent variables must simultaneously satisfy all of those equations.

All physiological solutions consist primarily of water. Therefore this outline of solution chemistry will begin with the equations describing the water dissociation equilibrium:



where K_w , the dissociation constant for water, is about 10^{-16} M (Harned and Owen 1958). Since $[H_2O]$ is large (about 56 M) K_w has negligible effect on $[H_2O]$; the term $K_w \times [H_2O]$ may be considered to be effectively constant and equation 1 rewritten as:



where K'_w is the 'ion product for water'. Its value is sensitive to temperature, osmolarity, solute concentrations, and ionic strength (Harned and Owen 1958).

Strong ions are those electrolytes which, for all practical purposes, are considered to be completely dissociated in physiological solutions. In vertebrates, the predominant strong ions are sodium (Na^+), potassium (K^+), magnesium (Mg^{++}), calcium

(Ca^{++}), chloride (Cl^-), and lactate (La^-). The organic ion lactate is a strong ion due to its large dissociation constant (1.36×10^{-5} Eq/l; $\text{pK}' = 4.87$). The difference between the sum of the concentrations of the strong base cations and the sum of the concentrations of the strong acid anions is called the strong ion difference, or [SID]:

$$(3) \quad [\text{SID}] = ([\text{Na}^+] + [\text{K}^+] + [\text{Mg}^{++}] + [\text{Ca}^{++}]) - ([\text{Cl}^-] + [\text{La}^-])$$

Weak acids and bases are those electrolytes which, by definition, dissociate only partially in physiological solutions. In the extra- and intracellular fluids of vertebrates there is a predominance of weak acids (primarily proteins and inorganic phosphate) over weak bases. For the sake of simplicity the total concentrations of intracellular weak acids and bases are pooled and represented by the expression 'total weak acid concentration', termed $[\text{A}_{\text{TOT}}]$.

In plasma, the value $[\text{A}_{\text{TOT}}]$ represents the relationship between the anion equivalency of plasma proteins and inorganic ions (i.e. the protein-ion complexes from which the dissociation of the ion is prevented or retarded). The $[\text{A}_{\text{TOT}}]$ of plasma proteins was initially quantified by Van Slyke et al. (1928) with the following relationship:

$$(1) \quad \text{A}_{\text{TOT}} = 0.78(\text{Alb-N})(\text{pH} - 5.16) + 0.48(\text{Glb-N})(\text{pH} - 4.89)$$

where Alb-N and Glb-N are gram of albumin and globulin nitrogen.

Knowing the plasma pH and the ratio of albumin to globulin in plasma, the $[A_{TOT}]$ per gram of protein nitrogen may be read from the nomogram of Van Slyke et al. (1928) and divided by 6.25 to give ions per gram of protein. In normal man the Alb:Glb ratio is 1.8 and $[A_{TOT}]$ is 0.243 mEq/g plasma protein (Van Slyke et al. 1928). This value is very close to the value of 0.245 determined empirically by Stewart (personal communication). Using an average plasma [protein] of 70 g/l for man, then:

$$(11) \quad [A_{TOT}] = 0.243 \text{ mEq/g} \times 70 \text{ g/l} = 17.0 \text{ mEq/l}$$

In terms of the dissociation of weak acid (HA) one can describe the relationship between H^+ and the number of anionic sites (A^-) by this dissociation equilibrium:

$$(4) \quad [H^+] \times [A^-] = K_A \times [HA]$$

where K_A is the weak acid dissociation constant. This K_A is thus a pooled value representing the relative contributions of physico-chemically active weak acids and bases in the intracellular fluids (see Table 7). It must be assumed that HA and A^- participate in no other reactions, such that the total quantity of substance 'A' per liter solution is a constant termed $[A_{TOT}]$:

$$(5) \quad [A^-] + [HA] = [A_{TOT}]$$

It is evident that the value for $[A_{TOT}]$ can only be changed by

external manipulation, therefore, $[A_{TOT}]$ is an independent variable. A manipulation of the concentrations of any other variables in the system will have no effect on $[A_{TOT}]$.

Carbon dioxide participates in a number of ionic equilibria in physiological solutions. The total carbon dioxide content of a solution is represented by dissolved CO_2 (CO_{2d}), carbonic acid (H_2CO_3), bicarbonate ion (HCO_3^-), and carbonate ion (CO_3^{--}).

Henry's Law describes the quantitative relationship between the concentration of CO_{2d} and the partial pressure of CO_2 (PCO_2) of the gas with which the solution is in equilibrium:

$$(6) \quad [CO_{2d}] = S \times PCO_2$$

where S is the CO_2 solubility coefficient. The value of S depends on temperature, solute concentrations and ionic strength and is $3.51 \times 10^{-5} \text{ Eq/l.mmHg}^{-1}$ in intracellular fluids at 37°C (Siesjo and Thews 1962). The value of $[CO_{2d}]$ is very small (1-4 mM) and can conveniently be neglected (Stewart 1981).

Dissolved CO_2 can react with water to form H_2CO_3 and at equilibrium:

$$(7) \quad [CO_{2d}] \times [H_2O] = K \times [H_2CO_3]$$

where K is the equilibrium constant. Since $[H_2O]$ is very large (about 56 Molar) it essentially remains constant. Substituting for $[CO_{2d}]$ from the preceding equation the quantitative relationship

may be expressed as:

8

$$(8) \quad [H_2CO_3] = K_{H_2CO_3} \times PCO_2$$

where $K_{H_2CO_3}$ is about 9×10^{-8} Eq/l/mmHg at $37^\circ C$, so that $[H_2CO_3]$ is usually less than 0.5% of $[CO_2d]$; it also can be neglected (Stewart 1981).

Bicarbonate (HCO_3^-) may be formed by the combination of CO_2d with OH^- ion, or from the dissociation of H_2CO_3 as described by the following 2 equilibria:

$$(9) \quad [CO_2d] \times [OH^-] = K_1 \times [HCO_3^-]$$

$$(10) \quad [H^+] \times [HCO_3^-] = K_2 \times [H_2CO_3]$$

The quantitative relationships describing $[HCO_3^-]$ equilibrium maybe simplified by combining (9) with (7) and (2) and combining the constants K_1 and K_2 to yield the relation:

$$(11) \quad [H^+] \times [HCO_3^-] = K_c \times PCO_2$$

Bicarbonate dissociates to form CO_3^{--} and H^+ , and at equilibrium:

$$(12) \quad [H^+] \times [CO_3^{--}] = K_3 \times [HCO_3^-]$$

where $K_3 = 6 \times 10^{-11}$ Eq/l in body fluids at $37^\circ C$.

The chemical reactions between the ionic constituents of physiological solutions may be considered to be in equilibrium at any given time. In addition to equilibria, the physico-chemical constraints of conservation of mass and electroneutrality must always be met. For purposes of analysis the equations for the individual reactions at equilibrium which fulfill the physico-chemical constraints imposed on the system are the following:

Water dissociation equilibrium:

$$(2) \quad [H^+] \times [OH^-] = K'_w$$

Weak acid dissociation equilibrium:

$$(4) \quad [H^+] \times [A^-] = K_A \times [HA]$$

Conservation of mass for 'A':

$$(5) \quad [HA] + [A^-] = [A_{TOT}]$$

Bicarbonate ion formation equilibrium:

$$(11) \quad [H^+] \times [HCO_3^-] = K_c \times PCO_2$$

Carbonate ion formation equilibrium:

$$(12) \quad [H^+] \times [CO_3^{2-}] = K_3 \times [HCO_3^-]$$

Electrical neutrality:

$$(13) \quad [SID] + [H^+] - [HCO_3^-] - [A^-] - [CO_3^{2-}] - [OH^-] = 0$$

Examination of these 6 equations will reveal that there are 6 dependent variables which must simultaneously satisfy all of the equilibria. The three independent variables are $[SID]$, $[A_{TOT}]$ and PCO_2 ; the 6 dependent variables determined by the three independent variables are thus $[HA]$, $[A^-]$, $[HCO_3^-]$, $[CO_3^{2-}]$, $[OH^-]$, and $[H^+]$.

These six equations can be rearranged and combined to obtain a fourth order polynomial to solve for $[H^+]$ (Stewart 1978, 1981, 1983):

$$(14) \quad [H^+]^4 + \{K_A + [SID]\} [H^+]^3 + \{K_A ([SID] - [A_{TOT}]) - (K_C \times PCO_2 + K'w)\} [H^+]^2 - \{K_A (K_C \times PCO_2 + K'w) + K_3 \times K_C \times PCO_2\} [H^+] - K_A \times K_3 \times K_C \times PCO_2 = 0.$$

where the physico-chemical constants used in solving this equation for skeletal muscle ICF are given in Table 7.

All of the independent and dependent variables do not have to be simultaneously measured in order to quantify all of the variable values. Indeed, if pH and PCO_2 are measured, the dependent variables in equations (2), (11), and (12) can be calculated. Similarly, if pH, [SID] and PCO_2 are measured the remaining unknown independent variable, $[A_{TOT}]$, and all the other dependent variables, can be calculated.

With the development of the pH and total CO_2 or PCO_2 electrodes, it became very convenient to describe the 'acid-base equilibria' of the blood plasma or intracellular environment in terms of only one independent variable, PCO_2 , and two dependent variables, $[H^+]$ and $[HCO_3^-]$. In his now classic paper, Henderson and coworkers (1924) described the equilibrium relationship

between $[H^+]$, PCO_2 and $[HCO_3^-]$ of equation (11) in logarithmic form as:

11

$$(17) \quad pH = pK' + \log ([HCO_3^-] / S \times PCO_2)$$

This relationship is usually referred to as the Henderson-Hasselbalch equation.

By definition, such results presented on their own can only describe a portion of the total physico-chemical equilibria; they can not be used to examine the mechanism behind the observed results. It was common practice, and still is to a large degree, to report the pH of blood, plasma, muscle homogenate, muscle extracts, and intracellular pH without also reporting the PCO_2 , total CO_2 or temperature, and as such these pH data are virtually meaningless. The reason the pH data on their own are meaningless is because pH is very dependent on temperature and on the other independent variables. The plentiful reports in the literature describing the 'pH-dependency' of biochemical reactions and physiological processes merely describe a relationship between the measured pH and the observed response(s) to changes in one or more of the independent variables. More often than not, these are omitted from the methods and results of the reports.

In addition to the physico-chemical relations existing in either the extra- and intracellular fluids, there are also physico-chemical interactions between extra- and intracellular fluids. These have been discussed by Manery (1954) and will be summarized as follows. (1) Electroneutrality must exist in each fluid compartment. (2) Osmotic equality exists between extra- and intracellular fluids;

12

however, under steady state conditions osmotic equilibrium is probably rarely attained but always approached. (3) Electrolyte inequality: The species and concentration of the electrolytes in the ECF differ from those in the ICF. The excess of strong basic cation concentration in cells (eg. greater [SID]) over that in plasma indicates that there is a higher concentration of weak anion equivalents within cells. These intracellular anion equivalents are in large part made up of high molecular weight colloidal, osmotically active particles which require more than one cation equivalent per mole to maintain electroneutrality. (4) Local concentrations of nondiffusible ions affect the distribution of diffusible ions according to the Gibbs-Donnan distribution. While the interaction between plasma and interstitial fluids is relatively simple, that between ECF and ICF is complicated by the effect of metabolic processes on ion movements. (5) Energy-yielding processes continuously alter the osmotic pressure, and the numbers of ionic equivalents such a way that simple equilibria are never established, but contribute to the maintenance of a complex steady state.

All of the preceeding considerations must be taken into account when analyzing the ionic status of a solution. It should be evident that 'acid-base' regulation is ion regulation, for without ion regulation there can be no 'acid-base' regulation. Cellular respiration and ventilatory gas exchange determine the PCO_2 of the system which in turn partially determines the equilibria between H^+ , OH^- , HCO_3^- , CO_3^{--} , and A^- ions. In addition, the concentrations of these same 5 ions, and $[HA]$, are simultaneously determined by the concentrations of strong ions and weak acids and bases within the solution.

Fifty years ago physiologists appear to have had a better working understanding of these fundamental relationships than present day physiologists and biochemists. Fenn (1936) attempted to explain his results on "the basis of the physico-chemical organization of the muscle" and realized that changes in muscle electrolytes were related to acid-base changes in blood. He referred to a "diffusion of acid" as "the chloride shift" and "a diffusion of base into the muscles" as "the potassium shift". Also, when frog muscle is exposed to high PCO_2 "potassium is driven from the blood into the muscle to neutralize the acid inside the muscle". While the principles for the changes in extra- and intracellular acidity may not have been fully understood, the ionic basis for acidity changes appear to have been recognized.

1.2.3 Biochemical Basis of Muscle Fatigue

1.2.3.1 Historical Perspective

The initial reports of major metabolic and ionic parameters in blood and muscle which have repeatedly been associated with fatigue in skeletal muscle are listed in Table 1. The following paragraph has been summarized from the excellent monograph on the historical development of muscle authored by Dorothy Needham (1971).

The biochemical basis for muscle fatigue has been under investigation for nearly two hundred years. Berzelius, in work published in Sweden in 1807, reported a marked acidification and accumulation of lactic acid in muscles from hunted stags. He noted that the lactic acid content of muscle is proportional to the extent to

TABLE 1

Biochemical factors within muscle which have been associated with skeletal muscle fatigue, and their discovery.

Factor	Initial Reports
acidification	Berzelius 1807/1840
lactic acid accumulation	Berzelius 1807; Ranke 1865
glycogen depletion	Nasse 1869
increase in Pi	Embden et al. 1914
inhibition of glycolysis	Meyerhof et al. 1927
creatine phosphate depletion	Eggleton & Eggleton 1927; Fiske & Subbarow 1927
adenine depletion	Parnas 1929
ATP depletion	Lundsgaard 1934
changes in cell permeability:	
increased $[Na^+]$,	Overton 1902; Berzelius 1912;
reduced $[K^+]$,	Mitchell & Wilson 1921; Fenn & Cobb 1936
reduced resting potential	Bernstein 1912;
reduced action potential	Hodgkin & Horowicz 1959b
increased $[H^+]$	Meyerhof & Lohman 1926; Furasawa & Kerridge 1927

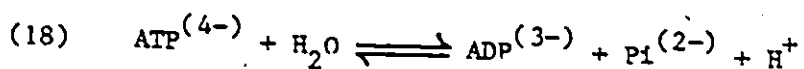
which it had been previously exercised. Nearly 60 years later Ranke (1865) described that muscle fatigue resulted from the injection of lactic acid into frogs which had been curarized to abolish nerve stimulation. Glycogen was first described in muscle by Claude Bernard in 1859, and ten years later Nasse (1869), finding that muscle glycogen was reduced after rigor, concluded that glycogen was the source of lactic acid in muscle. Later, in muscle extracts containing glycogen or hexosephosphates as substrate, Embden and coworkers (1914) observed an increase in the concentration of inorganic phosphate (P_i); and Meyerhof's group (1927) reported the inhibition of glycolysis simultaneously with P_i and lactic acid accumulation. These findings were soon followed by the discovery of creatine phosphate (CP) and its loss and subsequent recovery following muscle stimulation (Eggleton & Eggleton 1927; Fiske & Subbarow 1927). Parnas (1929) reported the depletion of muscle total adenine content as a result of stimulation and Lundsgaard (1934) later proposed that, during muscle contraction, CP breakdown was consistent with the resynthesis of adenosine triphosphate (ATP — the predominant source of total muscle adenine at rest) and the transfer of chemical energy. Within that time, ionic and electrochemical factors in muscle had also been identified and associated with muscle fatigue. These included the permeability of the muscle cell membrane to K^+ and Na^+ (Overton 1902), a reduction in the resting potential of the cell membrane (Bernstein 1912), and an increased intracellular sodium concentration ($[Na^+]$) and a decreased intracellular $[K^+]$ in directly stimulated muscles of the frog and rat (Fenn & Cobb 1936).

1.2.3.2 Metabolism and Energy Supply

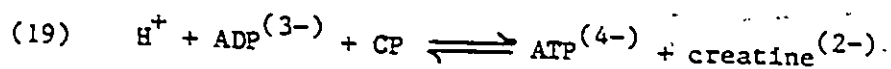
16

During high intensity exercise two major biochemical changes occur which have a profound influence on the physico-chemical properties of muscle. The first is the rapid degradation of CP to supply the energy required for muscular contraction. The reduction in CP with exercise effectively lowers the K_A of the total muscle weak acid pool by reducing its relatively large contribution to the K_A of resting muscle (see Table 14). The second is the large intracellular accumulation of La^- resulting from the increase in glycolysis. This increase in $[La^-]$ reduces the $[SID]$ (equation 3).

Energy for cellular reactions is derived from the catalytic hydrolysis of ATP (Bailey 1942):



to form adenosine diphosphate (ADP). The splitting of the terminal high-energy phosphate bond yields the energy required for muscle contraction, muscle relaxation, and maintenance of intracellular ion balance. A considerable proportion of the chemical energy in resting muscle is 'stored' in the high-energy phosphate bonds of CP. This reaction is catalyzed by the action of the equilibrium enzyme creatine kinase (Boyer et al. 1943):



The forward reaction requires both H^+ and ADP resulting from the hydrolysis of ATP (equation 18). When cellular ADP concentrations

increase and [ATP] decreases, ATP can also be produced by cytosolic myokinase (Kalckar 1943):



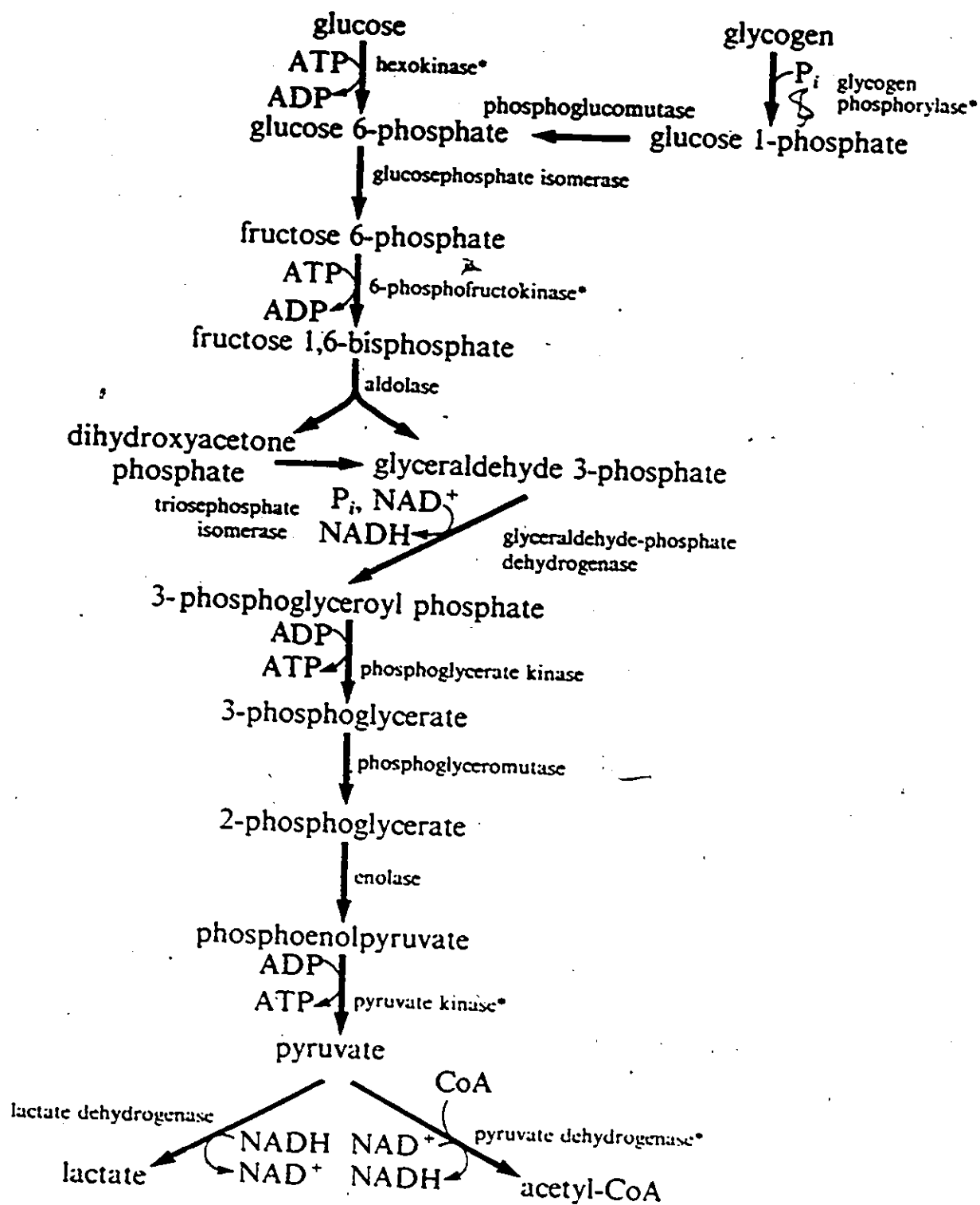
Adenosine monophosphate (AMP) is subsequently broken down to inosine monophosphate (IMP) and ammonia (NH_3) by the enzyme AMP deaminase (Smiley & Suelter 1967).

Average values for ATP and CP in resting muscle are about 5 and 20 $\mu\text{mole/g}$ wet weight. Glycolysis of 1 mole of glucose from glycogen results in the net production of 2 moles of ATP and 2 moles of pyruvate (Fig. 1). At accelerated rates of glycolysis, pyruvate accumulates and is converted to La^- by the catalytic action of the equilibrium enzyme lactate dehydrogenase. If pyruvate is channelled through the TCA cycle, oxidative phosphorylation yields an additional 34 moles of ATP.

Experimental evidence in intact muscle shows exercise-induced increases in ATP turnover rate are associated with a decrease in CP concentration and an increase in glycolytic activity (Hultman and Spriet 1986; Spriet, Soderlund, Bergstrom and Hultman 1986). However CP and ATP concentrations are still 30% and 80% of resting values at a time when exercised muscle is showing fatigue, i.e. a 45% reduction in power output (McCartney et al, 1986; Spriet et al. 1985a). Therefore reduced ATP concentrations and production do not appear to be causes of fatigue since its production and supply are relatively well maintained.

Decreases in the concentrations of glycolytic energy substrates

Fig. 1. A schematic representation of the glycolytic pathway in skeletal muscle. All enzymes can function physiologically in the reverse direction except those marked with an asterisk. From: Newsholme, E.A. and A.R. Leach. 1983. Biochemistry for the Medical Sciences. Chichester, England: John Wiley & Sons.



19

(glycogen and glucose) in muscle during exercise also do not appear to be the causes of fatigue. It has been shown that intramuscular glycogen stores need not be depleted in fatigued muscle (Spriet et al, 1985a) and that muscle may undergo significant glycogen depletion without the development of fatigue (Fitts et al. 1982). Cellular metabolic processes involved in ATP production may, however, be at least partially responsible for the decrement in muscle performance. Accumulation of the endproducts of glycolysis (La^-) and ATP hydrolysis (AMP, Pi , Mg^{++}) are intimately associated with fatigue (Fitts & Holloszy 1976; Sahlin et al. 1981; Hibberd & Trencham 1986). La^- , as a strong ion, exerts a major effect on the physico-chemical properties of fatigued muscle.

1.2.3.3 Events Related to Excitation-Contraction Coupling and Relaxation

The most important sequences of events in muscle contraction are the processes of excitation-contraction coupling and subsequent relaxation. The former event leads to force generation by the muscle, relaxation allows the muscle to recover (at least partially) so that the cycle of force generation can be repeated. All biochemical events occurring at the mitochondria, in the sarcoplasm or at the sarcolemma can be considered as leading toward these two essential processes of contraction and relaxation. An impairment of any one, or combination of, key biochemical events can have three major outcomes which will cause muscle fatigue. These are: (1) a reduction in the number of actomyosin cross-bridges formed; (2) a decrease in the rate of cycling of actomyosin cross-bridges; and (3) an increase in the relaxation time

20

of the muscle. These events may thus be considered to be the proximate causes of muscle fatigue, but the sequence of events leading to one or more of the fatigue-causing states must be examined to find those which exert major influences. The most common of these fatigue-associated factors, as they are presently understood, are briefly described below.

Cell membrane (sarcolemma) related events include changes in membrane permeability to electrolytes (including lactate), thus resulting in changes in the extra- and intracellular ion concentrations, $[SID]$, and resting membrane potential. Exercise induced changes in sarcolemmal permeability to K^+ (and possibly Na^+) have been realized since 1902 (Bernstein 1912; Overton 1902). Later, Fenn and Cobb (1936) showed a 50% decrease in muscle $[K^+]$ and a compensatory increase in $[Na^+]$ in directly stimulated skeletal muscles of the frog and rat. Subsequently Hodgkin and Horowicz (1959b) demonstrated that these changes reduce the resting membrane potential and the amplitude of the action potential. The decreased membrane excitability is linked to a diminished release of intracellularly sequestered Ca^{++} , resulting in reduced actin-myosin crossbridge formation and recycling (Sandow 1965; Fink et al. 1983).

Excitation-contraction coupling is initiated by depolarization of the sarcolemma caused by a neural stimulus transmitted to the neuromuscular junction. Sufficient membrane depolarization results in the development of a muscle action potential. Simply, the muscle action potential is associated with fluxes of Na^+ into, and of K^+ out of, the cells and leads to the release of sequestered Ca^{++} from the sarcoplasmic reticulum. The large increase in cytosolic free $[Ca^{++}]$ initiates the sequence of events leading to

contraction (Huxley 1969). Ca^{++} binds to high affinity Ca^{++} -binding sites on troponin C molecules of the contractile proteins. The binding of 4 Ca^{++} to one molecule of troponin C has been postulated (Ebashi & Endo 1968) to cause a conformational change in the molecular structure of troponin C which lifts the inhibition by tropomyosin of the myosin binding sites on the actin molecule. Thus the number of active actin-myosin crossbridges formed is proportional to the amount of Ca^{++} released from the SR. The strength of contraction is directly proportional to the number of actin-myosin cross-bridges formed, and thus upon the amount of Ca^{++} released from the SR to bind to troponin C (Caille et al. 1985; Hibberd & Trentham 1986). Mechanical work results from the cyclic interaction of the troponin, actin and myosin myofilaments coupled to the hydrolysis of ATP and release of ADP and P_i (Hibberd & Tretham (1986).

Relaxation of the sarcomeres is initiated by repolarization of sarcolemmal membranes due to the restoration of the ionic and electrochemical gradients across the membrane. The release of active actin-myosin crossbridges occurs by the pumping of Ca^{++} from the sarcoplasm into the SR by a Ca^{++} -ATPase (Huxley 1969). As Ca^{++} is removed, intracellular $[\text{Ca}^{++}]$ becomes low, Ca^{++} is released from its sites on troponin C and unmasks the inhibitory sites on the actin molecules. Myosin ATPase, the enzymatic component of the actin-myosin complexes, derives energy from the hydrolysis of ATP which causes conformational changes in the complexes. In the presence of low $[\text{Ca}^{++}]$ and ATP the myosin heads are released from actin active sites, the troponin inhibition of crossbridge formation is established, and relaxation results (Ebashi & Endo 1968; Hibberd & Trentham 1986).

22

An increase in intracellular $[H^+]$ is purported to exert its major effects as a causative agent in muscle fatigue by competitively inhibiting Ca^{++} -binding sites on troponin C, and by impairing the activities of Ca^{++} - and myosin-ATPases. Reduced tension development in the presence of high $[H^+]$ has been associated with: (1) decreased activity of the Ca^{++} -ATPases responsible for pumping Ca^{++} from the transverse tubular system and sarcoplasm into the extracellular fluids (ECF) and SR (Gonzalez-Serratos et al. 1978; Fabiato & Fabiato 1978; Fitts et al. 1982); (2) decreased activity of myosin-ATPase (Portzehl et al. 1969; Fabiato & Fabiato 1978); and (3) the binding of H^+ to the high affinity Ca^{++} -binding sites on troponin C (Williams et al. 1975). These combined effects will result in a reduction in the force of contraction by inhibiting both the contraction and the relaxation processes. However there is no direct evidence that H^+ does, in fact, participate in the events cited above; indeed the effects on enzyme activity are more likely the result of conformational changes of protein active-sites caused by the much larger changes in the concentrations of intracellular strong ions which occur in exercise.

The existence of a competition for H^+ and Ca^{++} for troponin and ATPase binding sites has been questioned by Fuchs (1974). Also, since $[H^+]$ is dependent on $[SID]$, PCO_2 and $[A_{TOT}]$, an effect of H^+ alone on the biophysical events of excitation-contraction coupling cannot be demonstrated. Recent studies indicate that the observed changes in muscle contractile properties may be explained in terms of the effects of the energy state of the muscle on the kinetics of Ca^{++} release and re-uptake and on the kinetics

of myofilament crossbridge attachment and detachment (Blanchi & Narayan 1982; Scales & Sabbadini 1979).

23

1.3 HISTORICAL DEVELOPMENT OF SKELETAL MUSCLE ION REGULATION

1.3.1 Muscle Fiber Composition and General Properties

Skeletal muscle was initially classified according to observed relationships between muscle fiber color and contractile properties (Ranvier 1873) and metabolism (Gleiss 1887). Gleiss (1877) used lactic acid production in electrical stimulation as a means of investigating the behavioural differences between mammalian slow red and fast white fibers, and between frog and toad muscles (Needham 1971).

The present classification of the three main skeletal muscle fiber types similarly depends upon the biochemical characteristics and contractile properties of the muscle fibers (Close 1972; Saltin and Gollnick 1983). The red fibers contract slowly when stimulated and are termed slow-twitch. Also, red fibers have a relatively high complement of oxidative enzymes and a high oxidative capacity. According to these properties red fibers may thus be classified as slow oxidative (SO) fibers. White fibers, on the other hand, have fast-twitch properties and have a relatively low oxidative capacity but a high glycolytic potential, eg. the ability to produce chemical energy (ATP) from glycolysis via the glycolytic pathway resulting in lactate accumulation. White fibers may thus be classified as fast glycolytic (FG).

There is a gradation of oxidative and glycolytic muscle fibers between SO and FG types. Most of these fibers have fast-twitch

properties and are thus termed fast oxidative glycolytic (FOG) fibers. The different muscle fiber types also differ in their fluid and electrolyte composition and resting membrane potential (Table 2), and metabolites, proteins, organelles and capillary supply (Table 3). Morphological studies have shown that SO fibers have a relatively small diameter and contain more sarcoplasm and mitochondria per unit area than FG fibers, which have a large diameter, high phosphorylase activity and low mitochondrial density (Kirkwood et al. 1986).

Skeletal muscle fibers are bounded by a membrane permeable to water, so the total muscle water consists of extra- and intracellular fluids. Intracellular fluid (ICF) thus consists of intracellular water plus all of the freely diffusible intracellular ions and molecules which it contains. Extracellular fluid (ECF) has been defined as a liquid which resembles plasma ultrafiltrate (Manery 1954) since it contains ions and small molecules which diffuse freely from the plasma. The extracellular fluid can be further divided into the interstitial fluids, water associated with connective tissue, and 'trapped' plasma (Manery 1954). Trapped plasma consists of plasma in the fine vasculature of the muscle, whereas interstitial fluid is the fluid present between the external surfaces of individual cell membranes (eg. the interstitial spaces). The interstitial spaces are very small and the interstitial fluid volume has been calculated (Manery 1954) to represent only about 22% of the total muscle extracellular fluid volume (ECFV). In resting muscle the ECFV amounts to 7-15% of the TTW, depending on the type of muscle.

The fact that muscle contains Na^+ , Cl^- , K^+ , Mg^{++} , Ca^{++} , La^- and phosphate was first reported in 1840 by

TABLE 2

The composition of mammalian skeletal muscle fibers at rest. I. Metabolites, fluid, electrolytes, membrane resting potential, contractile characteristics, and blood flows.

Parameter	Animal	SO	FOG	FG	Reference
creatine phosphate	human	52-56	57-67	57-71	3
	human	69-83	76-88		13
	rat	39-53	58-78	72-104	3, 6, 13
	cat	50-60		80-86	12
ATP	human	20-26	23-28	20-22	3, 13
	rat	17-25	25-28	26-31	3, 6, 13
	cat	14-18		28-32	12
Pi	rat		17		11
	cat	35-45		25-35	12
glycogen (gluc. units)	human	130-280	280-330	310-450	3
	rat	89-163	93-250	107-241	3, 6, 9, 11
lactate	human		16 (10-34)		1
	rat	10-14	6-14	7-11	6, 11
	cat	5-7		4-6	12
	human	23-37	13-23	13-23	3
triglyceride	rat	6-34	8-13	6-11	3, 9

... cont'd

TABLE 2 (cont'd)

Parameter	Animal	SO	FOG	FG	Reference
ECFV	rat	.53-.72	.33-.46	.34-.38	2, 4, 15
	human	0.38	0.26		1
ICFV	rat	2.72	2.64-2.75	2.58-2.63	2, 4, 15
	human	2.82	2.90		1
[Na ⁺]	human	7-51	12-88		14
	rat	13-40	10-26	12-16	2, 4, 5, 6, 15
[K ⁺]	human	120-191	131-175		14
	rat	129-157	150-165	167-179	2, 4, 6, 15
[Cl ⁻]	rat	27-30		19-26	4, 15
[Mg ⁺⁺]	human	11-19	10-15		14
	rat	12-14	16-18		6
[Ca ⁺⁺]	rat	1.6-2.8	2.9-3.7		6
Em	rat	-71	-81		15, 24
contraction time	rat	38-135	45-55	16-45	8, 10, 22, 23, 24
1/2 relaxation time	rat	65-210	35-45	15-50	10, 22, 23, 24
blood flows	rat	120-160	40-80	15-60	17, 18, 19
(anesthetized)	rat	7-23	6-12	3-8	20, 25
(conscious)	rat	28-40	13-19	6-14	25
	cat	12-28	7-11		21

Note: some values converted from wet weight to dry weight using a factor of 4.3.
 Fiber type composition, units and references are given the on following two pages.

TABLE 2 (cont'd)

Muscle fiber types:

animal	muscle	ZSO	ZFOG	ZFG	Reference
rat	see references 13 and 16				
cat	biceps brachii	5	20	75	12
	soleus	93	7	0	12
human	triceps brachii	19-60	40-81		14
	vastus lateralis	29-78	29-49	14-26	13, 14
	soleus	49-88	17-31	2-16	13, 14

Units: Metabolites in $\mu\text{mole/g}$ dry weightFluid volumes in ml/g dry weightIons in mEq/l intracellular fluid (ICF)Membrane resting potential (E_m) in mV

Contraction/Relaxation times in milliseconds

Blood flows in ml/min/100 g wet weight

TABLE 2 References

- | | |
|--|--------------------------------|
| 1. Sjogaard & Saltin 1982 | 2. Sreter & Woo 1963 |
| 3. Saltin & Gollnick 1983 | 4. Drahota 1961 |
| 5. Campion 1974 | 6. Chutkow 1973 |
| 7. Fregosi & Dempsey 1986 | 8. Staudte et al. 1973 |
| 9. Spriet et al. 1985b | 10. Witzmann et al. 1983 |
| 11. Favier et al. 1986 | 12. Meyer et al. 1985 |
| 13. Edstrom et al. 1982 | 14. Sjogaard 1983 |
| 15. Leader et al. 1984 | 16. Armstrong & Phelps 1984 |
| 17. Armstrong & Laughlin 1984 | 18. Laughlin & Armstrong 1982 |
| 19. Gorski et al. 1986 | 20. Mackie & Terjung 1983a & b |
| 21. Folkow & Halicka 1968 | 22. Woittiez et al. 1985 |
| 23. Fitts et al. 1982; Troup et al. 1986 | |
| 24. Segal et al. 1986 | 25. James et al. 1986 |

Table 3. The composition of mammalian skeletal muscle fibers at rest.

II. Myoglobin, capillary density, organelle volume density
enzyme activities.

Units: Myoglobin in mg/g dry weight

Capillary density: capillaries per mm^2

Organelle volume density in %

Organelle surface:volume ratio in $\mu\text{m}^2/\mu\text{m}^3$

Enzyme activities in $\mu\text{mole/gram wet weight/min @ 20-25}^\circ\text{C}$

- References:
1. Harms & Hickson 1983
 2. Kirkwood et al. 1986
 3. Edstrom et al. 1982
 4. Saltin and Gollnick 1983
 5. Hebisch et al. 1986
 6. Thomason et al. 1986
 7. Armstrong & Laughlin 1984
 8. Kjeldsen et al. 1984 (32 wk. old rats)
 9. Chi et al. 1986
 10. Hoppeler et al. 1985
 11. Stonnington & Engel 1973
 12. Kayer et al. 1986
 13. Andersen 1975
 14. Sillau 1986

TABLE 3

Parameter	Animal	SO	FOG	PG	Reference
myoglobin	rat	3	2	0.5	1
capillary density	human	287	-220-		13
	rat	392		135	14
M volume density	human		3-5		10
	rat	11-17		7-10	2, 12
M surface:volume	rat	5-8		6-9	2
SR volume density	rat	6.6		2.1	11
SR surface:volume	rat	1.8		4.5	11
phosphorylase	human	3	6	9	4
	rat	14	115	171	4
citrate synthase	human	11	9	7	4
	rat	20-30	17-41	7-12	1, 4, 5
phosphofructokinase	human	6-8	11-16		4
	rat	21	69	100	4
pyruvate kinase	rat	64	493	696	4
lactate dehydrogenase	human	60-110	180-260	160-220	4
	rat	42-51		775-830	9
succinate dehydrogenase	rat	7-10	2-9	2-7	1, 4
	rat	3-5	3-4	1-2	7
myosin ATPase	human	160		480-590	4
	rat	180-240	520-600	660-700	4, 6
creatine kinase	human	222		333	4
	rat	114		424	4
Na ⁺ -K ⁺ -ATPase	rat	120-130	115-135	149-173	8

° M = mitochondrial; SR = sarcoplasmic reticulum.

Berzelius. Liebig (1847) noted that muscle was rich in K^+ and poor in Na^+ while the reverse was true in the blood. Katz (1896) was the first to report that muscle tissue possessed nerves and blood vessels in addition to connective tissue and muscle fibers; he was also the first to measure accurately the ionic composition of muscle fibers from several animals. Studies on cell permeability (Overton 1902; Hober 1906) resulted in the first two theories which attempted to explain the different compositions of extra- and intracellular fluids: (a) the muscle fiber was enclosed by a semipermeable membrane resistant to the diffusion of sugar and some salts, but more permeable to potassium salts; and (b) the muscle fiber behaved like a colloidal suspension of gelatin and fibrin without a membrane (Ling's membrane theory, see Manery 1954). These studies also showed that muscular contraction was associated with the loss or gain of water from the muscle fibers to the spaces between them.

Fenn and coworkers (Fenn et al. 1934; Fenn and Cobb 1936) considered the sarcolemma to participate in transmembrane ion movements by virtue of its own enzymes and metabolic processes. Their pioneering investigations indicated that intracellular enzymatically controlled processes, together with physico-chemical processes, govern the active transport of inorganic ions (Na^+ , K^+ , Cl^- , Ca^{++} , Mg^{++}) and maintain concentration gradients. Manery (1954) stated that the inorganic ions "are now known to play a major role in the specific function of cells such as contraction in muscle and to act as enzyme catalysts in metabolic processes such as glycolysis (K^+ , Na^+ , Mg^{++})". These roles for inorganic ions were in marked contrast to static maintenance of osmotic pressure and electrical

neutrality attributed to them by Overton (1904) and Hober (1906).

29

Drahota (1961), using the extracellular Cl^- space to calculate ICFV in rat hindlimb muscles, made the first report of differences in the fluid and ionic composition of red and white muscles. Drahota showed that both the Cl^- and inulin spaces (and thus the ECFV) of soleus (a primarily SO muscle) was greater than in the primarily FG muscles, tibialis anterior (TA) and extensor digitorum longus (EDL). Also, the ICF of soleus had a higher $[\text{Na}^+]$ and $[\text{Cl}^-]$ but lower $[\text{K}^+]$ than the ICF of TA and EDL. Sreter and Woo (1963), using inulin as a measure of ECFV, confirmed and extended Drahota's initial observations to 12 skeletal muscles of the rat. Recently, Sjogaard (1983) has shown that these same relationships also occur in individual skeletal muscle fibers of man. Sreter and Woo (1963) suggested that these differences in ionic composition of red and white muscle "may be a factor in their different speed of contraction". White fibers, which have fast contractile properties, are easily fatiguable while red fibers, possessing slow twitch properties, do not fatigue easily (Close 1972) and are often termed 'fatigue resistant'.

1.3.2 Intramuscular Compartmentation of Ions

In superfused (in vitro muscle bath preparation) frog muscle, Fenn et al. (1934) reported that all of the muscle Cl^- diffused freely into the surrounding medium and concluded that Cl^- was absent from the ICF. Since they presumed that all of the Cl^- was extracellular, the calculated Cl^- space gave a measure of the volume of the muscle ECF compartment, or muscle ECFV. Using this measure, Fenn and Cobb (1936) were able to estimate the size and

30

composition of the intracellular compartment under various experimental conditions. Fenn (1936) concluded that the sarcolemma was impermeant to anions and that the large excess of cation equivalents over anion equivalents in the muscles is largely made up by proteins. With respect to the contribution of intracellular proteins in maintaining electrical neutrality Fenn was correct, however it is now known that Cl^- occurs intracellularly.

Comparison of intracellular $[\text{Cl}^-]$ with Cl^- activity measured with microelectrodes in barnacle (Hinke & Gayton 1971), frog (Kernan et al. 1974), mouse (Donaldson & Leader 1984) and rat (McCaig & Leader 1984) muscle fibers consistently show that between 80-90% of intracellular Cl^- is not detected by the electrodes (Table 4). Thus most of the intracellular Cl^- appears to be 'bound' or sequestered within the intracellular compartment. Indeed, the Cl^- content of intracellular organelles tends to be greater than that of the sarcoplasm in both frog and rat skeletal muscles (Gonzalez-Serratos et al. 1978; Sembrowich et al. 1982).

The initial studies in barnacle and frog muscle indicated that Cl^- may not be passively distributed across the sarcolemma. This was later confirmed for mammalian skeletal muscle by Dulhunty (1978). Recently it has been demonstrated that the muscle cells of frogs (Hironaka & Morimoto 1980) and rodent mammals (Dulhunty 1978) actively accumulate Cl^- under physiological conditions. These findings have been questioned by the studies of Cl^- activity in the mouse (Donaldson & Leader 1984) and rat (McCaig & Leader 1984). These workers found that the measured intracellular Cl^- activity was only slightly higher than that predicted by a Gibbs-Donnan equilibrium

Table 4. Intracellular compartmentation of ions in skeletal muscles at rest. Membrane resting potential, ion concentrations, activities, activity coefficients, % ion sequestered, % ion diffusible.

Units: Membrane resting potential (E_m) in mV

Total concentration and activity in mEq/l

Activity coefficient = ion activity/[ion]

Abbreviations: sartor. = sartorius

- References:
1. Hinke & Gayton 1971
 2. Kernan et al. 1974
 3. McLaughlin & Hinke 1968
 4. Kostyk et al. 1969
 5. Lee & Armstrong 1974
 6. Donaldson & Leader 1984
 7. McCaig & Leader 1984
 8. Cohen & Burt 1977
 9. Leader et al. 1984
 11. Juel 1986
 11. Maughan & Recchia 1985

TABLE 4

Ion	Animal	Muscle	Em	total conc.	activity	activity coefficient	Reference
Na ⁺	barnacle		-80	35	9	0.26	3
	frog		-85	13-29	5-13	0.38	4, 5, 11
	mouse	EDL	-73	38	16	0.42	6
	mouse	soleus	-70		8-16		11
	rat	EDL	-79	18-26	7.4	.28-.41	9
K ⁺	barnacle		-80	170-180	130-140	0.77	1, 3
	frog		-86	94-146	70-110	.48-.70	4, 5, 11
	mouse	EDL	-76	157	118-210	0.78	6, 10
	mouse	soleus	-70		168		10
	rat	EDL	-79	168-180	99	.55-.59	9
Mg ⁺⁺	frog			13-23	5-17	.30-.42	8, 11
Cl ⁻	barnacle		-72	30	30	1.0	1
	frog		-90		3.1		2
	mouse	EDL	-76	44	5.3	0.12	6
	rat	EDL	-79	19-26	4-6	.18-.24	7, 9

* Cl⁻ activity higher than predicted on the basis of a Donnan equilibrium.

32

(Hodgkin & Horowicz 1959a) and concluded that Cl^- was passively distributed. However their studies on mammalian muscle were performed at a temperature of $17-20^\circ\text{C}$ which would reduce the Cl^- pump activity, thus allowing the passive Cl^- efflux to predominate (Donaldson & Leader 1984). It is important to note that all of the above studies were conducted on isolated muscle preparations where the muscles were placed in a bath which was free of protein. The absence of protein (albumin) from the bathing medium substantially increases the anion permeability (Macchia et al. 1984) and also significantly reduces (by about 20%) the resting membrane potential (Shetty et al. 1985) of the sarcolemma. Consideration of the available data (Dulhunty 1978; Hironaka & Morimoto 1980; Donaldson & Leader 1984) suggests that Cl^- may not be passively distributed across the sarcolemma of skeletal muscle under physiological conditions, and that there is an active inward flux of Cl^- under physiological conditions.

Intracellular Na^+ was initially thought to be absent or in very small concentration in most tissues (Fenn 1936; Manery 1954) because of the use of the Cl^- space for measuring ECFV. Since some of the intramuscular Cl^- is intracellular, the Cl^- space, as used by Fenn, Manery and their contemporaries, thus overestimates ECFV and underestimates both the ICFV and the concentrations of intracellular substances. In some tissues Na^+ was measured to be in excess of that calculated by the Cl^- space and some Na^+ was deemed to be intracellular (Harris 1950). Like Cl^- , Na^+ has now been localized to the sarcoplasm and intracellular organelles (Sembrowich et al. 1982). Studies on skeletal muscles of barnacle and crab (Hinke 1959), frog (Lee & Armstrong 1974) and mouse (Donaldson &

Leader 1984) using Na^+ -sensitive microelectrodes have shown that only about 40% of the measured total intracellular $[\text{Na}^+]$ is free in the sarcoplasm (Table 4). This has led to the conclusions that significant amounts of Na^+ ions are 'bound' intracellularly to large molecules such as myosin (Lewis & Saroff 1957) or on the cellular surface, or are rendered effectively unavailable due to confinement within subcellular organelles (Gonzalez-Serratos et al. 1978; Sembrowich et al. 1982). Na^+ , together with K^+ , is capable of binding to myosin, but not to actin or serum albumin (Lewis & Saroff 1957). Na^+ binds to myosin more strongly than K^+ , and binding increases with increasing concentration of Na^+ or K^+ . The binding of Na^+ and K^+ to myosin also appears to be sensitive to temperature- and ion-related changes in the structure of imidazole and amino groups of myosin (Lewis & Saroff 1957).

Potassium (K^+) has always been considered to be in high concentration in the ICF (Berzelius 1840; Katz 1896). Some K^+ is closely associated with muscle glycogen stores (Hultman 1967; Patrick 1977) and with myosin (Lewis & Saroff 1957) while most is uniformly distributed in the sarcoplasm and intracellular organelles (Sembrowich et al. 1982). Hultman's (1967) data for humans shows that intracellular $[\text{K}^+]$ increases 25 μEq per 200 μg of glycogen, such that the maximum amount of K^+ bound to glycogen cannot be greater than 5-6% of total cell K^+ . This value is in keeping with the finding that only about 5% of the total muscle K^+ can not participate in a free ^{42}K exchange in resting muscle (Fischer et al. 1950). Ion activity measurements for K^+ in frog muscle (Lee & Armstrong 1974) and in mouse white muscle (Donaldson & Leader 1984),

however, indicate that about 25% of the intracellular K^+ is bound or compartmentalized so that it is not detected by ion selective electrodes (Table 4).

The intracellular concentrations of free Mg^{++} in most tissues studied have been calculated (Veloso et al. 1973) or measured by nuclear magnetic resonance (Gupta et al. 1984) to be about 0.5-1.0 mmol/l. Intracellular activities for Mg^{++} (Table 4) have been difficult to obtain due to marked interference effects from other cations. The concentration of ionic Mg^{++} is believed to be low in specific sites within the fiber, which would explain its catalytic effects in trace amounts (0.5-1.0 mEq/l), although the concentration of total intracellular Mg^{++} is considerably higher (Manery 1954; Gupta et al. 1984). A substantial portion of muscle Mg^{++} thus appears to, be bound to proteins or phosphate esters (Tabor & Hastings 1943; Maughan & Recchia 1985). However, of the total intracellular concentration of Mg^{++} (about 10 mmol/l) about 60% appears to be readily diffusable, at least in frog muscle (Maughan & Recchia 1985).

Intracellular Ca^{++} occurs in sufficiently high concentration that in the presence of the high intracellular phosphate concentrations precipitation would occur unless the concentration of free ionic Ca^{++} was very low (Manery 1954). Intracellular Ca^{++} is largely sequestered and morphologically separated from the phosphates. For example, Gonzalez-Serratos et al. (1978) have shown that the Ca^{++} content of the sarcoplasmic reticulum is 66-fold greater than that of the sarcoplasm. The important roles of Ca^{++} and phosphates on muscle function continue to be areas of active research (Hibberd & Trentham 1986).

Knowledge of the compartmentation of intracellular inorganic ions has been greatly facilitated by the technique of electron probe analysis of frog semitendinosus muscle (Gonzalez-Serratos et al. 1978) and rat soleus and gastrocnemius muscle (Sembrowich et al. 1982). In frog muscle the content of all major inorganic ions is greater in the terminal cisternae of the sarcoplasmic reticulum than their respective contents in the sarcoplasm; for Ca^{++} , notably, this difference is 66-fold. In rat muscle Cl^- appears to be evenly distributed through the sarcoplasm, sarcoplasmic reticulum and mitochondria, while the other strong ions (Na^+ , K^+ , Ca^{++} and Mg^{++}) showed an uneven distribution between cytoplasm and organelles which differed with muscle fiber type (Sembrowich et al. 1982).

1.3.3 Trans-Sarcolemmal Ion Movements and Membrane Potential

The initial 'membrane theory' required separation of extra- and intracellular compartments by a semipermeable membrane permeable to smaller cations (H^+ and hydrated K^+), but impermeable to anions and to the larger hydrated Na^+ ; K^+ was kept intracellular by large nonpenetrating anions, i.e. proteins (Overton 1902; Bernstein 1912). Bernstein suggested that, due to the high intracellular $[\text{K}^+]$, the 'sarcoplasmic membrane' was responsible for maintaining a potential difference between the inside and outside of the cell (outside positive and inside negative) and that changes in potential should alter the functional behaviour of the muscle. The requirement of external Na^+ for muscle excitation was first reported by Overton (1902), who suggested that there may be some exchange between intracellular K^+ and extracellular Na^+ .

An association between K^+ movement and change in pH was first reported by Mond and Netter (1930), and led to the suggestion of a K^+/H^+ exchange across the sarcolemma. Fenn and Cobb (1934) reported that the diffusion of K^+ from frog muscle was increased when the pH of the muscle bath was lowered, and that external K^+ must be added to give an equilibrium, but that an intracellular acidosis resulting from an increase in CO_2 reduced the loss of K^+ . Frog muscle in KCl solutions increased in volume and took up K^+ in excess of Cl^- . Fenn (1936) interpreted these results as the movement of Cl^- from the muscle bath into the muscle ECF and, that K^+ uptake into the cells occurred by the diffusion of undissociated KOH instead of by exchanging with H^+ . It was generally agreed at the time that K^+ could not enter with another anion since muscles were considered to be 'anion-impermeable'.

The impermeability of muscle to anions, and to Cl^- in particular, was challenged as early as 1927 by Winterstein and Hirschberg. They showed that Cl^- diffused through frog abdominal muscle and concluded that muscle is permeable to Cl^- (Fenn 1936). Wesselkina (1932) used the same method as Winterstein and Hirschberg to show that La^- could diffuse through muscle (Fenn 1936), and Conway and Kane (1934) demonstrated that La^- can diffuse into muscle ICF from the surrounding medium. Fenn (1936) maintained that the muscles were anion impermeable and explained these results as due to cell injury or to the diffusion of La^- from muscle as undissociated lactic acid (HLa).

Boyle and Conway (1941) extended the membrane theory to include free permeability to Cl^- and probably also to H^+ , OH^- ,

HCO_3^- but maintained impermeability to Na^+ , and phosphate and protein anions. This theory fit closely with the physico-chemical constraints of the system: the diffusible ions were distributed according to the Gibbs-Donnan laws; that electroneutrality existed on both sides of the membrane; and that the solutions on either side of the membrane were isosmotic (Manery 1954). However, Boyle and Conway maintained that the muscle cell was impermeable to Na^+ , in disagreement with the earlier reports of Overton (1902), Fenn et al. (1934) and Fenn (1936). Fenn et al. (1934) confirmed earlier suggestions that frog muscle contained intracellular Na^+ . This was undoubtedly difficult to show at the time, because with the Cl^- space used as a measure of ECFV, the cell was shown to contain no Cl^- and very little, if any, Na^+ . Under conditions of muscle stimulation (Fenn (1936) stated that "sodium without chloride appears to enter the cells in exchange for potassium". Thus, according to Boyle and Conway, cation (eg. K^+) accumulation occurred passively as the result of the intracellular deposition of impermeant anions.

Ussing (1947), in experiments on frog muscle using radio-sodium, suggested a membrane model in which extracellular K^+ exchanged for intracellular Na^+ without consumption of energy. The idea of a Na^+/K^+ exchange was an important development in our understanding of muscle physiology, however by not invoking energy consumption Ussing appears not to have accounted for the fact that both Na^+ and K^+ would be moving against steep concentration gradients. In his Croonian lecture Krogh (1946) suggested that the Na^+ equilibrium across the sarcolemma represents a 'steady state' which requires the continuous expenditure of energy to export Na^+

gained by inward diffusion. Based on the calculations of Boyle and Conway (1941), Krogh thought it improbable that K^+ was actively transported in skeletal muscle and that equilibrium was maintained by the outwardly directed active transport of Na^+ .

The energy requirement for maintaining the resting potential was subsequently shown. In resting muscle maintenance of the membrane potential does not appear to be dependent on oxygen supply or oxidative metabolism, but appears to be very dependent on glycolysis. In frog sartorius muscle, cyanide (a potent inhibitor of oxidative, but not glycolytic, metabolism) and anoxia did not produce a significant fall of the resting potential (Fenn et al. 1940; Ling & Gerard 1949). However iodoacetate, a potent inhibitor of glycolysis while having no effect on oxidative metabolism, resulted in a gradual fall of the muscle resting potential (Ling & Gerard 1949). The rate of fall was slowed by decreasing temperature or by the addition of external pyruvate, lactate, succinate or fumarate. This would seem to indicate that the energy required for the maintenance of the resting potential was ultimately derived from glycolysis. Iodoacetate and anoxia or cyanide together greatly increased the rate of fall of the resting potential, and this was further increased 2-fold during depletion of high-energy phosphates by stimulation (Ling & Gerard 1949). These results indicate that the energy required for maintaining the resting potential is, to a large degree, derived from ATP supplied by glycolysis.

Steinbach, in 1951, further modified the membrane theory to include permeability to Na^+ , requiring that some pumping device must be operating to keep intracellular $[Na^+]$ consistently low in

the face of constant inward diffusion from the high external $[Na^+]$. Kernan (1962) reported that frog muscle actively pumped sodium out of the cell, suggesting the the Na^+ pump was purely electrogenic with K^+ uptake being entirely passive. However Frumento (1965) later showed that there was some chemical coupling between K^+ and Na^+ pumping in muscle. The first direct evidence for the electrogenic pump's contribution to the resting membrane potential was shown in rat muscle by Locke and Solomon (1967) who showed that ouabain caused a significant depolarization of the resting membrane potential in vivo. In muscles with intracellular $[Na^+]$ elevated by prior stimulation, Horowicz and Gerber (1965) showed that an increase in external $[K^+]$ increases the rate of Na^+ efflux in such a way that the membrane potential remains above the K^+ potential. This latter phenomenon has been attributed to the operation of the Na^+ pump in an electrogenic fashion (Adrian & Slayman 1966). Azide, an inhibitor of oxidative phosphorylation, greatly reduces the the ouabain-sensitive K^+ influx and reduces the increase in Na^+ efflux induced by high external $[K^+]$ (Beauge & Sjodin 1976), indicating an energy requirement.

The sodium pump, also known as the membrane enzyme termed the $Na^+-K^+-ATPase$, has been shown to require monovalent cations (particularly Na^+ and K^+) for its activation (Sjodin 1971). In nearly all tissues examined the 'pump' appears to have a stoichiometry of 3 Na^+ transported outward for 2 K^+ transported inward for each ATP hydrolysed in the reaction (Schwartz et al. 1972; Thomas 1972). Thus operation of the ATPase appears to result in an electrogenic polarization of the sarcolemma which contributes to the

40

membrane potential (Kernan 1962; Frumento 1965; Akaike 1975). Cation coupling to the membrane ATPase in vertebrate skeletal muscle appears to be under metabolic control (Sjodin 1982). When ATP decreases there occurs a $\text{Na}^+:\text{Na}^+$ exchange in addition to the normal $\text{Na}^+:\text{K}^+$ exchange (Kennedy & DeWeer 1977). This has been interpreted to mean that the ATPase operates in two modes, the $\text{Na}^+:\text{K}^+$ or $\text{Na}^+:\text{Na}^+$, and that ATP depletion begins to limit the rates of exchange in these two modes (Sjodin 1982). It is evident that, during and following muscular activity, the sarcolemmal $\text{Na}^+:\text{K}^+$ -ATPase should play an important role in intracellular ion regulation and in regulation of the membrane potential. Activity induced increases in intracellular $[\text{Na}^+]$ and extracellular $[\text{K}^+]$ are expected to have a stimulatory effect on the enzyme activity and facilitate restoration of the intracellular environment and membrane potential.

Based on the findings of muscle fiber type differences in electrolyte composition (Drahota 1961; Sreter & Woo 1963), Sreter and Woo postulated that red fibers have a lower resting potential and a longer time course of action potential than white fibers. This was first shown to be true using isolated rat hindlimb muscles stimulated in a muscle bath (Yonemura 1967). The resting and action potential measured with glass micro-electrodes showed a greater resting potential and a larger action potential in fast-twitch white EDL than in slow-twitch red soleus. The differences in electrical properties between the fiber types were correlated with a greater intracellular $[\text{K}^+]$ and lower intracellular $[\text{Na}^+]$ in the EDL than in the soleus. It has also recently been reported that slow red soleus fibers

of the mouse have a significantly higher concentration of sarcolemmal $\text{Na}^+-\text{K}^+-\text{ATPase}$ than the fast-twitch EDL (Clausen & Hansen 1982; Abdel-Aziz et al. 1985). These observations appear to be related to the different contractile properties and rates of fatigue seen in muscles of differing fiber type.

1.3.4 Hydrogen Ion and pH in Skeletal Muscle

The first reported pH measurements of mammalian skeletal muscle were conducted by Michaelis and Kramsztyk (1914) on homogenates using a platinum/hydrogen electrode. Due to the nature of the electrode and the experimental conditions the pH values obtained were too alkaline; the authors realized that their technique had shortcomings. These initial attempts at measuring muscle pH were largely descriptive and not designed to answer questions related to muscle metabolism or physical chemistry, although theories regarding membrane permeability to H^+ and the nature of the transmembrane concentration difference were proposed.

The first reliable measurements of intramuscular pH were obtained using glass electrodes by Furusawa and Kerridge (1927) in cat gastrocnemius, cardiac and uterine muscles at rest and after electrical stimulation. Glass electrodes overcame the problem of oxidation/reduction effects on the platinum/hydrogen electrode. They reduced the problem of lactic acid and CO_2 production by freezing and mincing the dissected muscles in liquid nitrogen and measuring the pH of the homogenate at about 0°C . While the muscle homogenates were kept at 0°C the electrode was cooled to above 0°C to prevent excessive formation of condensate on the electrode, and thus the measurements

were probably made at between 2 and 5°C. The pH at 0°C was 7.04, which converts to 6.89 using a factor of -0.004 pH units/1°C (Furusawa & Kerridge 1927) or to 6.48 using a factor of -0.0152 pH units/1°C (Reeves & Wilson 1970).

The first careful studies of the effect of temperature on tissue pH were conducted by Rahn, Reeves and coworkers (Reeves & Wilson 1970; Malan et al. 1976; Reeves & Malan 1976). In various tissues from turtles, frogs and toads (including blood plasma and skeletal muscle) these workers have found a consistent relation between temperature (range 5 - 32°C) and extra- and intracellular pH which is about $(-0.016 \pm 0.003 \text{ pH units/1 } ^\circ\text{C})$. This value is significantly higher than the early reports on dog and cat skeletal muscle (Table 5) but in very good agreement with recent findings in mouse soleus (Aickin & Thomas 1977) and rat ventricle (Saborowski et al. 1973). It thus seems reasonable to apply a correction factor of -0.016 pH unit/1 °C change in temperature to convert reported pH values in the literature to a pH value at 37 °C. Care must be taken in the interpretation since in mammals, in contrast to ectotherms, the relation between temperature and pH at constant CO₂ content may not be linear (Reeves 1976). However, within the temperature range with which we are concerned this difference will not be great.

Examination of intracellular pH (pH_i) values 'corrected' to 37 °C shows that the pH at 37°C in a variety of vertebrate skeletal muscles ranges between 6.7 and 6.95 at physiological CO₂ concentrations in resting muscle (Table 6). Indeed these values are very similar to in vivo measurements of pH in vertebrate skeletal muscle using a variety of techniques (see Tables 5 & 6 of Roos & Boron

Table 5. The effect of temperature on the pH of animal tissues.

- References:
1. Hinke & McLaughlin 1967
 2. Boron and Roos 1976
 3. Malan et al. 1976
 4. Aickin & Thomas 1977
 5. Saborowski et al. 1973
 6. Furusawa & Kerridge 1927
 7. Carlstrom et al. 1928
 8. Spriet, Soderlund, Thompson & Hultman 1986

TABLE 5

animal	tissue	temperature range ($^{\circ}\text{C}$)	d pH/ 1°C	reference
barnacle	muscle	5 - 30	-0.008	1
"	"	30 - 40	-0.020	1
"	"	15 - 22	-0.006	2
bullfrog	plasma	5 - 32	-0.0206	3
"	sk. muscle	"	-0.0152	3
turtle	plasma	5 - 32	-0.0206	3
"	sk. muscle	"	-0.0186	3
"	heart	"	-0.0122	3
"	liver	"	-0.0233	3
"	sm. muscle	"	-0.0141	3
mouse	soleus	28 - 37	-0.018	4
rat	heart	21 - 37	-0.016	5
cat	blood	0 - 38	-0.009	6
cat	gastrocnemius	0 - 38	-0.004	6
dog	muscle juice	20 - 37	-0.007	7
human	vastus lateralis	0 - 37	-0.0105	8

Table 6. Resting muscle pH measurements in various animals 'corrected' from experimental pH to calculated pH at 37°C. The correction factor used was -0.016 pH unit/1°C (see text).

References: 1. Caldwell 1958

2. Galler & Moser 1986
3. Fenn 1928
4. Stella 1929
5. Root 1933
6. Fenn & Maurer 1935
7. Plontek & Herbst 1971
8. Gonzalez & Clancy 1986
9. Furusawa & Kerridge 1927
10. Wallace & Hastings 1942
11. Carlstrom et al. 1928
12. Burnell 1968
13. Sahlén et al. 1977
14. Spriet, Soderlund, Thompson & Hultman 1986

Note: Values in brackets () are the author's own corrected or measured value.

* Stella's (1929) correction using a PCO_2 of 20 mmHg.

TABLE 6

animal	tissue	method	T (°C)	PCO ₂ (mmHg)	pH	pH _{37°C}	ref.
crab	muscle	homogenate	20	?	7.21	6.938	1
"	"	pH electrode	20	?	6.99	6.727	1
"	"	"	20	3.5	7.14	6.868	2
frog	sk. muscle	?	22	?	7.20	6.96	3
"	"	?	22	20	6.90*	6.66	3
"	"	CO ₂ in vitro	18	18.5	7.0	6.696	4
"	"	CO ₂ in vitro	20	25	7.2	6.928	5
"	"	"	20	50	7.09	6.818	5
"	"	CO ₂ in vivo	20	25	6.95	6.678	6
"	"	"	20	35	6.90	6.628	6
"	"	dye	4	14	7.1	6.572	7
rat	tib. anterior	DMO	37	40		6.80	8
"	quadriceps	"	37	40		6.79	8
"	diaphragm	"	37	40		6.92	8
"	heart	"	37	40		6.83	8
cat	gastroc.	glass electrode	0	?	7.04 (6.89)	6.45	9
"	"	CO ₂	37??	50		6.89	10
dog	sk. muscle	press juice	20	?	7.03 (6.91)	6.76	11
"	neck muscle	DMO	37	29		6.84	12
human	qd. femoris	CO ₂ in vivo	37	40		6.95	13
"	v. lateralis	homogenate	0	2.6	7.50 (7.12)	6.912	14

Several investigators over the years have used the distribution of CO_2 in muscle to calculate pH_i (Table 6). The basis for the method is that dissolved CO_2 is freely diffusible across the cell membrane and will equilibrate on either side of the membrane according to physico-chemical constraints. The dissociation equilibrium of CO_2 on either side of the membrane can be used to calculate pH_i if external pH and CO_2 content is known. Fenn and Maurer (1935) realized that CO_2 or weak acid distribution methods give a pH value which lies somewhere in between external pH and pH_i . Using the Cl^- space to correct for the influence of external pH on the measured pH , they obtained a pH_i of 6.9 in frog muscle at room temperature with an intact PCO_2 (Table 6). This was the best early estimate of skeletal muscle pH_i . Wallace and Hastings (1942) used the same approach for in vivo cat skeletal muscle and obtained a pH_i of 6.89.

The weak acid distribution technique has culminated in the use of radiolabelled 5,5-dimethyl-2,4-oxazolidine-dione-2- ^{14}C (DMO) to estimate pH_i (Waddel & Butler 1959; Malan et al. 1976). The advantage of DMO over other weak acids is that it is nonvolatile under physiologic conditions, it has a pK of 6.1 at 37°C and has an ionic strength of 160 mM when used in a final concentration of 1 mmol/l (Roos & Boron 1981). The disadvantages of DMO are: that only one measurement per tissue can be made because the tissue is destroyed in the analysis; it depends on accurate measurement of the ECFV; and it yields an average pH of all of the intracellular compartments (Roos & Boron 1981). In a direct comparison of DMO and microelectrode measurements

of pH in barnacle muscle fibers, Boron and Roos (1976) and Hinke and Menard (1976) showed that the DMO method consistently gave a pH greater by about 0.05 than microelectrodes did.

The first direct measurements of pH_i were made by Caldwell (1954) by impaling single large muscle fibers of the crab with semimicro pH-sensitive glass electrodes; he reported a pH of 6.9 at 20° C. This value was not in agreement with a passive distribution for H^+ across the sarcolemma, and Caldwell concluded that there must be a cellular membrane mechanism whereby H^+ is actively transported across the sarcolemma. Similar findings followed in skeletal muscle of the rat (Carter et al. 1967) and frog (Kostyuk & Sorokina 1961). Glass microelectrodes are one of the most widely used tools for measuring pH_i and they appear to give reliable values (Aickin & Thomas 1977; Roos & Boron 1981). They are limited, however, in that they can not be used to record pH transients during muscular contraction since they will break. They have been used with success in following pH transients in a variety of tissues including skeletal muscle of mammals (Aickin & Thomas 1977) and invertebrates (Galler & Moser 1986) during and following extra- and intracellular ionic perturbations. Because of the drawbacks of the DMO and microelectrode for measuring pH in contracting muscle, the homogenate technique (Sahlin 1978; Spriet, Soderlund, Thompson and Hultman 1986) is the most widely used method of estimating muscle pH in stimulated muscle. Most of the initial drawbacks associated with this technique (discussed above) can be carefully controlled (Spriet et al. 1986).

Colorimetric techniques for measuring skeletal muscle pH_i have also been tried. In resting frog semitendinosus muscle Piontek

and Herbst (1971) reported a pH_i of 7.2 at $4^\circ C$ and 2% CO_2 . pH -sensitive dyes have also been used with some success to measure directional changes in pH_i during isometric contraction (Herbst & Piontek 1972). The problem with most dyes include metachromatic, protein and salt errors, and the presence of the dye can alter pH_i (Roos and Boron 1981). The primary advantage is its nearly instantaneous response to rapid changes in pH_i , a feature which has been used by Herbst and Piontek in exercising muscle (see Section 1.3.5).

The best tool currently available for measuring transients in intramuscular pH during contraction is nuclear magnetic resonance or NMR (Avison et al. 1986). In rat skeletal muscle at rest the pH is 7.01 (Ackerman et al. 1980; Kushmerick & Meyer 1985) and in humans values of 7.04-7.13 have been reported (Edwards et al. 1982; Wilkie et al. 1984). Once again, as with other techniques, the disadvantage of the NMR method is that the pH obtained is an average value reflecting the pH of all intracellular compartments as well as the contribution of muscle extracellular fluids (Avison et al. 1986).

1.3.5 Activity Induced Changes in Muscle and Blood

Short-term high intensity exercise, on which this dissertation is focussed, results in the changes listed in Table 1. The changes in metabolite concentrations are relatively easily explained in terms of the biochemical reactions of muscle metabolism. Changes in fluid and ionic composition, on the other hand, are more difficult to explain because of the complexity of fluxes occurring between intracellular compartments and between extra- and intracellular fluids.

The metabolic and ionic changes occurring with high intensity muscle activity (Section 1.2) may be summarized. They include the appearance of La^- , Pi , ammonium and glycerol in blood and a decrease in plasma [glucose]. Intracellularly, these changes are associated with: La^- production and accumulation from glycolysis; an increase in $[\text{Pi}]$ resulting from continued hydrolysis of CP and ATP, with the deamination of AMP as it accumulates from continued hydrolysis of ATP and ADP; an increased rate of triglyceride catabolism producing a rise in intracellular [glycerol]; and increased uptake of glucose by muscle. It is known that muscle was permeable to Pi and that Pi loss from muscle was increased by stimulation; Lundsgaard (1934) realized that the rate of loss of Pi from muscle paralleled the decrease in CP and the increase in intracellular $[\text{Pi}]$. Initial and continued muscular activity results in altered permeability of the sarcolemma resulting in the net flux of K^+ out of the cells and of Na^+ , Cl^- and water into the cells.

The increase in total muscle water upon stimulation was initially shown by Ranke (1865) and, Fletcher (1904) reported that water uptake by muscle was largely confined to the beginning of exercise. Hill and Kupalov (1930) concluded that a 48% increase in the vapour pressure of the whole muscle in extreme fatigue was due to increased osmotic pressure inside the fibers. Meyerhof (1930) reported that 75% of the change in osmotic pressure could be explained by the increased phosphates, lactic acid and ammonia in exercise. Using indirect muscle stimulation in anesthetized rats, Fenn and Cobb (1936) observed an increase of both the ECF and ICF; these changes were reversed during recovery. The increase in muscle ECFV was attributed

to the addition of an ultrafiltrate of plasma (water + Na^+ + Cl^-), perhaps caused by the increased capillary pressure. The increase in ICFV was considered to be due to increased concentrations of osmotically active metabolites in the muscle.

Mitchell and Wilson (1921) were the first to report that severe fatigue is accompanied by the loss of K^+ from frog muscle during stimulation and that K^+ was taken up during recovery. Using electrical stimulation of cat hindlimb muscle, Fenn et al. (1938) extended these observations to include a small increase in Cl^- , a gain of Na^+ which balanced the K^+ loss and Cl^- gain, an increase in water content, a possible decrease in Pi , and no significant change in Ca^{++} and Mg^{++} . In further studies on cats, Fenn (1938) reported that the loss of K^+ , and gain of water, Na^+ and Cl^- were increased if the number of tetani per second was increased. Fenn (1938), who was the first to quantify differences in K^+ loss and La^- accumulation in different muscle fiber types, noted that the soleus gained less La^- and lost less K^+ for a given amount of stimulation than the gastrocnemius. These findings were confirmed using the indirectly stimulated in situ rat hindlimb by Sreter (1963). Sreter also noted that the changes which occurred in the plantaris were intermediate to those which occurred in the white gastrocnemius and soleus, consistent with the mixed fiber type population of the plantaris. Sreter concluded that the progressive K^+ loss from the white, but not red, fibers "progressively alters the ionic gradients and ultimately limits the ability to perform work despite the continued stimulus".

Sembrowich et al. (1982) observed a loss of K^+ from all

compartments examined (sarcoplasm, mitochondria and sarcoplasmic reticulum) in fatigued rat muscles. In most compartments the K^+ loss was at least partially balanced by a gain in Na^+ . They concluded that these effects may have marked effects on the membrane potential and on the excitability of the sarcolemma. Ca^{++} was also elevated in all compartments, but most strikingly in the sarcoplasmic reticulum: the Ca^{++} content of the SR in gastrocnemius muscle increased from 8 to 135 μ mole/g dry wt. Sembrowich et al. (1982) suggested that the general elevation in $[Ca^{++}]$ was related to the fatigue state. They also showed a swelling of the transverse tubule system.

In view of the effects of extra- and intracellular $[K^+]$ and $[Na^+]$ on membrane potential, described by the Nernst equation (Hodgkin & Horowicz 1959b), intense exercise is associated with a significant reduction in the magnitude of both the resting potential and the action potential. This in turn is associated with a decrease in muscle tension development. Particularly during exercise, it is evident that the active Na^+-K^+ transport must be tightly regulated in order to maintain optimum muscle function (Clausen 1986). Maximal activity of the $Na^+-K^+-ATPase$ depends on the concentration of cytoplasmic ATP, on the concentrations of Na^+ and K^+ on either side of the sarcolemma, and on the mediators of acute hormonal control — insulin, epinephrine and norepinephrine (Clausen 1986). Hodgkin and Horowicz (1959b), in isolated frog sartorius, showed that electrical stimulation resulted in a sharp increase in the rate of $^{24}Na^+$ efflux from muscle, indicating an acute activation of the $Na^+-K^+-ATPase$ by muscle contraction. This has been

shown to be followed by a net uptake of K^+ by recovering skeletal muscle of dogs (Hazeyama & Sparks 1979; Hirche et al. 1980) and humans (McKelvie et al. 1986).

Perhaps the most important observation of the past 40 years is the direct association of extra- and intracellular pH changes with movements of ions across the cell membrane (Aickin & Thomas 1977; Galler & Moser 1986). These relationships had not previously been examined in skeletal muscle during and following contractile activity.

A reduction of muscle pH on stimulation has been consistently reported in the literature. Meyerhof and Lohman (1926) reported a change in pH from 7.11 at rest to 6.31 at fatigue in frog muscle extracts. Furusawa and Kerridge (1927) reported that exercised cat muscle had a pH_i of 6.11 compared to 6.89 at rest ($T = 37^\circ C$). Carlstrom et al. (1928) showed that the pH of dog muscle extracts was reduced to 6.57 after exercise from 7.02 at rest ($T = 20^\circ C$).

The pH changes in the early stages of activity were studied in frog muscle by the CO_2 method (Lipmann & Meyerhof 1930; Meyerhof et al. 1932; Hill 1940). The intercellular (between cells) pH changes of contracting muscles of the frog (Dubuisson 1939) and of rabbit and humans (Maison et al. 1938) were also studied at the onset of contraction using glass electrodes. Herbst and Piontek (1972) studied the same events in frog muscle using pH-sensitive dyes. All of these studies showed that there was an initial alkalosis associated with the onset of high intensity exercise correlated to the rapid breakdown of CP. The acidosis associated with the later stages of fatigue was attributed to the formation of lactic acid in excess of CP breakdown, so that the muscle became acid. This was accompanied by significant

decreases in the external pH of the medium during muscle contraction.

Dubuisson (1939) summarized the relations between muscle contractile events and intercellular pH changes in a carefully performed series of experiments on frog skeletal and smooth muscle as follows. The initial precontractile phase is associated with an alkalosis; at present this is explained by the rapid influx of strong cations (Na^+ and Ca^{++}) into the intracellular compartment during depolarization of the membrane potential and development of the action potential. This was followed by the contractile phase, which was associated with a drop in pH proportional to the amount of tension developed and attributed to ATP hydrolysis. The initiation of relaxation was accompanied by an alkaline phase presumed to result from CP hydrolysis and ATP resynthesis. The fourth and final phase of contraction was associated with acidification due to lactic acid formation. This schema of events also appears to be representative of muscle contraction in humans (Spriet, Soderlund, Bergstrom and Hultman 1986).

1.3.6 Dependence of Metabolism on Strong Ions

The organic and inorganic composition of muscle fibers determine its physico-chemical, biochemical and physiological characteristics. Changes in the concentrations of the constituents of extra- and intracellular fluids may be expected to alter the biochemical and physiological functions of muscle. From the preceeding discussion it is evident that the magnitude of ionic, metabolic and fluid changes in muscle fibers are related to the intensity and

duration of muscular activity. The fluid and ionic disturbances will in turn affect protein structure and function and, hence, cellular and organ function. The ionic composition of the intracellular fluids determine the solubility of colloids, the viscosity of the ICF, the integrity of the cellular membranes, and the rate of enzyme-catalyzed reactions.

Changes in the intracellular concentrations of strong ions may exert their effects on proteins in two ways: (1) by altering the equilibria between $[H^+]$, $[OH^-]$, $[A^-]$ and $[HA]$ and thereby changing the state of ionization of active sites on key enzymes, or their substrates, products and cofactors (Dixon & Webb 1979); and (2) by a direct requirement for a specific ion in an enzyme's active site in order for maximal catalytic activity to occur (Mildvan 1974). The former have been extensively studied in vitro and analyzed and interpreted in terms of a 'pH effect' on enzyme function (Dixon & Webb 1979); in these biochemical studies the underlying cause(s) for the 'pH effect' should be kept in mind.

Stadtman (1970) stated that "many regulatory enzymes are either dependent upon or are markedly affected by specific inorganic ions", therefore variations in the concentrations of specific ions may have "tremendous potential importance in the regulation of metabolism". In general, the requirements for divalent cations by many enzymes is widely recognized and, with a few exceptions, will not be discussed here. Instead, this section will attempt to show that the concentrations of K^+ and Na^+ can contribute to the regulation of some metabolic events in skeletal muscle during contraction. Specific attention will be given to regulatory enzymes which are known

54

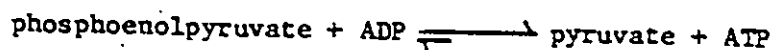
to occur in mammalian skeletal muscle and which are affected by physiological (as far as can be ascertained based on the in vitro nature of the experiments on muscle homogenates, muscle extracts and enzyme preparations) changes in inorganic ion concentrations, particularly those which are known to occur in muscle with exercise. A regulatory enzyme is one which "catalyzes a non-equilibrium reaction and whose activity is controlled by factors other than the substrate concentrations" (Newsholme & Start 1973).

Potassium has long been known to be important in metabolism. Lardy (1951) demonstrated, in experiments using liver particles in all- Na^+ or all- K^+ media, that K^+ was required to obtain maximum respiration. Lehninger and Kennedy (1948) showed that K^+ and/or Na^+ were essential for fatty acid oxidation by liver particles. Boyer et al. (1943) showed, in minced rat muscle, that K^+ is required for the incorporation of phosphate into creatine phosphate; without K^+ pyruvate oxidation continued at a rapid rate but no phosphate was fixed. In the presence of glucose, liver (Fenn 1939) and muscle (Kamminga et al. 1950) were shown to absorb K^+ from blood (Flock et al. 1938; Fenn 1939) or bathing medium (Kamminga et al. 1950) and this was correlated to the disappearance of glucose and Pi from the blood (Fenn 1939; Kamminga et al. 1950). Hultman (1967) showed that the K^+ content of glycogen-depleted human muscle in vivo increased 6-8% (from 400-430 $\mu\text{Eq/g dw}$ to 460 $\mu\text{Eq/g dw}$) when muscle glycogen stores were restored to 200 $\mu\text{g/g dw}$, such that 1 mmol of K^+ in cells was associated with 2 g of glycogen; it was postulated that K^+ may be required for glyconeogenesis.

In addition to its association with glyconeogenesis, K^+ was

also shown to be associated with glycolysis. During muscle contraction, the breakdown of glycogen and K^+ release were noted over 50 years ago (Fenn & Cobb 1936). More recently, Hultman (1967) reported an association between glycogen breakdown and K^+ release from skeletal muscle and between hepatic glucose output and K^+ release in man during exercise. The cell's ability to concentrate specific cations (eg. K^+) while simultaneously excluding other cations (eg. Na^+) may be important in the regulation of cellular metabolism and in the delay or prevention of fatigue during muscular contraction.

A direct involvement of K^+ in muscle glycolysis was first shown by Boyer et al. (1943) with the enzyme pyruvate kinase (in 1943 termed pyruvic phosphopherase). Pyruvate kinase catalyzes the reaction:



Pyruvate kinase had previously been shown to require Mg^{++} (Lohman & Meyerhoff 1934) and Boyer et al. (1943) showed that K^+ , or NH_4^+ , was required for maximal enzyme activity, and that Ca^{++} was strongly inhibitory. Kachmar and Boyer (1953) later showed that K^+ was not only stimulatory, but essential (NH_4^+ or Rb^+ could be substituted for K^+ but the required concentrations are not physiological) for the reaction. Enzyme activity was found to increase with increasing $[K^+]$ and increasing [phosphoenolpyruvate] to a maximum with 0.15 M K^+ . They also showed that lithium and Na^+ counteracted the K^+ activation presumably by competition with K^+ ; 25 mM Na^+ inhibited the K^+ activation by 5% at unphysiologically low $[K^+]$ (55 mM),

while 100 mM Na^+ inhibited by 20%. Whether this degree of inhibition would be physiologically significant at physiological K^+ and Na^+ concentrations is not known, and its implications in the regulation of glycolysis remain to be investigated.

During glycolysis, the catalytic conversion of fructose-6-phosphate to fructose-1,6-bisphosphate by vertebrate and mammalian muscle phosphofructokinase (PFK) was found to require K^+ for maximal activity (Paetkau and Lardy 1967) and to be better activated by K^+ than NH_4^+ , Rb^+ or Pi (Sugden and Newsholme 1975). At physiological $[\text{K}^+]$ (50 and 100 mM) Pi further activated the enzyme at non-inhibitory concentrations of ATP and NH_4^+ . The role of Pi appears to be that of a stabilizing agent to enzyme conformation and elevated free $[\text{Mg}^{++}]$ may also be stimulatory (Paetkau & Lardy 1967). Sugden and Newsholme concluded that elevated $[\text{Pi}]$ and $[\text{NH}_4^+]$ could be important in the regulation of glycolysis under conditions when the glycolytic flux is stimulated (during muscle contraction) by activating or de-inhibiting PFK.

Fructose-1,6-bisphosphatase (FBPase) is an enzyme closely associated with PFK and in fact catalyzes the reverse reaction of that catalyzed by PFK. It appears, at first glance, that it is an enzyme of gluconeogenesis. Recent evidence indicates that PFK and FBPase are involved in substrate cycling of fructose-1,6-bisphosphate and fructose-6-phosphate (Newsholme 1978), and this cycling may be important in increasing the sensitivity of the forward glycolytic flux to meet sudden increases in energy demand. FBPase from a variety of vertebrate tissues, including rabbit skeletal muscle, has been shown to

be activated by monovalent cations and especially physiologic⁵⁷ concentrations of K^+ (150 mM), and inhibited by AMP (Hubert et al. 1970).

Myokinase, which reversibly phosphorylates adenylic acid in vertebrate muscle:



is partially activated by Mg^{++} (Kalckar 1943). This enzyme is important in fatigue states where intracellular ATP production is low and ADP high, allowing for the synthesis of ATP from ADP. The resultant AMP is prevented from accumulating to excessive levels by the enzyme AMP deaminase.

AMP deaminase is more abundant in skeletal muscle than in any other tissue in which it has been found (Smiley & Suelter 1967). The enzyme catalyzes the reaction:



and is strongly activated by, but does not appear to require, K^+ and Na^+ , and elevated P_i is a poor inhibitor of the K^+ -activated enzyme (Smiley & Suelter 1967). These findings are important upon consideration of the role of the enzyme in muscle function during exercise. Thus, in contracting muscle when K^+ falls and Na^+ and P_i increase, Na^+ can replace K^+ with equal efficiency without inhibition by P_i . The enzyme is allosteric toward its substrate AMP such that in the presence of optimal $[K^+]$ (100 mM) its K_m (0.4 mM) is less than half that without K^+ .

The mode of action of monovalent cations on enzyme activity has not been rigorously studied and is open to speculation. Monovalent cations may be important for the maintenance of an enzyme conformation

necessary for optimum catalytic efficiency; the anionic field strength and nonhydrated size of the monovalent cation may be important factors in activation of the enzymes' active site; and the monovalent cation may act as a bridge between the enzyme and substrate (Nakashimi & Tuboi 1976).

2. METHODS

2.1 Introduction

The purpose of these studies was to examine the physico-chemical properties of skeletal muscle at rest and at the end of intense exercise. The relationships between glycolysis and lactate production on intracellular [SID] were examined, and the effects of changes in intracellular ion status on the regulation of metabolism during exercise were evaluated. Before the experiments designed to study these relationships could be conducted and evaluated, it was first necessary to modify existing, or develop new, methods to measure the parameters of interest.

2.2 Animals

All experiments described in the present thesis utilized adult male Sprague-Dawley rats (250-550 g body mass). Animals were maintained in healthy condition in a humidity- and light-controlled environment (12 h light, 12 h dark) and had free access to food and water. All animal handling and experimentation conformed to University guidelines for animal care; sacrificing of the animals was done as humanely as possible within experimental design. All experiments were conducted under approval of the University's Ethics Committee.

2.3 New Techniques

One of the purpose of these studies was to develop a working

model of trans-sarcolemmal ion movements between extra- and intracellular fluids. For these studies the isolated perfused rat hindlimb preparation was used almost exclusively. To be satisfied that the observed ion fluxes were representative of a healthy and viable muscle mass, we had to ensure that the artificial, single-pass, perfusion medium behaved physiologically. The suitability of the bovine erythrocyte perfusion medium for sustained muscle viability was initially demonstrated by Spriet et al. (1985a) during 30 min rest perfusions followed by 20 of perfusion during electrical stimulation. The respiratory and physico-chemical properties of the perfusion medium were subsequently shown to closely resemble those of rat blood (Appendix A; Lindinger et al. 1986).

Quantification of the intracellular concentrations of strong ions required that the ECFV, extracellular (plasma) ion concentrations, and total ion content be measured for each muscle sample. This led to the use of radio-labelled mannitol for measuring ECFV, and of instrumental neutron activation analysis for simultaneously measuring the contents of the major strong ions in muscle samples. These two techniques are fully described and discussed in Appendix B.

The third methodology developed is the use of homogenates of freeze-dried muscle to measure muscle pH and to determine the physico-chemical properties of skeletal muscle. These methods are described in detail in Chapter 3, and they form the foundation for which the interpretation of the results in the proceeding chapters is based.

2.4 Experimental Design

Two experimental designs were employed, the isolated perfused stimulated rat hindlimb, and exhaustive swimming exercise. Comparison of muscle metabolism and intracellular ion concentrations between these two exercise protocols forms the basis of Appendix C. We concluded that the metabolic changes in the stimulated perfused rat hindlimb were representative of intense exercise in vivo, and that the one pass perfusion system of the isolated hindlimb model permitted quantification of gas, ion and metabolite fluxes at constant arterial composition.

2.4.1 The Isolated Rat Hindlimb

The isolated, perfused and electrically stimulated rat hindlimb preparation used in the present studies was developed in this laboratory (Spriet et al. 1985a). Prior to surgery the animals were anaesthetized with sodium pentobarbital (60 mg/kg body mass); deep anaesthesia required a wait of 10-20 min before surgery could begin. Animals were sacrificed by a single intra-cardiac injection of sodium pentobarbital (40 mg/kg body mass) immediately prior to artificial perfusion and electrical stimulation of the hindlimb.

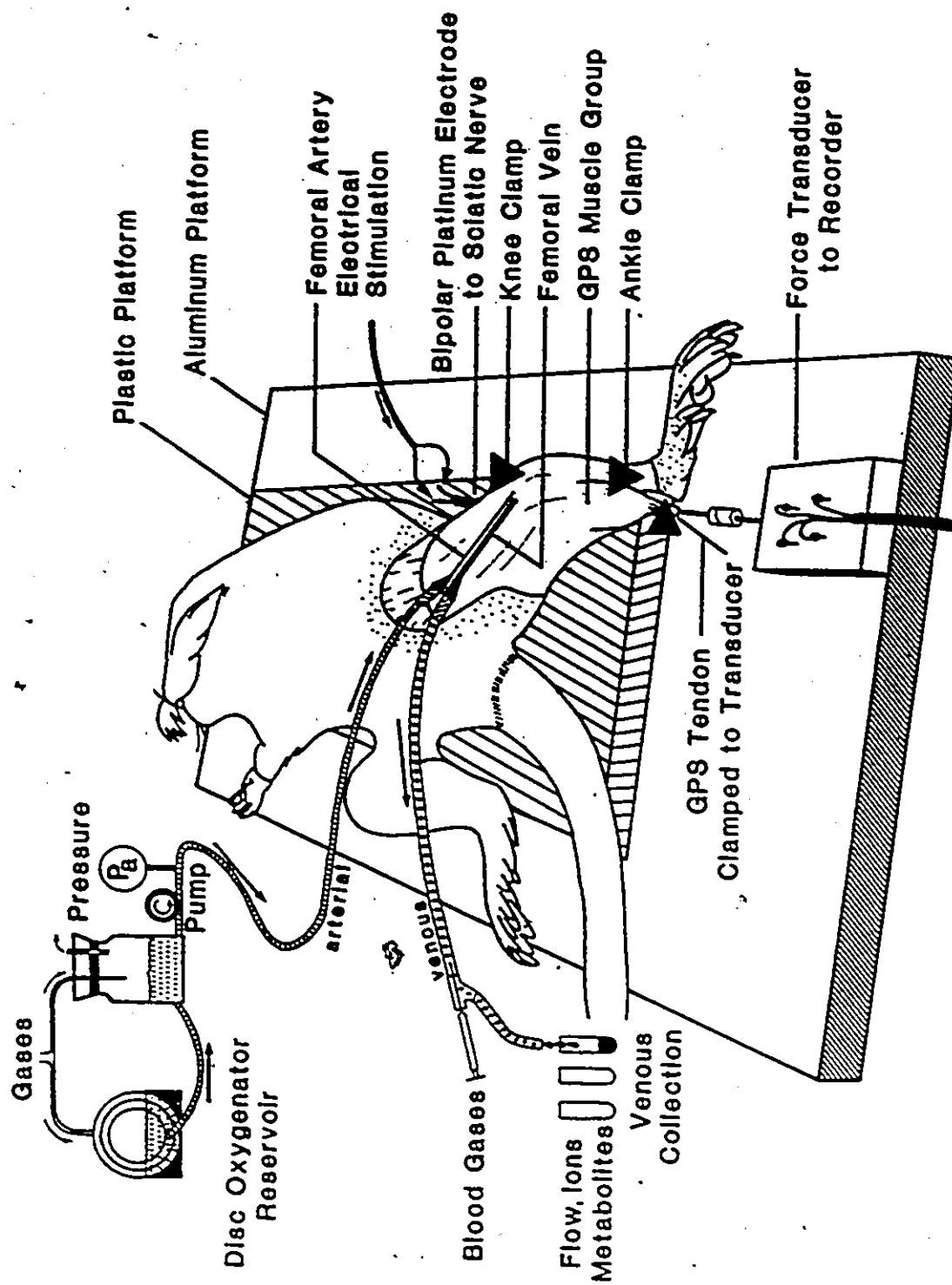
The initial hindlimb preparation (Spriet et al. 1985a) was modified to make it more suitable for quantifying the fluxes of respiratory gases, ions and metabolites between muscle and blood (Spriet, Lindinger et al. 1986). Initially the left hindlimb was perfused via the abdominal aorta and flow was restricted to the hindlimb, as much as was possible, by ligating several 'extraneous'

blood vessels. Following this procedure only 56% of the total perfused muscle mass was stimulated to contract via electrical stimulation of the sciatic nerve (Spriet et al. 1985a). This proportion of non-working to working muscle would have made the quantitative contribution of working muscles to arterial-to-venous concentration changes very difficult to assess. Subsequently, the catheters were inserted directly into the femoral artery and vein, just above the knee (Fig. 2). This preparation was nearly ideal for studies of muscle ion fluxes because the working muscle now represented 82% of the total perfused muscle mass (Spriet, Lindinger et al. 1986). Details of this preparation are also given in Appendix C.

2.4.2 Intense Swimming Exercise

The second design used live rats which were injected via a tail vein with ^3H -mannitol and ^{14}C -DMO (to measure ECFV and pH_i) three hours before the animals were sacrificed. These animals were divided into a control resting group and an exercise group. Initially, a separate group of rats were fitted with various masses of tail weights in order to cause exhaustion of the rat in about 5 min. In the Exercise group, swimming was performed to exhaustion (animal unable to surface for 15 s) with a tail weight corresponding to about 5% body mass of the rat. This permitted a direct comparison between the intense swimming and the electrical stimulation models. Since blood and muscle samples had to be obtained as soon as possible to the end of exercise, it was decided that these animals would be sacrificed by cervical dislocation. This procedure

Fig. 2. Schematic representation of the perfused stimulated rat hindlimb preparation as used in the present studies. GPS = gastrocnemius-plantaris-soleus muscle group; P_a = arterial pressure transducer.



was very rapid and effective, permitting blood sampling within 30 s of picking up the animal.

The intense swimming exercise protocol was developed for two major purposes. The first was to compare the intense tetanic electrical stimulation model with intense exercise in vivo to demonstrate the suitability of the isolated perfused stimulated rat hindlimb as a physiologically representative model of high intensity exercise (Appendix C). Intense swimming was chosen because it was simple to perform and very effective; trials indicated that the use of high-speed treadmill running would have necessitated training the animals, an effect which would have confounded interpretation of the results. The second reason was to assess the suitability of using DMO to measure rapid transients in muscle pH_i during exercise by comparing it with other techniques. The swimming protocol permitted both hindlimbs to be simultaneously sampled from resting and fatigued animals, thus yielding sufficient tissue to perform the several analyses required.

2.5 Statistics

Results are expressed as mean + standard error (SE). Ion concentrations are expressed in milli-equivalents per liter (mEq/l), a form which takes the ionic valency into consideration. Therefore, for monovalent ions $1 \text{ mmol} = 1 \text{ mEq}$, and for divalent ions $1 \text{ mmol} = 2 \text{ mEq}$. Differences between muscles and treatments were compared using analysis of variance. The Student's *t* test was used to compare means when a significant *F* ratio was obtained. Statistical significance was accepted at $p \leq 0.05$.

3 PHYSICO-CHEMICAL PROPERTIES OF SKELETAL MUSCLE AT REST AND FOLLOWING INTENSE EXERCISE

3.1 INTRODUCTION

The body fluid compartments may be analyzed as physico-chemical systems involving both dependent and independent variables. This chapter deals with the intracellular fluid compartment as such a system. Within any such system two fundamental laws of physical chemistry must be followed: the maintenance of electrical neutrality within the solution, and the conservation of mass for any given substance.

The physico-chemical variables which we can measure are categorized into dependent and independent variables. The independent variables are those which can only be changed by influences external to the system. The effect of changes in any other variable in the system, by definition, has no effect on an independent variable. As defined by the physico-chemical principles (see Section 1.2.2) outlined by Stewart (1978; 1981; 1983) the independent physico-chemical variables in ionic solutions are the PCO_2 , the total effective concentration of weak acids and bases ($[A_{TOT}]$), and the strong ion difference ($[SID]$). The PCO_2 can be easily measured using electrodes and $[SID]$ can be calculated from the measurements of the concentrations of strong ions in solution. In contrast, the variable $[A_{TOT}]$ cannot be directly, nor easily,

measured. Instead, with an understanding of the physico-chemical relationships governing the equilibria between the independent and dependent variables $[A_{TOT}]$ can be indirectly determined from simultaneous measurements of pH, PCO_2 and $[SID]$. This approach was developed using homogenates of freeze-dried muscles (of which the $[SID]$ was known) equilibrated to known concentrations of CO_2 and strong ions and is described in the present chapter. These measurements also permitted an evaluation of the dissociation constant for $[A_{TOT}]$ to be made and an appropriate value for mammalian skeletal determined. These physically effective values for $[A_{TOT}]$ and K_A permit the functional behaviour of skeletal muscle to be described in relation to its ionic status.

Functional differences (physiological and biochemical) between fiber types to a large extent reflect, and partly depend upon, the physico-chemical composition of the intracellular compartment. For example, slow twitch oxidative muscle fibers differ in their ionic composition from, and have a lower resting membrane potential than, fast twitch glycolytic muscle fibers (Sreter 1963; Yonemura 1967). They also have lower fatiguability associated with low myosin ATPase activity (Barany 1967; Brooke and Kaiser 1970), high oxidative capacity and low glycolytic potential (Saltin and Gollnick 1983; Spriet et al. 1985a) whereas the fast twitch fibers are highly fatigable, have high myosin ATPase activity, low oxidative capacity and a relatively higher glycolytic potential. These differences in physiological and biochemical characteristics may also be associated with differences in the physico-chemical properties of these muscle fibers.

During intense exercise, the increased rate of glycolysis

results in elevated rates of production of hexose-phosphates, pyruvate and lactate (Fig. 1). Muscles with a high proportion of fast twitch high glycolytic fibers show large changes in extra- and intracellular ionic composition (Sreter 1963; Sembrowich et al. 1982; Sjogaard et al. 1985) including increased $[H^+]$ and large accumulations of La^- (Sahlin et al. 1981; Spriet et al. 1985a). In contrast, muscles composed predominantly of slow twitch high oxidative fibers show significantly smaller changes in these variables. High intracellular $[H^+]$ during heavy exercise has often been implicated as a cause of muscle fatigue (Sahlin 1978; Hultman and Sahlin 1980). The loci for fatigue have been suggested to reside in excitation-contraction coupling (Fabiato and Fabiato 1978; Hultman and Sjoholm 1986), control of glycolytic flux at the level of phosphorylase (Chasiotis et al. 1983) and phosphofructokinase (Sahlin et al. 1981; Hultman and Sjoholm 1986), and impairment of ionic pumps and exchangers on the sarcoplasmic reticulum and sarcolemma (Nakamura and Schwartz 1972; Gunderson et al. 1983). The regulation of intracellular homeostasis during exercise necessitates the minimization, and ultimate correction of, associated large changes in intracellular ionic composition, such as increased $[La^-]$ and strong ion shifts.

The primary purpose of this study was to examine the physico-chemical composition of skeletal muscles taken from resting and exhaustively exercised animals. The present study also compares three methods for measuring intramuscular pH in resting and fatigued muscle:

- (1) the distribution of the weak acid 5,5-dimethyl-2,4-oxazolidine-dione-2- ^{14}C (pH-DMO); (2) measurement of pH on homogenates of freeze-dried muscle (pH-homog); and (3) and

calculation from measured independent physico-chemical variables (pH-SID). The effects of changes in the independent physico-chemical variables on the dependent variables are described. This chapter also discusses the implications of the differences in ionic composition for the inter-relationships between muscle fiber type, muscle metabolism, intracellular ionic and fluid contents and membrane potential.

3.2 METHODS

3.2.1 Animals

Male Sprague-Dawley rats ($n = 21$) weighing 430-530 g (478 ± 11 g, mean \pm SEM) were used for the study. The animals were housed in a humidity and light-controlled (12 h on, 12 h off) environment. Food, and water were available ad libitum. The animals were randomly assigned to two groups: resting non-exercised control rats ($n = 13$), and rats exercised to exhaustion by swimming with tail weights ($n = 8$).

3.2.2 Protocol

The pH_i of diaphragm and hindlimb muscles was measured using the distribution of ^{14}C -DMO (Malan et al. 1976; Milligan and Wood 1985) in conjunction with ^3H -mannitol as an ECFV marker (Page 1962; Appendix B). Animals were injected with 0.50 ml of a 0.9% saline solution containing 5.7 μCi of ^{14}C -DMO and 20.0 μCi of ^3H -mannitol (New England Nuclear) via a tail vein 2.5-3.5 h before blood and muscle samples were obtained. Handling stress was minimized

by allowing the rats to enter a small restraining chamber from which the tail could be vasodilated with warm water (50°C) to allow easy injection of the tracer solution.

Resting controls ($n = 13$) were quickly sacrificed by cervical dislocation. Both hindlimbs were skinned and prepared for muscle sampling. The abdomen was opened and a 2-3 ml blood sample obtained in a heparinized syringe from the abdominal aorta. The entire soleus (SL) and plantaris (PL) muscles, the medial (red) gastrocnemius (RG), and a large portion (0.3-0.5 g wet wt) of the superficial (white) gastrocnemius (WG) were removed from both legs. The diaphragm was exposed, dissected free of the thorax, and entirely removed. The muscle sample was immediately freeze-clamped with aluminum tongs cooled in liquid nitrogen. The muscle was wrapped in aluminum foil and stored in liquid nitrogen until analyzed. The total time for sacrifice, blood and tissue sampling was less than 5 min. The blood sample was immediately analyzed for pH, blood gases, ions and metabolites as described in Appendix A.

The exercise group rats ($n = 8$) were fitted with tail weights (amounting to 5% of body mass) and individually swum to exhaustion in a 35°C water bath. The bath was vigorously bubbled with air to prevent the animals from clinging to the sides of the bath and to ensure continuous exercise. The end point was determined by the animal's inability to remain at the surface of the bath for a 15 s period. The exhausted animal was removed from the water and immediately sacrificed by cervical dislocation. Blood and muscles were immediately sampled as described above.

3.2.3 Analyses

Each frozen muscle sample was pulverized in a stainless steel mortar under liquid nitrogen using a cooled stainless steel pestel. The muscle fibers were reduced to a powder while the connective tissue remained in strands. The connective tissue was dissected from the frozen powder and the sample divided into two parts. One part was weighed (Cohn roller balance) to determine tissue wet weight, and transferred to cooled polyethylene tubes for freeze-drying and determination of tissue dry weight. The remaining part was further divided for measurement of ^{14}C and ^3H radioactivity and for measurement of total tissue ion content. Since paired muscle samples were obtained from both hindlimbs from each rat, the muscle from one leg was used for one procedure while the sample from the other leg was used for the other procedures.

DMO-pH1 and ECFV. The frozen muscle for measurement of ^{14}C and ^3H radioactivity weighed from 100-200 mg wet wt. Immediately following measurement of the frozen tissue wet weight, the sample was placed into glass liquid scintillation vials containing 2.0 ml of tissue solubilizer (NCS, Amersham). When a clear solution was obtained (7-10 days) the solution was neutralized with 60 μl glacial acetic acid and 13 ml of scintillation fluor (OCS, Amersham) added. The samples were mixed, stored in a cold dark room for two days to reduce chemiluminescence, and counted for ^{14}C and ^3H in an LKB 1211 Rackbeta Scintillation Counter (Beckman) preprogrammed for standardization and quench correction. Plasma radioactivity was determined on 100 μl samples similarly prepared as the corresponding

muscle samples. Muscle ECFV, ICFV and pHi were calculated using standard equations (Malan et al. 1976).

Tissue ion content. The inorganic ion (Na^+ , K^+ , Mg^{++} , Ca^{++} and Cl^-) content ($\mu\text{Eq/g}$ dry wt.) of freeze-dried muscle was determined using instrumental neutron activation analysis, and the intracellular ion concentrations calculated as described in Appendix B. This procedure does not alter the composition of the tissue and the sample can subsequently be used for further analyses. Muscle lactate (La^-) was measured on extracts from these freeze-dried samples using enzymatic fluorometric techniques (Bergmeyer 1965).

3.2.4 Muscle homogenate titrations

The freeze-dried muscle samples remaining from ion analysis and from dry weight measurements were pooled for each muscle. This sample was divided into two 30-40 mg dry weight samples, where possible, for measurement of muscle homogenate pH during CO_2 and strong ion titrations of the solution. The muscle was weighed, added to 1.00 ml of the homogenizing solution (see next paragraph) within a 10 mm x 75 mm polyethylene test tube and dispersed using a glass rod. The tube was placed in a 37 °C water bath for equilibration to temperature and 10 μl of 2-octanol (an antifoam agent) and 10 μl of a rabbit muscle carbonic anhydrase (Sigma Chemical) solution (100,000 Units/1.0 ml homogenizing solution) were added. The carbonic anhydrase increased the rate of equilibration from 15-20 min to about 5 min during CO_2 titrations. The addition of 2-octanol and carbonic anhydrase had negligible effect on the physical parameters of

the homogenizing solution during strong ion titrations when compared to titration of the solution without 2-octanol and carbonic anhydrase. Equilibration of the homogenate to the gas mixtures was performed by passing a fine stream of bubbles from PE-50 tubing through the homogenate; the 2-octanol prevented foaming caused by the presence of muscle proteins.

The homogenizing solution consisted of 145 mM KCl, 10 mM NaCl and 5 mM sodium iodoacetate (Spriet, Soderlund et al. 1986). Since all of these compounds are strong ion pairs, the [SID] of this solution was zero, so that it did not interfere with the measurement of muscle pH. The iodoacetate blocks glycolysis at the phosphoglyceraldehyde dehydrogenase step (Carlson and Siger, 1960), and reduces the progressive acidification of the homogenate (Spriet, Soderlund et al. 1986). The pH of the solution was adjusted to near 7 (6.95-7.05) at 37°C by adding small amounts of dilute (0.02 N) NaOH. The solution may be stored for up to 2 months at 4°C.

Homogenate pH was monitored with a pH electrode (Radiometer model GK2421C, for micro-samples) connected to a Radiometer PHM 72 Mark 2 digital acid-base analyzer. The pH meter was calibrated with pH electrode calibration solutions warmed to 37 °C before each titration. Following temperature equilibration (about 5 min) the initial pH of the homogenate was recorded. In some trial experiments the homogenate was equilibrated for a further 5 min and the pH was found to decrease by less than 0.04 units, therefore 5 min was deemed sufficient time for equilibration. The homogenate was equilibrated to 0.03% CO₂ by bubbling with air for 5 min and the pH recorded when

a stable reading was obtained. The homogenate was titrated with increasing CO_2 by equilibration to 5%, 10% and 15% CO_2 in nitrogen. The ambient barometric pressure (P_b , in mmHg) was recorded and the PCO_2 (mmHg) calculated using the equation:

$$(21) \quad \text{PCO}_2 = ((P_b - 47) / 100) \times \% \text{CO}_2$$

where 47 mmHg is the value assigned to the partial pressure of water vapour at 37°C.

Immediately upon completion of the CO_2 titration the homogenate was re-equilibrated to air and titrated with strong ion (0.2 N NaOH) dispensed from a Gilson microburette in 5-20 μl aliquots. The homogenate pH was recorded following equilibration (about 5 min) to each addition. If the pH of the homogenate was above 6.5 prior to titration with Na^+ , the pH was first reduced by the addition of 5-20 μl 0.2 N HCl, the pH recorded and then Na^+ titration begun.

All muscle samples were treated in the preceding fashion. If there was insufficient muscle sample (i.e. only 20-40 mg dry weight) for two series of titrations, this first procedure was the only one used. When there was sufficient sample, the second muscle sample was titrated with increasing CO_2 (as before) and then equilibrated with 5% CO_2 (resting samples) or 15% CO_2 (exercised samples) for titration with strong ion (0.2 N NaOH).

3.2.5 Calculations from homogenate titrations

The physico-chemical relations describing the equilibrium for the ionic equivalency of weak acids, $[A_{\text{TOT}}]$, are given by the

following equations from Section 1.2.2 (Stewart 1981; 1983).

Weak acid dissociation equilibrium:

$$(4) \quad [H^+] \times [A^-] = K_A \times [HA]$$

where K_A is the weak acid dissociation constant.

Conservation of mass for 'A':

$$(5) \quad [HA] + [A^-] = [A_{TOT}]$$

Electrical neutrality:

$$(13) \quad [SID] + [H^+] - [HCO_3^-] - [A^-] - [CO_3^{2-}] - [OH^-] = 0$$

The concentrations of H^+ and OH^- are very small and are omitted from equation (13) for calculation purposes. The concentration of bicarbonate ion ($[HCO_3^-]$) is in turn described by the following equilibria:

Bicarbonate ion formation:

$$(11) \quad [H^+] \times [HCO_3^-] = K_c \times PCO_2$$

and carbonate ion (CO_3^{2-}) formation:

$$(12) \quad [H^+] \times [CO_3^{2-}] = K_3 \times [HCO_3^-]$$

where K_c is the apparent dissociation constant of bicarbonate formation and K_3 is the dissociation constant for carbonate formation. The value of K_c is thus the product of the apparent dissociation constant for CO_2 (K') and the CO_2 solubility coefficient.

The values for these constants are given in Table 7.

To calculate homogenate $[A_{\text{TOT}}]$ equations (4, 5 & 13) are combined and rearranged to give:

$$(23) \quad [A_{\text{TOT}}] = (([SID] - [\text{HCO}_3^-]) \times (K_A + [\text{H}^+])) / K_A$$

where the homogenate $[\text{HCO}_3^-]$ is calculated from equation (11).

The value for homogenate $[SID]$ is calculated from the whole muscle, not intracellular, strong ion content ($\mu\text{Eq/g}$ dry weight). The SID content is calculated from the contents of the strong ions using the equation:

$$(24) \quad SID = \text{Na}^+ + \text{K}^+ + \text{Mg}^{++}/2 - \text{Cl}^- - \text{La}^-$$

The Mg^{++} content is halved because about 50% of total intracellular Mg^{++} is non-diffusible (Maughan and Recchia 1985).

The homogenate $[SID]$ ($\text{mEq/l} = \mu\text{Eq/ml}$) is calculated as the product of the SID content (equation 24) and the muscle sample dry weight divided by the volume of the homogenate solution:

$$(25) \quad [\text{SID}]_{\text{homog}} = \text{SID} (\mu\text{Eq/g dry weight}) \times \text{dry weight (g)} / 1.02 \text{ ml}$$

A comparison of $[\text{A}_{\text{TOT}}]$ values calculated, using equation (7), from CO_2 and strong ion titrations for a given muscle sample show consistent differences, indicating the presence of unmeasured (and unaccounted for) ions. A correction factor was required to account for any unmeasured ions (UMI) and to yield consistent values for $[\text{A}_{\text{TOT}}]$ between titration methods. Equation (23) thus becomes:

$$(26) \quad [\text{A}_{\text{TOT}}] = (([\text{SID}] - [\text{HCO}_3^-] - [\text{UMI}]) \times (K_A + [\text{H}^+])) / K_A$$

where $[\text{UMI}]$ is the concentration of unmeasured ions in the homogenate and is calculated from a muscle UMI content of 70 $\mu\text{Eq/g}$ dry weight; the calculation of homogenate $[\text{UMI}]$ is the same as for homogenate $[\text{SID}]$ (equation 25). This procedure yields nearly identical $[\text{A}_{\text{TOT}}]$ values when $[\text{A}_{\text{TOT}}]$ was calculated from the two titration methods.

Titration with 0.2 N NaOH altered both the homogenate volume and homogenate $[\text{SID}]$, necessitating the re-calculation of homogenate $[\text{SID}]$ at each new equilibrium. The new homogenate $[\text{SID}]$ ($[\text{SID}]_n$) is equal to the product of the previous homogenate $[\text{SID}]$ ($[\text{SID}]_{n-1}$, $\mu\text{Eq/ml}$) and the previous homogenate volume (V_{n-1} , ml) plus the quantity of Na^+ (μEq) added, all divided by the new homogenate volume (V_n):

$$(27) \quad [\text{SID}]_n = ([\text{SID}]_{n-1} \times V_{n-1} + \text{Na}^+_{\text{added}}) / V_n$$

where the quantity of Na^+ added is the product of normality of the solution (eg. 0.2 Eq/l = 200 $\mu\text{Eq/ml}$) and the volume (eg. 0.010 ml) added:

$$(28) \quad \text{Na}^+_{\text{added}} = 200 \mu\text{Eq/ml} \times 0.010 \text{ ml} = 2 \mu\text{Eq}.$$

Calculation of muscle intracellular $[\text{A}_{\text{TOT}}]$ requires conversion of homogenate $[\text{A}_{\text{TOT}}]$ back to the tissue value and conversion to intracellular fluid:

Conversion of homogenate $[\text{A}_{\text{TOT}}]$ to tissue content:

$$(29) \quad \begin{aligned} \text{A}_{\text{TOT}} (\mu\text{Eq/g dry wt}) \\ = [\text{A}_{\text{TOT}}] (\mu\text{Eq/ml}) \times \text{homog. vol (ml)} / \text{sample dry wt (g)} \end{aligned}$$

Conversion to intracellular concentration $[\text{A}_{\text{TOT}}]_i$:

$$(30) \quad [\text{A}_{\text{TOT}}]_i = \text{A}_{\text{TOT}} (\mu\text{Eq/g dry wt}) / \text{ICFV (ml/g dry weight)}$$

No correction is made for the contribution of the ECFV to the A_{TOT} value because $[\text{A}_{\text{TOT}}]$ in plasma is only 17 mEq/l (Van Slyke et al. 1928) and trapped plasma within the muscle sample composes only 10-20% of the muscle ECFV, i.e. 1-2% of muscle total tissue water (Manery 1954).

each muscle was calculated from the intracellular concentrations of strong ions using the equation:

$$(31) \quad [SID] = [Na^+] + [K^+] + [Mg^{++}]/2 - [Cl^-] - [La^-]$$

This calculation assumes that free intracellular $[Ca^{++}]$ is very low and similar to free intracellular $[H^+]$, and that about 50% of total intracellular $[Mg^{++}]$ is bound (Maughan and Recchia 1985). Lactate is considered to be a strong ion because with a pK of about 3.8, it is about 99% dissociated under physiological conditions.

A pH_i was calculated for each muscle sample using (a) the intracellular [SID] (equation 31), (b) an intramuscular PCO_2 of 50 mmHg at rest, and the measured plasma PCO_2 in exercised rats, and (c) the calculated $[A_{TOT}]$ (equation 30). Values for the chemical constants used for muscle intracellular fluid are listed in Table 7. pH_i -SID was calculated using equation 14.

3.3 RESULTS

3.3.1 Performance

The mean time to fatigue of swimming rats was 4.4 ± 0.5 min. The composition of arterial blood in resting and fatigued rats is shown in Table 8. The significant increases in plasma PCO_2 , protein (weak acid) concentration, and $[La^-]$ (therefore reduced plasma [SID]) resulted in a significant acidification of the extracellular fluids.

TABLE 7

Physico-chemical constants used in the calculation of muscle ionic composition.

	value	reference
K'_w	$4.4 \times 10^{-14} \text{ (Eq/l)}^2$	Harned & Owen 1958
K_c	$2.34 \times 10^{-11} \text{ (Eq/l)}^2/\text{mmHg}^*$	Siesjo and Thews 1962
K_3	$6.0 \times 10^{-11} \text{ Eq/l}$	Edsall & Wyman 1958
K_A (rest)	$5.5 \times 10^{-7} \text{ Eq/l}$	this study
(exercise)	$4.0 \times 10^{-7} \text{ Eq/l}$	this study

* calculated from $K_c = K \times S$; where K , the apparent dissociation constant for $\text{CO}_2 = 7.41 \times 10^{-7} \text{ Eq/l}$; and S , the CO_2 solubility coefficient = $0.0351 \text{ mEq/l.mmHg}^{-1}$ at 37 C and intracellular ionic strength (Siesjo and Thews 1962).

TABLE 8

Composition of the arterial blood of rats at rest and at the end of intense swimming exercise. All animals sacrificed by cervical dislocation.

variable	units	mean \pm se or (range)	
		Rest (n = 13)	Exercise (n = 8)
pH		7.413 (7.401-7.426)	6.888* (6.863-6.914)
PCO ₂	mmHg	40 \pm 2	82 \pm 12*
[HCO ₃ ⁻]	mEq/l	25 \pm 1	15 \pm 2*
PO ₂	mmHg	81 \pm 3	48 \pm 12*
[Hb]	g/l	142 \pm 2	154 \pm 6*
[La ⁻]	mEq/l	1.5 \pm 0.4	20 \pm 1*
[Na ⁺]	mEq/l	130 \pm 0.3	154 \pm 2*
[K ⁺]	mEq/l	4.4 \pm 0.3	8.9 \pm 0.7*
[Cl ⁻]	mEq/l	94 \pm 1	95 \pm 1

Hb = hemoglobin; La⁻ = lactate

* indicates values significantly different ($p < 0.05$) from rest.

3.3.2 Muscle Fluids and Ions

81

In resting muscle, the relationships between muscle fiber types and fluid and ion contents are described and discussed in Section 1.3.1 and in Appendix B. The major differences are that $[K^+]_i$ is significantly lower in SL than in WG, and $[Na^+]_i$ and $[Cl^-]_i$ tend to be higher in SL than in WG. The concentrations of these ions determines the $[SID]_i$ of resting muscle.

The changes from rest to fatigue in intracellular strong ion concentrations and in muscle fluid volumes in rat hindlimb muscles are shown in Table 9. The quantitatively important changes in all muscles were the increases in $[La^-]_i$, $[Na^+]_i$, $[Cl^-]_i$ and muscle fluid volumes, and the reductions in $[K^+]_i$ and CP content. The increase in $[La^-]_i$ was responsible for 50%, 54%, 60% and 67% of the reduction in $[SID]_i$ in the SL, RG, PL and WG respectively; the balance of the fall in $[SID]_i$ was nearly all due to the loss of intracellular K^+ (Table 9). The increases in TTW and ICFV with exercise were not significant, however ECFV increased by 0%, 28% and 22% in RG, PL and WG respectively. CP contents were significantly reduced with exercise in all muscles: 37%, 58%, 67%, and 75% in SL, RG, PL and WG respectively (Table 9).

3.3.3 Effect of K_A

The value of K_A used in the equations has a marked effect on the calculation of $[A_{TOT}]$ (equation 26) and the intracellular dependent variables (equation 14). For example, when the K_A for the histidine groups of intracellular proteins of 1.5×10^{-7} Eq/l was used (Stewart 1981), there was a large difference in the two separately determined (by PCO_2 and strong ion titrations) $[A_{TOT}]$ values, and this calculated $[A_{TOT}]$ was about 30% greater

82

than the approximately 200 mEq/l predicted (Stewart 1981). Also, with NaOH titrations, the homogenate $[A_{TOT}]$ should decrease as the solution is titrated, as a direct result of dilution. With $K_A = 1.5 \times 10^{-7}$ Eq/l ($pK' = 6.82$), the homogenate $[A_{TOT}]$ for any given sample decreased to a greater extent than predicted and thus yielded erroneous values of $[A_{TOT}]$. In resting muscle, a $K_A = 5.5 \times 10^{-7}$ Eq/l ($pK' = 6.26$) gave the best consistent agreement between $[A_{TOT}]$ values separately determined by CO_2 and strong ion titrations, and yielded homogenate $[A_{TOT}]$ values consistent with the progressive dilution of the homogenate.

In resting and exercised muscle, the K_A values of 5.5×10^{-7} and 4.0×10^{-7} Eq/l ($pK' = 6.40$) (Table 7) were determined by iteratively changing the K_A to derive consistently similar values for muscle $[A_{TOT}]$ from CO_2 and NaOH titrations of the different muscles. As noted in the Methods, a $[UMI]$ equal to 13 mEq/l ICF also had to be used to obtain consistent values of $[A_{TOT}]$ for a given K_A in both resting and exercised muscles. The necessity of using this $[UMI]$ term indicated that there were anion equivalents contributing to the $[SID]$ which were not measured. The K_A 's are average values ($\pm 0.2 \times 10^{-7}$ and $\pm 0.4 \times 10^{-7}$ Eq/l at rest and exercise, respectively) which best represent $[A_{TOT}]$ from all of the titrations of resting and exercised muscles; only these average values (Table 7) were used in the calculations.

3.3.4 Muscle pH

Intracellular pH-SID of WG at rest, calculated (equation 14) from the three independent variables PCO_2 , muscle $[A_{TOT}]$ and intracellular $[SID]$, are compared to muscle pH-homog pH-DMO in Table

TABLE 9

Intramuscular fluid volumes and intracellular ion concentrations in rat hindlimb muscles at rest (R) and at the end of intense exercise (E).

variable	soleus		red gastroc.		plantaris		white gastroc.	
	R	E	R	E	R	E	R	E
TTW	766	776	760	778*	761	778*	758	777*
	± 7	± 6	± 3	± 5	± 2	± 3	± 3	± 3
PCPV	79	80	58	63	57	73*	64	78*
	± 14	± 14	± 10	± 10	± 8	± 12	± 10	± 18
ICPV	688	698	703	717	702	707	701	714
	± 13	± 14	± 11	± 14	± 8	± 10	± 13	± 14
CP	30	19*	40	17*	39	13*	44	11*
	± 4	± 4	± 4	± 5	± 4	± 4	± 5	± 5

(cont'd)

TABLE 9 (cont'd)

[Na ⁺]	7.2	9.0	9.6	13.3*	10.6	14.0	5.9	14.6*
	± 1.5	± 3.7	± 0.7	± 2.8	± 1.3	± 2.6	± 0.9	± 2.6
[K ⁺]	117	112	144	128*	136	123*	143	128*
	± 6	± 10	± 6	± 6	± 7	± 6	± 6	± 6
[Mg ⁺⁺]	24	21	31	29	29	28	31	26*
	± 1	± 1	± 1	± 2	± 2	± 2	± 2	± 3
[Cl ⁻]	8.5	12.8	5.1	9.3	5.9	9.1	8.7	11.2
	± 3.2	± 2.9	± 1.4	± 2.2	± 1.2	± 1.9	± 1.1	± 7.0
[La ⁻]	1.9	17.7	4.9	32.9*	7.0	35.7*	7.2	43.3*
	± 0.2	± 2.0	± 0.4	± 4.0	± 0.7	± 3.5	± 1.1	± 3.7

TTW = total tissue water; ECFV = extracellular fluid volume; ICFV = intracellular fluid volume. Units: fluid volumes (ml/kg wet wt.); strong ions (mEq/l intracellular fluid). * exercise (E) significantly different from rest (R).

TABLE 10

Comparison of white gastrocnemius pH values derived by the SID (pH-SID), DMO (pH-DMO) and homogenate (pH-homog) methods. The individual arterial PCO_2 , muscle $[A_{TOT}]$ and intracellular [SID] values used in the calculation of pH-SID are also shown (n = 17).

Sample	PCO_2 (mmHg)	$[A_{TOT}]$ (mEq/l)	[SID] (mEq/l)	pH-SID	pH-DMO	pH-homog
59	48.6	208	174.8	6.863	7.002	6.770
70	41.2	186	159.4	6.905	6.989	6.780
218	46.8	175	144.8	6.824	6.999	6.694
237	69.1	188	156.8	6.870	6.990	6.721
247	31.9	203	169.4	6.880	7.058	6.755
247 A	31.9	189	169.4	7.027	7.058	6.945
263	44.3	158	145.5	7.020	6.990	6.932
304	56.2	163	157.6	7.082	6.844	6.920
319	65.7	194	163.0	6.827	6.795	6.887
319 A	65.7	180	163.0	6.948	6.795	6.871
328	39.1	178	160.2	6.985	7.014	6.925
328 A	39.1	183	160.2	6.951	7.014	6.878
337	38.9	201	168.1	6.869	7.084	6.750
337 A	38.9	188	168.1	6.999	7.084	6.859
350	37.0	181	157.0	6.936	7.099	6.940
350 A	37.0	167	157.0	7.102	7.099	6.960
362	41.7	181	163.0	7.001	7.049	6.815
mean	45.5	184	161.0	6.946	6.998	6.847
sd	11.8	14	8.0	0.085	0.097	0.087
sem	2.9	3	2.0	0.021	0.024	0.022

sd = standard deviation, and sem = standard error of the mean.

Table 11

Intramuscular pH measured by DMO, SID and homogenate methods in rat hindlimb muscles.

Muscle	Condition	pH-DMO	pH-SID	pH-homog.
Soleus	Rest	$7.03 \pm .03$	$6.72 \pm .09$	$6.43 \pm .04$
	Exercise	$6.66 \pm .04^*$	$6.44 \pm .09$	$6.25 \pm .09^*$
Red gastroc.	Rest	$6.98 \pm .02$	$6.89 \pm .04$	$6.68 \pm .03$
	Exercise	$6.62 \pm .05^*$	$6.47 \pm .05$	$6.41 \pm .03$
Plantaris	Rest	$6.99 \pm .03$	$6.93 \pm .04$	$6.82 \pm .03$
	Exercise	$6.65 \pm .05^*$	$6.49 \pm .06$	$6.48 \pm .06$
Wh. gastroc.	Rest	$6.98 \pm .03$	$6.94 \pm .02$	$6.91 \pm .02$
	Exercise	$6.64 \pm .03^*$	$6.51 \pm .04$	$6.47 \pm .06$

Note: Significant difference between methods for rest values of SL, RG and PL.

* indicates values significantly different from the other two methods.

(rest, n = 10; exercise, n = 8).

10. There is good agreement between the three methods, but pH-homog 86 consistently yielded significantly lower values than pH-DMO and pH-SID.

Values of muscle pH determined for hindlimb muscles at rest and at the end of exercise are given in Table 11. Only in WG was there good agreement between the methods. At rest, pH-SID and pH-homog showed a significant decrease as the percentage of fast twitch fibers decreases (WG 100% fast twitch; SL 13% fast twitch; Armstrong and Phelps 1984). This trend was not evident with pH-DMO, and pH-DMO showed no significant differences between muscle fiber types at rest or after exercise.

Following exercise, muscle pH determined by all methods showed a significant decrease from resting values (Table 11). For a given method, at the end of exercise, there were no significant differences between the pH values of the different hindlimb muscles, except for SL with pH-homog. pH-DMO showed the least change from rest to exercise (about 0.35 units) of the three methods, and yielded significantly higher values than the other two methods. Both pH-SID and pH-homog showed similar pH reductions for a given muscle, and greater pH reductions in fast twitch muscles (WG and PL, $pH = -0.4$) than in slow twitch muscles (SL, $pH = -0.25$) (Table 11). In exercised muscles, pH-homog gave similar values to pH-SID in WG, PL and RG, but in SL pH-homog was significantly lower than pH-SID.

3.3.5 Physico-chemical Relationships in Muscle

The calculated intracellular ionic composition of rat hindlimb muscles at rest and following exercise are shown in Table 12. In resting animals, the SL had the lowest [SID]_i whereas there were no significant differences in [SID]_i between RG, PL and WG. The

$[A_{TOT}]_i$ of RG was significantly higher than that of SL and WG; there was no significant difference between SL, PL and WG $[A_{TOT}]$ at rest. It was assumed the intramuscular PCO_2 was identical in all muscles and approximately equal to the venous PCO_2 taken as 50 mmHg (Hogg et al. 1984). The lowest $[SID]_i$ values (in SL muscle) are associated with the lowest $[A^-]$, $[HCO_3^-]$ and $[OH^-]$, and the highest $[HA]$ and $[H^+]$, whereas the reverse is true in the WG.

The theoretical effects of changes in the independent physico-chemical variables on the dependent variables were calculated by computer using equation 14 and are shown in Fig. 3. The range of values for the independent variables are based on literature and experimental values, and represent the physiological range for mammalian skeletal muscle. Within these ranges, changes in PCO_2 (Fig. 3A) exert the least effect on the dependent variables while changes in $[SID]$ greatly affect the intracellular concentrations of the dependent variables (Fig. 3C). Changes in $[A_{TOT}]$ (Fig. 3B) exert an effect intermediate to those of changing PCO_2 and $[SID]$.

The majority of intracellular total weak acid, A_{TOT} , consists of creatine phosphate and proteins which contribute to the ionic status of the intracellular fluids. It is well known that changes in the ionization state of proteins affects protein structure and function, the biological activity of enzymes, and hence the rates of enzyme catalyzed reactions (Dixon & Webb, 1979). The ionization state of intracellular proteins are represented by the variables $[A^-]$ and $[HA]$. From Fig. 3 it is apparent that physiological changes in $[SID]$, compared to those of the other independent variables, have the greatest effect on $[A^-]$ and $[HA]$ and hence on the

Fig. 3. The effects of changes in the independent variables PCO_2 , $[\text{A}_{\text{TOT}}]$, and $[\text{SID}]$ on the concentrations of the dependent variables. The range of values for the independent variables are within the physiological range for skeletal muscle at rest and during exercise. Changes in PCO_2 (upper panel) exert the least effect on the dependent variables while changes in $[\text{SID}]$ (lower panel) exert the greatest effect. The plots were constructed using computer-derived values for the dependent variables, with constant or altered independent variables, using equation 14. The physico-chemical constants used in the equation are listed in Table 7; a K_A of 5.5×10^{-7} Eq/l for $[\text{A}_{\text{TOT}}]$ was used.

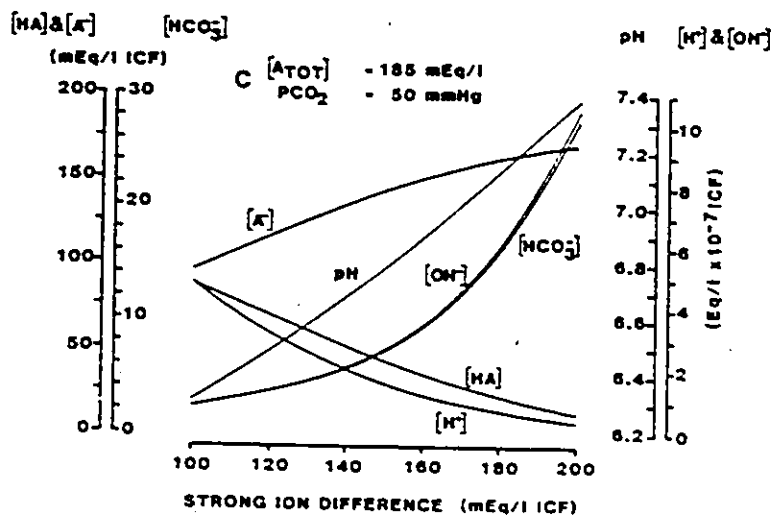
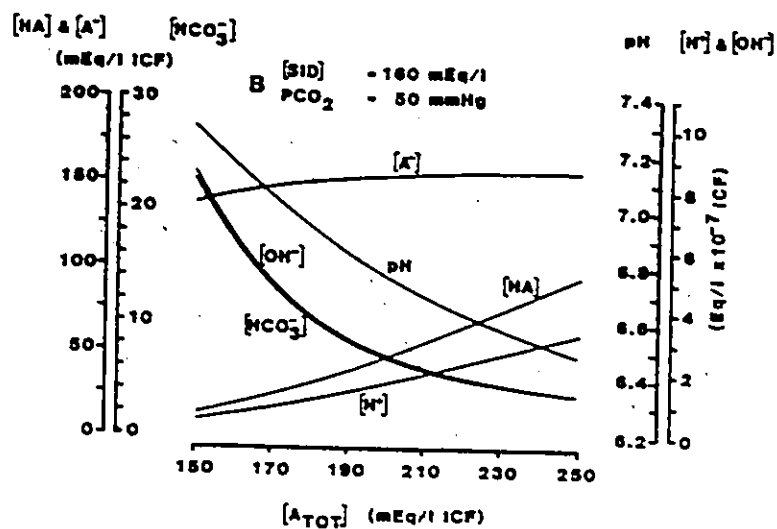
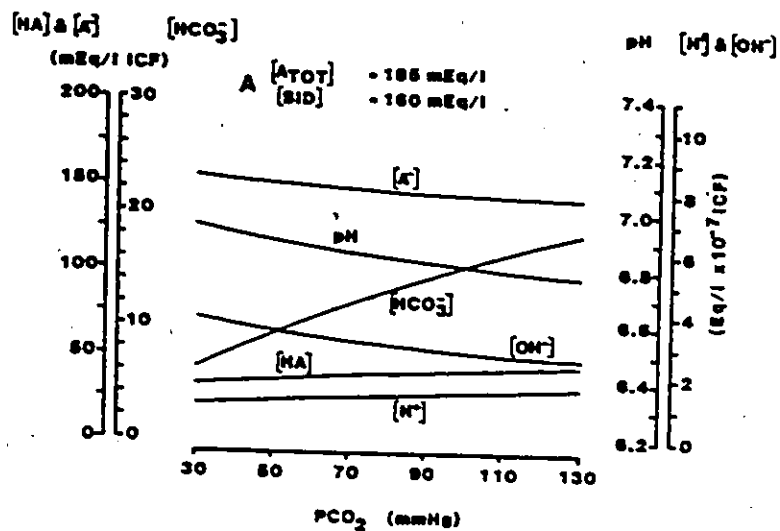
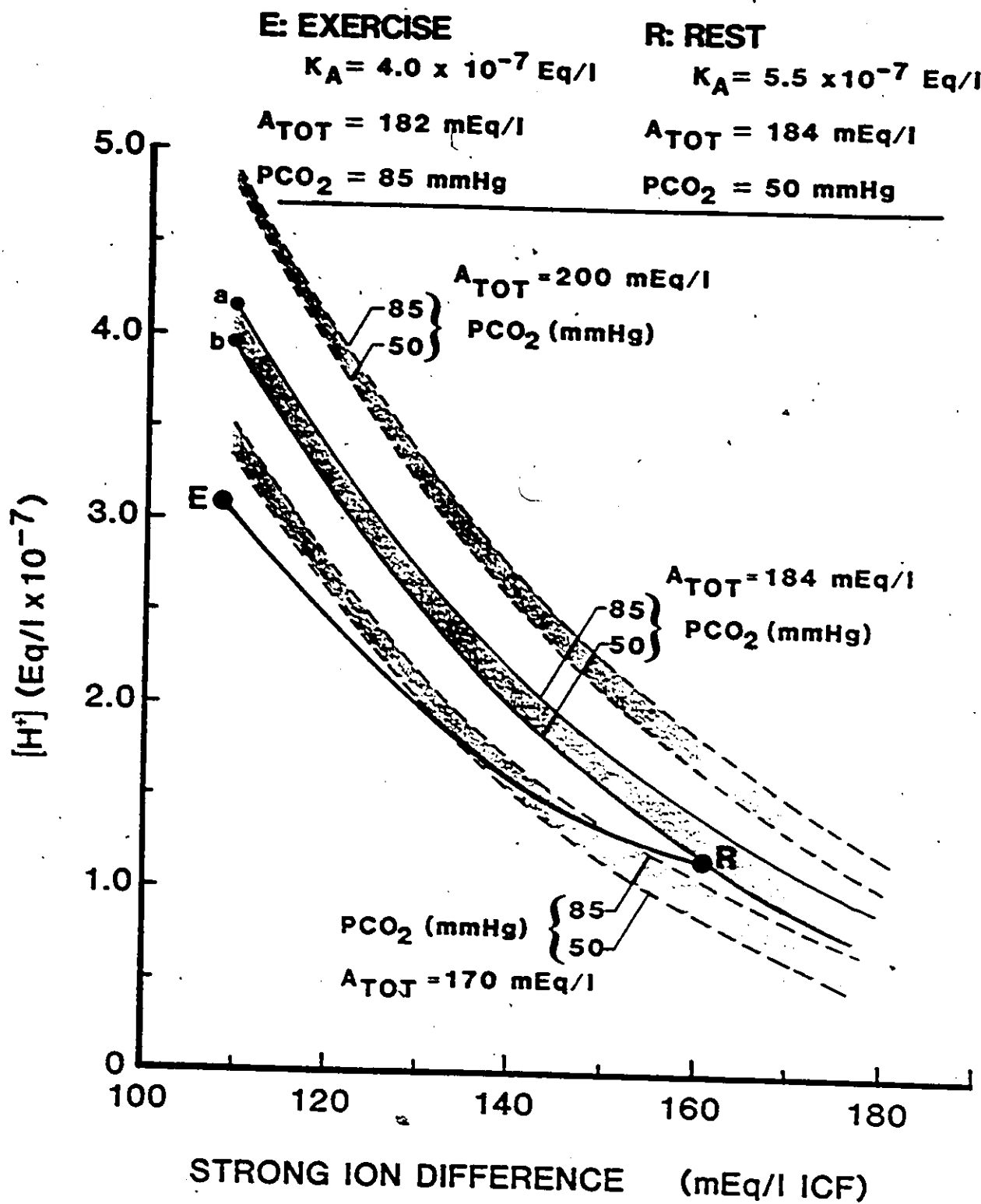


Fig. 5. The effects of changing PCO_2 , $[A_{TOT}]$, K_A and $[SID]$ on $[H^+]$ in the white gastrocnemius (WG) during intense swimming exercise. The three shaded regions represent the change in $[H^+]$ for $[A_{TOT}]$ values of 170, 184 and 200 mEq/l within the PCO_2 range of 50 - 85 mmHg at a K_A of 5.5×10^{-7} Eq/l (rested muscle K_A value). The $[A_{TOT}]$ values used represent the lower, mean, and upper limits in WG. Increasing the $[A_{TOT}]$ at any $[SID]$ increases $[H^+]$, however the effect is more pronounced at low $[SID]$. Compared to the effects of changing $[A_{TOT}]$ or $[SID]$, the effects of changing PCO_2 on $[H^+]$ are small. The effect of a 50 mEq/l reduction in $[SID]$ on the change in $[H^+]$, at any given $[A_{TOT}]$, is less if the initial $[SID]$ is high (180 mEq/l) than if it is low (140 mEq/l). The effect of increasing $[A_{TOT}]$ during a reduction in $[SID]$ would accentuate the increase in $[H^+]$.



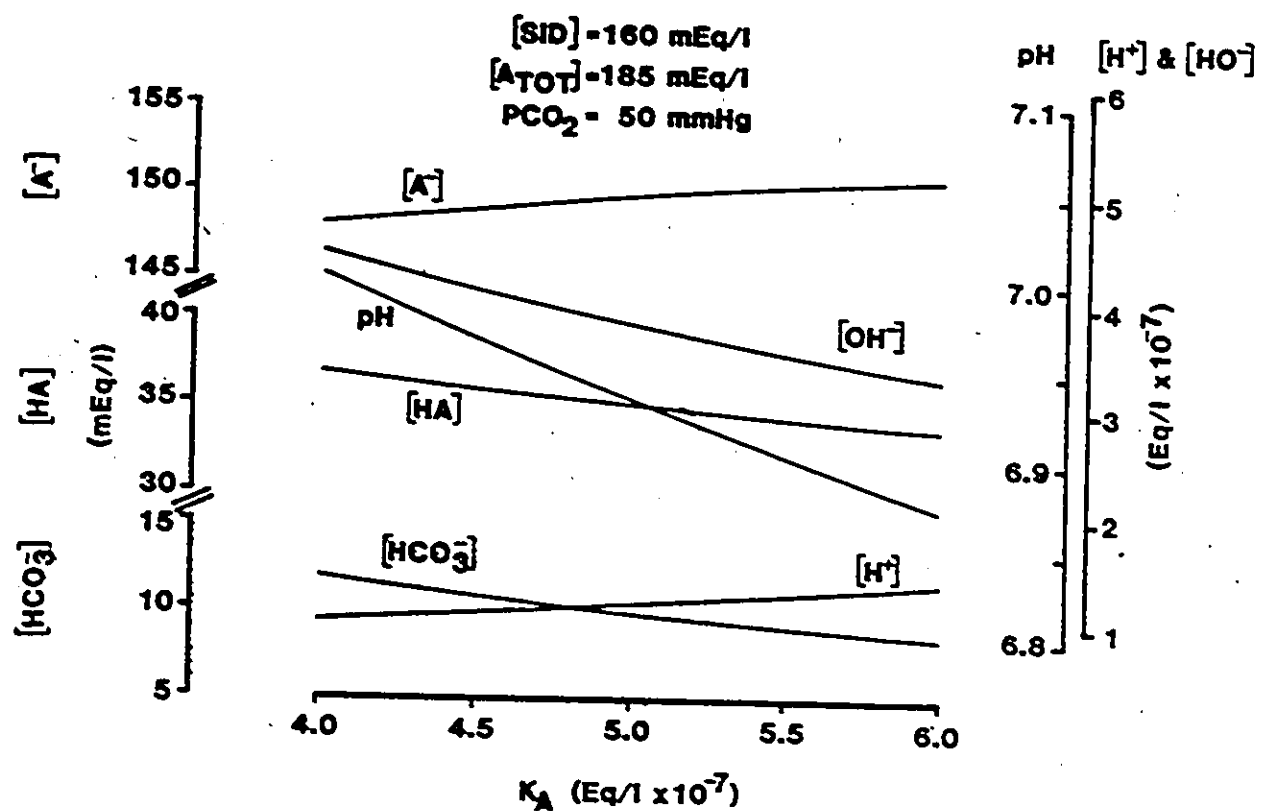


Fig. 6. The effects of physiological changes in the dissociation constant (K_A) for A_{TOT} on the concentrations of the dependent variables.

ionization state of intracellular proteins. Within intracellular fluids, changes in PCO_2 (Fig. 3A) have minimal effects on the ionization state of proteins.

In all muscles during exercise the PCO_2 increased and $[\text{SID}]$ decreased (Table 12); there were no significant changes in $[\text{A}_{\text{TOT}}]$. The 42 mmHg increase in PCO_2 (Table 8) would have had a relatively small effect on the dependent variables, whereas the changes in $[\text{SID}]$ would have a great effect (Figs. 3). These concepts are emphasized in a plot of intracellular $[\text{SID}]$ versus $[\text{H}^+]$ (Fig. 5), which was generated using the computer model of equation 14. For any given $[\text{A}_{\text{TOT}}]$ (shaded areas), increasing the PCO_2 from 50 to 85 mmHg (upper and lower limits of each shaded area) has relatively little effect on $[\text{H}^+]$ compared to the fall in $[\text{SID}]$ from 161 to 109 mEq/l.

The relative contributions of the changes in PCO_2 and $[\text{SID}]$ to the total change in $[\text{H}^+]$ can be calculated using measured values for the independent variables of WG as an example (Fig. 5). The total change in WG $[\text{H}^+]$ from rest (point R) to exercise (point E) averaged 2.02×10^{-7} Eq/l. At an $[\text{SID}]$ of 109 mEq/l and an $[\text{A}_{\text{TOT}}]$ of 182 mEq/l (from Table 12) the calculated change in $[\text{H}^+]$ due to increasing PCO_2 from 50 to 85 mmHg (assuming no change in K_A from rest to exercise) is the difference between points 'a' and 'b' in Fig. 5: $4.122 \times 10^{-7} - 3.954 \times 10^{-7} = 0.168 \times 10^{-7}$ Eq/l. Thus the contribution of increasing PCO_2 to the total change in $[\text{H}^+]$ was $(1 - 0.168/2.02) \times 100\% = 17\%$; the reduction in $[\text{SID}]$ accounted for the remaining 83%.

Perhaps the most important feature of Fig. 5 concerns the effect of reducing K_A from resting (point R) to fatigued muscle

TABLE 12

Skeletal muscle intracellular physico-chemical characteristics at rest and at the end of exercise.

Variable	Condition	MUSCLE			
		SL	RC	PL	WC
<u>Independent</u>					
(a) [SID]	Rest	137 \pm 5	172 \pm 4	162 \pm 5	161 \pm 3
(mEq/l)	Exercise	105 \pm 6*	120 \pm 6*	114 \pm 6*	109 \pm 4*
(b) [A _{TOT}]	Rest	184 \pm 11	203 \pm 9	190 \pm 7	184 \pm 4
(mEq/l)	Exercise	196 \pm 10	210 \pm 5	191 \pm 13	182 \pm 7
(c) PCO ₂	Rest	50	50	50	50
(mmHg)	Exercise	82 \pm 12*	82 \pm 12*	82 \pm 12*	82 \pm 12*
<u>Dependent</u>					
(d) [A ⁻]	Rest	134 \pm 7	165 \pm 6	152 \pm 6	151 \pm 3
(mEq/l)	Exercise	103 \pm 6*	113 \pm 5*	104 \pm 8*	101 \pm 4*
(e) [HA]	Rest	50 \pm 9	40 \pm 4	36 \pm 3	32 \pm 2
(mEq/l)	Exercise	95 \pm 7*	97 \pm 8*	87 \pm 9*	80 \pm 6*
(f) [HCO ₃ ⁻]	Rest	6.1 \pm 0.8	9.3 \pm 0.9	8.4 \pm 0.8	9.4 \pm 0.8
(mEq/l)	Exercise	5.9 \pm 0.7	6.3 \pm 0.7*	6.6 \pm 1.1*	7.2 \pm 0.4*
(g) [OH ⁻]	Rest	2.20 \pm .19	3.46 \pm .26	3.68 \pm .31	3.90 \pm .23
(Eq/lx10 ⁻⁷)	Exercise	1.26 \pm .14*	1.26 \pm .13*	1.40 \pm .18*	1.46 \pm .13*
(h) [H ⁺]	Rest	2.09 \pm .18	1.32 \pm .11	1.35 \pm .15	1.18 \pm .07
(Eq/lx10 ⁻⁷)	Exercise	3.71 \pm .36*	3.51 \pm .44*	3.41 \pm .44*	3.20 \pm .33*
(i) pH	Rest	6.72 \pm .04	6.89 \pm .04	6.93 \pm .04	6.94 \pm .02
	Exercise	6.44 \pm .04*	6.47 \pm .05*	6.49 \pm .06*	6.51 \pm .04*

All values are means \pm sem. All concentrations are for intracellular fluid. Asterisks denote exercise values significantly different ($p < 0.05$) from rest values. $n = 7$ for SL and RC at rest. $n = 7$ for SL, RC and PL with exercise.

$n = 13$ for PL and WC at rest. $n = 8$ for WC with exercise. SL = soleus;

PL = plantaris; RC = red gastrocnemius; WC = white gastrocnemius.

K_A at rest = 5.5×10^{-7} Eq/l; K_A with exercise = 4.0×10^{-7} Eq/l.

(point E) in preventing large increases in $[H^+]$. Point 'a' 93 represents the predicted $[H^+]$ in fatigued WC at a K_A of 5.5×10^{-7} . The difference between points 'a' (4.12×10^{-7} Eq/l; pH = 6.385) and E (3.20×10^{-7} Eq/l; pH = 6.51) shows how decreasing the K_A prevents larger changes in intracellular ion status caused by reductions in [SID] during intense exercise, i.e. lowering K_A has a "protective" effect. The effect of changes in K_A at constant PCO_2 , $[A_{TOT}]$ and [SID] on the dependent variables are shown in Figs. 6. Lowering the K_A reduces $[H^+]$ and $[A^-]$ and raises pH, $[OH^-]$, $[HCO_3^-]$ and $[AH]$ (Fig 6). The effect of changes in K_A on the ionization state of weak acids, i.e. $[A^-]$ and $[HA]$ are small.

3.4 DISCUSSION

The present study has examined the physico-chemical composition of rat hindlimb muscles at rest and following intense exercise. Total intracellular ion status is determined by the concentrations of strong ions, weak acids and bases ($[A_{TOT}]$), and CO_2 in the intracellular fluids. Changes in intracellular ion status cannot occur without a concomittant change in at least one of these three independent physico-chemical variables. Furthermore, a methodology for determining the contributions of $[A_{TOT}]$ and K_A to the intracellular ion status of muscle has been demonstrated. The results show that the independent variables may be used to calculate intracellular pH of skeletal muscle at rest and following exercise. There is a close association between changes in the ionic status of muscle during exercise and the physiological and biochemical

characteristics of the muscle.

3.4.1 Theoretical considerations

The ion status of any solution depends on the relative contributions of three important independent physico-chemical variables: PCO_2 , the $[\text{SID}]$, and the $[\text{A}_{\text{TOT}}]$ (Stewart 1978; 1981; 1983). The major assumptions in calculating the dependent variables of muscle ion status from the intracellular independent physico-chemical variables are: 1) that all of the important strong ions are measured and represented in the calculation of $[\text{SID}]$ (equation 14); 2) that all of the contributions of intracellular weak acids and bases to the physico-chemical equilibria are represented by $[\text{A}_{\text{TOT}}]$; and 3) that the intracellular PCO_2 (50 mmHg) is similar to that in the venous blood draining the muscle (Hogg et al. 1984).

The intracellular concentrations of strong ions reported in Table 9 are in agreement with previously reported values (Drahota 1961; Sreter 1963; Sembrowich et al. 1982). However, activity measurements of intracellular strong ions consistently yield lower values than those determined by chemical analysis (Donaldson and Leader 1984; Table 4). Those ions not detected by intracellular activity measurements appear to be bound to intracellular macromolecules or sequestered in subcellular compartments (Maughan and Recchia 1985; Sembrowich et al. 1982). The fact that the independent physico-chemical variables yielded values for $[\text{HCO}_3^-]$, $[\text{H}^+]$ and pH similar to those reported in the literature (Sahlin et al. 1978; Roos and Boron 1981) suggests that the electrically 'silent' components of the strong ion pool do contribute to the total intracellular ionic status.

Freeze-dried muscle is not usually used for the measurement of

muscle pH (Spriet, Soderlund, et al. 1986), and to our knowledge it has not previously been used for this purpose. However, in view of the major influences exerted by the independent physico-chemical variables, it seemed reasonable to assume that those quantities which determine pH in wet muscle homogenates should be the same as those which determine pH in homogenates of freeze-dried muscle.

It is useful first to examine briefly the coincidental manner in which the homogenate technique can be used to yield reasonable estimates of pH_i , but first a digression is necessary. Measurement of pH in muscle homogenates necessitates the dilution of the muscle sample (wet or dry) in a given volume of solution containing compounds to inhibit biochemical reactions which may otherwise lead to changes in pH (Spriet, Soderlund et al. 1986); these compounds have negligible effect on the homogenate pH (Spriet et al. 1986; present study). Thus muscle strong ions, $[A_{TOT}]$ and PCO_2 are all diluted, and the PCO_2 of the sample approaches equilibrium with air. Table 13 shows the effect of diluting 83 mg of wet muscle (or the equivalent 19.4 mg dry muscle) in 1.0 ml of solution (12-fold and 52-fold dilution respectively). In the case of the wet and dry muscle the total quantities of the strong ions and A_{TOT} are identical so that the effect of dilution on both samples is identical. Coincidentally, the $[H^+]$ (and thus pH) of the homogenate solution is very close to that predicted (from values for intracellular independent variables) to occur in vivo (Table 13). Of the calculated dependent variables in vivo and in the homogenate, only homogenate $[H^+]$ is similar to its in vivo predicted value, therefore the homogenate technique cannot be used to estimate any other dependent variable.

TABLE 13

Muscle physico-chemical variables in vivo and in homogenate solution; why the muscle homogenate technique works for estimating muscle pH. Values based on a 12-fold dilution of wet muscle or 52-fold dilution of dry muscle.

Variable		<u>in vivo</u>	in homogenate
[SID]	(mEq/l)	160	13.3
[A _{TOT}]	(mEq/l)	180	15.0
PCO ₂	(mmHg)	50	3.0
[A ⁻]	(mEq/l)	150	12.6
[HA]	(mEq/l)	30.5	2.36
[HCO ₃ ⁻]	(mEq/l)	10.4	0.69
[OH ⁻]	(Eq/l × 10 ⁻⁷)	3.93	4.29
[H ⁺]	(Eq/l × 10 ⁻⁷)	1.12	1.02
pH		6.951	6.989

Contrary to the premise of Madias and Cohen (1982) and Sahlin (1976) dilution of "buffered solutions" does exert a significant effect on the ratio of ion pairs in solution. From Table 12, the ratios of the ion pairs $[\text{OH}^-]:[\text{H}^+]$ and $[\text{A}^-]:[\text{HA}]$ in vivo are calculated to be 3.51 and 4.91, while in the homogenate solution the ratios are 4.19 and 5.37, respectively. This result is in direct contrast to statements by Hultman and Sahlin (1980): that "when a solution containing a non-volatile buffer is diluted or concentrated, practically no change will occur in pH because the concentration of free H^+ ions is negligible and the concentration of weak acids and their conjugates shows the same relative change", and Madias and Cohen (1982): "diluting a buffered solution has a negligible effect on the prevailing $[\text{H}^+]$ of the solution; because dilution lowers the concentrations of both components of a given buffer pair proportionately, their concentration ratio is not changed appreciably". The concentrations of weak acids and their conjugates do not, in fact, show the same relative changes with dilution. From the defining equations for these solutions only when a single weak acid is present, PCO_2 is zero, and the $[\text{SID}]$ value of close to $[\text{A}_{\text{TOT}}]/2$ are the concentration ratios constant; in any other situation, notably when PCO_2 is not zero and several weak acids and bases are present, dilution changes all ion concentrations and ratios (P.A. Stewart, personal communication). In the homogenate solution, where $[\text{A}_{\text{TOT}}]$ is less than $[\text{SID}]$ and PCO_2 is not zero, $[\text{SID}]$ is the predominant factor determining total intracellular ion status.

◆ Muscle $[\text{A}_{\text{TOT}}]$ is the most difficult of the three independent physico-chemical variables to measure. However, $[\text{A}_{\text{TOT}}]$

differs only slightly between different muscles and does not change significantly with strenuous exercise (Table 12). Also, because $[A_{TOT}]$ exerts only a moderate effect on muscle ion status (Figs. 3B & 5), a small difference (± 10 mEq/l) between the actual and assumed $[A_{TOT}]$ values used to calculate the intracellular dependent variables will not significantly alter estimations of intracellular ionic status.

An important factor in the calculation of pH-SID is the K_A of the total intracellular weak acid pool. The major intracellular substances contributing to the apparent K_A of muscle are given in Table 14. The histidine residues of intracellular proteins are the primary contributors to the K_A (about 50%) and CP is next in importance (about 25%) in resting muscle. With the exception of CP with a high K_A of 3.16×10^{-5} Eq/l, all of the substances have K_A 's in the order of 2×10^{-7} Eq/l. Thus, given the contribution of the large K_A for CP and the quantity of CP in muscle, the experimentally determined K_A of 5.5×10^{-7} Eq/l in resting muscle is reasonable. The effects of changing the value of K_A on $[H^+]$ and $[A_{TOT}]$ are given by equations 14 and 23. If $[H^+]$ is known and the equation solved for $[A_{TOT}]$, then an increase in K_A reduces the value of $[A_{TOT}]$. If $[A_{TOT}]$ is known and the equation is solved for $[H^+]$, then a change in K_A exerts minimal effects on the dependent variables (Fig. 6).

In the present study K_A decreased with exercise (Table 7), and thus had the effect of preventing larger increases in intracellular $[H^+]$ (Figs. 5 & 6). At rest, the primary substances contributing to the K_A are the histidine residues of intracellular proteins

which have an apparent acidic dissociation constant (K_a) of 1.78×10^{-7} Eq/l, creatine phosphate, with a relatively large K_a of 3.16×10^{-5} Eq/l, and Pi with an apparent K_a of 1.66×10^{-7} Eq/l (Table 14). During intense exercise the concentrations of proteins remain relatively unchanged, but CP may decrease by 75% (Table 9). The hexose-phosphates and inorganic phosphate contribute to the $[A_{TOT}]$ and K_A of the intracellular fluids (Table 14), and the substantial increase in these compounds during intense exercise (Sahlin et al. 1983; McCartney et al. 1986) are expected to increase the $[A_{TOT}]$. Therefore, during intense exercise, the contribution of CP to the K_A is greatly reduced while that of Pi and the hexose-phosphates increased. These combined effects would contribute to the lowering of K_A , as we have found (Table 7), with little or no apparent change in the calculated $[A_{TOT}]$ from rest to exercise (Table 12). A reasonable, assumed value of $[A_{TOT}]$ for calculation of intracellular ionic status is therefore justified.

3.4.2 Comparison of methods for muscle pH

The values for muscle pH at rest and exercise calculated from $[SID]$ and the distribution of DMO (Table 11) are within the range of values tabulated by Roos and Boron (1981) from a variety of mouse and rat skeletal muscles in which pH_i was measured both in vitro and in vivo using microelectrodes and weak acid distribution techniques. However, muscle pH-homog gave significantly lower values than the two other techniques. The reasons for this discrepancy are not known, but may be related to muscle fiber type and possibly muscle protein composition. There exists the possibility that this discrepancy may have affected the calculation of muscle $[A_{TOT}]$ from titration of RG

TABLE 14

Acidic dissociation constants (@ 25°C) of intramuscular weak acids and bases, and their contents and relative abundance in muscle.

Substance	pKa	Ka (Eq/l $\times 10^{-7}$)	mmol/kg dry wt. at rest	% abundance
histidine	pK ₂ = 6.04 pK ₃ = 9.33 app = 6.75	1.78	130-150	46-53
CP	4.5	316	68-83	24-29
PI	pK ₂ = 7.198 pK ₃ = 12.375 app = 6.78	1.66	36-41	13-14
ATP	6.97	1.07	21-27	7-10
ADP	6.75	1.78	2.7-3.7	1
G-6-P	6.11	7.76	1.0-2.5	1
total			283	

CP = creatine phosphate; PI = inorganic phosphate;

G-6-P = glucose-6-phosphate.

Adapted from Hultman and Sahlin (1980); dissociation constants from Robinson and Stokes (1970) and Hultman and Sahlin (1980),

app = apparent dissociation constant.

and SL muscle homogenates. In resting and exercised muscle, pH-DMO may overestimate pH_i (Table 11). In resting barnacle muscle, pH-DMO overestimated the pH_i measured simultaneously with microelectrodes by 0.05 units (Hinke and Menard 1976; Boron and Roos 1976). This is the magnitude of the difference between pH-DMO and pH-SID in WG and PL at rest (Table 11); so that pH-SID represents the average pH of the pooled intracellular fluid reasonably well. The reason for the progressive discrepancy between muscle pH methods with increasing proportion of slow twitch fiber in the muscle is unknown at this time. A combination of factors including the contribution of whole muscle [SID], the effects of sample dilution, and the volatility of CO_2 may be responsible.

With the probable exception of intracellular microelectrode measurements of pH, all other techniques of estimating pH_i , including pH-SID, yield an average value representing an assumed "total intracellular compartment". The major contributors to this compartment are the cytosol (70%-90% by volume), endoplasmic reticulum (2%-7%) and mitochondria (7%-17%) (Stonnington and Engel 1973). The same is true for intracellular strong ion concentrations determined by methods other than electron microprobe analysis or with ion specific microelectrodes (Appendix B). Nonetheless, there is good agreement between techniques of measuring 'average' intracellular pH and microelectrode pH measurements (Roos and Boron 1981), so that these 'average' techniques will continue to be valuable in assessing the state of the intracellular environment following perturbations to the system. In addition to the pooled intracellular environment, pH-homog also contains the contribution of the extracellular compartment to the

measured pH, and thus tends to overestimate pH_i (Sahlin 1978; Spriet, Soderlund et al. 1986). In the present study, in comparison to the other methods intracellular pH estimated from the distribution of DMO during large non-steady-state ionic disturbances of short duration gave higher pH values and appeared to underestimate the change in pH_i (Table 11). This observation is inconsistent with previous findings concerning the relatively long equilibration time (10 - 15 min) for DMO across cell membranes (Roos and Boron 1981; Milligan and Wood 1985), since incomplete equilibration of DMO across the sarcolemma should yield lower estimates of intracellular pH when external pH is lowered.

3.4.3 Effects of changing the independent variables

Two important features of intramuscular ion regulation involve changes in the ionization state of weak acids: (a) changes in $[A^-]$ and $[HA]$ are less at high values of $[A_{TOT}]$ than at low values of $[A_{TOT}]$ (Fig. 3B), and less at high values of $[SID]$ than at low values of $[SID]$ (Fig. 3C); (b) changes in $[HCO_3^-]$ and $[OH^-]$ are greater at low values of $[A_{TOT}]$ and high values of $[SID]$ (Fig. 3). High initial values of $[A_{TOT}]$ and $[SID]$ may therefore prevent large changes in $[A^-]$, $[HA]$ and $[H^+]$ (Fig. 3) during intense muscular activity. Resting muscles possess values for the independent variables $[SID]$ and $[A_{TOT}]$, i.e. 161 mEq/l and 184 mEq/l. (Table 12), which lie near the points of inflexion of the $[HCO_3^-]$, $[OH^-]$ and $[H^+]$ curves in Figs. 3B and 3C. With intense muscular activity there is a reduction in $[SID]$ (Table 12), such that the muscle ICF moves to the left on the curves of Fig. 3C. These changes are in the direction which will minimize changes in $[A^-]$,

$[HA]$, $[OH^-]$ and $[H^+]$, and hence will result in a minimum of perturbation of the ionization state of intracellular weak acids and bases.

$[H^+]$ is the ionic variable in lowest concentration (Table 12), and changes in $[H^+]$ with changes in the independent variables are always less than those of the other dependent variables (Fig. 3). Why then is so much importance given to $[H^+]$? While it is recognized that the $[H^+]$ of a solution is associated with certain states of ionization of proteins (Dixon and Webb 1979), there is no direct evidence that the $[H^+]$ of a solution exerts a direct effect on protein structure and function. As pointed out by Stewart (1978; 1981; 1983), the only way to change $[H^+]$ is by changing the concentrations of one or more of the strong ions, by changing the PCO_2 , or by changing the concentration of weak acids. The effects of these changes are not only a change in $[H^+]$, but also changes in all of the other dependent variables. Therefore, because $[H^+]$ depends on the independent variables, it is incorrect to postulate an exclusive pH-dependency of any given response on a change in the ionic status of a system.

3.4.4 Significance

There are major differences in the ionic composition of skeletal muscle at rest and following exercise which are related to muscle fiber type population and to muscle function. The $[SID]$ at rest and following exercise (Table 12) reflects the intracellular concentrations of strong ions (Table 9). The relatively low $[SID]$ and high $[H^+]$ in resting SL, compared to fast twitch muscle, results from the significantly lower $[K^+]$ and higher $[Cl^-]$ in this

tissue than in the other muscles. Following exercise, the [SID] in all muscles was similar (Table 12), therefore the decrease in [SID] was greater in fast twitch WG (-52 mEq/l) than in slow twitch SL (-32 mEq/l); correspondingly, the increase in $[\text{H}^+]$ was greater in WG ($2.02 \times 10^{-7} \text{ Eq/l}$) than in SL ($1.62 \times 10^{-7} \text{ Eq/l}$). Despite this greater change in [SID] in fast twitch muscles, $[\text{H}^+]$ did not reach the higher concentrations seen in SL. Indeed, $[\text{H}^+]$ following exercise was directly proportional to the fiber type composition of the muscles, with WG having the lowest and SL having the highest $[\text{H}^+]$ (Table 12). A high [SID] in resting muscle has a protective effect against large changes in $[\text{H}^+]$ caused by ionic disturbances.

The major contributor to the reduction in [SID] in all muscles was the increase in $[\text{La}^-]$ (Table 9). The increase in $[\text{La}^-]$ contributed 50% and 67% to the fall in [SID] in SL and WG respectively; the reduction in $[\text{K}^+]$ was responsible for an additional 20%-30%. This fall in [SID] was the major contributor to changes in the concentrations of the intracellular dependent ionic variables (Fig. 3; Table 12). Muscles with a relatively high glycolytic capacity (WG and PL) produce and accumulate La^- at a high rate during intense exercise (Table 9; Spriet et al. 1985a), and should incur the greatest disturbance in ion status. During and following intense exercise the predominant mechanisms for ionic regulation appear to be a high rate of La^- movement from muscle to blood (Table 8; Spriet, Lindinger et al. 1986) and a reduction in La^- production by glycolysis (Spriet, Lindinger et al. 1986; McCartney et al. 1986).

An important factor in this apparent regulation of glycolytic rate with sustained high intensity exercise may be changes in [SID],

and even more directly, changes in the relative intracellular concentrations of Na^+ and K^+ . Within the glycolytic pathway (Fig. 1) in vitro at least one key regulatory glycolytic enzymes, pyruvate kinase (Boyer et al. 1943; Kachmar and Boyer 1953) is known to have a requirement for, or their activity is allosterically modified by, changes in the concentrations of the monovalent cations Na^+ and K^+ . Pyruvate kinase catalyzes the conversion of phosphoenolpyruvate plus ADP to pyruvate plus ATP, and is maximally activated at high $[\text{K}^+]$ (150 mEq/l) and low $[\text{Na}^+]$ (Kachmar and Boyer 1953). It is well established that intracellular $[\text{Na}^+]$ increases and $[\text{K}^+]$ decreases during muscle contraction (Sreter 1963; Sembrowich et al. 1982. The magnitude of reduction in $[\text{K}^+]$ and increase in $[\text{Na}^+]$ seen at the end of intense exercise in WG (Table 9) may significantly inhibit pyruvate kinase activity (Kachmar and Boyer 1953), however whether or not this degree of inhibition of catalytic activity significantly affects flux through the system has not yet been determined. A significant inhibition of pyruvate kinase would result in reduced pyruvate and lactate production, as well as fall in glycolytic ATP production.

The mechanism of these allosteric regulatory effects of monovalent cations on enzyme activity appears to be mediated through structural and conformational changes in active site residues (see Section 1.3.6). Given that the intracellular protein pool is adequately represented by $[\text{A}_{\text{TOT}}]$, and the concentrations of ionized and unionized forms of the proteins by $[\text{AH}]$ and $[\text{A}^-]$, it is evident that exercise induced changes in $[\text{K}^+]$ and $[\text{Na}^+]$ (Table 9) and $[\text{SID}]$ (Table 12) have a marked effect on the protein ionization state

represented by the changes in $[A^-]$ and $[HA]$ (Fig. 3). The largest changes in $[A^-]$ and $[AH]$ occurred in WG, while the SL showed the smallest changes (Table 12).

3.4.5 Summary and Conclusions

Intracellular ionic status at rest and following exercise in muscles of differing fiber type composition can be estimated with reasonable accuracy from measurements of the three independent quantities PCO_2 , $[A_{TOT}]$ and $[SID]$.

Changes in $[SID]$ are responsible for the bulk of the changes in intracellular acid-base state in skeletal muscle during exercise.

Changes in intracellular $[SID]$ during exercise exert the largest influence of any of the independent variables on protein ionization state, and hence protein structure and function.

Highly fatiguable fast twitch muscles such as WG and PL have a higher resting $[SID]$ and a lower resting $[H^+]$ than slow twitch SL. The high resting $[SID]$ in WG may effectively prolong continued muscle function during exercise by protecting the intracellular fluids from large changes in protein ionization state and $[H^+]$ as $[SID]$ is reduced.

The three major protective effects against incurring large changes in protein ionization state and $[H^+]$ during exercise-induced falls in $[SID]$ which a muscle may utilize are: (1) a high resting $[SID]$; (2) a decrease in K_A ; and (3) no change in $[A_{TOT}]$.

4 SKELETAL MUSCLE ION FLUXES IN THE STIMULATED,
 PERFUSED RAT HINDLIMB

4.1 INTRODUCTION

It has previously been shown that electrical stimulation of the perfused rat gastrocnemius-plantaris-soleus (GPS) muscle group resulted in a 45% reduction in isometric tension development in 5 min (Spriet et al. 1985a). This degree of fatigue was associated with significant reductions in the intramuscular contents of creatine phosphate (CP), adenosine triphosphate (ATP) and glycogen. However, at the end of the 5 min of stimulation there still remained substantial supplies of CP, ATP and glycogen within the working muscles (Spriet et al. 1985a), suggesting that depletion of metabolic substrates and high energy phosphates was not solely responsible for the observed decrement in force production.

Intracellular ions appear to play extremely important roles in numerous cellular activities including glycolysis (Kachmar and Boyer 1953; Krebs et al. 1959; Paetkau and Lardy 1967) and muscle contraction (Donaldson 1983; Hultman and Sjöholm 1986). Therefore, an investigation of intra- and extracellular ion changes during muscle activity was appropriate. As Stewart (1981; 1983) has shown, the concentrations of weak ions in solution are dependent on the independent variables PCO_2 , [SID], and the total concentration of weak acids and bases ($[A_{TOT}]$) (see Section 1.2.2). The strong ions are, for practical purposes, always fully dissociated in solution. [SID] is defined as the difference between the sum of the

concentrations of the strong base cations (Na^+ , K^+ , Mg^{++}) and the strong acid anions (Cl^- , La^-).

In Chapter 3, increases in the intracellular concentrations of La^- and Na^+ and reduced $[\text{K}^+]$ were demonstrated in vivo to have a direct and profound effect on intracellular weak ion status, and impairment of enzyme function was suggested. Also, a decrement in membrane potential caused by accumulation of K^+ in the extracellular spaces coupled with a reduction in intracellular K^+ concentration during exercise (Tibes et al. 1977; Hirsche et al. 1980; Sjogaard et al. 1985) may contribute to a reduced action potential and impairment of excitation/contraction coupling by reducing the amount of Ca^{++} released per impulse (Bigland-Ritchie and Woods 1984). The purpose of the present study was to demonstrate the magnitude and importance of changes in intra- and extracellular strong ions, including La^- , to metabolic, ion, and sarcolemmal-mediated mechanisms of fatigue in skeletal muscle during intense exercise. The present study employed the isolated, perfused, electrically stimulated rat hindlimb described in detail in the Appendices and by Spriet, Lindinger et al. (1986).

4.2 METHODS

Male Sprague-Dawley rats weighing 423 ± 5 g ($n=16$) were used. The animals were fed Purina laboratory chow ad libitum and housed in a controlled environment with 12 h of day and night. The animals were divided into two groups: perfused resting (421 ± 8 g, $n=7$) and perfused stimulated (424 ± 6 g, $n=7$). Two animals were not perfused and used for control measurements only. Three to 5 hours prior to

tissue sampling the rats were injected via a tail vein with 0.5 ml 0.9% saline solution containing 25 μ Ci of 3 H-mannitol (New England Nuclear) for determination of muscle extracellular and intracellular fluid volumes (ECFV and ICFV respectively) as described in Appendix B.

4.2.1 Experimental Protocol

The surgical preparation and electrical stimulation protocol are described in detail in Appendix C and by Spriet, Lindinger et al. (1986). The prepared rat was placed in a 37°C perfusion chamber and the left hindlimb perfused with a bovine erythrocyte perfusion medium (Appendix A), with the characteristics shown in Table 15.

Each resting muscle group was perfused for 25 min at a flow rate of 2.0 ml.min⁻¹ then the gastrocnemius, plantaris, soleus (GPS) muscles sampled. The samples were immediately freeze-clamped and stored in liquid nitrogen for later analysis. The exercise group was perfused for 20 min at resting flow rates, and then for 5 min at a flow rate of 7-8 ml.min⁻¹ while being electrically stimulated. At these flow rates tissue oxygen consumption was independent of perfusate flow rate. Arterial and venous perfusate was sampled via syringe at 5 min intervals during rest and at 1 min intervals during exercise. The working GPS muscles were sampled (as described above) at the end of the stimulation period. The elevated perfusion flow rate and electrical stimulation were continued until all muscles were sampled, about 90 s.

4.2.2 Analytical Procedures

Arterial and venous perfusate samples were analyzed for gases, pH, plasma ions and metabolites as described in Appendix A. Muscle fluid volumes and ion concentrations were analyzed as described in

TABLE 15

Characteristics of the arterial perfusate; ion concentration are for plasma. Values are the mean \pm SD of 55 measurements on 16 batches of perfusate.

PCO ₂	38.7 \pm .3 mmHg	[Na ⁺]	153.1 \pm .4
pH	7.438 \pm .004	[K ⁺]	5.43 \pm .02
[HCO ₃ ⁻]	21.0 \pm .2	[Cl ⁻]	114.0 \pm .4
[H ⁺]	36.5 nmol/l	[Lactate ⁻]	0.91 \pm 0.04
[NVA]	1.4 \pm .1	[Ca ⁺⁺]	2.58 \pm .02
[Hemoglobin]	13.5 \pm .1 g/dl	[SID]	46.2
Hematocrit	37.9 \pm .3 %	[Glucose]	3.95 \pm .07
O ₂ sat'n	99.2 \pm .2 %	[Albumin]	41 \pm 1 g/l
³ H-mannitol	160 uCi/l		

Non-volatile acid ([NVA]) and [HCO₃⁻] were calculated using the nomogram (Fig. A-3). All units, except pH, mEq/l unless indicated.

Appendix B; muscle lactate was determined using enzymatic fluorometric techniques (Bergmeyer 1965).

A term usually referred to as 'base excess' or 'base deficit' is often calculated in ionic disturbances in plasma (Siggaard-Andersen 1963; Severinghaus 1965). These terms represent the theoretical quantity of strong base cation or strong acid anion, respectively, which has been added to the venous blood plasma responsible for the change from arterial plasma 'acid-base' status from a defined starting point ($\text{pH} = 7.40$; $\text{PCO}_2 = 40 \text{ mmHg}$). In the present study we have referred to the theoretical amount of strong acid anion added to plasma during muscle stimulation as non-volatile acid (NVA) to avoid confusion associated with the other terminology. With respect to the perfused hindlimb preparation, the plasma non-volatile acid concentration ($[\text{NVA}]$) represents the theoretical quantity of strong acid anion which must be added to the perfusate to account for the change in perfusate pH and $[\text{HCO}_3^-]$ from defined perfusate values of pH (7.4), PCO_2 (40 mmHg) and $[\text{HCO}_3^-]$ (20 mEq/l) where $[\text{NVA}] = 0 \text{ mEq/l}$. It must be realized that the removal of strong base cation from the plasma is equivalent to the addition of strong acid anion, and is thus reflected as an increase in $[\text{NVA}]$. Under conditions of alkalosis (in Chapter 5), $[\text{NVA}]$ may be negative, indicating the net removal of strong acid anion from the plasma from the pre-defined values.

Muscle pH_i was calculated from equation 14 using $[\text{SID}]$ determined in the present study and $[\text{A}_{\text{TOT}}]$ values determined in Chapter 3 (Table 12). Intramuscular PCO_2 of resting muscle was assumed to be 50 mmHg (Hogg et al. 1984); that of stimulated muscle

was assumed to be 70 mmHg, i.e. about 10-15 mmHg higher than in the venous plasma draining the muscle. This large muscle to plasma PCO_2 difference reflects CO_2 diffusion from regions of high PCO_2 to low PCO_2 . Any difference in actual muscle PCO_2 from these values will be small and will not significantly affect the calculated values of the dependent variables (see Chapter 3).

The potassium equilibrium potential (E_K in units of mV), used as an estimate of the resting membrane potential of resting and stimulated muscles, was estimated using the Nernst equation (Hodgkin and Horowicz 1959):

$$(32) \quad E_K = RT/F \ln([K^+]_e/[K^+]_i)$$

where $RT/F = 26.7$ mV at 37°C , $[K^+]_e$ is the ECF K^+ concentration (assumed equal to that of interstitial fluids), and $[K^+]_i$ is the ICF K^+ concentration.

4.3 RESULTS

4.3.1 Performance

The flow rates employed in the present study were $0.3 \text{ ml} \cdot \text{min}^{-1} \cdot \text{g}^{-1}$ at rest and $1.5 \pm 0.1 \text{ ml} \cdot \text{min}^{-1} \cdot \text{g}^{-1}$ during stimulation. Arterial perfusion pressures increased from 80-120 mmHg at rest to 173 ± 15 mmHg at the start of stimulation and to 223 ± 7 mmHg at the end of stimulation. Hindlimb oxygen uptake increased from $2.9 \pm 0.2 \mu\text{mole} \cdot \text{min}^{-1}$ at rest to a constant $15 \pm 1 \mu\text{mole} \cdot \text{min}^{-1}$ during stimulation. Glucose uptake by the hindlimbs increased from an average of $0.35 \mu\text{mole} \cdot \text{min}^{-1}$ at rest to $0.52 \mu\text{mole} \cdot \text{min}^{-1}$ during

stimulation.

The peak isometric tension generated by the GPS muscle group was 2.85 ± 0.10 kg, which occurred immediately at the start of stimulation (Fig. 8). Tension decreased by 24% and 45% after 2 and 5 min of stimulation. The rate of decline in tension in the first min of stimulation averaged 471 g/min compared to 222 g/min during the next 3 min and 137 g/min in the final min of stimulation.

4.3.2 Perfusate

There were no significant changes with time in venous perfusate variables during the last 10 min of rest perfusion, indicating that the perfusion medium and perfused muscles were in a steady state.

Electrical stimulation reduced venous pH from 7.403 to $7.304 \pm .008$ at the 4th min, then increased slightly during the last min of stimulation (Fig. 9A). Venous PCO_2 increased to 53.2 ± 1.5 mmHg after 3 min and remained elevated during the last 2 min (Fig. 9B). Venous $[HCO_3^-]$ (not shown) remained unchanged between 20.4 and 20.9 mmol/l during stimulation. Venous [SID] increased significantly by 2 mEq/l and 3 mEq/l within the first and third min of stimulation, respectively (Fig. 9C); the elevated venous [SID] was maintained throughout the remainder off the stimulation period.

The fluid shifts into perfused muscles during stimulation (calculated from the change in arterial to venous protein concentration) are shown in Fig. 9D. The magnitude of the increases in these protein concentrations reflect the shifts of fluid from the perfusate into the extra- and intracellular spaces of the muscle, since in maximally vasodilated rat hindquarters perfused at high flow

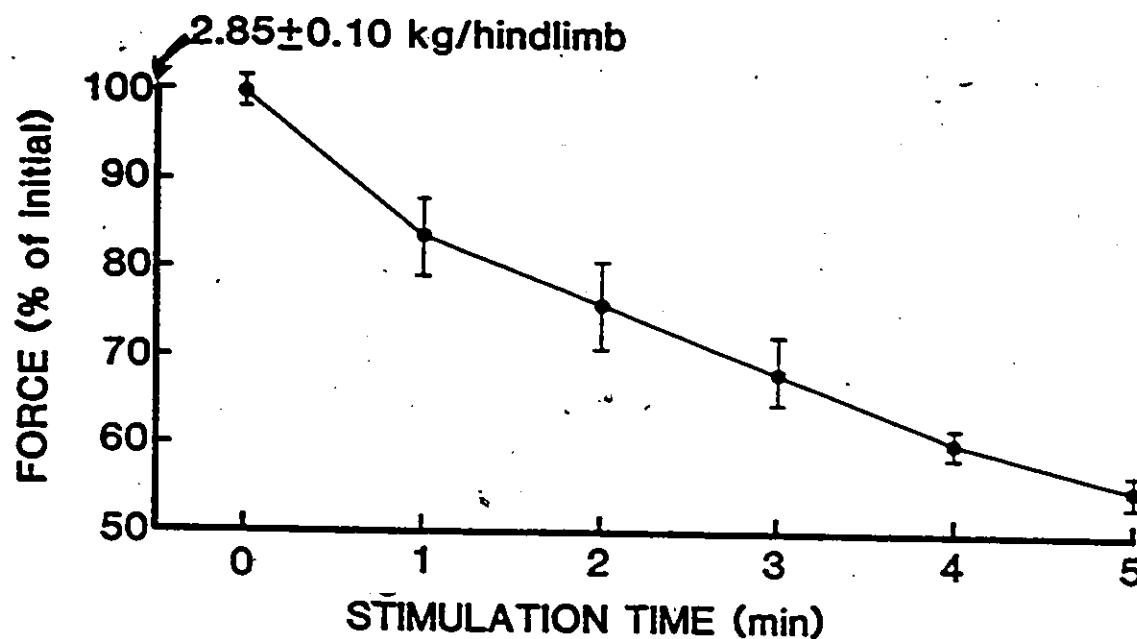


Fig. 8. Isometric tension generated by the perfused hindlimb during 5 min of electrical stimulation. Initial force was 2.85 ± 0.10 kg/hindlimb ($n=7$). Perfusion flow rate was 8.0 ± 0.3 ml/min and perfusion pressure was 220 ± 7 mmHg during stimulation. Resting flow rate was 1.6 ± 1 ml/min with a pressure of 170 ± 15 mmHg. All values are significantly different from rest (0 min).

Fig. 9. Venous pH (A), PCO_2 (B), strong ion difference ([SID]) (C), and plasma fluid shift (D) during 5 min of electrical stimulation. The fluid shifts were calculated from the arterial to venous change in plasma protein concentration. Asterisks indicate values significantly different from rest value (0 min).

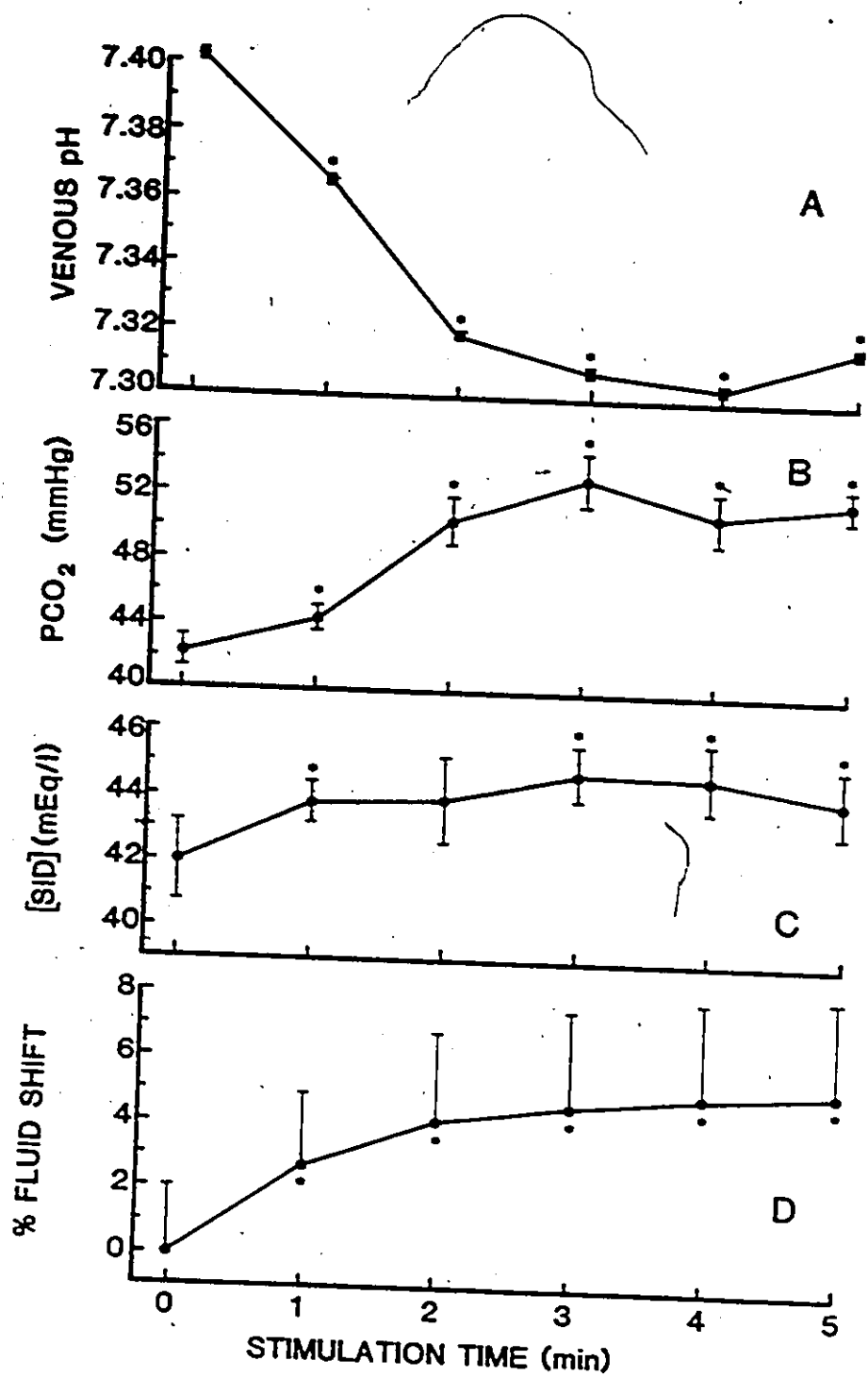
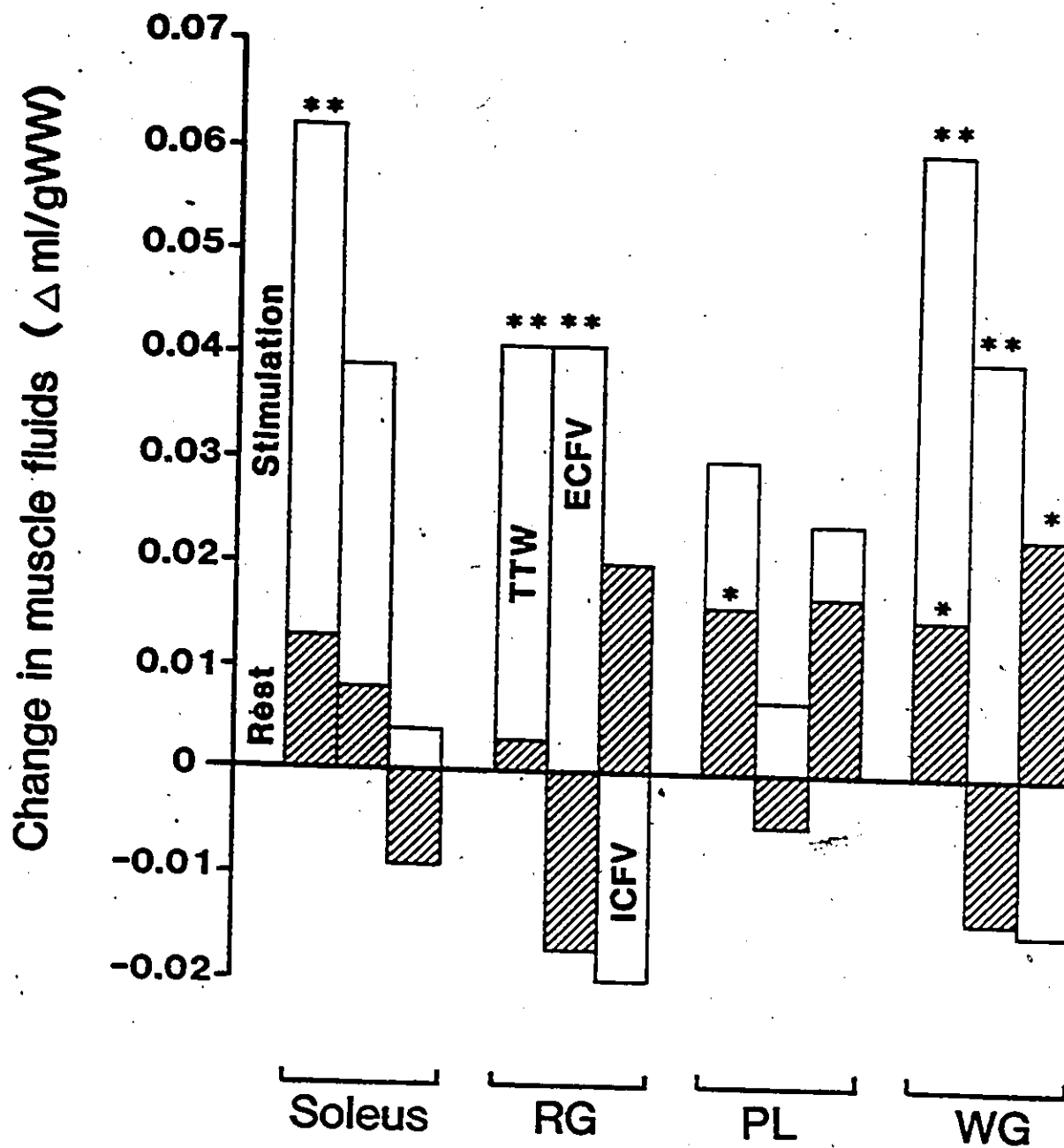


Fig. 10. Changes in muscle total tissue water (TTW), extracellular and intracellular fluid volumes (ECFV, ICFV) during rest perfusion (hatched bars) and stimulation (open bars). The net fluid shift from control rest conditions (right hindlimb muscles) to the end of stimulation is the sum of the two bars, signs considered.



rates, albumin has a reflection coefficient close to 1 (Rippe and Haraldsson 1986). The hemoconcentration corresponded to a 2.5% and 5% reduction in plasma volume during the first and fifth minute of stimulation, respectively (Fig. 9D). The arterio-venous protein concentration difference was paralleled by proportionate increases in hematocrit and hemoglobin concentration during stimulation.

Perfusion of resting muscles resulted in a 0.5-2% increase in TTW of all muscles, significant only in PL and WG (Table 16, Fig. 10). There were no significant changes in ECFV or ICFV during perfusion of resting muscles except for a significant 3.3% increase in WG ICFV. Five min of electrical stimulation resulted in a 2-6% increase of TTW and a 7-36% increase in ECFV of all muscles, with the change being significant in the SL, RG and WG. There were variable, but not significant, changes in the ICFV of all muscles.

Arterio-venous ion and metabolite concentration differences cannot be used to quantify the fluxes of ions and metabolites between muscle and perfusate because the fluid shifts also contribute to their concentration. To correct for the fluid shifts at each time point, the venous concentration of the substance is multiplied by the factor:

$$(1 - ([Pr]v - [Pr]a) / [Pr]a)$$

where $[Pr]a$ and $[Pr]v$ are the arterial and venous plasma protein concentrations, respectively. The data presented in Figures 11, 12 and 13 have been corrected for the fluid shift so that the actual net movement of ions across the hindlimb could be quantified with greater accuracy.

Stimulation caused significant increases in fluid shift-corrected venous plasma $[NVA]$, $[La^-]$, $[K^+]$, and a

significant decrease in $[Cl^-]$ (Fig. 11). $[NVA]$ increased rapidly by 3 mEq/l during the first 2 min of stimulation and remained elevated (Fig. 11A). $[La^-]$ increased slowly by 2.3 mEq/l during the first 4 min of stimulation (Fig. 11B). The increase in $[La^-]$ accounted for only 20% of the rise in $[NVA]$ during the first min of stimulation, but $[La^-]$ fully accounted for the elevated $[NVA]$ during the final three min of stimulation. $[K^+]$ peaked at 110% of resting values within 2 min of stimulation and remained elevated (Fig. 11C). $[Cl^-]$, and $[Na^+]$ (not shown), progressively decreased during stimulation, so that by 4 min $[Cl^-]$ was 96% of pre-stimulation values (Fig. 11D); the decrease in venous plasma $[Na^+]$ at the end of stimulation was not statistically significant.

The net fluxes between perfusate and perfused muscles of the 4 major strong ions and of NVA during 5 min of stimulation are plotted in Fig. 12. A positive net flux (calculated as the product of A-V difference and flow rate) represents an 'uptake' by muscle, and a negative flux represents 'release' from muscle. All values during stimulation are significantly different from rest (time 0). As indicated by Fig. 12, Na^+ and Cl^- were taken up, and K^+ and La^- released, from muscle at high rates during stimulation. There was also a marked increase in the rate of appearance of NVA, which at the end of the first min of stimulation exceeded that of La^- by a factor of 12; this was reduced to a factor of 2 during the fifth min of stimulation.

The total change in perfusate ions and NVA during the 5 minutes of stimulation are summarized in Fig. 13. The uptakes of Na^+ and Cl^- by muscle were equal (peaked at about 7.4

Fig. 11. Venous plasma non-volatile acid ([NVA]), [lactate],
[K⁺] and [Cl⁻] concentrations, corrected for fluid shifts,
during 5 min of electrical stimulation. Asterisks indicate values
significantly different from rest (0 min). Plasma [Na⁺]
followed a course similar to that of [Cl⁻].

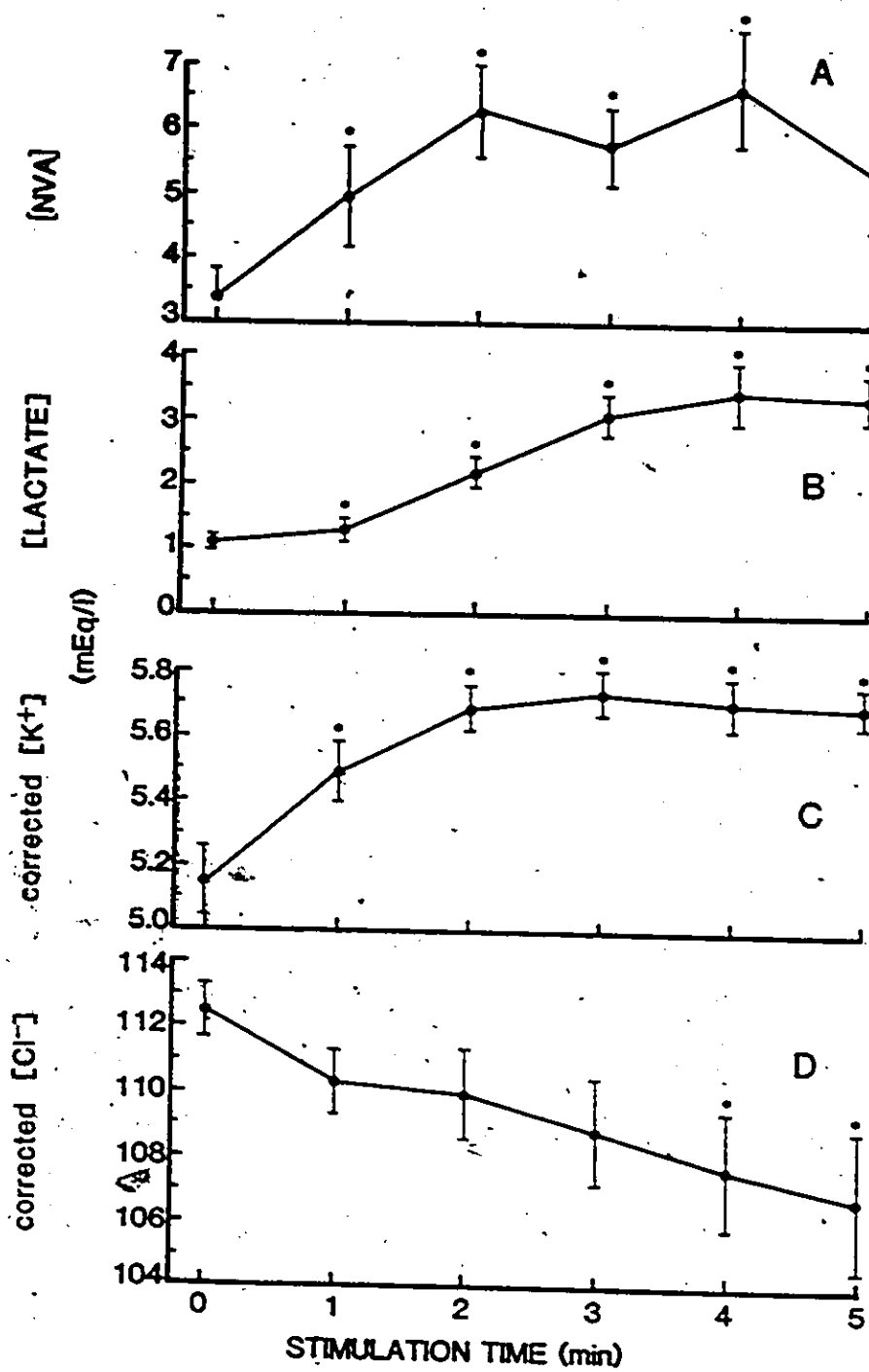


Fig. 12. Ionic fluxes and appearance rate of non-volatile acid (NVA) in the perfusate during 5 min of electrical stimulation. A positive flux is indicative of an uptake of ion by perfused muscle, while a negative flux represents an efflux of ion from perfused muscle. All values are significantly different from rest (0 min).

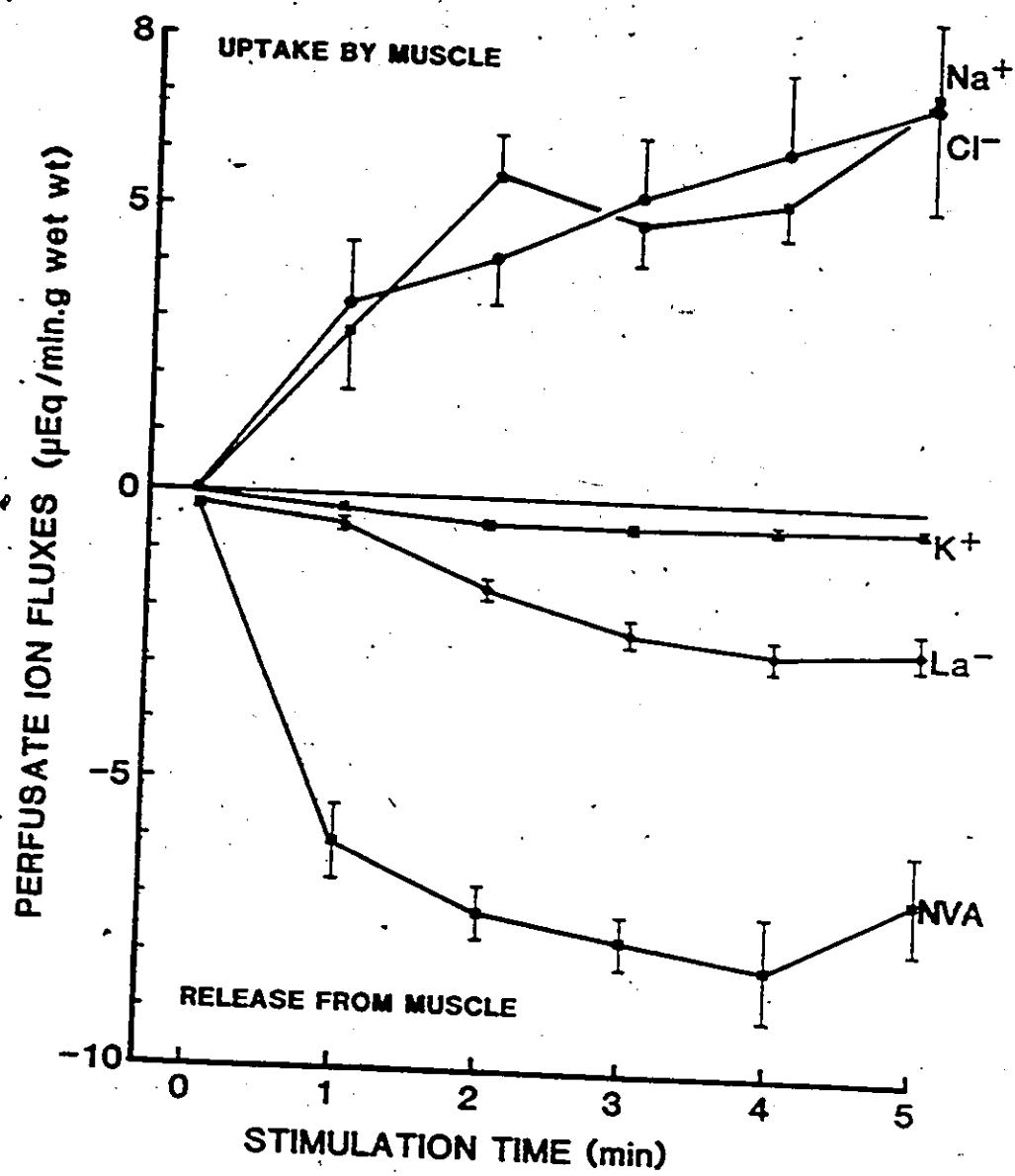
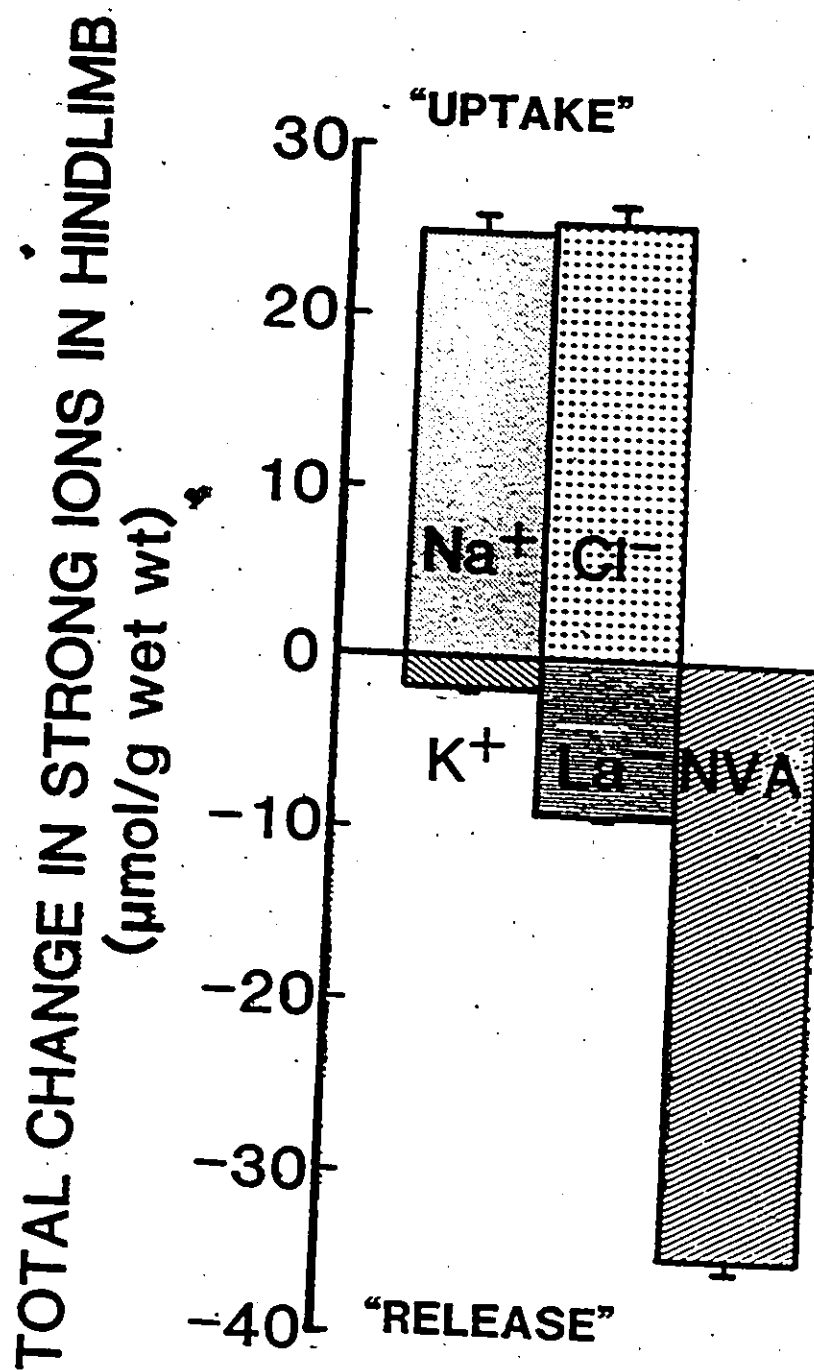


Fig. 13. A summary of the total change in perfusate strong ions and non-volatile acid (NVA) during 5 min of electrical stimulation. All values are significantly different from 0.



$\mu\text{Eq}/\text{min} \cdot \text{g}^{-1}$) and represent the largest flux of strong ions between muscle and perfusate. The total flux of Na^+ exceeded that of K^+ by a factor of 14, while La^- exceeded that of K^+ by a factor of 5, and the appearance of NVA was 4-fold greater than that of La^- .

4.3.3 Muscle Ions

Total muscle ion contents measured using instrumental neutron activation analysis were corrected for the quantity of ion in the muscle ECFV (Appendix B) to obtain the intracellular ion concentrations ($[]_i$, in mEq/l ICF) shown in Table 16. Perfusion of resting muscle resulted in small (7-14%) significant reductions in $[\text{K}^+]_i$, significant decreases (14-32%) in $[\text{Mg}^{++}]_i$, significant increases in $[\text{Cl}^-]_i$, and no change in $[\text{Na}^+]_i$. The combined changes in intracellular ion concentrations resulted in a significant reduction (9-20%) in $[\text{SID}]_i$, and hence increased intracellular $[\text{H}^+]$ calculated from physico-chemical variables in all muscles (Table 18).

Because of the readjustment of intracellular ion status during perfusion of resting muscles, changes during stimulation will be described relative to the values at the end of resting perfusion. Stimulation significantly reduced (8-19%) $[\text{K}^+]_i$, with the loss increasing in proportion to increasing glycolytic capacity of the muscle ($\text{WG} > \text{PL} > \text{RG} > \text{SL}$) (Table 16, Fig. 14). $[\text{Na}^+]_i$ and $[\text{Cl}^-]_i$ increased up to 25% in SL, RG and WG muscles, and increased significantly (56%) in the PL. $[\text{Mg}^{++}]_i$ was significantly reduced by 16-20% in all muscles but SL, while total $[\text{Ca}^{++}]_i$ showed variable changes with stimulation (Table 16, Fig. 14).

TABLE 16

Muscle total tissue water (TTW), extracellular fluid volume (ECFV), intracellular fluid volume (ICFV), and intracellular strong ion concentrations in control rest, and rest perfused, and stimulated perfused hindlimb muscles.

SL = soleus; RG = red gastrocnemius; PL = plantaris; WG = white gastrocnemius.

All values are mean \pm SE. Muscle fluid volumes in ml/g wet wt. Ion concentrations in mEq/l intracellular fluid. ^a indicates control rest mean (n=16) significantly different ($P \leq 0.05$) from perfused rest mean (n=7).

Asterisks (*) indicate perfused stimulated mean (n=7) significantly different from perfused rest mean.

TABLE 16

	CONTROL REST				REST PERFUSED				STIMULATED PERFUSED			
	SOL	RG	PLT	WG	SL	RG	PL	WG	SL	RG	PL	WG
TTW	.785	.775	.772	.770	.798	.778	.788 ^a	.785 ^a	.847 [*]	.816 [*]	.802	.830 [*]
	± .004	± .003	± .003	± .002	± .011	± .003	± .009	± .008	± .019	± .011	± .009	± .023
ECPV	.113	.096	.097	.085	.121	.079	.092	.071	.152	.120 [*]	.099	.111 [*]
	± .008	± .006	± .005	± .007	± .005	± .012	± .011	± .006	± .024	± .020	± .018	± .021
ICPV	.672	.678	.675	.684	.663	.698	.692	.707 ^a	.667	.678	.699	.692
	± .007	± .007	± .006	± .007	± .009	± .011	± .006	± .008	± .021	± .020	± .023	± .021
[La ³⁺]	1.46	1.46	2.09	2.08	1.52	1.37	1.20	2.64	3.42 [*]	15.3 [*]	16.8 [*]	28.2 [*]
	± .21	± .11	± .22	± .19	± .20	± .25	± .19	± .24	± .85	± 3.2	± 4.1	± 2.8
[K ⁺]	120.0	142.2	149.4	156.8	104.6 ^a	132.2	127.7 ^a	140.6 ^a	96.3	114.0 [*]	103.7 [*]	117.5 [*]
	± 3.7	± 6.0	± 4.6	± 4.9	± 5.5	± 2.7	± 4.3	± 5.4	± 9.9	± 5.1	± 6.3	± 4.4
[Na ⁺]	12.9	9.2	9.2	8.1	14.5	10.8	7.9	7.8	15.5	12.9	14.9 [*]	10.2
	± 1.2	± 0.9	± 0.7	± 0.7 ^a	± 3.0	± 2.3	± 1.6	± 1.6	± 1.9	± 1.4	± 1.3	± 2.0
[Cl ⁻]	13.5	9.7	8.6	7.7	20.4 ^a	13.7 ^a	12.4 ^a	10.7 ^a	22.3	13.1	23.1 [*]	12.0
	± 0.9	± 1.1	± 0.9	± 0.9	± 3.2	± 2.4	± 1.0	± 0.8	± 2.2	± 2.2	± 3.7	± 1.8
[Mg ⁺⁺]	27.2	33.1	35.7	36.9	18.5 ^a	28.4 ^a	24.7 ^a	27.8 ^a	20.5	23.7 [*]	20.8 [*]	22.2 [*]
	± 1.5	± 1.4	± 1.5	± 1.6	± 1.0	± 2.2	± 1.2	± 0.9	± 1.3	± 0.5	± 0.8	± 2.3
[Ca ⁺⁺]	2.41	2.88	3.71	3.73	2.64	3.14	3.19	4.21	3.69 [*]	3.54	3.88 [*]	3.28 [*]
	± .23	± .20	± .21	± .23	± .14	± .26	± .21	± .38	± .28	± .24	± .25	± .34

Fig. 14. The total change in the intracellular concentrations of strong ions in hindlimb muscles after 5 min of electrical stimulation. La^- accumulation is plotted reversed to show its close association with K^+ efflux. Muscle work is associated with increased concentrations of Na^+ , Cl^- and La^- and reduced concentrations of Mg^{++} and K^+ within the muscle cells.

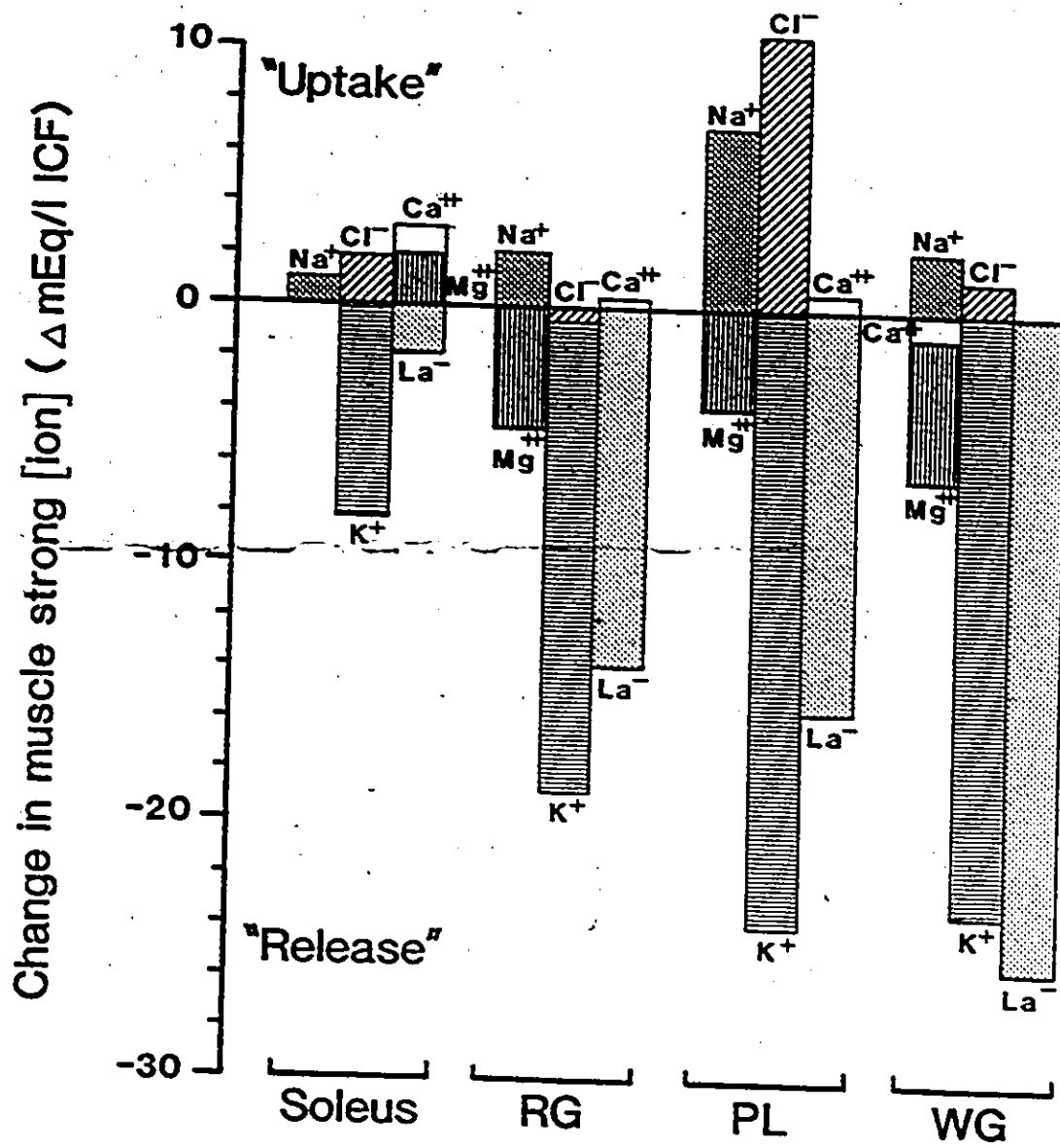


TABLE 17

Total flux of ions across the sarcolemma in hindlimb muscles during 5 min of electrical stimulation, and the percent contribution to the entire hindlimb flux (from Fig. 13).

Muscle	K ⁺	Na ⁺	Cl ⁻
Soleus	-2.30	+0.28	+0.53
Red gastrocnemius	-4.05	+0.47	-0.13
Plantaris	-14.97	+4.36	+6.68
White gastrocnemius	-70.03	+15.27	+3.94
Total GPS	-91.35	+20.38	+11.02
Total hindlimb	-2.26	+30.9	+31.5
% GPS to hindlimb	4,042	66.0	35.0

Units are $\mu\text{mol}/\text{muscle}$ per 5 min; +ve = uptake by muscle; -ve = loss from muscle. The calculations were made as follows: $\text{ION flux} = ([\text{ion}]_{\text{rest perfused}} - [\text{ion}]_{\text{stimulated perfused}} (\text{mEq/g wet wt})) \times \text{muscle wt (g)}$. The [ion] in mEq/g wet wt was obtained by dividing the [ion] in mEq/l ICF by the ICFV (values from Table 16). The muscle weights used were calculated from Table C-2.

TABLE 18

Muscle strong ion difference ([SID]) and calculated intracellular dependent variables, and K^+ equilibrium potential in control rest hindlimbs, and in rest perfused and stimulated perfused hindlimb muscles.

Units: [SID], $[A^-]$, [HA], and $[HCO_3^-]$ in mEq/l; $[OH^-]$ and $[H^+]$ in nmol/l; K^+ equilibrium potential (E_K) in millivolts.

SL = soleus; RG = red gastrocnemius; PL = plantaris; WG = white gastrocnemius. * indicates control rest mean (n=16) significantly different ($P \leq 0.05$) from perfused rest mean (n=7).

Asterisks indicate perfused stimulated mean (n=7) significantly different from perfused rest mean. For calculations: (1) PCO_2 for control rest and perfused rest was 50 mmHg; for stimulated perfused, 70 mmHg. (2) $[A_{TOT}]$ assumed constant at 184 mEq/l, 205 mEq/l, 190 mEq/l and 184 mEq/l for SL, RG, PL and WG, respectively (Chapter 3).

TABLE 18

	CONTROL REST				REST PERFUSED				STIMULATED PERFUSED			
	SL	RG	PL	WG	SL	RG	PL	WG	SL	RG	PL	WG
[SID]	131.5	156.7	166.5	174.1	104.6 ^a	142.0 ^a	134.0 ^a	150.1 ^a	98.2 [*]	110.4 [*]	89.1 [*]	98.6 [*]
	± 4.6	± 6.3	± 4.8	± 5.2	± 11.2	± 2.5	± 5.2	± 4.6	± 5.6	± 6.2	± 6.5	± 6.0
[A ⁻]	127	151	157	160	125	138	129	143	95	106	86	94
[HA]	57	54	34	24	82	67	61	41	89	99	104	90
[HCO ₃ ⁻]	4.7	5.9	10.0	14.1	2.6	4.3	4.5	7.4	3.2	4.4	3.4	4.3
[OH ⁻]	177	223	374	532	99	164	171	277	85	118	90	116
[H ⁺]	248	198	118	83	443	269	257	159	515	374	487	381
pH _i -SID	6.61	6.70	6.93	7.08	6.35	6.57	6.59	6.80	6.29	6.43	6.31	6.42
E _K	-81	-85	-87	-88	-79	-85	-84	-87	-74	-79	-76	-79

The total changes in intracellular ion concentrations during 5 min of stimulation (Fig. 14) are compared to the total perfusate ion fluxes (Fig. 17) in Table 17. The quantity of K^+ lost from the GPS muscles greatly exceeds (by a factor of 49) that which can be accounted for by the increase in venous plasma $[K^+]$. The uptake of 20.4 $\mu\text{mol Na}^+$ and of 11.0 $\mu\text{mol Cl}^-$ by the GPS group accounted for 80% and 42% of the observed decrements in venous plasma $[Na^+]$ and $[Cl^-]$.

4.3.4 Muscle $[SID]$ and $[H^+]_i$

A increase in $[H^+]_i$ will result from one or a combination of these three events: a reduction in $[SID]$, an increase in PCO_2 and/or an increase in $[A_{TOT}]$ (Section 1.2.2). The changes in intracellular ion concentrations resulting from electrical stimulation (Fig. 14) significantly reduced $[SID]_i$ by 22%, 34% and 35% in RG, PL and WG, respectively (Table 18). The relative contributions of the 20 mmHg rise in PCO_2 (assumed) and the decreases in $[SID]_i$ to the increase in $[H^+]_i$ can be determined by calculating the dependent variables at PCO_2 's of 50 and 70 mmHg and at resting and stimulated muscle $[SID]_i$'s. It was also assumed that $[A_{TOT}]$ for each muscle remained unchanged (Section 3.1) during stimulation. The contribution of the increase in $[La^-]_i$ to the reduction in pH-SID accounted for 53%, 48%, 37% and 55% of the total decrement in $[SID]$ in the SL, RG, PL and WG respectively. Through its effect on decreasing $[SID]$, the increase in $[La^-]_i$ was thus directly responsible for increasing $[H^+]$ by 48%, 86%, 59%, and 74% in the SL, RG, PL and WG respectively, during 5 min of high intensity exercise. The contribution of the increase in PCO_2 to the increase in $[H^+]$

was greater in slow twitch muscles (13% and 8% in SL and RG) than in fast twitch muscles (4% in both PL and WG).

4.3.5 Membrane potential

The calculated K^+ equilibrium potential of resting muscle is larger with increasing glycolytic capacity of the muscle (-88 mV in WG, -81 mV in SL; Table 18), reflecting the lower $[K^+]_i$ in SL (slow oxidative fibers) and higher $[K^+]_i$ in WG (fast glycolytic fibers). There was no change in the potentials during perfusion at rest. However, at the end of electrical stimulation, the combination of elevated extracellular $[K^+]$ and reduced $[K^+]_i$ increased (made less negative) the K^+ equilibrium potential of all muscles by about 10% (Table 18).

4.4 DISCUSSION

The present study has shown that high intensity exercise results in large changes in extra- and intracellular strong ion concentrations. The exercise-induced changes in extra- and intracellular strong ion concentrations, which caused changes in intracellular weak ion concentrations, are associated with factors linked to muscle fatigue. The 45% reduction in muscle performance during 5 min of stimulation (Fig. 8) was associated with large changes in protein ionization state ($[A^-]:[HA]$ ratio), a 2-fold increase in WG and PL $[H^+]_i$, and a 6-10% decrease in the K^+ equilibrium potential of the GPS muscles (Table 18).

Several major chemical events are associated with intense contractile activity in skeletal muscle: increased CO_2 production and release (Fig. 10); reduced $[Na^+]_i$, increased $[K^+]_i$,

increased $[La^-]_i$, and reduced $[SID]_i$ (Tables 16 & 18); altered protein ionization stage (Table 18); and increased $[H^+]_i$ (Table 18). Similar changes have been documented by several investigators (Sahlin 1978; Tibes et al. 1977; Hirsche et al. 1980; Sjogaard et al. 1985), and their significance will be discussed below.

4.4.1 Fluid balance

The changes in muscle fluid volumes and ionic composition during perfusion of resting muscle (Fig. 10, Table 16) indicated that initially a nonsteady-state existed between the muscles and the arterial perfusate. Examination of the venous effluent at 3 min intervals during resting perfusions showed that after the initial 10-15 min of perfusion, venous perfusate electrolyte composition remained constant. Therefore the muscles and perfusate were in a new steady-state for at least 5 min prior to the start of stimulation.

The increase in muscle TTW during exercise was due mainly to an increase in muscle ECFV (Table 16), a finding consistent with the observations that the interstitial concentrations of osmolytes increases during exercise (Tibes et al. 1977; Hirsche et al. 1980). The observed increase in TTW is similar to that found in previous studies in stimulated rat (Sreter 1963) and rabbit (Tibes et al. 1977) hindlimb muscle, and in human quadriceps muscle during intense dynamic knee extension (Sjogaard et al. 1985). Sreter (1963) reported that the increase in muscle TTW was also associated with a small increase in ICFV of stimulated soleus and gastrocnemius muscles. In the present study ICFV (Fig. 10) did not change significantly, perhaps due to the one-pass perfusion used in the present study compared to the intact circulation used in Sreter's work. In contrast to the findings by both

Sreter (1963) and the present study, the largest increases in fluid occurred in the ICPV of working muscle in humans conducting maximal dynamic knee extension exercise for 6 min (Sjogaard et al. 1985). The reason for these differences are not known, but they may be due in part to a larger muscle to ECF $[La^-]$ difference in human muscle than in rat muscle, causing a larger flux of fluid into the ICF of human muscle.

4.4.2 Ion Balance

Muscle stimulation resulted in increased $[La^-]$, $[Na^+]$ and $[Cl^-]$, and decreased $[K^+]$ and $[Mg^{++}]$ within the intracellular muscle compartment (Table 16; Fig. 15), along with increased $[K^+]$ and $[La^-]$, and reduced $[Na^+]$ and $[Cl^-]$ in venous plasma (Figs. 12 & 13). Skeletal muscle contraction in man (Sjogaard et al. 1985) and in isolated or in situ stimulated muscle preparations (Fenn and Cobb 1936; Sreter 1963; Tibes et al. 1977; Hirche et al. 1980) has also been shown to cause an increase in venous plasma $[K^+]$ and a decrease in venous plasma $[Na^+]$ and $[Cl^-]$. These changes have been attributed to incomplete re-uptake of K^+ , and higher influx of $[Na^+]$ and $[Cl^-]$ during muscle contractions (Tibes et al. 1977; Hirche et al. 1980; Sjogaard 1983).

The reasons for the large discrepancy between the observed K^+ flux into perfusate, and muscle concentrations (Table 4) may be two-fold. First, the erythrocytes are capable of removing a significant proportion of K^+ added to the circulation from exercising muscle (McKelvie, Lindinger and Heigenhauser, Appendix D). Second, Tibes et al. (1977) have demonstrated that interstitial $[K^+]$ in working muscle may be at least 2-fold greater than plasma

[K⁺]. The differences between perfusate and muscle Na⁺ and Cl⁻ fluxes are in reasonably good agreement given the contributions of interstitial fluids and inactive tissues. The contributions of the red blood cells to ion balance were not assessed in the present study, however a complete accounting of ion fluxes between muscles and perfusate requires that those analyses should be performed.

Lactate accounted for only a small proportion of the theoretical total acid anion load ([NVA]) to the venous plasma perfusate during the initial two minutes of muscle stimulation (Fig. 12). Because of the large differences in A-V [NVA], the apparent flux of NVA from stimulated muscle always greatly exceeded that of the major contributing strong anion La⁻. This suggests that some proportion of the net strong anion, i.e. La⁻, efflux from muscle is not measured as a change in plasma [La⁻]. At least part of this may result from the movement of La⁻ from plasma into inactive tissues (erythrocytes) in exchange for another strong anion, perhaps Cl⁻. For example in man following high intensity exercise, the erythrocytes may carry 32% of the total blood La⁻ load (Appendix D).

In frog sartorius muscle Adrian (1974) has estimated that a single action potential can reduce the interstitial [Na⁺] by 0.5 mEq/l and increase [K⁺] by 0.28 mEq/l. In Adrian's study, assuming that the ECFV averaged 100 ul/g wet muscle, the increase in ECF K⁺ content is 0.028 μmol/g wet muscle while intracellular Na⁺ would increase by 0.05 μmol/g wet muscle. In the present study the total theoretical K⁺ efflux and Na⁺ influx from muscle during 5 min stimulation of the WG can be estimated by multiplying the number of stimuli by the Na⁺ and K⁺ fluxes/impulse reported by Adrian

(1974). During 5 min of stimulation there were 10 action potentials every 2 s for a total of 1,500. Using a WG ECFV of 100 $\mu\text{l/g}$ wet wt, the total theoretical increase in ECF K^+ content is 42 $\mu\text{mol/g}$, and the decrease in Na^+ is 75 $\mu\text{mol/g}$. From Table 17 the amount of K^+ loss from WG was 33.4 $\mu\text{mol/g}$ (80% of theoretical) while the increase in $[\text{Na}^+]_i$ was 7.3 $\mu\text{mol/g}$ (10% of theoretical). Therefore, during the intervals between action potentials, only 20% of the K^+ was pumped back into the cells while 90% of the Na^+ was pumped back out into the ECF. These persistent fluxes of Na^+ and K^+ may be due to inadequate or impaired Na^+/K^+ ATPase pump activity (Milner-Brown and Miller 1986), in the face of increased sarcolemmal conductances of K^+ and Na^+ , at a time when ATP demand is very high. The result is reduced resting membrane potential and reduced rates of action potential propagation resulting in a decrease in muscle contractile force (Dulhunty 1982; Bigland-Ritchie and Woods 1984; Milner-Brown and Miller 1986).

Total $[\text{Mg}^{++}]_i$ decreased significantly with exercise (Table 16, Fig. 15). The free and diffusible Mg^{++} content of skeletal muscle has been measured to be 40-50% of total Mg^{++} (Cohen and Burt 1977; Hess and Weingart 1981; Maughan and Recchia 1985), while Mg^{++} bound to CP and ATP contribute an additional 19% and 27% respectively (Cohen and Burt 1977). The large reductions in intramuscular CP and ATP during heavy exercise (McCartney et al. 1986) should contribute to an increase in free $[\text{Mg}^{++}]_i$ (Cohen and Burt 1977; Hultman and Sjöholm 1986) which favors the efflux of Mg^{++} from the cell. Since free Mg^{++} competes with Ca^{++} for the binding sites on troponin (Donaldson and Kerrick 1975), an increase in free Mg^{++} in exercise

could reduce the number of active actomyosin cross-bridges formed. Therefore Mg^{++} efflux, to keep free $[Mg^{++}]_i$ low, may be beneficial to the maintenance of force generation during the development of fatigue.

4.4.3 $[SID]$ and $[H^+]_i$

WG forms the largest portion of perfused, stimulated and sampled muscle mass in the rat hindlimb preparation (Table C-2 of Appendix C) and may be considered as representative of stimulated rat hindlimb muscle (Wottiez et al. 1985). Using stimulated WG as an example, the decreases in $[K^+]_i$ and increases in $[La^-]_i$ contributed 45% and 50%, respectively, to the reduction in $[SID]_i$ (Tables 16 & 18). CO_2 release from muscle was increased during stimulation (Fig. 9) indicating an increase in muscle PCO_2 , and $[A_{TOT}]$ does not change with exercise (Chapter 3). Therefore the major factors contributing to the change in intracellular acid-base status during exercise are the increase in PCO_2 , the reduction in $[SID]_i$, and the decrease in K_A . The decrease in K_A from 5.5×10^{-7} Eq/l to 4.0×10^{-7} Eq/l appears to result primarily from the decrease in muscle CP content during intense exercise (Chapter 3). In SL, CP content is not significantly changed during 5 min of stimulation (Spriet et al. 1985a) and therefore the K_A in SL would not be expected to change significantly. In the calculations of the dependent intracellular variables a K_A of 5.5×10^{-7} Eq/l was used for SL because CP concentrations remained elevated, whereas a K_A of 4.0×10^{-7} Eq/l was used for the other muscles (Table 18).

Hindlimb muscle $[H^+]_i$, calculated from independent

physico-chemical variables, at the end of 5 min stimulation were about 2-fold higher than those at rest in all muscles except SL, which showed only a small increase (Table 18). Using the WG as an example, the relative contributions of increased PCO_2 and reduced $[\text{SID}]_i$ to the total change in $[\text{H}^+]_i$ from the resting perfused state to the end of stimulation ($2.215 \text{ Eq/l} \times 10^{-7} \text{ Eq/l}$) can be estimated as follows: the 20 mmHg increase in PCO_2 accounted for 4% ($0.094 \times 10^{-7} \text{ Eq/l}$), and the 51.5 mEq/l decrease in $[\text{SID}]$ accounted 94% ($2.082 \times 10^{-7} \text{ Eq/l}$). The contribution of the rise in $[\text{La}^-]$ can similarly be estimated and was calculated to account for 74% of the increase in $[\text{H}^+]_i$ in WG. Thus, compared to the reduction in $[\text{SID}]_i$, physiological increases in PCO_2 appear to have relatively little effect on pH_i during exercise; the increase in $[\text{La}^-]_i$ is the major contributor to changes in the total ionic status of the intracellular fluids.

Muscle CO_2 production is high during exercise, but CO_2 does not appear to accumulate to any great extent within the cells (Sahlin et al. 1983) despite large increases in intracellular PCO_2 . Intracellular $[\text{HCO}_3^-]$ is only about 10 mmol/l at rest and may be reduced to below 3 mmol/l in heavy exercise (Table 18; Sahlin et al. 1983). From physico-chemical principles $[\text{HCO}_3^-]_i$ is not only dependent on PCO_2 , but also on $[\text{A}_{\text{TOT}}]_i$ and $[\text{SID}]_i$ (Fig. 3); therefore changes in $[\text{HCO}_3^-]$ do not have to parallel changes in PCO_2 and, as in heavy exercise, their changes may be opposed (Table 18).

What factors are responsible for the increase in muscle CO_2 output and venous PCO_2 ? Muscle metabolism is increased

substantially in the stimulated perfused rat hindlimb, with glycolysis contributing only 23% to the elevated metabolic rate in the first 5 min of stimulation (Spriet et al. 1985a). Thus with aerobic metabolism contributing about 77% to the elevated metabolic rate, a substantial increase in PCO_2 should result. The rapid and large reduction in $[SID]_i$ also appears to contribute to the elevation in PCO_2 with exercise; this makes the assumption that the intracellular compartment of the muscle is behaving as a partially closed system. In explanation, the rapid reduction in $[SID]_i$ determines (by physico-chemical equilibria outlined in Section 1.2.2) that $[HCO_3^-]_i$ must decrease; the equilibrium relationships show that reduced $[SID]$ together with reduced $[HCO_3^-]$ must be associated with an increase in PCO_2 . Therefore, in exercising muscle, there appears to be a disequilibrium for CO_2 , with muscle behaving as a partially closed system, and with $[SID]$ partially determining the PCO_2 (i.e. PCO_2 is behaving like a dependent variable with respect to $[SID]$). The relative contributions of increased metabolism and reduced $[SID]$ to the elevation in PCO_2 cannot be distinguished at this time.

4.4.4 Significance

Muscle fatigue may result from one or a combination of three key processes occurring within muscle: inhibition of metabolism, reduction in the number of actomyosin crossbridges formed and decreased in the rate of cross-bridge cycling, and membrane depolarization causing reduced action potentials. As discussed in Chapters 1 & 3, exercise-induced changes in the concentrations of $[Na^+]_i$ and $[K^+]_i$, and in $[SID]_i$, may indirectly decrease the activities of key

glycolytic enzymes by altering active site conformation and by exerting direct allosteric effects.

The strength of contraction is directly proportional to the number of actomyosin crossbridges formed and to the quantity of Ca^{++} released from the sarcoplasmic reticulum (SR) to bind to troponin C (Ebashi 1976). Relaxation of the sarcomeres is initiated by repolarization of sarcolemmal membranes and active uptake of Ca^{++} from the sarcoplasm (Ebashi 1976). A decrease in ATP production and turnover with decreasing [SID] may reduce the ATP supply required by myosin ATPase for relaxation of the active actomyosin complex (Kushmerick 1983). Increased intracellular $[\text{H}^+]$ has been postulated to exert its major effects on the modulation of free Ca^{++} concentrations of extra- and intracellular fluids, thereby affecting the force of contraction. Changes in ion status associated with increased $[\text{H}^+]$ have been implicated in decreased activity of the Ca^{++} ATPases required for pumping of Ca^{++} into the ECF or SR (Nakamaru and Schwartz 1972; Fabiato and Fabiato 1978), decreased activity of myosin ATPase, and binding to the high affinity Ca^{++} -binding sites on troponin C (Fabiato and Fabiato 1978; Donaldson 1983; Hultman and Sjöholm 1986). The first two events result in an increase in sarcomere relaxation time while the latter event results in reduced rates of crossbridge formation and recycling. Of particular relevance to these 'pH effects', Chapter 3 has shown that conditions causing an increase in $[\text{H}^+]$ also causes an increase in $[\text{HA}]$ and a decrease in $[\text{A}^-]$ (Fig. 3), reflecting changes in the ionization state of intracellular proteins. It is proposed that any conformational or electrostatic alterations (Nakashimi and Tuboi 1976;

Woodbury 1974) could also be imposed on the enzymes and proteins involved with the contraction process per se.

The concentration of inorganic phosphate P_i increases markedly as ATP and CP is hydrolyzed during intense muscular contraction (Wilkie 1986). In the intracellular fluid P_i exists in monobasic and dibasic forms ($H_2PO_4^-$ and HPO_4^{2-} , respectively), therefore conditions associated with an increase in $[H^+]$ will also be associated with a decrease in the dibasic form and an increase in the monobasic form of P_i (Cooke & Pate 1985; Wilkie 1986). Recent evidence strongly suggests that increases in $[P_i]$ during intense muscular contraction is directly responsible for some of the inhibition of force generation (Hibberd et al. 1985), and it seems likely that the resultant high $[H_2PO_4^-]$ associated with changes causing an increase in $[H^+]$ may be a direct inhibitor of the actomyosin ATPase system (Wilkie 1986).

Reduced trans-sarcolemmal Na^+ and K^+ differences during muscle activity depolarize the muscle cells. This depolarization may decrease the magnitude of the muscle action potential and reduce Ca^{++} release (Bigland-Ritchie and Woods 1984; Caille et al. 1985), decrease free intracellular $[Ca^{++}]$, and thus contribute to the decline in force during muscle activity (Juel 1986; Section 1.3.3). Using the WG as an example, the increase in ECF $[K^+]$ during 5 min of electrical stimulation was calculated (equation 32) to be responsible for only 29% of the change in the potassium equilibrium potential; the decrease in ICF $[K^+]$ was responsible for the balance.

4.4.5 Summary and Conclusions

The two events which appear to have the greatest effect on muscle performance during intense exercise are the large decrease in $[K^+]_i$ and the marked accumulation of La^- within muscle cells.

These two major ion perturbations reduce intracellular $[SID]$ and the K^+ equilibrium potential, both of which are intimately associated with muscle fatigue. Correction of the ionic disturbances would be directed towards restoration of normal muscle ion status and muscle function. In particular, recovery from fatigue requires a critical readjustment of intramuscular electrolyte balance, which is energy dependent. The loss of muscle contractile force at a time when cellular ATP stores are depressed may be beneficial by preventing the muscle rigor associated with a large fall in ATP. Muscle fatigue may provide a means for the self-preservation of muscle cells.

MODULATION OF SKELETAL MUSCLE METABOLISM AND ION FLUXES

BY ALKALOSIS

5.1 INTRODUCTION

During high intensity exercise, glycolysis contributes significantly to the total energy production of the working muscles. The intramuscular accumulation of lactate (La^-) and hydrogen ions (H^+) associated with this type of exercise have been implicated as causes of muscular fatigue (Hermansen and Osnes 1972; Spriet et al. 1985b; Hultman and Sjöholm 1986). In support of this theory it has been shown that artificially induced acidosis is associated with an increased rate of decline of initial force, a decreased rate of glycolysis and a lower rate of La^- release in rat muscle preparations (Spriet et al. 1985b) and exercising humans (Sutton et al. 1981). Conversely, La^- release from contracting muscle appears to be enhanced in conditions of extracellular alkalosis, and in particular with high ECF $[\text{HCO}_3^-]$ (Mainwood and Worsley-Brown 1975; Seo 1984) resulting in increased concentrations of La^- in the blood (Sutton et al. 1981; Davies et al. 1986).

Artificial acidosis is traditionally induced by the addition of excess Cl^- (strong acid anion) to, or the removal of Na^+ (strong base cation) from, the extracellular fluids. Alkalosis, on the other hand, is typically induced by the addition of Na^+ to the ECF. The present study tested the hypothesis that changes in the strong ion composition of the extra- and intra-cellular fluids influences the regulation of metabolism in contracting skeletal muscle.

There appear to be two components to the enhanced release of

La^- from muscle in alkalotic conditions. A non-ionic (HLa) component is thought to be related to the $[\text{H}^+]$ of the ECF, while an ionic (La^-) component may be associated with extracellular $[\text{HCO}_3^-]$ (Hirche et al. 1975; Mainwood and Worsley-Brown 1975; Seo 1984; Mason et al. 1986). A combination of low extracellular $[\text{H}^+]$ and high $[\text{HCO}_3^-]$ (metabolic alkalosis) is associated with a high rate of $[\text{La}^-]$ efflux, and low extracellular $[\text{H}^+]$ with normal $[\text{HCO}_3^-]$ is associated with a lower rate of La^- release. The lowest rates of La^- release are seen when ECF $[\text{H}^+]$ is high and $[\text{HCO}_3^-]$ low, i.e. metabolic acidosis (Hirche et al. 1975; Seo 1984; Spriet et al. 1985b). In exercising humans, metabolic acidosis is also associated with reduced plasma $[\text{La}^-]$ (Jones et al. 1977; Sutton et al. 1981; Kowalchuk et al. 1984).

According to physico-chemical principles, the acid-base status of a solution is dependent upon three independent variables: the PCO_2 , the total concentration of weak acids and bases ($[\text{A}_{\text{TOT}}]$), and the strong ion difference ($[\text{SID}]$) (Stewart 1981; 1983; Section 1.2.2). Disturbances of ion status caused by changes in $[\text{A}_{\text{TOT}}]$ and $[\text{SID}]$, but where PCO_2 is unchanged, are referred to as metabolic. Respiratory disturbances, on the other hand, are caused by changes in PCO_2 . Metabolic disturbances appear to exert significant effects on muscle La^- release and the change in $[\text{NVA}]$. The implication is that changes in the concentrations of strong ions other than La^- in the ECF and ICF directly affect the movement of the strong ion La^- between body fluid compartments. Under conditions of elevated intramuscular La^- production and accumulation, La^- released

from muscle to blood is expected to be the primary contributor to the¹⁴¹ rise in [NVA].

The present study used an isolated, perfused rat hindlimb preparation (Spriet et al. 1985a) to examine the effects of induced alkalosis on skeletal muscle metabolism and performance during 5 min of electrical stimulation. The model served as a closed metabolic and ionic system, enabling precise measurements to be made of: (1) the energy sources utilized and the metabolites produced by the working muscle; (2) the ionic fluxes between muscle and perfusate; and (3) the changes in intracellular ion concentrations in hindlimb muscles, during tetanic stimulation. Isometric force production by the gastrocnemius-plantaris-soleus (GPS) muscle group was also measured.

The aims of the present study were four-fold: (1) to examine the effects of alkalosis on the isometric tension development of rat skeletal muscle; (2) to assess the relative contributions of the major energy sources to force production during alkalosis and control conditions; (3) to compare the effects of respiratory (reduced extra- and intramuscular PCO_2) and metabolic (increased extra- and intramuscular [SID]) alkalosis on the rates of La^- release and other strong ion fluxes from working muscle; and (4) to test the hypothesis that alkalosis reduces the degree of intracellular ionic disturbances in exercising muscle.

5.2 METHODS

Male Sprague-Dawley rats weighing 405 ± 6 g ($n=50$) were used. The animals were fed Purina laboratory chow ad libitum and housed in a controlled environment with 12 h of day and night. Six groups of

experiments were conducted to establish both baseline and exercise parameters: control acid-base status (C), resting (n=7); C exercise (5 min stimulation; n=11); metabolic alkalosis (MALK) resting (n=6); MALK exercise (n=12); respiratory alkalosis (RALK) resting (n=5); and RALK exercise (n=9). The control animals from these groups were used for the comparison of muscle performance and metabolism only; this was because these control experiments were being conducted prior to the time when ion flux analyses was performed in this lab. The appropriate controls for the ion fluxes and intracellular ion concentrations at rest (n = 7) and during stimulation (n = 7) are those presented in the preceeding chapter (Chapter 4).

Arterial perfusate gases, and plasma ion and metabolite concentrations for each condition are listed in Table 19. The arterial perfusate was prepared to simulate conditions of RALK by reducing the PCO_2 of the solution, whereas MALK was simulated by increasing the [SID] (by addition of $NaHCO_3$) of the solution. Reduced PCO_2 alone (RALK) had no effect on $[HCO_3^-]$ but decreased $[H^+]$, whereas an increase in [SID] (MALK) caused a reduction in $[HCO_3^-]$ and a decrease in $[H^+]$.

Surgical preparation, perfusion and stimulation protocols, perfusate and muscle sampling protocols, perfusate analyses, and statistics were performed as described previously (Chapter 3; Appendix C). Muscle intracellular ion and metabolite contents ($\mu Eq/g$ wet wt, and $\mu mol/g$ dry wt, respectively) was determined as described in Appendix B; muscle extra- and intracellular fluid volumes were not measured in the alkalotic hindlimbs, therefore intracellular concentrations were not calculated. Therefore, muscle intracellular

TABLE 19

Composition of the arterial perfusate in controls, respiratory alkalosis (RALK), and metabolic alkalosis (MALK).

	CONTROL (n=16)	RALK (n=14)	MALK (n=18)
[Na ⁺]	153 ± 2	149 ± 1	161 ± 2 ^{a,b}
[Cl ⁻]	124 ± 2	122 ± 1 ^a	121 ± 1 ^a
[K ⁺]	5.4 ± 0.2	5.5 ± 0.1	5.7 ± 0.1
[Mg ⁺⁺] ^c	2.2 ± 0.2	2.1 ± 0.1	1.9 ± 0.1
[Ca ⁺⁺] ^d	2.6 ± 0.2	3.0 ± 0.1	3.2 ± 0.1
[La ⁻]	0.91 ± 0.04	0.85 ± 0.05	0.94 ± 0.06
[SID]	37.2 ± 0.6	34.7 ± 0.5 ^a	48.0 ± 0.7 ^{a,b}
PCO ₂ (mmHg)	38.7 ± 0.8	26.6 ± 1.2 ^a	38.3 ± 0.9 ^b
[NVA]	1.4 ± 0.4	1.2 ± 0.2	-10.4 ± 1.4 ^{a,b}
[HCO ₃ ⁻]	21.0 ± 0.5	19.8 ± 0.5	29.1 ± 0.8 ^{a,b}
pH	7.438 ± 0.009	7.566 ± 0.017 ^a	7.570 ± 0.006 ^a
[glucose] (g/l)	40 ± 7	42 ± 2	43 ± 2
[albumin] (g/l)	41 ± 2	41 ± 3	38 ± 2
[hemoglobin] (g/l)	135 ± 2	127 ± 2	132 ± 1
hematocrit (%)	37.9 ± 0.3	37.4 ± 0.4	37.1 ± 0.3

Units are mEq/l unless otherwise indicated. [SID] calculated as:

$$[\text{SID}] = [\text{Na}^+] + [\text{K}^+] + [\text{Ca}^{++}] - [\text{Cl}^-] - [\text{La}^-]$$

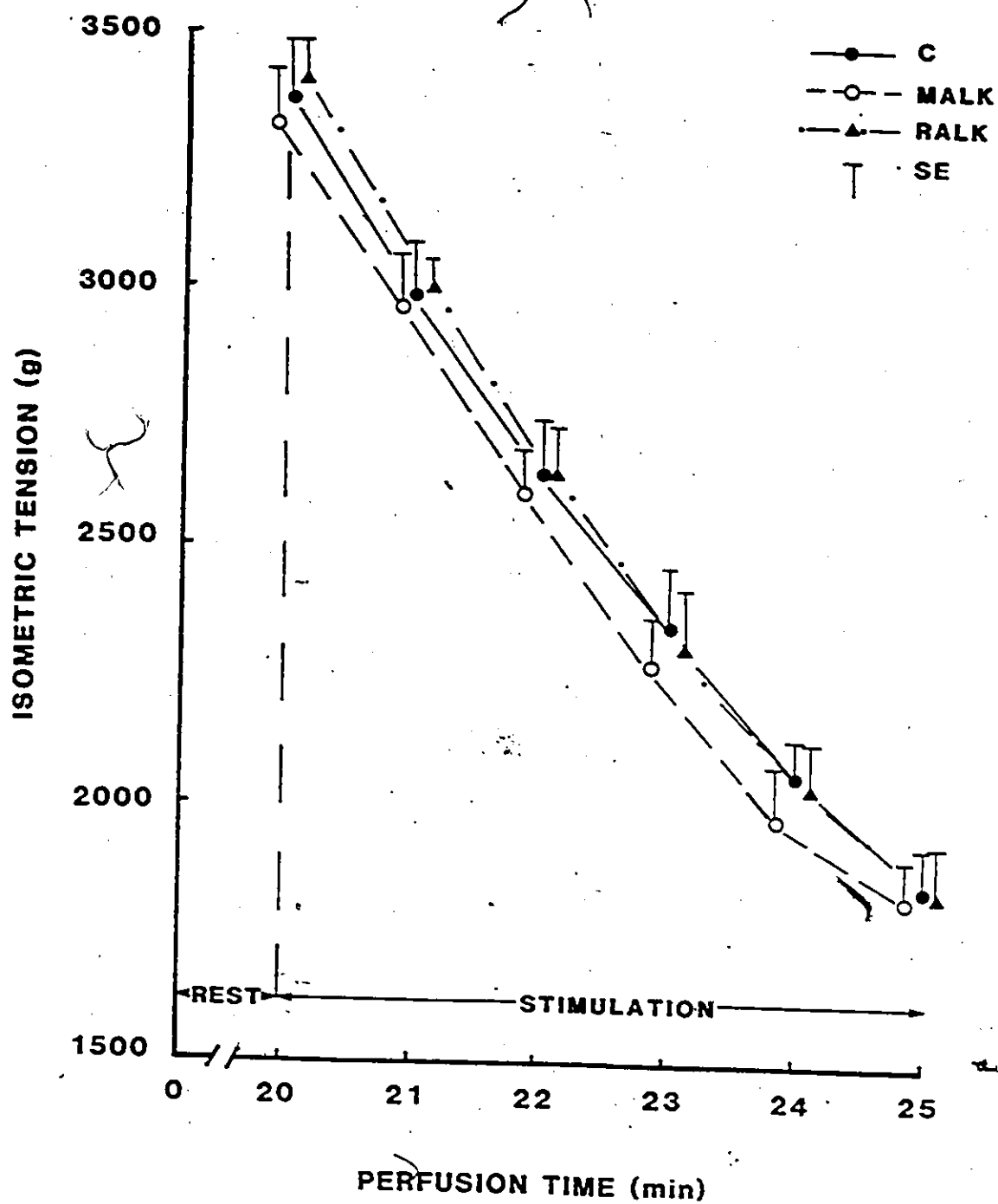
a significantly different from control

b significantly different from RALK

c total Mg⁺⁺ concentration of plasma

d ionized Ca⁺⁺ concentration of plasma

Fig. 15. Isometric tetanic tension generated by the gastrocnemius-plantaris-soleus muscle group during 5 minutes of electrical stimulation. C, control; MALK, metabolic alkalosis; RALK, respiratory acidosis.



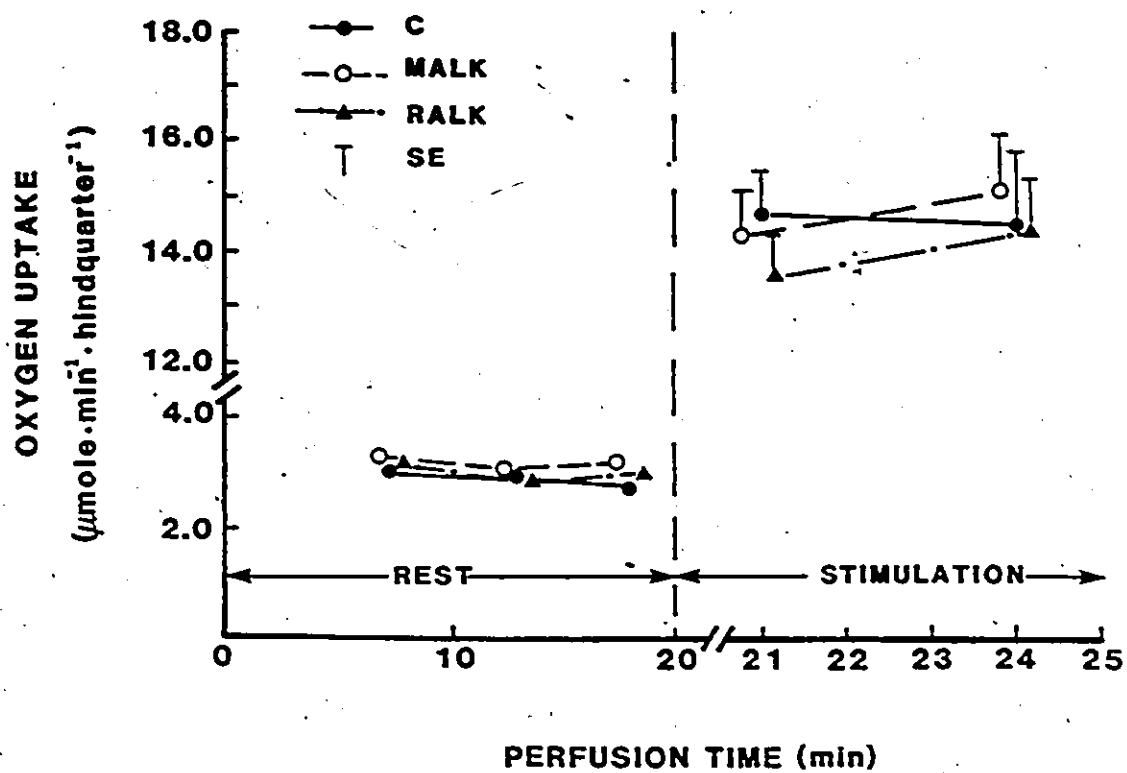


Fig. 16. Hindlimb oxygen uptake at rest and during stimulation. Definitions as in Fig. 15. Standard error of the means at rest were equal to the size of the symbols.

ion contents were calculated using mean muscle ECFV values listed in Table 16 for the appropriate condition (control rest; rest perfused; stimulated perfused).

5.3 RESULTS

5.3.1 Performance and Metabolism

Arterial perfusion pressures at resting flow rates were similar (80-130 mmHg) in the three conditions. During stimulation at flow rates of $7.5 \text{ ml} \cdot \text{min}^{-1}$, the arterial perfusion pressures increased to 129 ± 16 , 139 ± 15 , and 189 ± 25 mmHg during C, MALK, and RALK conditions, respectively.

The peak isometric tension generated by the GPS muscle group during C was 3367 ± 107 g (Fig. 15). Tension decreased to 79% and 55% of peak tension after 2 and 5 min of stimulation. Tensions developed during MALK and RALK were not significantly different from C.

Oxygen uptake by perfused hindlimb at rest and during stimulation were not affected by alkalosis (Fig. 16). The rate of O_2 uptake was stable during the final 15 min of rest perfusion and throughout the 5 min of stimulation in all conditions.

Hindlimb glucose uptake was minimal both at rest and during electrical stimulation in all conditions. During 5 min of stimulation, total glucose uptake by the hindlimb was 2.6, 3.9, and 6.0 umoles in the C, MALK, and RALK groups, respectively.

Samples of non-working muscle were taken following 20 min of perfusion in each condition to examine the effects of perfusion in the resting state. In all cases, no significant differences were observed in the intramuscular concentrations of glycogen, La^- , CP, and ATP

in hindlimb muscles: representative data from the PL muscle are shown in Table 20.

No significant differences were observed in intramuscular concentrations of ATP and CP between conditions (Fig. 17). Following stimulation, concentrations of CP and ATP fell by 60-80% and 25-40%, respectively, in both the PL and WG while in SL, CP decreased by 20-50% and ATP remained unchanged. Alkalosis had no effect on the depletion of CP and ATP stores in any muscle.

Stimulation resulted in a large decrease in glycogen content and increased La^- content in the PL and WG muscles (Fig. 18). Both alkalotic conditions were associated with decreased La^- accumulation in WG and PL; this was significantly different from control conditions in the PL. Glycogen and La^- contents in SL muscle were not affected by alkalosis.

5.3.2 Venous Perfusate

Venous plasma pH, PCO_2 and [NVA] from perfused resting muscle were constant during the final 5 min of the 20 min perfusion; steady state values are represented by time 0 min in Fig. 19. Venous plasma $[\text{HCO}_3^-]$ (calculated from the nomogram, Fig. A-3) was 19.9 ± 0.5 , 19.7 ± 0.5 and 26.5 ± 0.6 mEq/l for C, RALK and MALK at rest; these values did not change significantly during 5 min of stimulation. During stimulation, the reduction in venous pH was accompanied by increases in PCO_2 and [NVA] (Fig. 19). During the first min of stimulation, venous pH was reduced to a greater extent in both RALK and MALK; at the end of the stimulation period the reduction in pH with MALK was significantly greater than with RALK, and the change with RALK was significantly greater than in C (Fig. 19A).

TABLE 20

Muscle fuel and metabolite contents of plantaris at rest in
in controls and in alkalosis.

	Glycogen	Lactate	CP	ATP
PP	128 \pm 5	4.7 \pm 0.5	93 \pm 3	30 \pm 1
C	125 \pm 9	5.0 \pm 0.5	89 \pm 5	31 \pm 1
MALK	139 \pm 15	4.2 \pm 0.8	88 \pm 4	30 \pm 1
RALK	124 \pm 7	6.4 \pm 1.5	105 \pm 9	28 \pm 2

Units: $\mu\text{mol/g}$ dry weight.

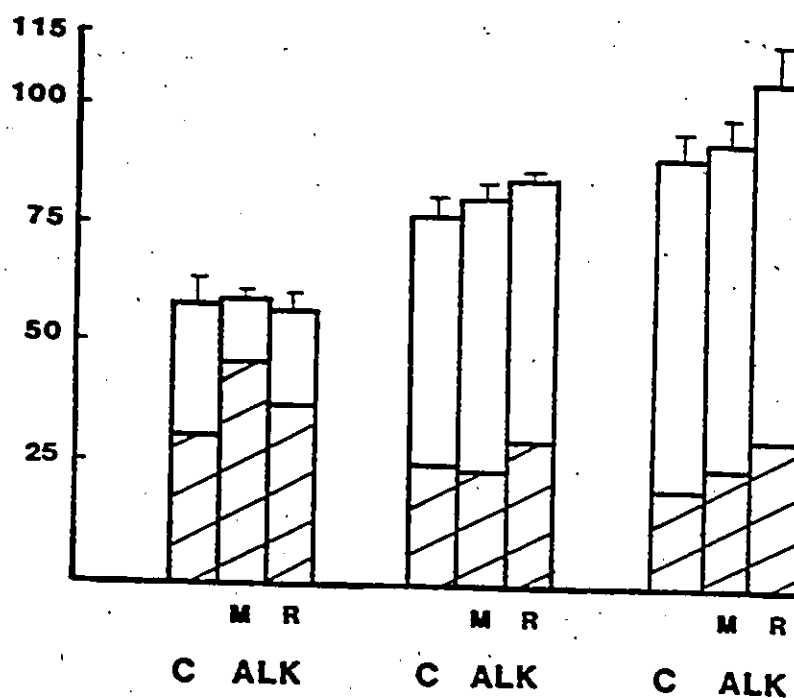
Values are means \pm SE for preperfusion (PP) and post-20
min of rest perfusion in control (C), metabolic alkalosis
(MALK), and respiratory alkalosis (RALK) conditions.

PP, n = 18; C, n = 7; MALK, n = 6; RALK, n = 5.

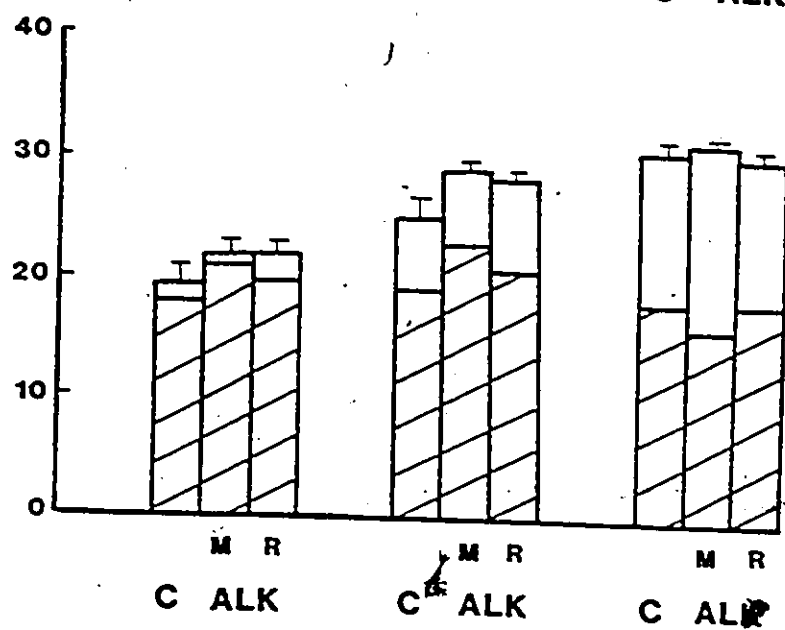
Fig. 17. Muscle creatine phosphate (CP) and adenosine triphosphate (ATP) contents at rest and following 5 minutes of stimulation.

Preperfusion contents are represented by the total height of the bars, and nonhatched sections represent CP or ATP utilized during stimulation. Definitions as in Fig. 15.

MUSCLE CREATINE PHOSPHATE

 $(\mu\text{mole} \cdot \text{g}^{-1} \text{ dry wt})$ 

MUSCLE ATP

 $(\mu\text{mole} \cdot \text{g}^{-1} \text{ dry wt})$ 

SOLEUS

PLANTARIS

WHITE GAST

Fig. 18. Muscle glycogen and lactate contents at rest and following 5 minutes of stimulation. Preperfusion glycogen contents are represent by the total height of bars, and preperfusion lactate contents are represented by the height of hatched sections.

Nonhatched sections represent glycogen utilized and lactate accumulated during stimulation. * Significantly different from C; + significantly different from metabolic alkalosis.

Definitions as in Fig. 15.

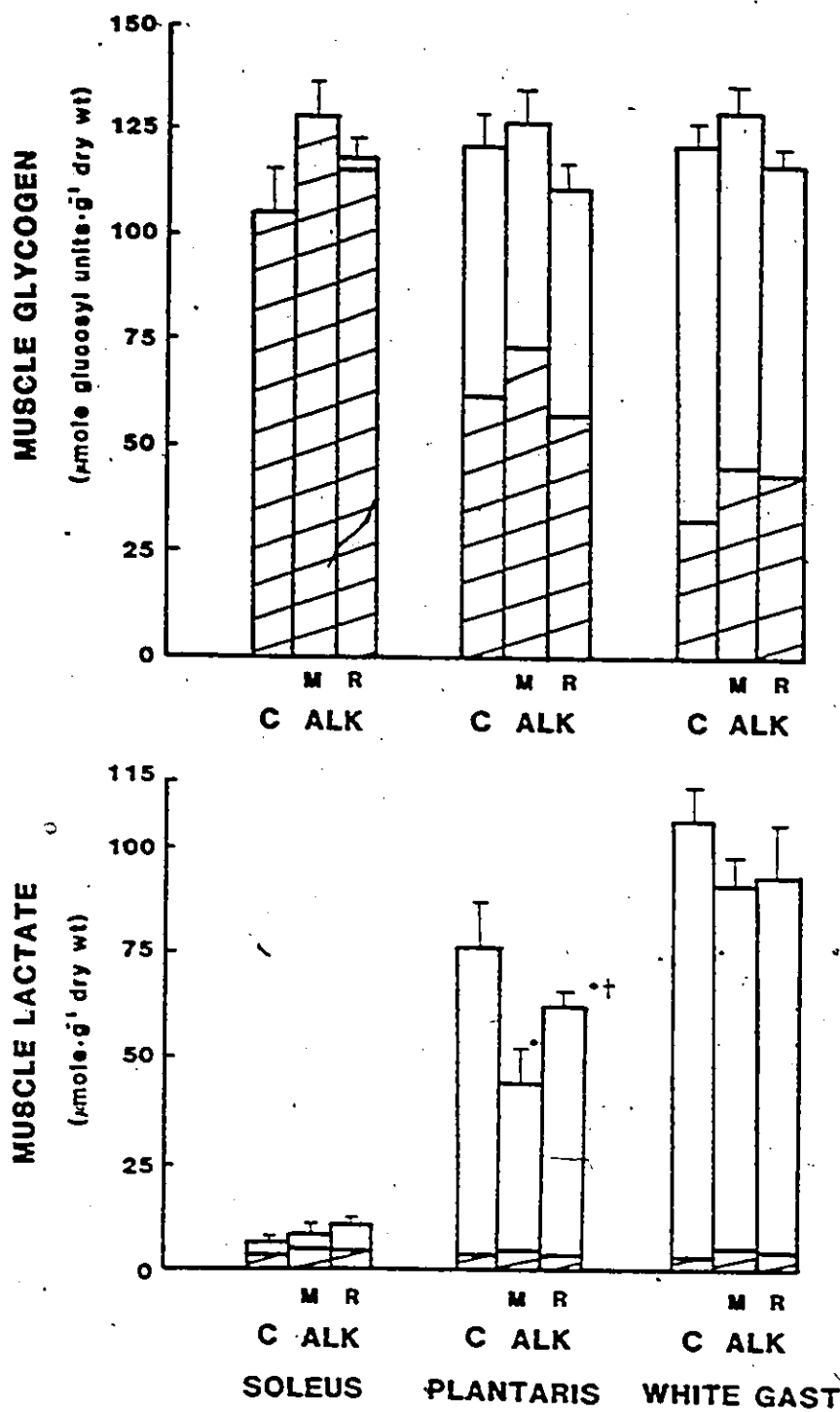


Fig. 19. The change in venous pH, PCO_2 and [NVA] in the stimulated rat hindlimb in controls (shaded areas, from Chapter 4), MALK (squares) and RALK (circles). Pre-stimulation mean \pm SE is given in each panel for the three perfusate conditions. * indicates mean is significantly different from control; ** indicates MALK mean is significantly different from RALK mean. Definitions as in Fig. 15.

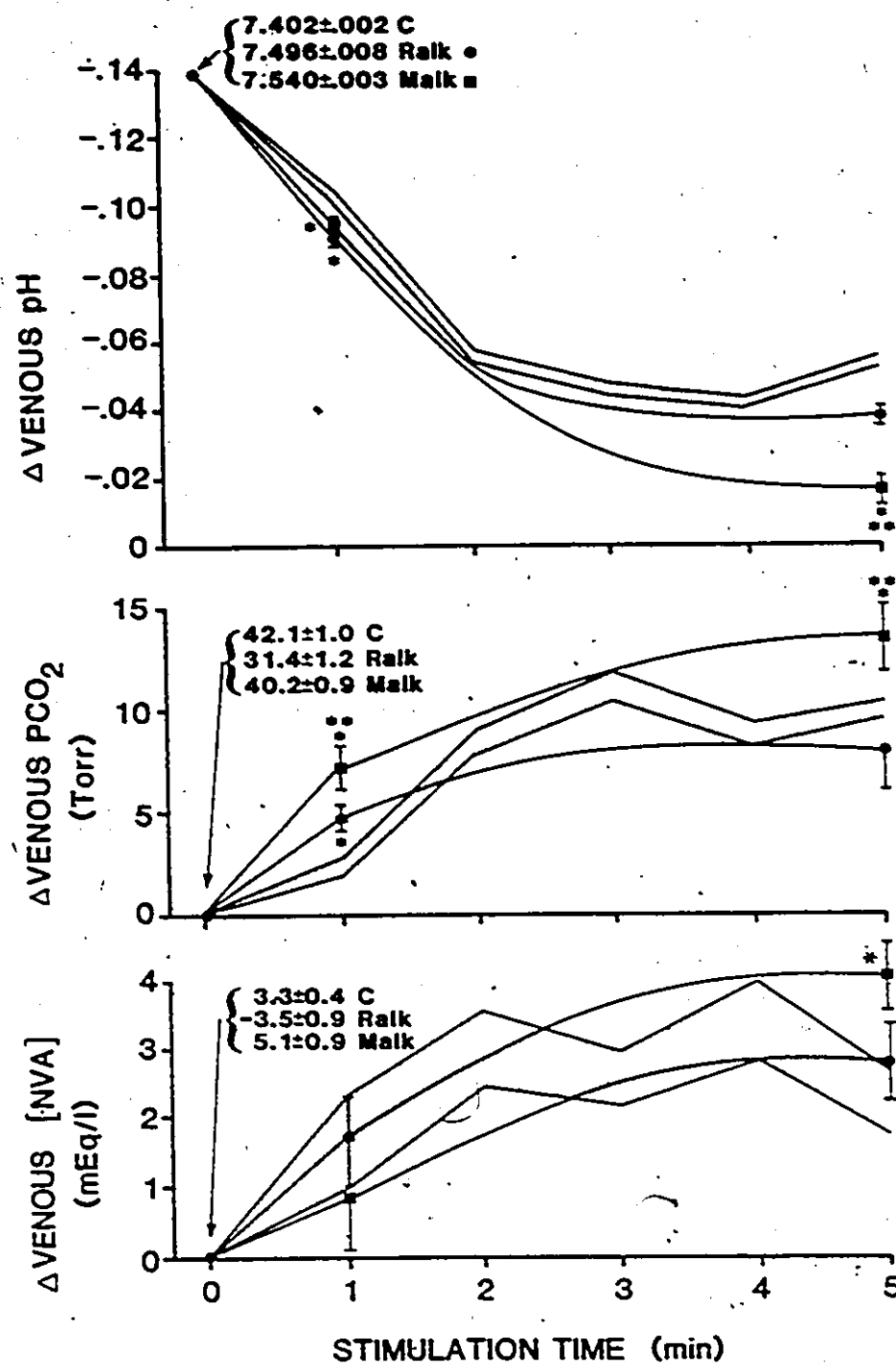
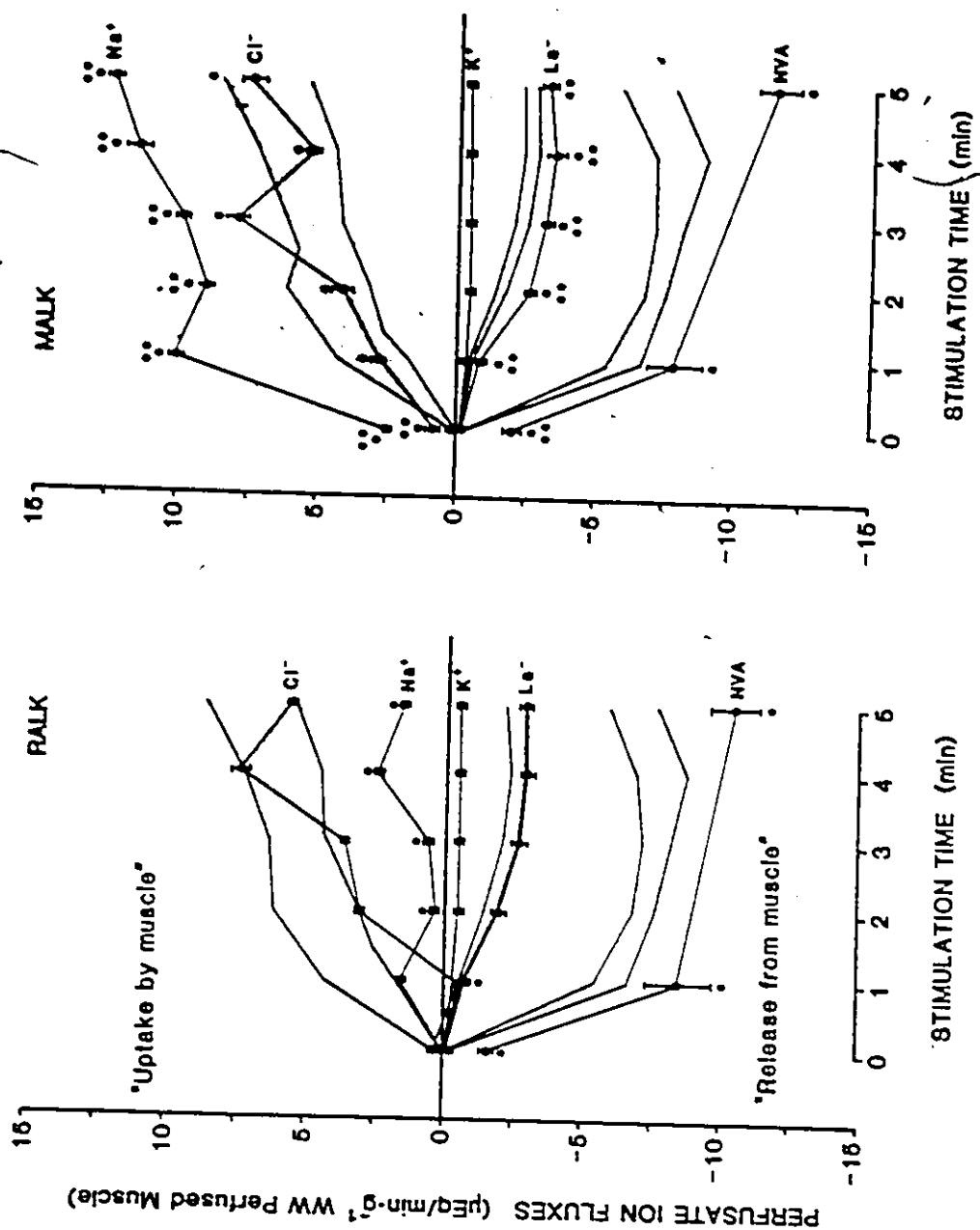


Fig. 20. The net fluxes of strong ions and apparent non-volatile acid anion (NVA) in the stimulated perfused hindlimb as a function of duration of stimulation in RALK and MALK. The controls (from Chapter 4) are indicated by the shaded regions; the shaded region above the 0 line represents both the Na^+ and Cl^- fluxes; the corresponding control fluxes for K^+ and NVA are indicated below the 0 line. A positive flux is representative of an uptake of ion by muscle, while a negative flux is indicative of a release of ion from muscle. * indicates mean is significantly different from control; ** indicates MALK mean is significantly different from RALK mean. Definitions as in Fig. 15.



During the first min of stimulation, the increase in venous PCO_2 with MALK and RALK was 3-fold and 2-fold greater than that of C, respectively (Fig. 19B). For the remainder of the stimulation, venous PCO_2 in RALK was the same as C; however with MALK, venous PCO_2 remained significantly elevated during stimulation. Venous plasma [NVA] increased more in MALK than in RALK, this difference was significant at the end of stimulation (Fig. 19C). The venous plasma [NVA] during stimulation in both alkalotic conditions were not significantly different from C.

5.3.3 Ion Fluxes

During the final 5 min of the 20 min resting perfusion, the net fluxes of Na^+ , Cl^- , K^+ , La^- and NVA between muscle and perfusate were significantly greater in RALK and MALK than in C (time 0 min, Fig. 20). This reflects the greater perfusate to muscle concentration differences for the alkalotic media compared to the control medium, and suggests that the alkalotic perfusates and muscle may not have been in a steady state at the start of stimulation. In RALK, compared to C, there were no significant differences in the fluxes of Cl^- , K^+ and La^- ; however Na^+ influx was significantly reduced (2- to 3-fold), and the apparent NVA efflux was significantly greater. In MALK, compared to C, there were no significant differences in the fluxes of Cl^- and K^+ during stimulation (Fig. 20); however Na^+ influx and La^- and NVA effluxes were significantly greater than in C. In MALK compared to RALK, the net flux of Na^+ and Cl^- from perfusate to muscle was significantly greater, while the fluxes of K^+ , La^- and NVA from muscle to venous perfusate were similar in both alkalotic conditions.

154

The total change in strong ions and NVA during 5 min of electrical stimulation in RALK and MALK, relative to that of C, are summarized and compared in Fig. 21. With RALK, the fluxes of Na^+ and Cl^- from perfusate to muscle were reduced compared to C, while the fluxes of La^- and NVA were significantly greater in RALK than in C. In MALK, however, the fluxes of Na^+ and Cl^- from perfusate to muscle were significantly greater than both C and RALK; and the fluxes of K^+ and La^- from muscle were significantly greater than in both C and RALK. The apparent fluxes of NVA in both alkalotic conditions were similar, and were both significantly greater than in C.

5.3.4 Relationships Between Lactate and NVA

In all conditions the rate of appearance of NVA in venous plasma of stimulated muscle exceeded that of La^- (Fig. 21). In C, the ratio of NVA: La^- flux averaged 3.8, significantly lower than the ratios of 4.6 and 4.3 in RALK and MALK respectively. Since venous $[\text{La}^-]$ was significantly higher with alkalosis, the increase in NVA: La^- ratios were due solely to increased apparent fluxes of NVA in the alkalotic conditions.

The relationships between the maximum measured fluxes of La^- and NVA from stimulated hindlimb and arterial pH, $[\text{HCO}_3^-]$, $[\text{Na}^+]$ and $[\text{NVA}]$, in conditions ranging from metabolic and respiratory acidosis (data from Spriet et al. 1985b) to controls (Spriet et al. 1985b; Chapter 4; present study) to MALK and RALK, are shown in Figs. 22 and 23. In all studies the fluxes of La^- and NVA were maximal at 3-5 min of stimulation (see Fig. 20), and these values were used to describe the relationships. Only the

Fig. 21. A summary of the ion fluxes in the perfused rat hindlimb during 5 min of stimulation in RALK and MALK. Control fluxes (from Chapter 4) are indicated by the lightly shaded regions. A positive flux is representative of an uptake of ion by muscle while a negative flux is indicative of a release of ion from muscle. * indicates mean is significantly different from control; ** indicates MALK mean is significantly different from RALK mean.

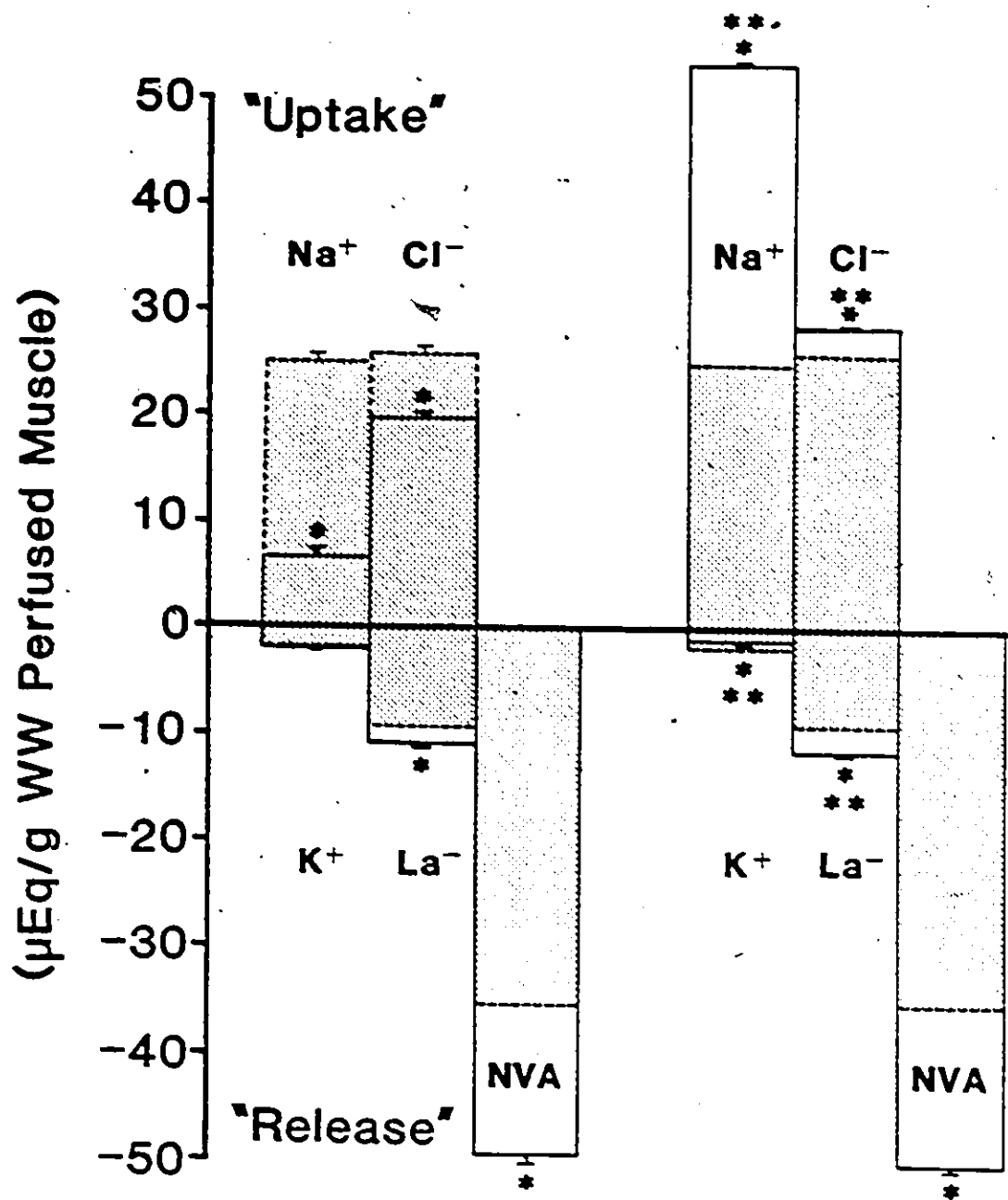


Fig. 22. The significant linear relationship ($p < 0.05$) between the net La^- flux and the apparent net flux of NVA during stimulation of the perfused rat hindlimb over the physiological range (pH 7.15 - 7.57; PCO_2 27 - 63 mmHg; $[\text{HCO}_3^-]$ 13 - 27 mEq/l) of arterial perfusate compositions. Data from Spriet et al. (1985b), Chapter 4, and the present study. The line of identity (La^- flux = NVA flux) is shown by the dashed line. MA = metabolic acidosis; RA = respiratory acidosis; C = controls; RK = respiratory alkalosis; MK = metabolic alkalosis.

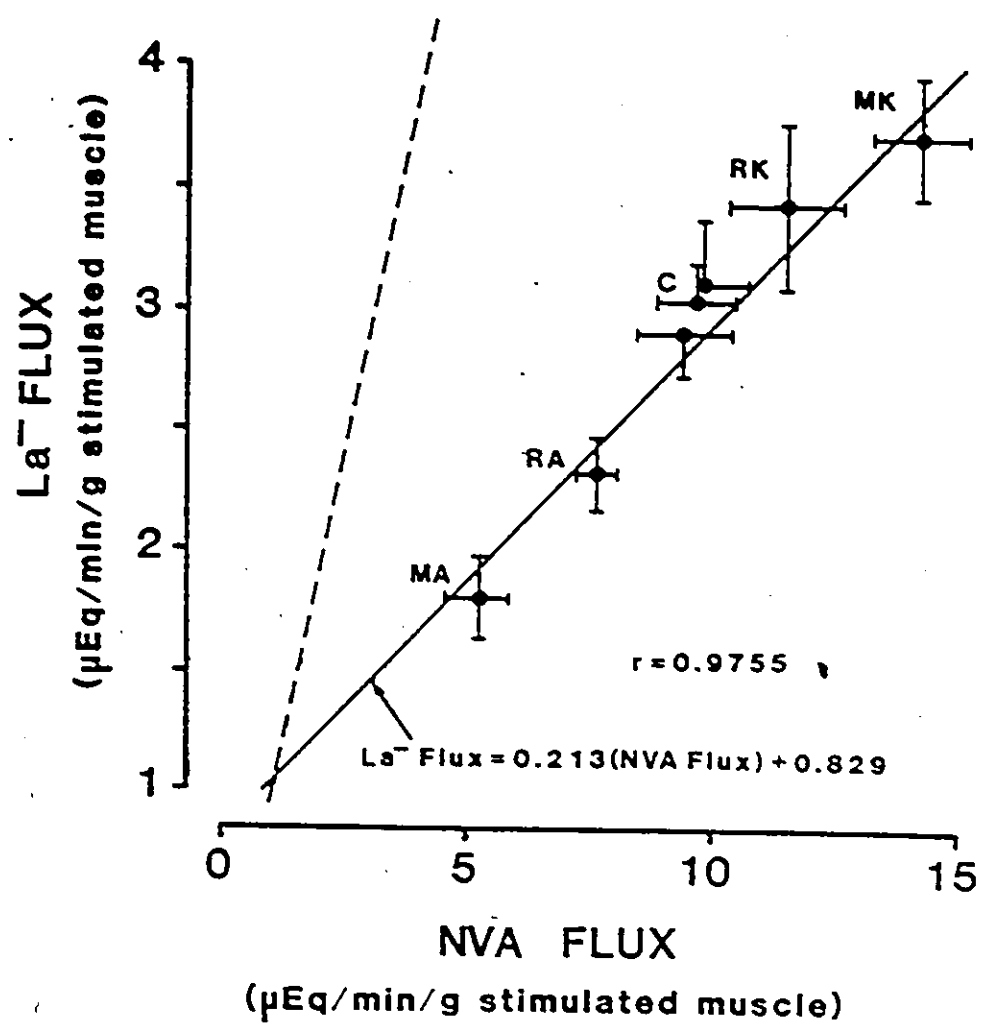
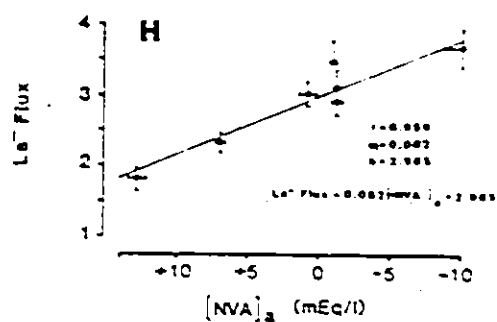
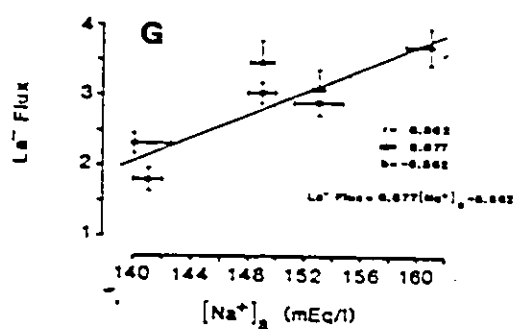
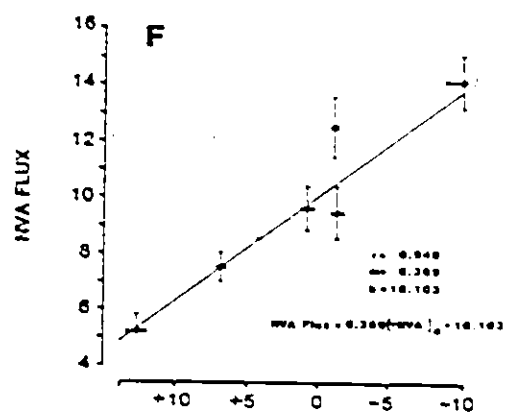
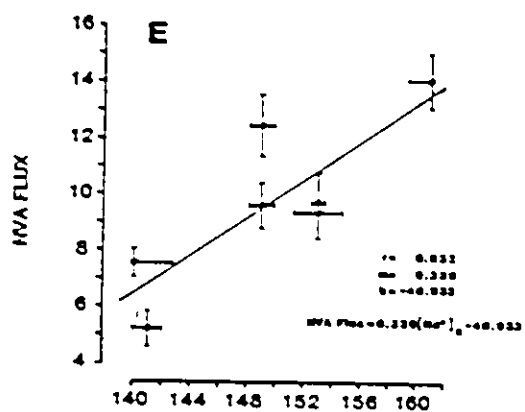
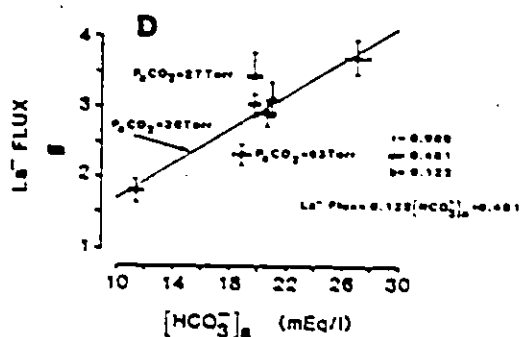
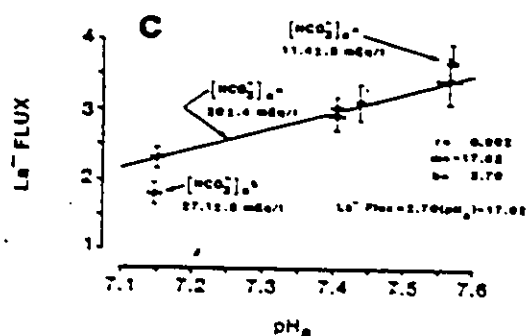
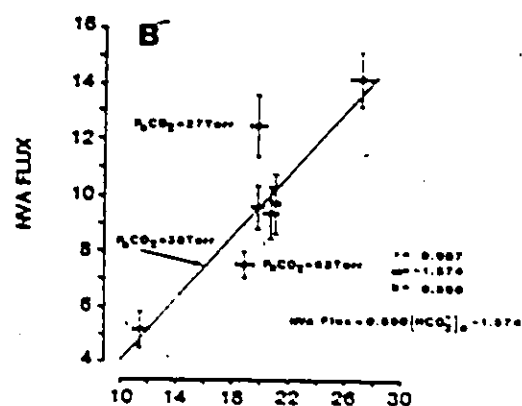
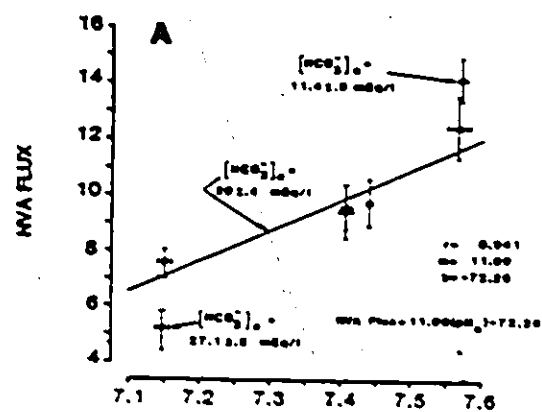


Fig. 23. The significant ($p < 0.05$) linear relationships between the apparent flux of NVA and the La^- flux with arterial perfusate pH , $[\text{HCO}_3^-]$, $[\text{Na}^+]$ and $[\text{NVA}]$ over the physiological spectrum of arterial perfusate compositions. The regression coefficient (r) and equation describing each relationship is given in the appropriate panel. Values for acidic perfusates (squares = metabolic acidosis; triangles = respiratory acidosis) are from Spriet et al. (1985b); alkalosis values (diamonds = respiratory alkalosis; stars = metabolic alkalosis) are from the present study; and control values (circles) are from Spriet et al. (1985b), Chapter 4, and the present study. In panels F and H, positive $[\text{NVA}]$ (to the left of 0 on the abscissa) represents acidotic perfusates, while negative $[\text{NVA}]$ (to the right of 0 on the abscissa) represents alkalotic perfusates.



mean maximal values (\pm standard error), from each different condition in each study, are indicated in the figures.

Analysis of the flux data from all of the above conditions showed that there was a significant linear relationship between the apparent NVA flux and the measured La^- flux (Fig. 22) during muscle stimulation. Furthermore, La^- and NVA fluxes increased linearly as a function of increasing arterial $[\text{Na}^+]_a$, $[\text{NVA}]_a$, $[\text{HCO}_3^-]_a$ and pH_a (Fig. 23); these relationships are all significant ($p < 0.05$) by least squares linear regression. The order of increasing efflux of La^- and NVA from exercising muscle is metabolic acidosis < respiratory acidosis < C < RALK < MALK.

5.3.5 Muscle Fluid and Ion Fluxes

During perfusion of resting muscle, both alkalotic media resulted in significant increases in TTW (7%-12%), and in the intracellular contents of Na^+ (110%-170%) and Cl^- (35%-400%). Intracellular La^- and total Ca^{++} contents were increased in RALK but not in MALK (Table 21). The increases in TTW, Na^+ and Cl^- contents were significantly greater than in C. For the C group (control rest, rest perfused and stimulated perfused), values for muscle total tissue water and intracellular ion contents are presented in Appendix C.

Electrical stimulation resulted in further significant increases (from perfused resting values) in TTW (6%-7%) of RG, PL and WG in both RALK and MALK (Table 21). La^- content increased significantly above rest perfused values in all muscles in all conditions (Table 21) as described above (Fig. 18). Intracellular, K^+ contents were significantly reduced by 7%-17% in RG, PL and WG,

whereas intracellular Na^+ and Cl^- increased by 5%-70%. The smallest changes in intracellular ion contents during stimulation occurred in SL, whereas the greatest changes occurred on PL and WG. Stimulation also resulted in small decrements in total intracellular Mg^{++} and produced variable changes in total intracellular Ca^{++} .

The exercise-induced changes in intramuscular strong ions during 5 min of electrical stimulation are summarized and compared in Fig. 24. Compared to controls, the main findings are that MALK and RALK resulted in significantly less La^- accumulation in all muscles, and there was significantly less K^+ and Mg^{++} depletion in all muscles in both RALK and MALK. As shown in Chapter 4 and Appendix C, the increase in La^- and the reduction in K^+ contents accounted for over 90% of the decrease in SID content during stimulation. The significantly reduced K^+ and Mg^{++} depletions, and significantly reduced La^- accumulations in alkalotic muscles (Table 21) compared to C (Appendix C), accounted for the significantly lower reduction of SID content with alkalosis (comparisons summarized in Fig. 24).

The major differences between RALK and MALK during stimulation were increased Na^+ and Cl^- influx to SL with MALK, while Na^+ and Cl^- influx to other muscles was less with MALK (Table 21; Fig. 24). In the fast-twitch muscles (PL and WG) K^+ depletion was less with MALK than with RALK, this difference was highly significant in WG. La^- accumulation was significantly less only in PL with MALK compared to RALK. Mg^{++} depletion in slow twitch muscles (SL and RG) was significantly greater with MALK than with RALK, while in PL and WG the degree of Mg^{++} depletion tended to be

TABLE 21

Muscle total tissue water (TTW, ml/g dry wt) and strong ion contents ($\mu\text{equiv/g dry wt}$) in right hindlimb muscles before perfusion (Control Rest), after 20 min rest perfusion (RP) of the left hindlimb, and after 20 min rest perfusion followed with 5 min tetanic electrical stimulation (STIM) of the left hindlimb in conditions of respiratory (RAIK) and metabolic alkalosis (MALK).

a RP mean significantly different from control RP mean (from Table C-5).

b, MALK-RP mean significantly different from RALK-RP mean.

c STIM mean significantly different from control stim mean (from Table C-5).

d MALK-STIM mean significantly different from RALK-STIM mean.

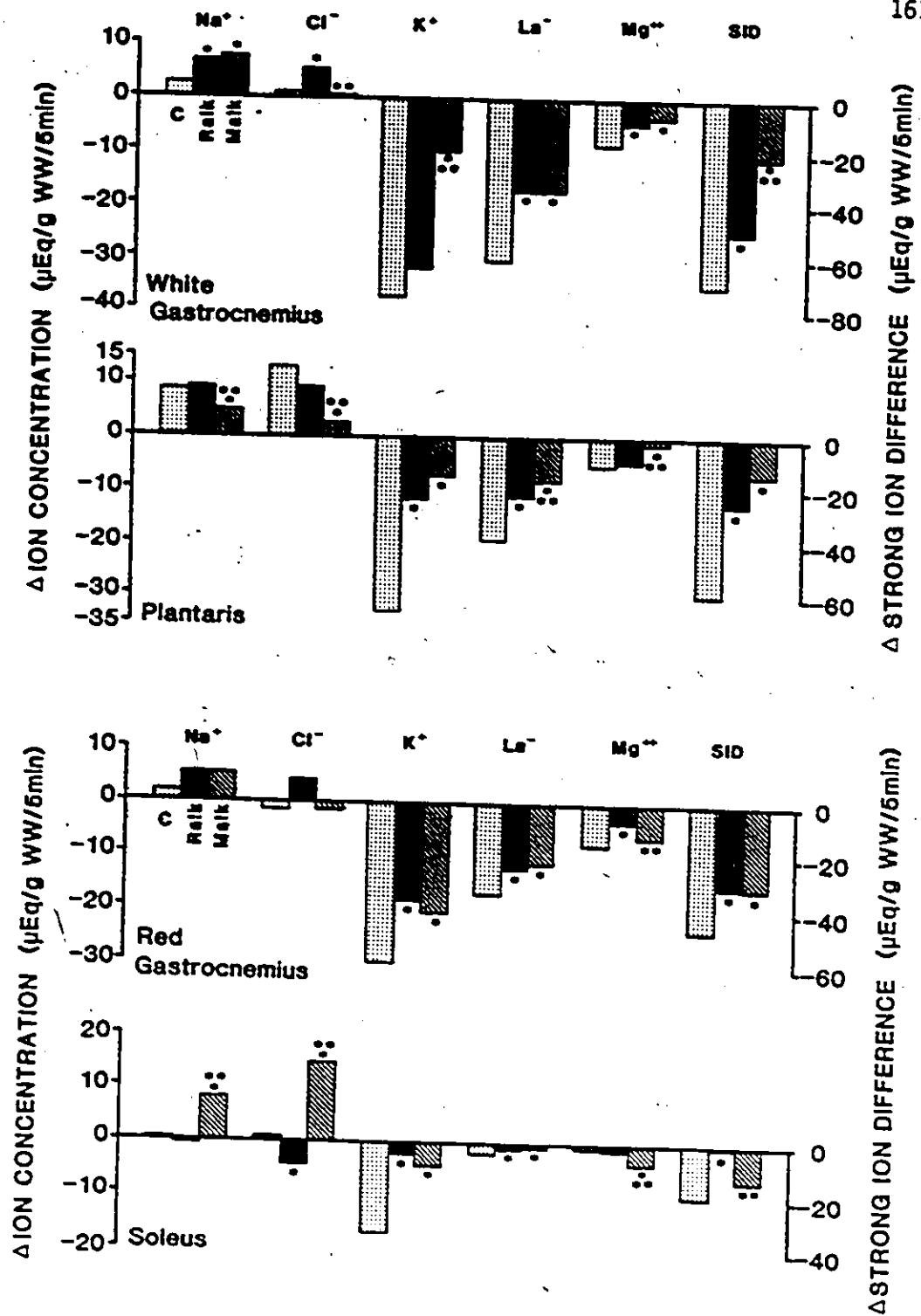
TABLE 21

Muscle/	Condition	TTW	La-	K+	Na+	Cl-	Mg++	Ca++
SOLEUS								
	Control Rest (n=13)	3.80 ± .09	5.08 ± 0.87	333 ± 8	69.2 ± 7.2	49.7 ± 6.1	66.1 ± 2.4	8.1 ± 0.6
	RAIK-RP (n=6)	4.25 ± .20	6.07 ± 0.69	282 ± 14	187 ± 30	182 ± 15	72.6 ± 4.8	16.0 ± 1.3
	RAIK-STIM (n=9)	4.55 ± .26	10.77 ± 1.62 ^C	295 ± 16	196 ± 28	170 ± 15	69.8 ± 7.6	13.1 ± 2.0
	HALK-RP (n=6)	4.06 ± .14	3.82 ± 0.68 ^{ab}	323 ± 12 ^b	136 ± 17	67.0 ± 15.7 ^b	66.7 ± 8.2	6.9 ± 1.5
	HALK-STIM (n=13)	4.30 ± .40	9.22 ± 2.12 ^C	315 ± 12	186 ± 16	151 ± 13	49.7 ± 6.7	10.8 ± 1.3
RED GASTROCNEMIUS								
	Control Rest (n=13)	3.47 ± .07	5.32 ± 1.16	365 ± 11	27.8 ± 4.4	22.9 ± 3.3	78.5 ± 2.3	8.0 ± 0.6
	RAIK-RP (n=6)	4.00 ± .20	8.00 ± 1.38	388 ± 16	108 ± 31	87.9 ± 25.6	90.8 ± 5.8	12.4 ± 1.2
	RAIK-STIM (n=9)	4.44 ± .29	70.5 ± 8.2	323 ± 18	147 ± 10	119 ± 12	82.0 ± 6.7	16.7 ± 2.3
	HALK-RP (n=6)	3.59 ± .23	3.25 ± 0.79 ^{ab}	383 ± 14	96.6 ± 15.8	67.7 ± 8.6	85.9 ± 4.7	9.4 ± 1.0
	HALK-STIM (n=13)	4.27 ± .12	65.8 ± 9.1	326 ± 14	138 ± 14	77.3 ± 9.9 ^d	65.1 ± 6.7	7.0 ± 1.0

TABLE 21

Muscle/	Condition	TTW	La-	K+	Na+	Cl-	Hg++	Ca++
PLANTARIS								
	Control Rest (n=13)	3.37 ± .06	4.86 ± 0.69	378 ± 7	27.4 ± 3.7	15.2 ± 1.4	79.4 ± 3.9	8.9 ± 0.5
	RALK-RP (n=6)	3.77 ± .19	6.80 ± 0.59	365 ± 15	91.6 ± 11.3	76.9 ± 8.1 ^C	94.2 ± 4.7	12.4 ± 1.7
	RALK-STIM (n=9)	4.17 ± .14	62.5 ± 3.6 ^C	335 ± 9	147 ± 17	132 ± 13	77.4 ± 7.9	11.7 ± 1.1
	HALK-RP (n=6)	3.71 ± .18	4.18 ± 0.83 ^b	367 ± 19	103 ± 18	70.1 ± 6.6	69.6 ± 5.8 ^b	8.7 ± 1.5
	HALK-STIM (n=13)	3.90 ± .11	48.6 ± 8.4 ^C	341 ± 14	129 ± 14	84.7 ± 13.8 ^d	65.0 ± 6.6	7.3 ± 0.5
WHITE GASTROCNEMIUS								
	Control Rest (n=13)	3.27 ± .19	5.55 ± 1.01	400 ± 9	23.1 ± 4.3	14.0 ± 1.5	86.4 ± 2.8	8.9 ± 0.4
	RALK-RP (n=6)	3.36 ± .12	10.1 ± 1.9	440 ± 9	71.9 ± 15.1	61.0 ± 12.6	94.0 ± 6.1	10.3 ± 0.8
	RALK-STIM (n=9)	4.25 ± .17	100.5 ± 7.6 ^C	355 ± 24	120 ± 17	99.5 ± 13.9	87.1 ± 8.8	10.7 ± 1.5
	HALK-RP (n=6)	3.51 ± .15	4.48 ± 0.53 ^{ab}	380 ± 16 ^b	60.3 ± 16.1	63.9 ± 11.3	83.9 ± 7.5	8.0 ± 1.4
	HALK-STIM (n=13)	4.05 ± .10	94.8 ± 7.3 ^C	369 ± 16	105 ± 14	72.8 ± 11.5	75.0 ± 5.7	7.5 ± 0.8

Fig. 24. The change in intracellular contents of strong ions and SID expressed as fluxes in perfused rat hindlimb muscles during 5 min of stimulation. Control fluxes (C, light shading) are from Chapter 4. * indicates mean is significantly different from control; ** indicates MALK mean is significantly different from RALK mean.



reduced in MALK, compared to RALK. The reduction in SID content of WC with MALK was significantly less than with RALK (Fig. 20A), the change in SID of PL and RG was similar in both alkalotic conditions (Fig. 20B & C), while in SL the reduction in SID was significantly greater with MALK than with RALK (Fig. 20D).

5.4 DISCUSSION

The present study demonstrated that alkalosis did not significantly affect hindlimb tension generation during stimulation. Muscle glycolysis and La^- production in alkalosis were not significantly different from controls, but alkalotic hindlimb muscles accumulated significantly less La^- , and released significantly more La^- than controls. The highest rates of La^- and NVA efflux from muscle was observed in MALK (Figs. 20 & 21); La^- efflux rate in MALK and RALK exceeded that of controls by 25% and 17%, while NVA efflux in MALK and RALK averaged 40% and 45% greater than in C, respectively.

5.4.1 Ion Fluxes in Resting Muscle

During perfusion of resting muscle, the elevated ion flux rates in the alkalotic conditions, compared to C, was most likely associated with the initial large imbalance in perfusate to muscle ion concentration differences compared to rat blood or control perfusate (Table 19). Evidently, 20 min of perfusion may not have allowed time for the establishment of a new steady state between muscle and blood with MALK. The relative small magnitude of these fluxes in resting versus stimulated muscle should not seriously alter the interpretation of the results. Particularly in MALK, perfusate fluxes of Na^+ and

Cl^- reflect the large increases in the intracellular contents of these ions in all muscles (Table 21).

5.4.2 Ionic Changes in Stimulated Muscle

Five min of electrical stimulation resulted in reductions in venous plasma volume, pH, $[\text{Na}^+]$, $[\text{Cl}^-]$ and $[\text{SID}]$ and increases in venous $[\text{La}^-]$, $[\text{K}^+]$ and $[\text{NVA}]$ (Figs. 19-21). The corresponding changes in muscle were increased TTW, increased contents of La^- , Na^+ and Cl^- , and reduced contents of K^+ and SID (Table 21; Fig. 24). These changes are characteristic of contracting muscle under a variety of conditions (Tibes et al. 1977; Sjogaard et al. 1985; Appendix C).

In the present study, exercise-induced intracellular K^+ depletion was significantly reduced in alkalotic conditions compared to controls (Table 21; Fig. 24). Similar findings have been reported in superfused frog sartorius muscles following stimulation (Mainwood and Lucier 1972). In the present study muscle K^+ depletion was associated with only a 0.35 mEq/l increase in venous plasma $[\text{K}^+]$ compared to the 0.53 mEq/l change seen in controls.

During perfusion with alkalotic media, the combined effects of reduced intracellular K^+ depletion and reduced intracellular La^- accumulation in exercising muscle was responsible for a significant reduction in the exercise-induced decrease in SID , compared to controls (Fig. 24). Estimates of the intracellular concentrations of dependent variables from intracellular contents of strong ions cannot readily be made in this study because intracellular fluid volumes (ICFV) of the alkalotic muscles were not determined. However, based on the effects of changes in intramuscular $[\text{SID}]$ on the

concentrations of the intracellular dependent variables presented in Chapters 3 and 4, the significantly reduced decrement in SID content of stimulated alkalotic muscles must be associated with a smaller increase in intracellular $[H^+]$. In stimulated WG, assuming that the ICFV changed to the same extent in MALK as in C (Table 11), then the change in $[SID]_i$ in MALK (estimated as $130-100-30$ mEq/l) is calculated to reduce intracellular pH by 0.20 units; this is much less than the 0.36 pH unit decrease calculated for control WG (Table 11).

5.4.3 Mechanism for Trans-Sarcolemmal La^- Efflux

Intramuscular La^- accumulation results when the rate of glycolytic pyruvate production exceeds the rate of pyruvate oxidation (Fig. 1). Therefore, regulation of intracellular $[La^-]$ in exercising muscle requires that: (1) La^- production is reduced; (2) La^- oxidation is increased; or that La^- be transported from the intracellular to the extracellular fluids. Lactate elimination during heavy exercise consists primarily of transport across the sarcolemma into the ECF (Hermansen & Vaage 1977; Astrand et al. 1986).

The enhanced flux of La^- from perfused stimulated muscles with alkalosis in the present study confirms previous work suggesting that alkalosis increases the rate of La^- release from superfused frog muscle (Mainwood et al. 1972; Seo 1984), in perfused dog hindlimb (Hirche et al. 1975) and in man (Jones et al. 1977; Kowalchuk et al. 1984; Davies et al. 1986). In the present study, reductions in glycogen contents were similar in the three conditions, but alkalosis was associated with less accumulation of La^- , and total La^- release was increased (Table 22). Total hindlimb La^- release increased from 38% of total La^- production in C, to 48% in RALK and

TABLE 22

Lactate released from muscle, muscle lactate, and total lactate produced during 5 min of stimulation.

	Lactate released	Muscle lactate	Total lactate
C	54.2 (38.3)	87.4 (61.7)	141.6
MALK	74.3 (54.6)	61.9 (45.4)	136.2
RALK	68.6 (47.6)	75.4 (52.4)	144.0

Units: $\mu\text{mol/hindlimb per 5 min}$; calculated from group means. Bracketed values are percent of total lactate produced in each condition. Assumptions: plantaris muscle represents nonsampled working muscle (see Table C-2); nonworking muscle involvement was constant throughout stimulation; lactate metabolized was minimal due to single-pass perfusion. Definitions as in Table 20.

55% in MALK (Table 22); this effect was greatest in highly glycolytic (WG and PL) muscles than in primarily oxidative (SL and RG) muscles (Fig. 24). In a study of imposed acidosis (Spriet et al. 1985b) the opposite effect was seen, with a greater reduction in La^- release being found in metabolic acidosis (MA) than in respiratory acidosis (RA).

The rate of La^- efflux from muscle during exercise in the stimulated perfused rat hindlimb is significantly correlated with the arterial composition of the perfusate (Fig. 23). In this context it must be remembered that the arterial PaCO_2 , $[\text{A}_{\text{TOT}}]_{\text{a}}$ and $[\text{SID}]_{\text{a}}$ determine the $[\text{H}^+]_{\text{a}}$, $[\text{HCO}_3^-]_{\text{a}}$, and $[\text{NVA}]_{\text{a}}$ composition of the arterial perfusate. In the metabolic disturbances the changes in the dependent variables are caused by changes in $[\text{SID}]$ primarily due to altered $[\text{Na}^+]_{\text{a}}$. In the respiratory disturbances, the changes in the dependent variables result from the change in PCO_2 . Increased rates of La^- efflux, in the stimulated perfused rat hindlimb preparation, are associated with increased pH_{a} (Fig. 23C), increased $[\text{HCO}_3^-]_{\text{a}}$ (Fig. 23D), increased $[\text{Na}^+]_{\text{a}}$ (Fig. 23G) and decreased $[\text{NVA}]_{\text{a}}$ (Fig. 23H). A 1.0 mEq/l increase in $[\text{HCO}_3^-]_{\text{a}}$ was associated with a 7.2% increase in La^- (Fig. 23D), and a 1.0 mEq/l increase in $[\text{Na}^+]_{\text{a}}$ or $[\text{NVA}]_{\text{a}}$ was associated with a 3.6% increase in La^- efflux (Fig. 23G & H). These findings are supported by previous work using a number of muscle preparations which have described the La^- flux in terms of the $[\text{H}^+]_{\text{a}}$ or $[\text{HCO}_3^-]_{\text{a}}$ (both dependent variables) of the blood (Mainwood et al. 1972; Hirche et al. 1975; Sutton et al. 1981; Seo 1984; Davies et al. 1986). The results presented in Fig. 23, and by other

investigators, cannot be used to determine cause-and-effect relationships unless the La^- efflux is plotted against an independent variable such as $[\text{Na}^+]$. In the present study, La^- efflux was increased 12.6% by changes in independent variables which caused a 0.1 unit increase in ECF pH (Table 19), a finding consistent with that of Mainwood & Worsley-Brown (1975) in frog sartorius.

Relatively small changes in arterial ion concentrations are capable of evoking relatively large changes in La^- efflux rates. These findings are supportive for primarily ionic mechanisms of La^- efflux (Benade & Heisler 1978; Hultman et al. 1985). The close association between La^- efflux and arterial pH (Fig. 23C) suggests that La^- flux across the sarcolemma may be sensitive to altered conformation of ionizable groups at ionic La^- -transporting sites (Kuret et al. 1986). Further evidence for a primarily ionic mechanism for trans-sarcolemmal La^- flux is provided by the finding that 4-acetamido-4'-isothiocyanostilbene-2,2'-disulfonic acid (SITS) inhibits the influx of La^- into perfused rat hindlimb muscles by about 30% (Kuret et al. 1986). This ~~was~~ suggestive of a $\text{La}^-/\text{HCO}_3^-$ or La^-/Cl^- exchange, or that the La^- flux is coupled to the $\text{Cl}^-/\text{HCO}_3^-$ exchanger (Aickin & Thomas 1977) of mammalian skeletal muscle.

The results of the alkalotic and acidotic rat hindlimb perfusion studies suggest that ionic disturbances, i.e. altered $[\text{HCO}_3^-]$, $[\text{OH}^-]$ and $[\text{H}^+]$, associated with changes in perfusate PCO_2 (RA, RALK) also exert a powerful effect on La^- flux (Fig. 23D). Increasing the PCO_2 from 27 mmHg to 63 mmHg, at constant $[\text{HCO}_3^-]$, is associated with a 30% reduction in La^-

efflux from stimulated perfused rat hindlimb. This suggests that changes in PCO_2 , through alteration of the concentrations of extra- and intracellular dependent variables may also affect carrier-mediated ionic transport process. The movement of La^- out of muscle may also be partially due to the electroneutral diffusion of undissociated $H^+ + La^-$ across the cell membrane, secondary to ion-induced changes in membrane conductance to La^- and other ions.

5.4.4 NVA Flux from Muscle

The appearance of NVA in the extracellular fluids results from the apparent addition of strong acid anion to the blood. Similar to the La^- fluxes, the apparent efflux of NVA from stimulated perfused rat hindlimb increases with increasing pHa (Fig. 23A) and increasing $PaCO_2$ (Fig. 23B) at constant $[HCO_3^-]_a$, and NVA flux increases with increasing plasma $[Na^+]_a$ and whole blood $[NVA]_a$ (Fig. 23E & F). There was a highly significant correlation between La^- flux and the NVA flux (Fig. 23), with the La^- flux into plasma accounting for 21% of the NVA flux into whole blood. This discrepancy strongly suggests that the red blood cells may be responsible for removing La^- from plasma in exchange for another strong anion such as Cl^- , or in cotransport with a strong cation such as K^+ , as has been demonstrated in humans (Appendix D).

Theoretically, exercise-induced changes in venous whole blood $[NVA]$ must be due to the combined effects of La^- (and/or other strong anion) fluxes from, and of Na^+ (and/or other strong cation) into, inactive tissues such as nonworking muscle and red blood cells. The directions of these fluxes would cause an increase the apparent quantity of strong acid anion added to the blood. The magnitudes of

these fluxes, in alkalosis, are indicated in Figs. 20 and 21. In MALK, the magnitudes of the Na^+ influx and La^- efflux can fully account for the apparent NVA flux (Fig. 21); however in RALK these fluxes account for only 36% of the NVA flux. In RALK, the unaccounted 74% of the NVA flux may be partially accounted for by an uptake of La^- by inactive tissues (erythrocytes, non-contracting muscle; Appendix D) and balanced by the release of other strong acid anions such as Cl^- . The rate of Cl^- uptake in RALK was significantly lower than in C (Fig. 21), indicating that Cl^- may have been released, relative to controls. If Cl^- was simply not taken up to the same extent in RALK as in C, then the reduced Cl^- flux in RALK accounted for a further 22% of the NVA flux; if, on the other hand, Cl^- was exchanged for La^- then an additional 22% of the NVA flux can be accounted for.

5.4.5 Intracellular Ion Regulation During Exercise

Several mechanisms have been suggested for the apparent "regulation of intracellular pH" in muscle and other tissues. Most mechanisms require the trans-membrane movements of strong ions in exchange for a weak ion of the same charge, or with an ion of opposite charge. For example, "regulation" of pH_i in acid-loaded muscle cells requires external HCO_3^- (Aickin and Thomas 1977; Boron 1977; Boron et al. 1978) and Na^+ (Aickin and Thomas 1977; Boron et al. 1981) and internal Cl^- (Boron et al. 1978). The apparent stoichiometry for these ion fluxes appears to be about 2 H^+ "neutralized" for 1 Na^+ entering, and 1 Cl^- leaving, the cell (Boos and Boron 1981). There is, at the present time, no direct evidence that pH_i is regulated, or even that it should be

regulated, because there is no evidence which can demonstrate an exclusively $[H^+]$ -dependent response within a physico-chemical system. As Stewart (1981; 1983) has pointed out, a number of simultaneous changes in the ionic status of a solution must simultaneously occur to cause a change in $[H^+]$, and one of more of these simultaneous changes could just as easily be responsible for the apparent "pH effect".

$[H^+]$ is dependent on [SID] (Stewart 1981; 1983), therefore trans-sarcolemmal movements of strong ions are expected to affect the $[H^+]$ of both the extra- and intracellular fluids within muscle. During MALK, arterial ECF [SID] is reduced by the addition of the strong base cation Na^+ to the plasma (Table 19); in turn Na^+ leaves the ECF and enters the ICF as a new equilibrium for Na^+ is established (Table 21). During perfusion of the resting muscles with media made alkalotic by increasing $[Na^+]_a$, the $[H^+]$ of the venous plasma should increase as venous [SID] is reduced (Na^+ uptake by muscles), and the $[H^+]$ of the ICF should be reduced as intracellular [SID] is increased. During exercise, the venous [SID] is reduced by the addition of La^- to, and the removal of Na^+ from, the arterial capillary plasma; the resultant decrease in [SID] of the ECF and an increase in [SID] of the ICF causes an increase in $[H^+]$ of the ECF, while the $[H^+]$ of the ICF is reduced. The direction of strong ion fluxes during exercise therefore appear to reduce the increment in intracellular $[H^+]$ at the expense of the ECF.

5.4.6 Muscle Performance and Metabolism

In the present study, coincident with the lack of effect of alkalosis on force production during 5 min of stimulation, O_2

TABLE 23

Energy released from the hindlimb during 5 min of stimulation.

Energy released (joules) as a function of:					
	oxygen	lactate	CP	total	percent
	consumed	produced	utilized	energy	of
				released	C energy
C	36.8	12.7	3.8	53.3	
	(69.1)	(23.8)	(7.1)		
MALK	37.0	12.3	4.1	53.4	100.2
	(69.3)	(23.0)	(7.7)		
RALK	34.9	13.0	3.8	51.7	97.0
	(67.5)	(25.1)	(7.4)		

C, control (n = 11); MALK, metabolic alkalosis (n = 12);
 RALK, respiratory alkalosis (n = 9). Values are per stimulated
 hindlimb and calculated from group means of oxygen utilization,
 creatine phosphate (CP) utilization, and lactate production.
 Bracketed values are percent of total energy released in each condition.
 Calculations based on 1.0 ml oxygen = 20.9 joules, 1.0 mg lactate =
 1.0 joules, and 1.0 umol CP = 0.05 joules (Margaria 1976).
 Assumptions: calculations based on oxygen and CP utilized and lactate
 produced above resting values; oxygen uptake reaches maximal values
 instantly; plantaris muscle represents nonsampled working muscle;
 nonworking muscle involvement constant throughout stimulation;
 efficiency of energy releasing pathways unchanged by alkalosis;
 lactate metabolized was minimal due to single-pass perfusion system.

uptake and metabolic fuel utilization were found to be similar in all three conditions, with 25% of the total energy production being accounted for by anaerobic glycolysis (Table 23). Steinhagen et al. (1976) also reported that MALK had no effect on force production during 12 min of intense isotonic exercise in blood-perfused dog gastrocnemius muscle. Several studies of humans exercising maximally for less than 2 min have also shown that alkalosis has a minimal effect on maximum power output and endurance (McCartney et al. 1983; Katz et al. 1984; Kowalchuk et al. 1984).

In contrast, perfusion of the stimulated hindlimb with acidotic media resulted in reductions in muscle glycogen utilization and La^- accumulation as well as a reduced rate of La^- efflux from contracting muscles (Spriet et al. 1985b). Skeletal muscle pH_i has been shown to increase by 0.07 pH unit for each 0.10 pH unit increase in extracellular pH during perfusion with alkalotic media (Burnell 1968; Heisler 1975). The similar rates of glycolysis and of La^- production under the present alkalotic conditions support in vitro work showing that key regulatory enzymes are less susceptible to changes in activity caused by factors associated with decreased intracellular $[\text{H}^+]$ than with increased $[\text{H}^+]$ (Gevers and Dowdle 1963; Danforth 1964; Trivedi and Danforth 1966).

There is agreement that alkalosis is associated with an increased rate of appearance of La^- in plasma. However, there is controversy as to whether the increase in plasma $[\text{La}^-]$ is due to an increase in the rate of glycolysis or to an increase in the rate of La^- release from muscle (Sutton et al. 1981; Katz et al. 1984; Davies et al. 1986). Previous studies of induced extracellular

alkalosis in humans also reported an increase in the appearance of plasma La^- during exercise (McCartney et al. 1983; Katz et al. 1984; Davies et al. 1986), but intramuscular $[\text{La}^-]$ was not measured. In the present study, $[\text{La}^-]$ in venous perfusate was also greater during exercise in the alkalotic conditions, but muscle La^- accumulation was lower, and the total La^- production was similar in all conditions (Table 22). Glycogen utilization was also similar (Fig. 18), indicating that approximately 90% of the glycogen degraded was metabolized anaerobically in each condition. This suggests that alkalosis has little effect on glycolytic rate during exercise conditions where glycolysis is maximally or near-maximally stimulated, and that the increase in plasma $[\text{La}^-]$ during alkalosis is due to an increased rate of La^- release from muscle.

Acidosis was associated with an increased rate of muscle fatigue in this preparation (Spriet et al. 1985b), and it was expected that alkalosis might increase initial force output or reduce the rate of muscle fatigue. The fact that it did not (Fig. 15) may have been due to a lack of effect on rate limiting enzymes or to non-metabolic factors. At the high stimulation rates used in the studies, failure of force generation may have been due to maximal recruitment of motor units or maximal transmission of action potentials. If the mechanisms involved in excitation-contraction coupling were maximally activated, a change in intracellular ionic status would not be expected to improve performance.

There appear to be two opposing forces responsible for the lack of observable differences in muscle metabolism and performance in alkalosis. The first effect, which was expected to be stimulatory with

respect to muscle performance, involved the intracellular alkalosis resulting from the accumulation of strong basic cation (Na^+) within the resting muscle perfused with alkalotic medium (Table 21). As mentioned in Chapter 3, the resulting increase in intracellular $[\text{SID}]_i$ in the resting perfused muscle should exert a 'protective' effect against large changes in $[\text{H}^+]_i$ and protein ionization state. The opposing force is the negative allosteric effect that increased intracellular $[\text{Na}^+]_i$ may exert on key regulatory enzymes of glycolysis thus, in alkalosis, glycolytic flux may have been impaired.

With muscle stimulation, the reduction in intracellular $[\text{SID}]_i$ responsible for the increase in $[\text{H}^+]_i$ during high intensity exercise, was associated with a significant decrease in $[\text{K}^+]_i$ and a significant increase in $[\text{Na}^+]_i$ (Chapters 3 and 4). Two key regulatory glycolytic enzymes, pyruvate kinase and phosphofructokinase, require 150 mEq/l $[\text{K}^+]_i$ for maximal activation in vitro (Kachmar and Boyer 1953; Paetkau and Lardy 1967). Furthermore, the activity of at least one of the enzymes (pyruvate kinase) is significantly inhibited by increased $[\text{Na}^+]_i$. In vivo it was suggested that glycolysis may have been inhibited by about 20% due to reduced $[\text{K}^+]_i$ during intense swimming exercise, since in that study there were no significant increases in $[\text{Na}^+]_i$ (Chapter 3). In the isolated hindlimb preparation (Chapter 4), however, stimulation was associated with significant increases in intracellular $[\text{Na}^+]_i$, and these increases were even more pronounced in the present study (Table 21; Fig. 24). Therefore, in alkalosis, it is possible that the reduced glycogen utilization may be due to inhibition of glycolysis by high $[\text{Na}^+]_i$. The effect of reduced activities of regulatory enzymes may

be due to alterations in protein conformation or of electrostatic interactions between enzymes and substrate, product, activators or inhibitors (Nakashima and Tuboi 1976; Woodbury 1974). Changes in $[SID]_i$ have a marked effect on the ionized concentrations ($[A^-]$ and $[HA]$) of intracellular weak acids, indicative of alterations in the ionization state of intracellular proteins (Chapter 3). Therefore, in the present study, the large increase in $[Na^+]_i$ during perfusion with alkalotic media may have negated any beneficial effect that the increased $[SID]_i$ may have on minimizing the exercise-induced changes in the concentrations of other dependent variables. On the other hand, it is also possible that glycolysis was maximally activated by stimulation under control conditions (C) and could not be increased further by alkalosis.

In some situations, alkalization of the body fluids has been reported to protect against exercise-induced acidosis (Wilkes et al. 1983). In a recent study, Costill et al. (1984) examined the effects of alkalosis on repeated bouts of maximal exercise and reported that endurance was enhanced during the fifth work bout performed to exhaustion when muscle pH prior to the bout was higher than during the control. Also, during exercise at 95% of VO_{2max} , endurance capacity is increased by sodium bicarbonate ingestion (Jones et al. 1977; Sutton et al. 1981). The beneficial effects of alkalosis in this situation may be explained, at least in part, by the effects of Na^+ ingestion on increasing the $[SID]$ of extra- and intracellular body fluids; any increase in plasma $[HCO_3^-]$ are rapidly corrected by ventilation relative to the elevation in plasma $[Na^+]$. It was shown in Chapter 3 that an initially high $[SID]_i$ is associated with a

lower $[H^+]_i$, and that for a given fall in $[SID]_i$ with exercise the change in the ratio of $[A^-]:[HA]$ and in $[H^+]_i$ is much less than at low initial $[SID]_i$.

5.4.7 Summary and Conclusions

Initial tension development and muscle performance was not improved with alkalosis, since the rate of tension decline was identical in the three conditions. This result was not expected because performance was impaired with acidosis (Spriet et al. 1985b) and, in vivo, alkalosis has been associated with increased speed (Wilkes et al. 1983) and endurance (Jones et al. 1977; Sutton et al. 1981; Costill et al. 1984).

Intramuscular La^- accumulation in the control condition was 15-20% greater than in alkalotic conditions, suggesting that muscle La^- accumulation was not a major factor contributing to fatigue during alkalosis.

The rate of La^- efflux from stimulated muscle is enhanced under conditions of alkalosis; this contributes to the reduction in intracellular La^- accumulation.

The combination of reduced falls in $[K^+]_i$ and increased $[La^-]_i$ in alkalosis was responsible for a reduced fall in $[SID]_i$, thereby decreasing the effects of large falls of $[SID]$ on intracellular dependent variables.

Alkalosis, and particularly MALK, was associated with a large increase in $[Na^+]_i$, which not only contributed to increasing $[SID]_i$, but may have had an inhibitory effect on glycolytic enzymes.

Since the development of the pH electrode early in the 20th century, the measurement of pH by physiologists and biochemists has become a routine procedure, probably because it is relatively easy to measure. However, this ease of measurement may have falsely led investigators to conclude that many physiological and biochemical responses to events which changed pH were in fact 'pH-dependent'. Muscle fatigue, a prime example, has long been associated with an increase in intramuscular $[H^+]$, and many biochemical and physiological changes associated with impaired muscle performance have been interpreted as the 'result' of increased $[H^+]$. As pointed out by Stewart (1981; 1983), and in the preceeding chapters, one cannot change the $[H^+]$ of a solution independently of other changes; specifically, an alteration in the $[H^+]$ of a solution can only occur by changing one or more of the independent variables PCO_2 , $[A_{TOT}]$ and $[SID]$. Since these quantities are seldom reported, or even measured, it was (and still is) very convenient to measure the pH of an experimental solution and describe the events which occur in terms of a 'pH-dependency'. While a pH- or H^+ -dependency may in fact exist, one can not make such a conclusion because the factors responsible for the apparent 'pH-effect' have not been examined and themselves eliminated as causative agents. pH alone is a relatively unimportant physico-chemical measurement, but it is a useful indicator of the ionic status of a solution when measurements of at least two of the independent variables are also made.

In the future much research will have to be conducted to bridge the gap between apparent pH effects and our new realization of biochemical and physiological cause-and-effect relationships. It will be convenient to continue to measure and report pH, but all of the variables responsible for, and associated with, pH must also be reported. Experimental results must be interpreted with respect to changes in the independent variables, for any one of several combinations of changes in these variables can produce a given pH, $[H^+]$, $[HCO_3^-]$ or $[A^-]$.

6.2 Inter-Relationships Between Ion Balance and Regulation of Skeletal Muscle Metabolism During Exercise

Moderate to intense exercise results in muscular fatigue. Several lines of recent evidence show conclusively that fatigue is associated with alterations of extra- and intracellular electrolyte status of muscle (Sjogaard et al. 1985; Heigenhauser et al. 1986). The present studies have demonstrated that changes in extra- and intracellular PCO_2 and in the relative concentrations of strong ions profoundly affect extra- and intracellular electrolyte status of muscle at rest and during exercise. The evidence suggests that the onset of fatigue may be delayed, and that fatigue during and following exercise may be ameliorated by critical regulatory adjustments of ionic status which are energy dependent. The onset of fatigue may be rapid, or the recovery from fatigue delayed, when energy supplies are severely limited.

The present studies have shown that intense muscular exercise, both in vivo and in vitro, caused an increased production and

release of CO_2 and La^- . Intense exercise was also associated with a 10%-30% reduction in $[\text{K}^+]_i$, 30%-120% increased $[\text{Na}^+]$ and $[\text{Cl}^-]$, and a substantial accumulation of intracellular La^- .

The relative contribution of exercise-induced increases in PCO_2 to changes in the concentrations of dependent variables has been shown to be minor (about 4%-15%) compared to the changes responsible for the reduction in $[\text{SID}]_i$; there were no changes in $[\text{A}_{\text{TOT}}]$. About 90% of the associated increase in $[\text{H}^+]_i$ was due to the decrease in $[\text{SID}]_i$. Theoretically, high PCO_2 in resting muscle ($[\text{A}_{\text{TOT}}]$ and $[\text{SID}]$ constant) results in an increase in $[\text{HCO}_3^-]_i$ (Fig. 4A), therefore the decrease in $[\text{HCO}_3^-]_i$ seen in exercise was due solely to the reduction of $[\text{SID}]_i$.

The two major contributors to the reduction in $[\text{SID}]_i$ during intense exercise were decreased $[\text{K}^+]_i$ and increased $[\text{La}^-]_i$. The increase in $[\text{La}^-]_i$ contributed 50%-80%, and the decrease in $[\text{K}^+]_i$ contributed 15%-45%, to the reduction in $[\text{SID}]_i$. The increases in $[\text{Na}^+]_i$ and $[\text{Cl}^-]_i$ during exercise nearly balanced each other, and in terms of their contributions to changing $[\text{SID}]_i$ they can conveniently be ignored. The potential effects of changes in $[\text{Na}^+]_i$ on the regulation of metabolism must, however, be kept in mind.

Exercise-induced reductions in $[\text{SID}]_i$ were responsible for a 2- to 4-fold decrease in the ratio $[\text{A}^-]:[\text{HA}]$, which represents the ionized state of intracellular proteins in solution -- contractile, enzymatic and structural. It is proposed that these large changes in $[\text{A}^-]:[\text{HA}]$ must be accompanied by small changes in protein structure which alter active site conformation, and hence protein function. In

the past, such conformational and functional changes were usually ascribed to direct effects of pH on the proteins (Woodbury 1974). Also, alterations of the ionic state of substrates, products, inhibitors and activators may also influence catalytic activity of the enzymes involved; the pH-related effects of Pi on phosphorylase activation (Chasiotis 1983) and on relaxation of contractile elements (Cooke and Pate (1985) provide good examples of these effects. In the next few paragraphs I will briefly outline some of the key processes in contracting skeletal muscle which may be affected by changes in the ionization state of proteins which have been demonstrated to be 'affected by changes in pH'.

Glycolytic rate is thought to be very closely associated with the rate of muscular contraction (Wilkie 1981); indeed, the initial regulation of glycogenolysis at the level of phosphorylase (Fig. 1) and the activities of contractile proteins are both modulated by variations in intracellular free $[Ca^{++}]$. The release of Ca^{++} from the sarcoplasmic reticulum into the sarcoplasm upon muscle cell stimulation resulting in actin-myosin crossbridge formation and muscular contraction. Phosphorylase, the flux-generating enzyme of glycogenolysis, is converted to the active 'a' form by Ca^{++} -activation of the enzyme phosphorylase kinase (Cohen 1981). Thus phosphorylase activity appears to increase simultaneous to formation and cycling of actin-myosin crossbridges. ATP, in the presence of myosin ATPase, is required for the release of actin-myosin crossbridges. Therefore, at times of maximal muscular contraction, ATP derived from the stimulation of glycogenolysis is able to contribute to the energy supply of the muscle.

Several of the contractile proteins and enzymes are 'pH-sensitive' and probably undergo conformational changes in conditions which cause a reduction in pH. A decrease in pH has been associated with reduced activities enzymes of these enzymes and proteins involved in excitation-contraction coupling: (1) the Ca^{++} -ATPase responsible for pumping Ca^{++} from the sarcoplasm at the initiation of the relaxation cycle (Fabiato and Fabiato 1978; Gonzalez-Serratos et al. 1978; Fitts et al. 1982); (2) decreased activity of myosin ATPase resulting in impairment of actin-myosin crossbridge release (Portzehl et al. 1969; Fabiato and Fabiato 1978); and (3) reduced Ca^{++} effect on troponin C (Williams et al. 1975). The combined effects of these events is a reduction in the force of contraction by inhibiting the formation, cycling rate, and release of actin-myosin crossbridges. Further evidence in support of reduced Ca^{++} pumping and binding in fatigued muscle are higher intracellular concentrations of free (Fitts et al. 1983) and total (Tables 12 & 18; Gonzalez-Serratos 1978) Ca^{++}].

The activity of phosphorylase does not appear to be 'pH-sensitive' (Chasiotis 1983), however low pH has been reported of have an 'inhibitory effect' on the enzyme phosphorylase b kinase (Krebs et al. 1959; Chasiotis et al. 1983). Inhibition of phosphorylase b kinase reduces the rate of transformation of inactive phosphorylase b to phosphorylase a and thereby reduces the rate of glycogenolysis (Hultman and Sjoholm 1986).

Conditions associated with low intracellular pH have also reported to cause an inhibition of glycolysis at the level of phosphofructokinase (PFK), a key regulatory enzyme in that it may be

important in increasing the sensitivity of the forward glycolytic flux to meet sudden increases in energy demand (Challiss et al. 1984). This has led to the suggestion that the rate at which energy is supplied by glycolysis may be limited by the inhibition of PFK by the accumulated products of glycolysis — La^- and H^+ (Edwards 1981; Hultman and Sjöholm 1986). PFK activity is highest at high $[\text{K}^+]$ (120–150 mEq/l — Paetkau and Lardy 1967), and exercise-induced reductions in $[\text{K}^+]_i$ may reduce PFK activity. In exercising muscle the concomitant increase in $[\text{Pi}]$ and $[\text{NH}_4^+]$ may partially de-inhibit PFK (Snugden and Newsholme 1975). The effects of exercise-induced increases in $[\text{Ca}^{++}]$, $[\text{Pi}]$ and $[\text{Na}^{++}]$ on the activities of pyruvate kinase, phosphoglucosmutase, and AMP-deaminase are described in Section 1.3.6.

It has long been realized that exercise is associated with a reduction in $[\text{K}^+]_i$ and increases in $[\text{Na}^+]_i$, $[\text{Cl}^-]$ and H_2O (Fenn 1936). Therefore, conditions associated with reduced pHi also appear to be associated with a general increase in membrane permeability to strong ions and water. Again, alterations in the ionization state of membrane-bound transporting proteins may be involved. In fatigued muscles fibers, the elevated free $[\text{Ca}^{++}]$ associated with high $[\text{H}^+]_i$ appears to 'promote' K^+ conductance (Fink et al. 1983); the suppression of K^+ conductance after Ca^{++} removal indicates a Ca^{++} -activated increase of the K^+ conductance (Fink et al. 1983), perhaps mediated through the Ca^{++} -activated K^+ channels. It is conceivable that similar events may be involved in the increased Na^+ and Cl^- conductances, however this does not appear to have been investigated.

183

The large increase in $[Na^+]$ in 'metabolic' alkalosis (Table 21) in resting muscle indicates that these membrane permeability effects warrant further study.

The magnitudes of the exercise-induced decreases in $[K^+]_i$ and increases $[Na^+]$ and $[Cl^-]$ are sufficient to reduce the magnitude of both the resting membrane potential and the muscle action potential (Hodgkin and Horowicz 1959a & b). Depolarization of the membrane may be associated with an impairment of excitation-contraction coupling at the level of the sarcolemma (Dulhunty 1982) and at the contractile proteins (Mainwood and Zepetnek 1985; Hibberd and Trentham 1986).

6.3 Conclusions

The magnitude of the changes in the intracellular concentrations of strong ions during intense exercise are sufficient to explain the impairment of muscle force production at all levels of muscle function: the plasma membranes, the enzymes of metabolism, and contractile proteins. These ionic changes may exert direct effects, as in the case of Na^+ and K^+ on the membrane potential and glycolytic enzymes, or they may exert their effects through a reduction of the $[SID]_i$. The increase in $[La^-]$ is the single most important contributor to the reduction in $[SID]_i$ of both the extra- and intracellular fluids. The reduction in $[SID]_i$ has major effects on the concentrations of the dependent variables and on the ionic state of proteins, enzymes, substrates, products, inhibitors and activators.

Alkalosis ameliorates the exercise-induced reduction in $[SID]_i$ by enhancing the removal of La^- from muscle and by increasing

[Na⁺]. The potential beneficial effects of the higher [SID]_i during exercise in alkalotic conditions may be offset by the potentially detrimental effects of high [Na⁺]_i on the activities of glycolytic enzymes and on depolarization of plasma membranes.

6.4 Future Directions

The greatest drawback of the isolated perfused rat hindlimb preparation is that a single perfusate perfusing a diverse population of stimulated and inactive muscle groups and fibers does not permit the precise quantitative correlations between extra- and intracellular events required to elucidate the mechanisms of skeletal muscle ion transport, its regulation, and the integrated regulation of metabolism.

However, the isolated rat hindlimb preparation is presently the most physiological in vitro muscle preparation currently being used to examine muscle function in isolation from external or confounding influences. Most of these 'influences' directly result from non-physiological perfusion models including perfusion with blood-free media at elevated flow rates, elevated oxygenation, reduced or no plasma volume expanders, and superfused preparations. The next major confounding factor is the use of intact or recirculating muscle perfusion systems. While these preparations are more physiological than single-pass systems, they do not permit the precise control of arterial variables required to investigate these mechanisms.

The next line of technical sophistication is to use the same physiological perfusion system to perfuse a single muscle, of essentially homogenous fiber type composition, in isolation from all other muscles, with minimal removal of the muscle from skeletal or

connective tissue elements. This is currently being conducted in our laboratory; the muscles which are being isolated are the tibialis anterior and extensor digitorum longus (primarily FG fibers) and the soleus (primarily SO fibers) of the white rabbit.

Using this new preparation, the changes in arterial to venous perfusate composition should be directly reflected in quantitatively identical changes in intracellular composition. Unidirectional ion and metabolite fluxes can be quantified accurately in a variety of experimental conditions using radiotracer techniques. Studies on resting muscle, or in muscle recovering from fatigue, will utilize micro-electrode techniques to measure changes in the electrophysiological and ionic properties of the muscle. The effects of ion transport inhibitors, channel blockers and a wide variety of stimulatory and inhibitory drugs can be used to study their effects on muscle metabolism and ion balance at rest, during different exercise intensities, and during recovery from exercise.

The results of the present studies have shown that a re-examination of enzymes purported to display a 'pH-dependency' will be critical to our understanding of enzyme function and metabolic regulation. A critical examination of the effects of changes in strong ion concentrations, and of the interactions between their physiological concentrations, on the activities of metabolically important enzymes is due. Undoubtedly these studies can be conducted using the techniques of conventional benchtop biochemistry. Some of the published literature may contain sufficient information to reconstruct the experimental conditions described to exert the 'pH-effect' and permit interpretation of the results in physico-chemical terms, but it seems

186
as though much basic biochemistry may have to be repeated in a more
physiological context and with the fundamentals of physical chemistry
kept in the forefront.

APPENDIX A

ACID-BASE AND RESPIRATORY PROPERTIES OF A BUFFERED BOVINE ERYTHROCYTE PERFUSION MEDIUM

Michael I. Lindinger, George J.F. Heigenhauser and Norman L. Jones

Published: Can. J. Physiol. Pharmacol. 64:550-555 (1986).

ABSTRACT

Current research in organ physiology often utilizes in situ or isolated perfused tissues. We have characterized a perfusion medium associated with excellent performance characteristics in perfused mammalian skeletal muscle. The perfusion medium consisting of Krebs-Henseleit buffer, bovine serum albumin, and fresh bovine erythrocytes was studied with respect to its gas carrying relationships and its response to manipulation of acid-base state. Equilibration of the perfusion medium at base excess of -10, -5, 0, 5, and 10 mmol.L⁻¹ to humidified gas mixtures varying in their CO₂ and O₂ content was followed by measurements of perfusate hematocrit, hemoglobin concentration, pH, P_{CO₂}, C_{CO₂}, P_{O₂}, and % oxygen saturation. The oxygen dissociation curve was similar to that of mammalian bloods, having a P₅₀ of 32 Torr, Hill's constant "n" of 2.87 ± 0.15, and a Bohr factor of -0.47,

showing the typical Bohr shifts with respect to CO_2 and pH. The oxygen capacity was calculated to be 190 ml.L^{-1} blood. The carbon dioxide dissociation curve was also similar to that of mammalian blood. The in vitro non-bicarbonate buffer capacity (ΔHCO_3^- , pH^{-1}) at 0 base excess was -24.6 and $-29.9 \text{ mmol.L}^{-1}.\text{pH}^{-1}$ for the perfusate and buffer, respectively. The effects of reduced oxygen saturation on base excess and pH of the medium were quantified. The data were used to construct an acid-base alignment diagram for the medium, that may be used to quantify the flux of non-volatile acid or base added to the venous effluent during tissue perfusions.

INTRODUCTION

Perfused organ (Neely et al. 1975) and tissue (Ruderman et al. 1971; Watson, 1983; Idstrom et al. 1985; Spriet et al. 1985) systems have become important tools of physiological research, allowing investigators to use a more controlled approach to studying regulatory mechanisms than can be obtained in vivo. Many studies have not reported the gas-carrying properties, buffering capacity and ionic composition of the perfusion medium employed. This tends to limit the extent to which these studies may be extrapolated to evaluate physiological control mechanisms existing in vivo. Precise characterization of mammalian blood and other media used to perfuse isolated or in situ tissues would allow a more accurate assessment of respiratory and acid-base changes, since changes in any of these variables will directly affect muscle metabolism and acid-base regulation.

The present report describes the oxygen and carbon dioxide carrying characteristics and the buffering capacity of a perfusate that was found to be associated with improved physiological characteristics in the isolated, perfused rat hindlimb electrically stimulated to contract for 20 min (Spriet et al. 1985). The perfusion medium consisted of fresh bovine erythrocytes suspended in Krebs-Henseleit buffer. The studies were performed at a single hemoglobin concentration, a value corresponding to the mean rat blood hemoglobin concentration and hematocrit.

METHODS

Perfusion Medium

The perfusate was composed of Krebs-Henseleit buffer (Krebs and Henseleit 1932), containing 24 mM sodium bicarbonate, 50 g.L⁻¹ dialyzed bovine serum albumin (Cohn fraction V), 5.6 mM glucose, 0.14 mM free fatty acids (bound to albumin), 2.5 mM calcium chloride, 22 uM choline chloride, and fresh bovine erythrocytes to give a final hemoglobin concentration ([Hb]) of 140 g.L⁻¹. Sodium pyruvate was added to give an initial lactate/pyruvate ratio of 10-15. For this study bovine blood was collected from eight cattle of different strains, and the erythrocytes washed as described by Spriet et al. (1985). Briefly, fresh bovine blood was collected directly into an ice-cold acid-citrate-dextrose anticoagulant solution. After centrifugation the erythrocytes were washed with 30-40 volumes of Krebs-Henseleit buffer containing 30 mM bicarbonate and 10 mM glucose. Washed erythrocytes were passed through a column of glass beads to

remove fibrin and fibrinogen and, prior to the addition of the buffer portion of the perfusion medium, were passed through an intravenous blood-line filter (Abbott Laboratories). The buffer was initially passed through a 22- μ m filter (millipore) then added to the erythrocytes. A preliminary study was performed to determine if erythrocytes obtained from the different strains of cattle used showed varying responses to acid or base titration. These perfusion media showed identical changes in measured acid-base variables and P_{50} using red cells prepared from six cattle (2 bulls and 4 cows of 3 different strains).

Protocol

Heparin was not required to prevent coagulation of the perfusate because the washing procedures effectively removed the clotting factors. Glycolytic inhibitors were also not used because of their effects on acid-base status (Nunn 1959) and their potential to displace the O_2 dissociation curve (Sommerkamp et al. 1961). As a result, lactate was produced by erythrocytes at a rate of 0.24 ± 0.04 mmole. L^{-1} .h $^{-1}$ at 37°C. In order to minimize the acidifying effects of lactate production, perfusate samples were equilibrated to experimental conditions for no longer than 0.5 h (see below).

The base excess of 0 mmol. L^{-1} for the perfusion medium was defined at pH 7.40 and P_{CO_2} 40 Torr (Severinghaus 1965). Aliquots (5.0 ml) of the perfusion medium or of the buffer without red cells were transferred to chilled glass test tubes. 1.0 ml of sodium bicarbonate, lactic acid (molarity determined by titration with standard NaOH), or HCl of appropriate molarity were added to achieve

base excess values of 0, ± 5 , ± 10 and ± 25 mmol.L⁻¹. These 6.0 ml aliquots were mixed and kept in an ice-water bath until ready for gas equilibration. Addition of equimolar amounts of lactic acid or HCl to the perfusion medium resulted in an identical shift in acid-base status. Each aliquot was transferred to a 37°C temperature regulated tonometer (Instrument Laboratories IL 237) for 10 min and equilibrated to humidified gas mixtures of known P_{O_2} and P_{CO_2} (balance nitrogen) delivered by two Wosthoff gas mixing pumps in parallel. The gas flow into the tonometer was regulated at 300 ml.min⁻¹ to prevent dehydration of the blood. The gas mixtures were used to obtain aliquots of the perusate with a combination of P_{CO_2} 's of 20, 40, or 60 Torr with oxygen saturations of 50, 75, or 100% for each of the 5 base excess levels between -10 and 10 mmol.L⁻¹. Only a limited number of equilibrations were performed using base excess of ± 25 mmol.L⁻¹.

Following equilibration, each aliquot was utilized for 4 replicates of each measurement described below. A 700 μ l sample was drawn using a gas-tight Hamilton syringe for measurement of pH, P_{CO_2} , P_{O_2} , $\%O_2$ saturation, and [Hb]. An additional 200 μ l sample was taken to measure total- CO_2 content ($[C_{CO_2}]$). Additional measurements for completion of the O_2 and CO_2 dissociation curves were obtained by equilibrating aliquots of the perfusion medium at 0 base excess, pH 7.4 at the half-saturation of oxygen (P_{50}), and at constant P_{CO_2} (40 Torr) or P_{O_2} (35 Torr) while permitting the O_2 and CO_2 content, respectively, to change. This data was used to determine the

relationships between base excess, pH and oxygen saturation, and of the non-bicarbonate buffering capacity of the perfusate and buffer. Only those measurements made at an oxygen saturation of 95-100% were used to construct the perfusate acid-base alignment nomogram.

Animals

In order to compare perfusate variables to the in vivo condition, rat blood acid-base, ion, and metabolite status was also determined. Male Sprague-Dawley rats (354 ± 18 g, mean \pm SD, $n = 4$) were anaesthetized (sodium pentobarbital, 6 mg.100 g⁻¹ body wt) and blood samples obtained by cardiac puncture. The samples were immediately analyzed for whole blood and plasma acid-base state, and later for electrolytes and substrates (Table A-1).

Analytical Methods

Perfusate and rat blood pH, P_{CO_2} and P_{O_2} were measured at 37 °C using electrodes (Radiometer BMS3 MK2 blood micro system coupled to a Radiometer PHM72 MK2 digital acid-base analyzer). The pH electrode was calibrated for each aliquot of the perfusate using precision buffers (Radiometer S1500 & S1510). The P_{CO_2} and P_{O_2} electrodes were calibrated using known gas mixtures (Linde Medical Gas, Union Carbide). Oxygen saturation and [Hb] were measured using a Radiometer OSM2 hemoximeter calibrated with precision Hb standards (Radiometer S2100) and known oxygen mixtures. No spectral differences between bovine Hb (Sigma) and the Radiometer Hb standards were detected at the wavelengths (506.5 and 600.0 nm) used in the OSM2 hemoximeter, therefore oxygen saturation characteristics were believed to be accurately represented. CO_2 content of whole

blood and plasma was measured using a Corning 965 CO_2 analyzer; each sample was bracketed with freshly made NaHCO_3 standards calibrated to known solutions of HCl to increase precision. The Corning 965 CO_2 analyzer acidifies the sample, causing the rapid release of all CO_2 . The resulting change in the electrical properties of the solution is measured and converted to a value of CO_2 by an electrometric transducer.

Separate samples were used for the determination of the concentrations of protein, glucose, lactate, free fatty acids, and ions. Protein, glucose, lactate, and free fatty acids were measured as described by Spriet et al. (1985a). Na^+ and K^+ concentrations were measured using ion selective electrodes (Radiometer KNA1 sodium/potassium analyzer) calibrated using Radiometer standard solutions. Chloride was determined by coulometric titration (Buchler-Cotlove chloridometer), and total calcium and magnesium were measured by atomic absorption spectrophotometry (Varian AA-1275). Plasma $[\text{HCO}_3^-]$ was calculated using the equation:

$$[\text{A-1}] \quad [\text{HCO}_3^-] = C_{\text{CO}_2} - S \cdot P_{\text{CO}_2}$$

where C_{CO_2} was measured in plasma and S (solubility coefficient for CO_2) was 0.0306 at 37°C (Severinghaus 1965).

The perfusate acid-base alignment nomogram was constructed from data collected from 60 aliquots of the perfusion medium equilibrated to 95-100% oxygen saturation, with complete analysis performed on 4 samples from each aliquot. The procedure employed was

essentially that described by Siggaard-Andersen (1963). At pH 7.4 and P_{CO_2} 40 Torr the base excess of the perfusate was always within $\pm 2 \text{ mmol.L}^{-1}$ and curve-shifting to "normalize" data (Weiskopf 1983) was not required.

RESULTS

The perfusate composition (Table A-1) and respiratory properties (Table A-2) closely resembled that of rat blood. Perfusate [Hb] was within the ranges reported for both species. The P_{50} at pH 7.4 was in the lower range for rats but higher than that reported for cattle. The Bohr factor ($\Delta \log P_{50} \cdot \Delta pH^{-1}$) and oxygen capacity for the perfusate was low compared to rat blood, but similar to bovine blood. Bovine red cell diameter was at the lower range of reported values for the rat.

The mean O_2 dissociation curve of the perfusion medium within the physiologic pH range is shown in Fig. A-1. Hill's n , a value which classically describes the slope of the oxygen dissociation curve, was calculated to be 2.87 ± 0.15 at pH 7.4; this value is within the mammalian range of 2.8-3.0 (Antonini and Brunori 1971). High pH and low P_{CO_2} resulted in shifts of the curve to the left, while low pH and high P_{CO_2} shifted the curve to the right. The combined Bohr effect at 0 base excess and 37°C was described by the significant ($P < 0.05$) linear relationship:

[A-2] $\log P_{50} = 5.065 - 0.475(pH); (r = 0.979, n = 17)$

TABLE A-1

Chemical composition of the perfusion medium compared to rat blood at 37°C.

parameter	perfusate (n = 40)	rat blood (arterial)	reference
pH	7.41 \pm 0.009	7.347	Lahari 1975
P _{CO₂} (Torr)	40.5 \pm 0.91	40.7	"
HCO ₃ ⁻	22.3 \pm 0.79	24.9	"
Na ⁺	140 \pm 0.4	140	this study
		151	Gahlenbeck et al. 1968
		145	Schloerb et al. 1967
Cl ⁻	119 \pm 0.6	103	" ; this study
K ⁺	5.7 \pm 0.28	5.8	this study
		4.7	Gahlenbeck et al. 1968
		4.62	Schloerb et al. 1967
Ca ⁺⁺	2.6 \pm 0.05	2.34	this study
Mg ⁺⁺	1.0 \pm 0.04	0.98	this study
glucose	5.6 \pm 0.17	5.2	this study
		7.8	Goodman et al. 1983
lactate	1.0 \pm 0.07	1.2	this study
		1.28	Goodman et al. 1983
pyruvate	0.6 \pm 0.05		
protein (g/L)	50.0 \pm 1.1	49	this study
		60	Cotlove et al. 1951

Values are mean \pm SE. All units are mmol.L⁻¹ unless otherwise noted.

TABLE A-2

In vitro respiratory characteristics of bovine and rat bloods and the perfusion medium at 37°C.

parameter	cattle	rat	perfusate
Hct		0.422	0.393
[Hb] (g.L ⁻¹)	87-145	120-175	140
P ₅₀ (Torr) @pH 7.4	28-32	38	32
$\Delta \log P_{50} / \Delta pH$ (Torr/pH)	-0.49	-0.52	-0.47
O ₂ capacity (ml.L ⁻¹)	150-220	200-230	190*
RBC diameter (μm)	5.9	6.0-7.5	5.9

references: Cattle: Albritton 1952; Bartels and Harms 1959; Bartels et al. 1963; Hilpert et al. 1963; Huisman and Kitchens 1968; Rat: Albritton 1952; Bullard et al. 1966; Gahlenbeck et al. 1968; Gray and Steadman 1964; Hall 1966; Lahari 1975; Lechner 1976.

* calculated from [Hb] x 1.36, (Altman and Dittmer 1971).

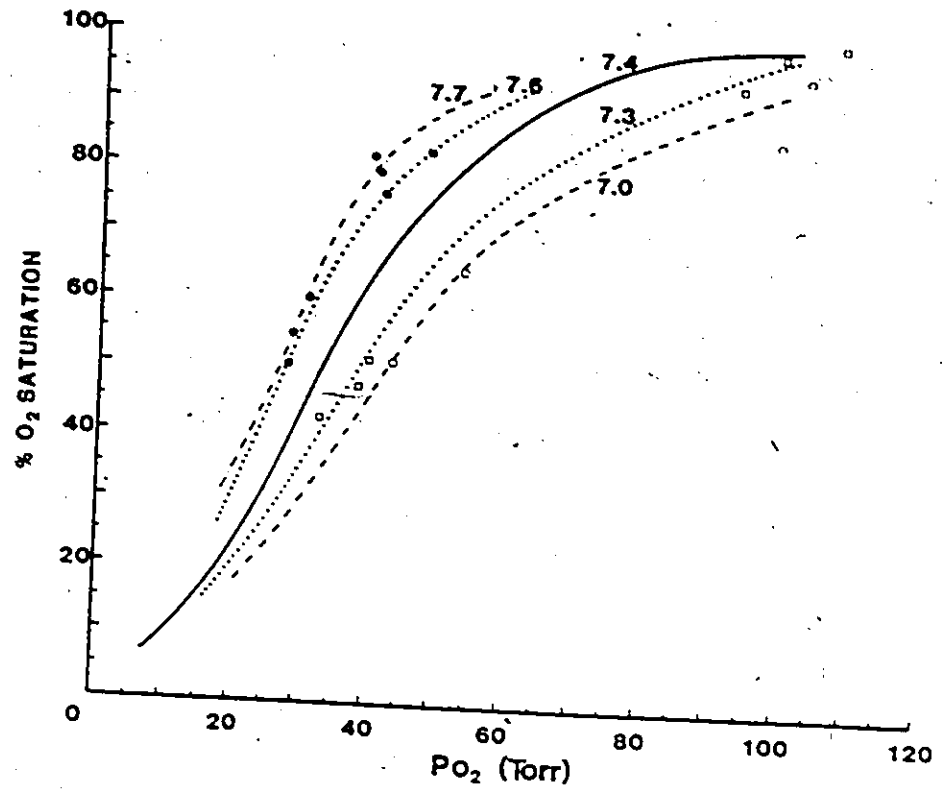


Fig. A-1. The effect of pH on shifting the perfusate O_2 dissociation curve at 37°C . Each point on the graph represents the mean of four individual determinations.

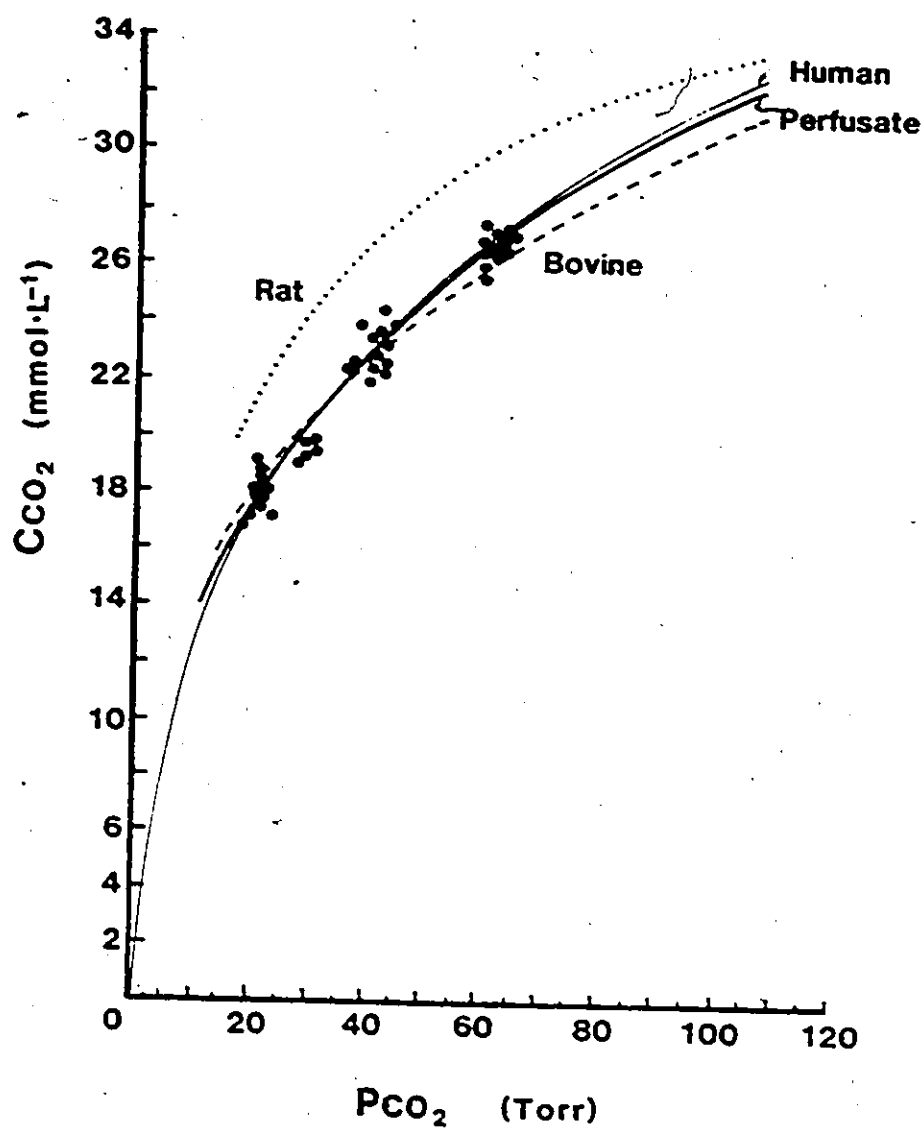


Fig. A-2. Perfusate CO₂ dissociation curve (heavy solid line and n = 40 points) compared to CO₂ dissociation curves for bovine (Bartels and Harms 1959) and rat (Brodie and Woodbury 1958; Gray and Rauh 1958; Nichols 1958) bloods at 37°C.

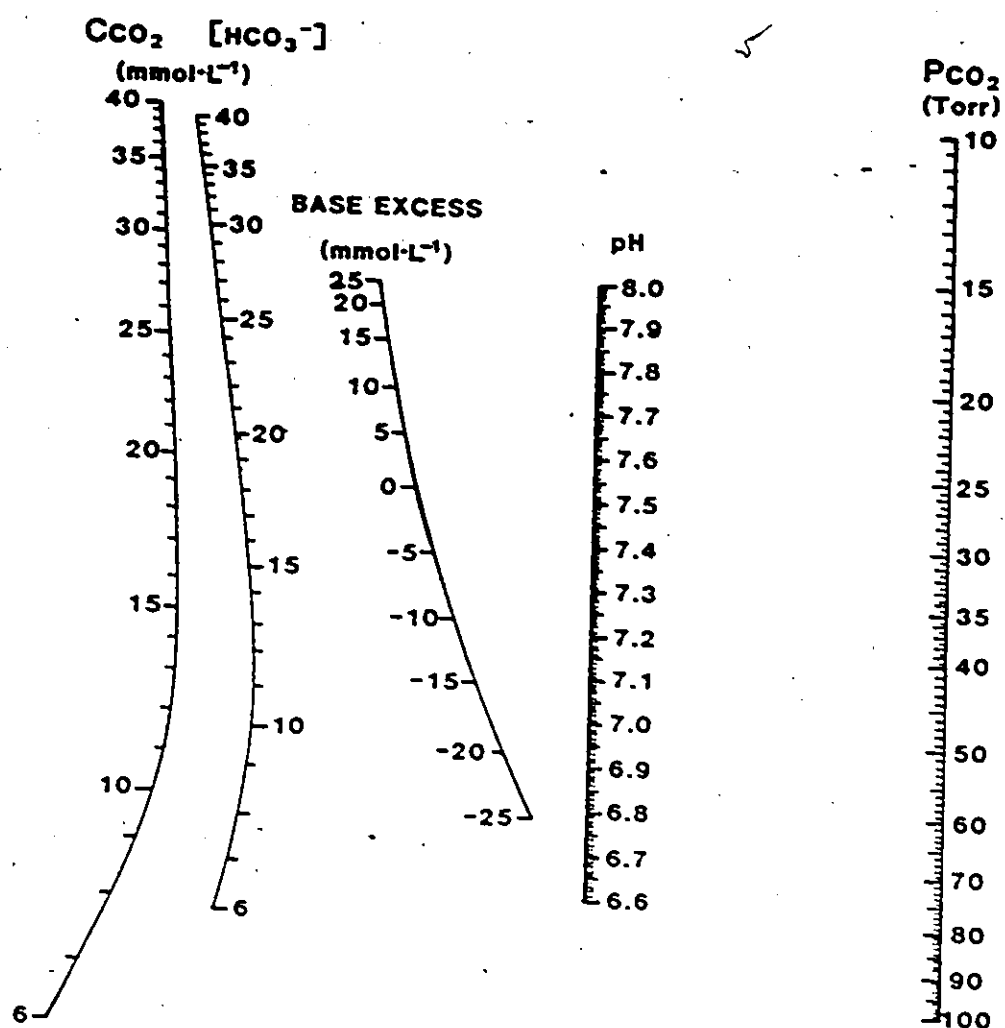


Fig. A-3. The acid-base alignment diagram for the perfusate at 95-100 % O₂ saturation, [Hb] = 140 g.L⁻¹, and 37°C.

The carbon dioxide dissociation curve for the perfusate was similar to bovine blood in vitro, but to the right of the curve for rat plasma in vivo (Fig. A-2).

The relationships between HCO_3^- and pH of the perfusate at base excess values of -10, -5, 0, 5, and 10 mmol.L⁻¹ are given in Table A-3. There was a significant correlation between the slopes of these linear relations (B = nonbicarbonate buffer capacity) and base excess (BE), expressed by the equations for perfusate:

$$[A-3] \quad B = 0.48 \pm .03 \cdot \text{BE} - 23.38 \pm 0.8 \quad (r = 0.961; P < 0.05)$$

and for buffer (non-erythrocyte portion):

$$[A-4] \quad B = 0.48 \pm .07 \cdot \text{BE} - 27.76 \pm 1.3 \quad (r = 0.942; P < 0.05)$$

where B is the slope of the buffer line in mmol.L⁻¹.pH⁻¹.

The acid-base data collected from the series of tonometered perfusate samples were used to construct the acid-base alignment diagram (Fig. A-3). The errors incurred in the construction of the alignment diagram do not exceed $\pm 5\%$ for each scale when the perfusate acid-base status is aligned on the diagram.

Effect of Oxygen Saturation on Base Excess

Increasing oxygen saturation produced significant linear decreases in both the base excess and pH of the perfusion medium,

TABLE A-3

The equations expressing the relationships between $[\text{HCO}_3^-]$ and pH of the perfusate whole blood (WB) and buffer (P) at 37°C for 5 values of base excess (BE) ($\text{mmol}\cdot\text{L}^{-1}$).

The equations are in the form $[\text{HCO}_3^-] = a - B(\text{pH})$, where the slope, B, is the non-bicarbonate buffer capacity.

BE	n	equations	r
10	22	WB $[\text{HCO}_3^-] = 164.84 - 18.26(\text{pH})$	-0.965
		P $[\text{HCO}_3^-] = 197.56 - 21.86(\text{pH})$	-0.984
5	24	WB $[\text{HCO}_3^-] = 181.88 - 21.12(\text{pH})$	-0.890
		P $[\text{HCO}_3^-] = 222.09 - 25.83(\text{pH})$	-0.912
0	40	WB $[\text{HCO}_3^-] = 204.01 - 24.56(\text{pH})$	-0.951
		P $[\text{HCO}_3^-] = 247.93 - 29.87(\text{pH})$	-0.961
-5	24	WB $[\text{HCO}_3^-] = 194.82 - 24.10(\text{pH})$	-0.959
		P $[\text{HCO}_3^-] = 235.83 - 29.18(\text{pH})$	-0.965
-10	24	WB $[\text{HCO}_3^-] = 210.09 - 28.85(\text{pH})$	-0.935
		P $[\text{HCO}_3^-] = 255.02 - 32.61(\text{pH})$	-0.941

resulting from proton release from hemoglobin. Thus the base excess value determined for a sample of venous perfusate at an oxygen saturation (S_{O_2}) less than 95% ($P_{O_2} < 35$ Torr) must be corrected to a value corresponding to that occurring at an S_{O_2} of 100% to calculate the correct base excess. In order to calculate base excess (BE) and pH at 100% S_{O_2} from lower values of oxygen saturation, the following equations were derived from those measurements at perfusate oxygen saturations at 50%, 75% and 100% at each level of base excess:

$$[A-5] \quad BE_{100} = BE_m - ([100\% - S_{O_2}] \times 0.222),$$

$$r=0.957, P<0.05,$$

where BE_{100} is base excess at 100% S_{O_2} and BE_m is the BE measured from the alignment diagram;

$$[A-6] \quad pH_{100} = pH_m - ([100\% - S_{O_2}] \times 0.004),$$

$$r = 0.973, P<0.05,$$

where the subscripts have the same meaning as above. The alignment diagram thus allows the acid-base changes from artery to vein to be converted to an equivalent amount of hydrogen ions added to or removed from the perfusate.

DISCUSSION

In view of the important influences that the gas carrying

capacity and acid-base characteristics of an organ perfusate exert on the viability and function of the perfused tissue in question, there is a surprising lack of information regarding these properties in many previous reports. Investigations of the effects of extracellular fluid disturbances on tissue metabolism requires quantitative data on perfusate buffering and gas carrying capacity. This information enables accurate estimates of non-volatile acid (NVH^+) release from tissue and organ preparations to be made. This report presents a description of the medium associated with improved performance in the rat hindlimb. The present studies were all conducted using a single hemoglobin concentration approximating the mean value found in most mammals (Altman and Dittmer 1971). Since the perfusate can easily be made up to achieve the desired hemoglobin concentration and hematocrit, inclusion of other hemoglobin concentrations into the alignment diagram (Siggaard-Andersen 1963; Weiskopf et al. 1983) was not required.

Gas Transport

Since Ruderman's (1971) initial characterization of the rat hindquarter as a model for mammalian skeletal muscle metabolism, human erythrocytes have been used in various perfusion media (Ruderman et al. 1980). In early experiments in our laboratory, conducted with rejuvenated time-expired human red cells in Krebs-Henseleit buffer, a number of problems were encountered including abnormally low P_{50} , excessive accumulation of lactic acid, and depletion of 2,3-DPG, ATP and glucose, as reported also by Ruderman et al. (1980). Human red cell dimensions may be up to 50% greater than rat red cells, therefore

media containing human red cells may have difficulty in perfusing the capillary beds in rat skeletal muscle. This drawback does not apply to media employing bovine red cells which are comparable in size to the rat erythrocyte (Table A-2). Ideally, it would be preferable to use blood from the same species as the tissues to be perfused, a technique used by Watson (1983) for cat hindlimb perfusions. However, when using small animals and single-pass perfusion systems the large amount of blood required for perfusions often necessitates the use of blood from another mammalian species.

The magnitude of the pH (and PCO_2 , not shown) induced shifts in the O_2 dissociation curve (Fig. A-1) was similar to that reported for mammalian blood (Lenfant 1973). This effective Bohr effect results from the combination of the specific separate effects of both pH and P_{CO_2} on the oxygen affinity of hemoglobin (Kilmartin and Rossi-Bernardi 1973; Tyuma 1984). It is clear that a decrease in pH and an increase in P_{CO_2} will facilitate both oxygen unloading from hemoglobin at the tissues and CO_2 uptake by deoxyhemoglobin. These features of the perfusion medium, combined with the normal P_{50} and steep sigmoid shape of the O_2 dissociation curve of the perfusion medium (Hill's n of 2.87), suggested that the perfusate should behave satisfactorily with respect to tissue O_2 uptake.

Indeed, the perfusate need not be maintained hyperoxic nor used a high flow rates to ensure adequate oxygen uptake by isolated perfused rat hindlimb muscles during high intensity electrical stimulation via the sciatic nerve (Lindinger and Heigenhauser,

unpublished observations). The preparation in current use (Spriet, Lindinger et al. 1986) differs slightly from that previously described (Spriet et al. 1985a) in that arterial and venous catheters are inserted into the femoral vessels. As a result of this refinement the total amount of tissue perfused averages 6.5 g with 5.35 g (or 82%) being stimulated to contract, for a 400 g rat. With a typical resting perfusion flow rate of $0.3 \text{ ml} \cdot \text{min}^{-1} \cdot \text{g}^{-1}$ the oxygen uptake averaged $0.32 \text{ } \mu\text{mol} \cdot \text{min}^{-1} \cdot \text{g}^{-1}$ perfused tissue. During the 5 min of stimulation flow rates were increased to $1.5 \text{ ml} \cdot \text{min}^{-1} \cdot \text{g}^{-1}$ and oxygen uptake increased to $2.58 \text{ } \mu\text{mol} \cdot \text{min}^{-1} \cdot \text{g}^{-1}$ of stimulated muscle. These flow rates are within the physiological range for these tissues in vivo (Armstrong and Laughlin 1984) and in situ (Mackie and Terjung 1983). Folkow and Halicka (1968) reported similar values of muscle flow and oxygen extraction in in situ resting and electrically stimulated soleus and gastrocnemius muscles of the cat. These oxygen extractions are also similar to those reported by Spriet, Lindinger et al. (1986) using hyperoxic perfusion medium at the same flow rates, indicating that these flows and normoxic oxygenation parameters were adequate for tissue perfusion and oxygen supply. This was supported by the absence of changes in muscle concentrations of phosphocreatine, ATP and lactate during 20 min perfusions of resting muscle (Lindinger and Heigenhauser, unpublished observations). A recent study investigating the oxygen dependence of energy metabolism in rat skeletal muscle (Idstrom et al. 1985) initially showed that basal metabolism could not be maintained at an in situ rate without the use of red cells in the

perfusate. Yet in their characterization of the oxygen dependence of energy metabolism they did not use erythrocytes in the perfusion medium and consequently had to use elevated flow rates and high P_{O_2} to maintain oxygen delivery at a rate at which depletion of phosphocreatine did not occur. Clearly, perfusion media without erythrocytes do not supply adequate O_2 to the tissues to meet metabolic demands unless unphysiologically high flow rates and P_{O_2} are used.

Acid-Base

The recent development of acid-base nomograms for dog (Scott-Emuakpor et al. 1976) and swine (Weiskopf et al. 1983) bloods has shown clear species differences in acid-base characteristics. The perfusate whole blood acid-base alignment diagram (Fig. A-3) was derived from measurements made at an oxygen saturation of 95-100% and was designed to quantify changes in perfusate acid-base state as it passed through the tissues. The diagram permits rapid and accurate determination of the entire acid-base status with the direct measurement of only two acid-base variables, usually pH and whole blood or plasma C_{CO_2} or P_{CO_2} . Since whole blood is used to perfuse the tissues, changes in acid-base state and base excess of the venous perfusate should be obtained from measurements on whole blood. The perfusate non-bicarbonate buffer capacity over a range of base excess values (Table A-3) was within the range reported for mammals (Altman and Dittmer 1971; Lahari 1975). The perfusate buffer system responded as expected to disturbances of acid-base balance induced by metabolic and respiratory acidosis and alkalosis,

as shown by the alignment diagram (Fig. A-3).

The presence of erythrocytes in perfusion media appears to play another role in addition to its important gas-carriage and buffering roles. Recent studies (Watson 1983) have shown that both protein and blood (erythrocytes plus normal electrolytes) are required in perfusion media in order to prevent abnormal and excessive transcapillary water exchange within the perfused tissues. This is important in studies using perfused tissues, where changing concentrations of strong electrolytes may influence acid-base homeostasis and, in turn, metabolism.

ACKNOWLEDGEMENTS

The authors acknowledge with appreciation the technical assistance of Dr. M. Ganagarajah, and thank Drs. D.G. McDonald and C.M. Wood for the loan of equipment. This work was supported by grant MA-7675 from the Medical Research Council of Canada.

APPENDIX B

INTRACELLULAR ION CONTENT OF SKELETAL MUSCLE MEASURED BY INSTRUMENTAL NEUTRON ACTIVATION ANALYSIS

M.I. Lindinger and G.J.F. Heigenhauser

Submitted to: J. Appl. Physiol.

ABSTRACT

The intracellular contents of sodium (Na^+), potassium (K^+), calcium (Ca^{++}), magnesium (Mg^{++}), and chloride (Cl^-) in rat hindlimb muscles (soleus, plantaris, white and red gastrocnemii) were measured by instrumental neutron activation analysis (INAA) and atomic absorption spectrophotometry (AAS). Muscle extracellular fluid volume (ECFV) was determined using ^3H -mannitol, ^{14}C -mannitol, ^3H -polyethylene glycol (PEG, mol. wt. 900, PEG-900) or the chloride (Cl) method and intracellular fluid volume (ICFV) calculated. Rats were anesthetized with sodium pentobarbitol. The muscles were biopsied, frozen in liquid nitrogen, freeze-dried, weighed and transferred to vials for analysis. For a given muscle, ion contents measured by the two methods showed a consistent small difference which could not be explained. The PEG-900

space and the Cl method yielded a larger ECFV than did mannitol; it is concluded that PEG-900 and Cl overestimate ECFV. There were significant differences in total tissue water (TTW), ECFV, ICFV and intracellular ion contents between the different muscle types. The fast glycolytic muscles (white gastrocnemius, plantaris) had lower TTW (758 ml/g WW) and ECFV (6.5-8.5% TTW) but the highest ICFV; the soleus (slow oxidative fibers) had the highest total tissue water (TTW) (766 ml/g WW) and ECFV (10-15% TTW) but the lowest ICFV. The fast-twitch white gastrocnemius and plantaris muscles have a higher intracellular content of K^+ , and lower Na^+ and Cl^- than the slow-twitch soleus muscle. The technique of INAA provides a rapid and accurate means of determining intramuscular electrolyte state in small samples of tissue.

INTRODUCTION

Knowledge of the ionic composition of the extra- and intracellular fluids is a prerequisite to understanding the effects of fluid and electrolyte (and acid-base) disturbances of the extra- and intracellular fluids on the physiological function of muscle. The physiological properties directly involved include the resting membrane potential (Dulhunty 1978; Hodgkin and Horowicz 1959; Wareham 1978; Yonemura 1967), membrane depolarization and action potential propagation (Hodgkin and Horowicz 1959; Milner-Brown and Miller 1986), size of the action potential (Yonemura 1967), membrane transport properties (Clausen 1986), intracellular enzyme function (Snugden and Newshome 1975), and ultimately the strength of muscle contraction.

Ideally, the analysis of intramuscular ionic composition involves the simultaneous measurement of the total muscle ion content and of the extra- and intracellular fluid volumes. This permits the ion content of the muscle extracellular space to be determined, and this value, when subtracted from the total muscle ion content, yields an average ion content for the intracellular fluid compartment.

Several other methods are currently used for the determination of intracellular ion concentrations in skeletal muscle. These include electron microprobe analysis (Gupta and Hall 1981; Sembrowich et al. 1982), the use of ion-selective electrodes (Aickin and Thomas 1977, Donaldson and Leader 1984; Hnik et al. 1976), flame photometry (Cotlove et al. 1951; Sreter and Woo 1963), and AAS (Jaweed et al. 1982). Most of these techniques require elaborate tissue preparation; in contrast, INAA can be performed with a minimum of sample handling. Furthermore, INAA permits the entire spectrum of strong ions in a single small sample of lyophilized tissue to be measured simultaneously. While INAA has been used for analyzing muscle in the past (Bergstrom 1962), the technique appears to have been neglected. This may be the result of difficulties in sample preparation, the poor detection limits of older detection and analytical equipment (generally less than 5% efficient), and the relative unavailability of facilities for irradiating samples and for the subsequent detection and quantification of the ions within that sample.

The ideal ECF marker is one which equilibrates rapidly throughout the entire ECFV, does not penetrate into cells, is not adsorbed by connective tissue, and is not rapidly degraded and

excreted (Corlove 1954; Manery 1954; McIver and Macknight 1974). Such compounds commonly employed include non-metabolized or slowly metabolized saccharides (inulin, mannitol, sucrose) and more recently, polyethylene glycol. The Cl space (Graham et al. 1967) has also been used extensively, but consistently yields values which differ from those obtained simultaneously by other techniques. When used properly, the inulin space yields what is considered to be the "gold standard" for ECFV. However, to be used properly the inulin must first be passed through a column to remove the numerous low molecular weight particles resulting from normal degradation (Manery 1954; Walsh et al. 1984). These low molecular weight particles can easily lead to an overestimate of the ECFV, since they appear to be readily taken up by some cells. Inulin also requires a relatively long distribution time of 2-3 h, and may thus underestimate ECFV (Page 1962). In our search for a reliable and easily used marker of skeletal muscle ECFV we tried mannitol and PEG-900, and simultaneously measured the Cl space.

The present study presents an analysis of intracellular fluid volume and ion content of different mammalian skeletal muscle fiber types. In particular, we report the use of instrumental neutron activation analysis (INAA) for the simultaneous measurement of all major ion species in small samples of muscle. The mannitol space of skeletal muscle provides a good estimate of tissue extracellular fluid volume (ECFV), while the Cl space and PEG-900 space both overestimate ECFV. Mannitol appears to be stable, does not readily break down into low molecular weight particles, and does not appear to be metabolized

by skeletal muscle.

METHODS

Animals

Male Sprague-Dawley rats (weight 330-410 g) were used for all experiments. The animals were fed Purina lab chow ad libitum and housed in a temperature-, humidity- and light-controlled (12 h on, 12 h off) environment. The animals were anesthetized with sodium pentobarbital (6 mg.100 mg⁻¹ body wt i.p.). The skin covering the hindlimbs was carefully stripped away and samples of the white and red gastrocnemii (WG, RG), plantaris (PL) and soleus (SOL) muscles removed, freeze-clamped and stored in liquid nitrogen. Total time for biopsies of all muscles and freezing did not exceed 2 min. There was minimal or no bleeding onto the biopsied muscles, reducing the possibility of blood contamination of the sampled tissues. Blood samples were drawn from the abdominal aorta and plasma ions were measured with ion selective electrodes (Na⁺, K⁺, Ca⁺⁺) or titration (Cl⁻) as described previously (Lindinger et al. 1986).

Determination of Muscle Ion Content.

Introduced in 1936 by de Hevesi and Levi, INAA is most widely used for the analysis of trace elements in many substances (Heydorn 1984). The technique also affords an accurate, sensitive and precise method to measure the major elements in muscle tissue (Bergstrom 1962; Heydorn 1984). INAA utilizes neutrons generated by nuclear fission or other neutron sources to activate the elements within the sample

introduced close to the nuclear reactor core. The induced activity is proportional to the half-lives of the radio-isotopes, the duration of irradiation and the quantity of element irradiated (DeSote et al. 1972; Heydorn 1984). Following correction for the amount of ion (or element) present in the ECF space of muscle tissue, a measurement of the mean intramuscular ion content can be obtained. In the present study 'content' and 'concentration' have their usual meanings: content refers to the quantity of a substance in a specified mass (eg. $\mu\text{Eq/g}$) and concentration refers to the quantity of a substance in a specified volume (eg. mEq/l).

The white and red gastrocnemii, plantaris and soleus muscles from the right hindlimbs of 26 rats (391 ± 4 g) were used for comparison of muscle element contents determined by INAA and AAS. Frozen muscle tissues were finely ground with a cooled stainless steel mortar and pestle under liquid nitrogen and connective tissue dissected out. A 30-200 mg sample of the ground muscle was weighed and then freeze-dried to a powder within acid-washed (0.5% nitric acid and distilled water rinsed) polyethylene vials. Muscle TTW was determined from the difference between wet and dry muscle weights.

The freeze-dried muscle (6-45 mg) within the acid-washed vial was transported to the nuclear reactor core via pneumatic lines (McMaster University Nuclear Reactor, Hamilton, Ontario). The tissue was irradiated with thermal neutrons (flux density = $5 \times 10^{12} \text{ ncm}^{-2} \cdot \text{sec}^{-1}$) for 10 min. The vials were returned from the core and the tissues were then transferred to pre-weighed, acid-washed, unirradiated vials in order to eliminate any isotopic

activity present in the irradiated vials. The delay time involved in the transport of the vial from the reactor core, transfer of the irradiated tissue into the fresh vial and positioning of the vial on the detector for counting was kept constant at 150 s. The activated elements within the muscle sample were counted for 10 min using a hyper-pure germanium detector. The detector was 8% efficient, having a full width half maximum resolution of 2.1 KeV at the 1332 KeV cobalt peak, and was coupled to a Canberra multichannel analyzer (Series 40 or Series 90).

Irradiation of a suitable standard (citrus leaves, National Bureau of Standards # 1572), done in triplicate, permitted the quantity of an element (A) in the tissue to be calculated from the fundamental relations described by equation B-1 (Heydorn 1984):

$$(B-1) \quad \frac{\text{quantity of A in sample}}{\text{quantity of A in standard}} = \frac{\text{radiation intensity of A in sample}}{\text{radiation intensity of A in standard}}$$

To take into account the rate of radioactive decay (λ), the neutron flux (Φ), the neutron capture cross section (σ), the irradiation time (t_i), the delay time (t_d), the counting time (t_c), the mass of standard tissue irradiated (W_k), the mass of the (unknown) sample (W_u), and the elemental content of the standard tissue (ppm_k) equation B-1 takes the following form (DeSote et al. 1972):

$$(B-2) \quad \text{ppm}_u = \text{ppm}_k \cdot \frac{W_k}{W_u} \cdot \frac{N_u}{N_k} \cdot \frac{[(1-e^{-\lambda t_i})(1-e^{-\lambda t_d})(1-e^{-\lambda t_c})]_k}{[(1-e^{-\lambda t_i})(1-e^{-\lambda t_d})(1-e^{-\lambda t_c})]_u}$$

where ppm_u is the content of element in the unknown, and N_u and N_k are the number of atoms of radionuclide in the unknown and standard. For calculations, the term:

$$(P_u - (B_1 + B_2)/2) / (P_k - (B_1 + B_2)/2)$$

is substituted for N_u/N_k in equation B-2, where P_u and P_k are the peak readings for the unknown and standard and B_1 and B_2 are background readings on either side of the respective peak readings from the multichannel analyzer for the gamma rays being measured. For this calculation we utilized a computer program.

Recoveries were performed on a sample of 25 tissues, weighing between 25 and 75 mg dry weight, on which the elemental composition had been determined previously by INAA. To these samples was added 200 μ l of a solution containing known concentrations of Na, K, Cl, Mg and Ca. The vials were sealed and the elemental composition of the solution determined using the same procedure. Following subtraction of the elemental concentration of the added solution, the tissue recoveries for Na, K, Cl, Mg and Ca were $111 \pm 6\%$, $104 \pm 7\%$, $104 \pm 12\%$, $108 \pm 7\%$, and $105 \pm 4\%$ respectively.

To validate the ion contents measured by INAA the muscle sample were assayed for ion content using AAS. The previously irradiated muscle samples from 26 hindlimbs were given 3 to 8 weeks to allow for decay of radioactivity. These muscle samples and citrus

leaves standards were dissolved in 4.0 ml of 50% nitric acid at 80°C for 24 hours. The concentrations of Na^+ , K^+ , Ca^{++} and Mg^{++} in the supernatant were measured after appropriate dilution and ionization suppression by AAS (Varian AA-1275). Chloride could not be measured directly using acidified samples and therefore is not included in the comparison.

Measurement of Extracellular Fluid Volume.

A separate group of 13 rats (385 ± 4 g) were injected via a tail vein with 25 μCi ^3H -mannitol (New England Nuclear) dissolved in 0.5 ml 0.9% NaCl for measurement of muscle ECFV. After 2-3 h for equilibration of the solution in the body fluids, the rats were anesthetized, muscles from each hindlimb were sampled as described above, and a blood sample was taken to determine plasma ions and radioactivity. Muscle ion concentrations were determined from samples of the contralateral leg, using the technique of INAA. The right leg was always sampled first; 7 right leg muscle samples and 6 left leg muscle samples were used for INAA; the reverse was used for determination of muscle radioactivity. There were no differences in muscle ions, or ECFV between right and left leg samples. Plasma and muscle La^- were determined as described previously (Lindinger et al. 1986).

A 50-200 mg sample of wet muscle and 0.1 ml of plasma from these rats were dissolved in 2 ml tissue solubilizer (NCS, Amersham) per sample. After a clear solution was obtained (7-10 days), the solution was neutralized with 60 μl glacial acetic acid and 13 ml of

fluor (OCS, Amersham), was added. Samples were counted for ^3H in an LKB 1211 Rackbeta Scintillation Counter (Beckman) preprogrammed for standardization and quench correction. Muscle ECFV was calculated using equation B-3:

$$(B-3) \quad \text{ECFV (ml/g d.w.)} = (\text{dpm/g d.w.}) / (\text{dpm/ml ECF})$$

where dpm is disintegrations per minute of the tritium label in dry weight (d.w.) muscle and in extracellular fluid (ECF).

In this group of 13 animals, ECFV was also determined by the Cl method -- equation B-1 (Graham et al. 1967), using an intracellular Cl^- concentration ($[\text{Cl}^-]_i$) derived from the relationship between membrane potential (E_m) and plasma $[\text{Cl}^-]_e$ -- equation B-4 (Hodgkin and Horowicz 1959a):

$$(B-4) \quad \text{ECFV} = (\text{Cl}_t - \text{TTW}[\text{Cl}^-]_i) / ([\text{Cl}^-]_e - [\text{Cl}^-]_i)$$

$$(B-5) \quad \ln[\text{Cl}^-]_i = F/RT(E_m) \ln[\text{Cl}^-]_e$$

where F, R, and T are the Faraday, gas constant, and absolute temperature respectively, and the other symbols are as defined above. The E_m for SOL, PL, RG, and WG were taken as -76, -78, -80, and -82 mV respectively (Wareham 1978).

For comparison of ECFV measured by mannitol or PEG-900, another group of rats ($n=4$, mean wt = 408 g) were injected via a tail vein with 0.5 ml 0.9% sodium chloride (NaCl) solution containing 25

$\mu\text{Ci } ^3\text{H-PEG } 900$ and $5 \mu\text{Ci } ^{14}\text{C-mannitol}$ (New England Nuclear).

After 3 h equilibration, the rats were anesthetized with sodium pentobarbital. A resting arterial blood sample (1.0 ml) was collected from the right femoral artery and the SOL, PL, RG, and WG were sampled as described above. Plasma and tissue radioactivity were measured and tissue ECFV calculated as described above.

Calculation of Intracellular Ion Concentration .

The intracellular ion concentrations were calculated from total muscle ion contents measured by INAA and from muscle ECFV measured by mannitol space. Following measurement of total ion content (ion_T) in the muscle tissues, the quantity of ion in the muscle extracellular space (ion_{ECF}) was subtracted from the total to obtain the mean intracellular ion content (ion_i) in $\mu\text{Eq/g d.w.}$:

$$(B-6) \quad \text{ion}_i = \text{ion}_T - \text{ion}_{\text{ECF}}$$

where ion_{ECF} in $\mu\text{Eq/g d.w.}$ for each individual muscle was determined as:

$$(B-7) \quad \text{ion}_{\text{ECF}} = \text{ion}_{\text{plasma}} (\mu\text{Eq/ml}) \times \text{ECFV (ml/g d.w.)}$$

In equation B-7 the plasma ion concentration is used, and not the interstitial fluid ion concentration calculated from the plasma ion concentration according to the Donnan equilibrium (Manery 1954). This is done because only about 10% of the total muscle ECFV is composed of

the interstitial fluids, the remainder being primarily trapped plasma (Manery 1954).

The ICFV for each muscle was calculated as the difference between the TTW and the ECFV. The intracellular ion contents (uEq/g d.w.) from equation B-6 were converted to units of concentration (mEq/l of ICF) by:

$$(B-8) \quad [\text{ion}]_{\text{ICF}} \text{ (mEq/l ICF)} = \text{ion}_i / \{ (w.w./d.w.) \times (\text{ICFV, ml/g w.w.}) \}$$

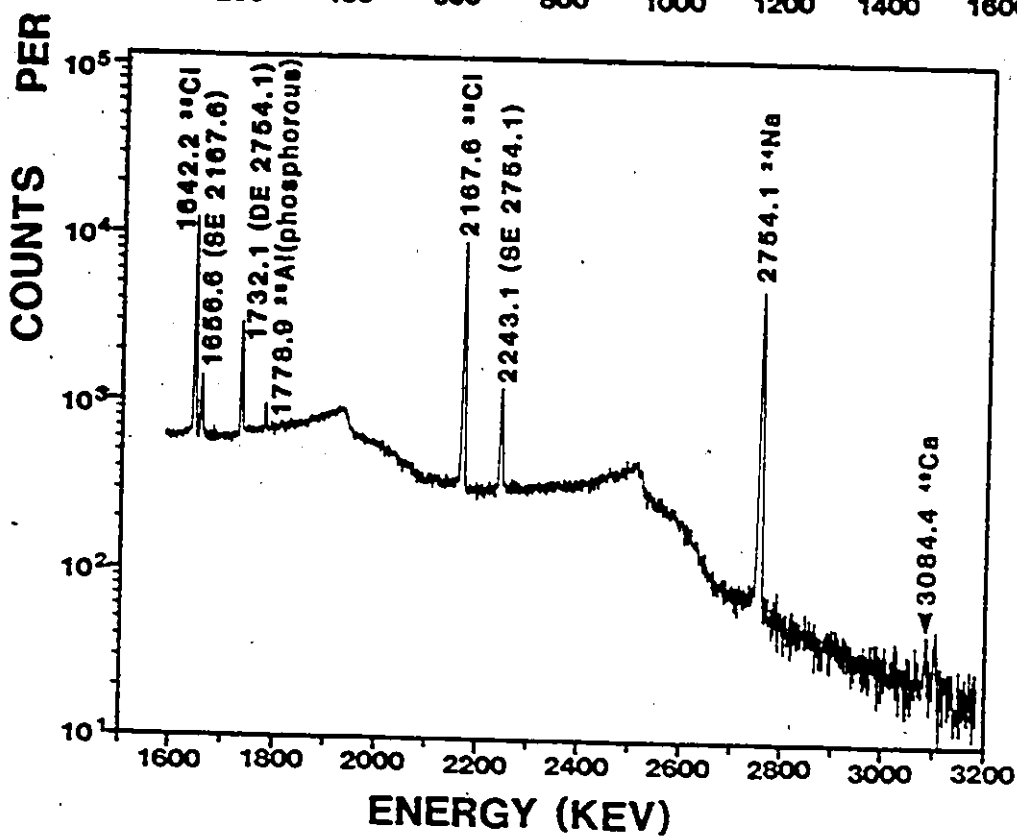
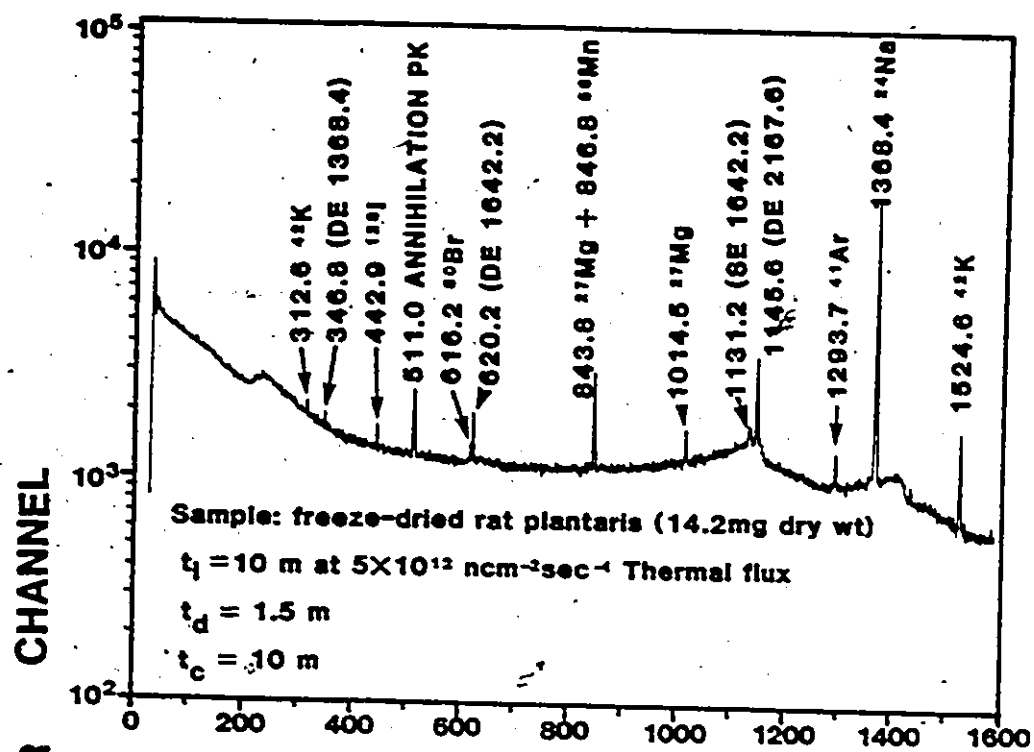
Statistics

Results are expressed as mean \pm SE. Ion contents and concentrations are expressed in equivalents (Eq), a form which takes the ionic valency into consideration. For monovalent ions 1 mmol = 1 mEq, and for divalent ions 1 mmol = 2 mEq. Differences between treatments and among muscles for comparison of INAA vs AAS methods were determined using repeated measures analysis of variance. Differences between muscles for intracellular ion content and for ECFV or ICFV were determined by analysis of variance. The Student-Newman-Keuls test was used to compare means when a significant F ratio was obtained. Statistical significance was accepted at $P \leq 0.05$.

RESULTS

The INAA energy spectrum of the activated elements within a sample of rat plantaris muscle is shown in Fig. B-1. The detectable

Fig. B-1. Instrumental neutron activation analysis energy spectrum of rat muscle elements. Energy peaks are indicated for all elements detected following a 10 minute irradiation. The single (SE) and double escape (DE) energies are obtained by subtracting 511.0 (value of annihilation energy) from the designated energy, once for a SE peak and twice for a DE peak. The spectrum was obtained using a hyper-pure germanium detector coupled to a Canberra 8100 multichannel analyzer and plotted using computer graphics. t_i =irradiation time; t_d =delay time; t_c =counting time; m=minutes.



elements following 10 min irradiation of 6-45 mg freeze-dried tissue are indicated. Some elements of interest have more than one main energy, as can be seen for Na^{24} , Cl^{38} , K^{42} , and Mg^{27} . Generally, the energy having the highest relative intensity is used for the calculation of elemental content since this peak will give the highest signal:noise ratio. Peaks with interfering energies cannot be readily used, i.e. Mg^{27} at 843.8 keV has 100% relative intensity but has interference from manganese (Mn^{56}) at 846.8 keV; therefore, the Mg^{27} peak at 1014.5 keV having 40% relative intensity is used. The aluminum (Al) peak in muscle tissue (see Fig. B-1) is believed to represent primarily muscle phosphorus (P) concentration arising from the $^{32}\text{P}(\text{n}, \alpha) ^{28}\text{Al}$ interference reaction of $^{27}\text{Al}(\text{n}, \gamma) ^{28}\text{Al}$, since intracellular [Al] is very low and [P] is high. At present we have not exploited the possibilities of measuring either phosphorous or aluminum.

The intracellular ionic contents of muscles from 26 hindlimbs determined by INAA and by AAS are compared in Table B-1. Both methods showed that there were significant differences between muscle fiber types with respect to their ionic content: the SOL had significantly higher Na^+ and Cl^- contents and significantly lower K^+ , Ca^{++} and Mg^{++} contents than the WG. With an increasing proportion of fast twitch fibers (ie. from SOL to RG to PL to WG; Armstrong and Phelps 1984), there is a reduction in Na^+ and Cl^- contents and an increase in K^+ , Ca^{++} , and Mg^{++} contents.

Repeated measures analysis of variance revealed that there was

a significant systematic difference with respect to technique (INAA vs. AAS) across all fiber types for Na^+ , K^+ and Ca^{++} , but not for Mg^{++} . In general, AAS yielded values for Na^+ that were 16-30% higher, for K^+ that were 4-8% lower and for Ca^{++} that were 18-30% lower than INAA values (Table B-1). A contrast test showed that there was no interaction between fiber type and technique for all elements compared.

Also measured, simultaneous with the above elements, by INAA were the muscle elemental contents of Mn, bromine (Br) and iodine (I) (Table B-1). These values have not been corrected for their ECF contents since their concentrations in the plasma are very low and were not measured. The contents of these three elements were significantly lower in WG than in SOL.

Table B-2 compares values from this study for TTW, ECFV and ICFV in rat hindlimb muscles obtained with mannitol, PEG-900 and the Cl method with literature values obtained using inulin, PEG-900, Cl space, sucrose, and raffinose. As shown previously (Kobayashi and Yonemura 1967; Sreter and Woo 1963) the TTW and ECFV of slow-twitch red muscle (SOL) is greater than in fast-twitch white muscle (WG). In the present study, values of ECFV and ICFV obtained using either ^3H - or ^{14}C -mannitol (Tables B-2 and B-3) agreed well with reported values using inulin. PEG-900 consistently yielded a significantly higher ECFV and lower ICFV than mannitol in all tissues. Measurements of ECFV using Cl space (present study; Cotlove 1954; Vernadakis and Woodbury 1964) clearly overestimate ECFV and underestimate ICFV as measured by mannitol or inulin, particularly in

TABLE B-1

Intracellular ion content of rat hindlimb muscles determined by instrumental neutron activation analysis (INAA) and by atomic absorption spectroscopy (AAS) on the same muscle samples. Values are mean \pm SE (n=26), units are $\mu\text{equiv}\cdot\text{g}^{-1}$ dry wt.

TABLE B-1

Tissue	Na ⁺	K ⁺	Ca ⁺⁺	Mg ⁺⁺	Cl ⁻	Mn ⁺⁺	Br ⁻	I ⁻
Soleus								
INAA	65.7	338.4	8.31	73.8	49.7	4.15	3.71	0.31
	± 4.7	± 8.0	± 0.55	± 2.6	± 3.2	± 0.56	± 0.35	± 0.02
AAS	77.7	325.2	6.84	77.9				
	± 4.5	± 11.4	± 0.30	± 1.2				
Red gastrocnemius								
INAA	27.2	374.9	10.59	96.8	23.3	3.76	3.21	0.37
	± 3.6	± 15.7	± 0.52	± 2.2	± 2.1	± 0.45	± 0.30	± 0.03
AAS	37.0	341.6	7.39	93.8				
	± 3.9	± 17.9	± 0.45	± 2.1				
Plantaris								
INAA	25.0	380.5	9.61	90.6	18.2	1.77	3.23	0.25
	± 2.2	± 9.4	± 0.46	± 2.3	± 1.6	± 0.27	± 0.30	± 0.03
AAS	33.4	359.6	6.08	87.5				
	± 3.5	± 13.1	± 0.39	± 2.2				
White gastrocnemius								
INAA	21.3	404.9	10.13	98.2	14.9	2.04	2.38	0.22
	± 2.1	± 9.6	± 0.59	± 1.5	± 0.9	± 0.29	± 0.20	± 0.02
AAS	24.9	390.3	7.39	95.0				
	± 2.0	± 13.9	± 0.49	± 2.3				

TABLE 8-2

Comparison of rat muscle total tissue water (TTW), extracellular fluid volume (ECFV) and intracellular fluid volume (ICFV).

MUSCLE	n	TTW (ml/kg d.w.) (±TTW)	ECFV (ml/kg d.w.) (±TTW)	ICFV (ml/kg d.w.) (±TTW)	METHOD	REFERENCE
Soleus	4	3505(9)	15.5(0.5)	84.5(0.5)	Mannitol	This study
	4		22.1(1.9)	77.9(2.1)	PEG-900	This study
	13	3310(98)	22.0(2.7)	78.1(2.9)	Cl space	This study
	5	3440(40)	21.0	79.0	Inulin	1
			23.9	76.1	Cl space	1
	26	3444(3)	16.3	83.7(0.4)	Inulin	2
	18	3386(56)	18.5(0.2)	81.5	Inulin	3
Plantaris	4	3292(8)	9.0(0.4)	91.0(0.5)	Mannitol	This study
	4		10.7(0.9)	89.2(1.0)	PEG-900	This study
	13	3200(40)	11.8(1.3)	88.4(1.4)	Cl space	This study
	26	3248(3)	10.3	89.7(0.2)	Inulin	2
Red gastroc.	4	3367(13)	8.6(0.7)	90.7(0.5)	Mannitol	This study
	4		12.3(1.2)	87.7(1.2)	PEG-900	This study
	13	3190(30)	13.0(1.3)	87.0(1.4)	Cl space	This study
	18	3320(3)	12.0(0.1)	88.0	Inulin	2

...continued

TABLE B-2

References

1. Drahota 1961
2. Sreter and Woo 1963
3. Kobayashi and Yonemura 1967 .
4. Vernadakis and Woodbury 1964
5. Law and Phelps 1966
6. Leader et al. 1984

Table 2 (cont'd)

White gastroc.	4	3386(13)	6.5(0.6)	93.5(0.4)	Mannitol	This study
	4		8.4(0.8)	91.6(0.6)	PEG-900	This study
	13	3150(50)	12.4(0.2)	87.6(0.3)	Cl space	This study
	18	3316(3)	9.1(0.1)	90.9	Inulin	2
Whole gastroc.	18	3326(3)	10.0(0.1)	90.0	Inulin	2
	16	3458(2)	15.0(0.2)	85.0(0.1)	Cl space	4
	12		10.0(0.3)		Inulin	5
	14		12.0(2.2)		Sucrose	5
	18		10.7(0.6)		Raffinose	5
BDL	5	3100(18)	18.6	81.4	Cl space	1
	5		14.8	85.2	Inulin	1
	26	3289(2)	10.7	89.3(0.2)	Inulin	2
	17	3367(29)	15.2(1.0)	84.8	Inulin	3
	4	3310(30)	12.4	87.6(0.6)	Inulin-60 min	6
	4	3500(40)	19.9(0.8)	80.1	Inulin-160 min	6
	4	3310	15.5	84.5(0.6)	PEG-900-60 min	6
	4	3500	29.1(1.4)	70.9	PEG-900-160 min	6

Note: Values in brackets () are standard errors of the mean. Values for Sreter and Woo (1963) and Vernadakis and Woodbury (1964) were converted from wet wt to dry wt using the following factors: soleus, 4.505; plantaris, 4.292; red gastrocnemius, 4.367; white gastrocnemius, 4.386; whole gastrocnemius, 4.377.

TABLE B-3

Muscle total tissue water (TTW), ECFV, ICFV, and intracellular ion concentrations from 13 rat hindlimbs.

TTW	ECFV	ICFV	[Na ⁺]	[K ⁺]	[Cl ⁻]	[Mg ⁺⁺]	[Ca ⁺⁺]	[La ⁻]
(ml/kg wet wt.)			(mmol/l intracellular fluid)					
Soleus								
766	79	688	17.2	117	18.5	24.2	2.42	1.1
± 6	± 14	± 13	± 1.5	± 6	± 3.2	± 1.4	± 0.30	± 0.2
Red gastrocnemius								
760	58	703	9.6	124	15.1	31.3	2.91	1.9
± 3	± 10	± 11	± 0.7	± 6	± 1.4	± 1.5	± 0.33	± 0.4
Plantaris								
761	57	702	10.6	136	10.9	28.9	2.71	2.0
± 2	± 8	± 8	± 1.3	± 7	± 1.2	± 1.5	± 0.36	± 0.7
White gastrocnemius								
758	64	701	9.6	143	8.7	31.2	3.50	2.5
± 2	± 10	± 13	± 0.9	± 6	± 1.1	± 1.9	± 0.64	± 1.1

muscles having a low TTW (WG and PL). In contrast to the present study using PEG-900 in fast-twitch white muscle, Leader et al. (1984) obtained a very high ECFV in rat extensor digitorum longus (EDL) using PEG-900 equilibrated for 160 min.

The concentrations of intracellular ions in the ICF from 13 hindlimbs are shown in Table B-3. These values were calculated from intracellular ion contents determined by INAA and from muscle ECFV measured by the distribution of ^3H -mannitol. The differences in intramuscular fluid content and ion concentrations between the muscle types is clearly apparent. Muscle fiber types having a high glycolytic potential (fast-twitch WG) had a significantly higher ICFV, $[\text{K}^+]$ and $[\text{Mg}^{++}]$ and lower TTW, ECFV, $[\text{Na}^+]$ and $[\text{Cl}^-]$ than muscles with a high proportion of oxidative fibers (slow-twitch SOL).

DISCUSSION

Measurement of intracellular ions

In the present study, we report the results of a practical adaptation of the technique of INAA from its more common biological use in trace element research (Heydorn 1984) to the investigation of the major ion species within mammalian skeletal muscle. Although we are not the first to do so (see Bergstrom 1962), this practical method has not yet come into widespread usage. Also, in this study, we have compared the suitability of INAA methods for analysis of the elemental composition of a complex tissue with that of the more widely used method of AAS. Perhaps INAA may be unsuited to investigators who

cannot gain ready access to nuclear reactor facilities. However, once the sample is in a freeze-dried powdered form, research nuclear reactor facilities can readily perform these analyses.

The accuracy of the values determined for intracellular contents of Na^+ , K^+ , Ca^{++} , Mg^{++} , and Cl^- depends critically on the measured or assumed values for the extracellular space and on the respective ion concentrations in the ECF. This is particularly true for Na^+ and Cl^- , because their ECF concentrations are relatively high. The values for intramuscular ion contents ($\mu\text{Eq}\cdot\text{g}^{-1}$ dry wt) reported in Table B-1 are similar to those reported by McCaig and Leader (1984) and Sembrowich et al. (1982). Values expressed as intramuscular ion concentrations (Table B-3) are also similar to previously reported values (Donaldson and Leader 1984; Jaweed et al. 1982; McCaig and Leader 1984). However, there were consistent differences between technique (INAA vs. AAS) with respect to measured values for Na^+ , K^+ and Ca^{++} in all muscles (Table B-1). The reasons for these discrepancies are unclear and possible sources are discussed below. Nonetheless, the values reported by either technique are within the range of previously reported values.

At present the major techniques for ion analysis in muscle are AAS (Jaweed et al. 1982) and flame photometry (Cotlove et al. 1951; Sreter and Woo 1963). While both of these methods can be performed readily, they have a number of disadvantages. The major drawbacks of the techniques are associated with ionization problems and chemical interferences which can only be corrected by the addition of

appropriate ionization suppression agents to the solutions, a potential source of contamination and dilution errors. Contamination and dilution errors may also result during acid dissolution and subsequent dilution of the solution to a concentration appropriate for AAS or flame photometric determination. Individual dilutions usually must be made for each element to be analyzed and all of the solutions analyzed separately. This can easily result in orders of magnitude increases in the number of samples to be processed. Also, anions such as chloride cannot be directly measured by AAS or flame photometry.

INAA has a number of advantages over other commonly used methods of intracellular elemental analysis, perhaps the most important being that all major ion species within a single tissue sample can be determined simultaneously. This greatly reduces sample handling and sources of contamination, and greatly increases the number of tissues which can be analyzed in a given time. The short irradiation time used poses no radiation hazard when proper handling precautions are taken, nor does it destroy the freeze-dried tissue as does AAS. Thus, once the radiation levels in the tissue have subsided (1-2 weeks), the tissue may be used subsequently for other types of analyses or stored indefinitely. Also, because only a small amount of the total tissue sample is required for the analysis, many other analyses may be performed on the remaining muscle sample. Tissue for INAA can be used wet and unpreserved and, so long as reference values for extracellular fluid volume and ion concentrations are available, intracellular composition can be determined easily. In the wet state, however, the oxygen in the tissue fluids will give a higher background

energy which may slightly reduce the precision of the measurements. One disadvantage of INAA, as well as AAS and flame photometry, is that it can not yield information about the intracellular compartmentalization of the elements being examined. Those studies require the use of electron microprobe analysis (Gupta and Hall 1981; Sembrowich et al. 1982) or ion-selective microelectrodes (Aickin and Thomas 1977; Donaldson and Leader 1984; McCaig and Leader 1984).

The potential sources of error in INAA include variations in neutron flux density and counting errors; both topics are discussed in detail by Bergstrom (1962) and Heydorn (1984). Variations in flux density are not likely to affect the present results due to the short duration of the activation and frequent checks using standards. Counting errors may be the greatest source of error in INAA. These include statistical errors in peak and background determinations for the samples and standards. Since the error of a single determination is proportional to the square root of the total number of counts, elements detected and counted with a low peak:background ratio will have a greater counting error or variability. In our study, this appeared to be the case for Ca, where the counting error ranged from 5-20% depending on the sample size. For all other major elements, the standard error of counting was $\leq 5\%$.

Ion-selective microelectrodes are not suited for following ion transients in contracting skeletal muscle due to probable breakage of the electrode and high background noise. Additionally, each ion to be studied requires a specific microelectrode; thus, numerous electrodes may be needed for a single study. While electron

microprobe analysis is a good technique for investigation of ion shifts between the various intracellular compartments (Sembrowich et al. 1982) and between the cytosol and the interstitial fluids (Gupta and Hall 1981), the procedure is susceptible to contamination from sectioning and coating of specimen material. It is also very time consuming and requires the use of specialized electron microscopy equipment.

Measurement of extracellular fluid volume

Inulin is one of the most widely used markers of ECFV in a variety of tissues and is considered to be a reliable method against which other techniques have been measured (Cotlove 1954; Drahota 1961; Glasby 1985; Leader et al. 1984; Manery 1954). Due to its high molecular weight (5000), it does not readily penetrate cell membranes. Inulin is also not metabolized by most tissues but is readily taken up by macrophages in kidney, liver, spleen and skin (White and Rolf 1957; McIver and Macknight 1974) and may thus overestimate ECFV in those tissues. The present study compared three methods for estimating ECFV in skeletal muscle, mannitol, PEG-900, and Cl space.

The main reason for using mannitol in this study was a high level of labelled low molecular weight impurities in the labelled inulin available. In the past this necessitated repurification of inulin to high molecular weight fractions using Sephadex G-50 (Walsh et al. 1984). Failure to remove low molecular weight compounds results in abnormally high values for ECFV. Despite the fact that mannitol is of much lower molecular weight (182.2) than inulin, it gave muscle ECFV values very similar to those from inulin reported by

other authors (Table B-2). In contrast, Page (1962) has shown that inulin substantially underestimates the mannitol space in cat heart papillary muscle. Page (1962) provides convincing evidence that mannitol: 1) is the smallest carbohydrate ECF marker that is impermeable to cells, 2) is not adsorbed to extracellular components, and 3) is highly representative of muscle ECFV. Furthermore, Glasby (1985) has shown that in the dog only cells of the liver (and possibly the kidneys) are significantly penetrated by mannitol.

The PEG-900 space yielded values for ECFV significantly greater than the mannitol space in rat hindlimb muscles (Table B-1). The PEG-900 space in rat EDL (Leader et al. 1984) and the PEG-1000 space in mammalian kidney and liver slices (McIver and Macknight 1974) have also been shown to be significantly greater than the corresponding inulin space. Furthermore, Leader et al. (1984) showed that the PEG-900 space in isolated rat EDL increased from 697 to 1019 ml.kg^{-1} dry wt in 100 min (see Table B-2).

The present study showed that the Cl space yielded an ECFV which was 8-35% greater than previously reported values for the inulin space (Table B-2). Others have reported that the distribution of inulin in the Cl space of muscle is only about 80% complete in 3 hours (Cotlove 1954; Drahota 1961; Vernadakis and Woodbury 1964). Assuming that inulin is fully distributed within the ECFV of muscle after 3 hours, the corollary of these observations is that ECFV measured by the Cl method is too large and that Cl^- is not passively distributed across the sarcolemma. According to the distributions of both mannitol and inulin in heart muscle (Page 1962), Cl^- also

appears not to be passively distributed in this tissue. In the calculation of ECFV by the Cl method (equation B-2), the intracellular $[Cl^-]$ must be calculated first from the extracellular $[Cl^-]$ and the resting membrane potential (equation B-3). Using values for E_m of -76, -78, -80, and -82 mV for the SOL, RG, PL and WG respectively (Wareham 1978), the intracellular Cl^- concentrations calculated using equation 5 yielded mean values of 4.64, 4.28, 3.95 and 3.65 $mEq.l^{-1}$ respectively in muscles from the 13 hindlimbs in which mannitol space was measured (Table B-3). These calculated $[Cl^-]_i$ values are significantly lower than those in muscle in this and other studies (Donaldson and Leader 1984; McCaig and Leader 1984; Page 1962). If, however, the $[Cl^-]_i$ values reported in Table 3 are substituted in the Cl method equation (equation B-2), much lower Cl space values are obtained which are in keeping with the ECFV measured using mannitol or inulin. With present techniques one cannot say with certainty whether or not Cl^- is passively distributed across the sarcolemma. Microelectrode techniques have provided evidence both for (McCaig and Leader 1984) and against (Dulhunty 1978; Hironaka and Morimoto 1980) the passive distribution of Cl^- in skeletal muscle.

We conclude, that the mannitol space is a valid and reliable measure of ECFV in skeletal muscle. Also, mannitol does not pass into the skeletal muscle cell nor is it metabolized to any appreciable extent over a 3 hour period (Page 1962). In contrast, PEG-900 and the Cl method both overestimate ECFV in skeletal muscle. PEG-900 may accomplish this by entering the ICF of skeletal muscle cells, as has

been suggested for PEG-1000 in kidney and liver (McIver and Macknight 1974). The apparent problems with the CI method are inherent in the assumptions and calculations.

In summary, we have shown that muscle ion and fluid concentrations are closely associated with muscle fiber type and oxidative capacity. INAA has been shown to be a simple and useful method, while being sufficiently accurate and precise to measure changes in intramuscular ion concentrations in the mmol range, despite the apparent discrepancy with AAS values.

Acknowledgements

The authors thank Dr. S. Landsberger and the staff of the McMaster University Nuclear Reactor for their technical assistance. We also thank Dr. L. Spriet, Dr. M. Ganagarajah and S. Peters for their work in the laboratory, Dr. D.G. McDonald for the use of the Varian AA-1275, Dr. R. Roberts for assistance with the statistical analysis, and Drs. N.L. Jones and P.A. Stewart for critical reading of the manuscript.

APPENDIX C

EFFECTS OF INTENSE SWIMMING AND TETANIC ELECTRICAL STIMULATION
ON SKELETAL MUSCLE IONS AND METABOLITES

Michael I. Lindinger, George J.F. Heigenhauser and Lawrence L. Spriet

Submitted to: Journal of Applied Physiology

ABSTRACT

The purpose of this study was to compare changes in ions and metabolites in four different rat hindlimb muscles in response to intense swimming exercise in vivo (263 ± 33 s) (SWUM), and to 5 min (300 s) of tetanic electrical stimulation of the perfused rat hindlimb (STIM). Hindlimbs of the STIM group were perfused with a bovine erythrocyte perfusion medium. The exercise-induced changes in muscle metabolites, and increased muscle total tissue water, were similar in both groups. With exercise, in both groups, soleus (SL) contents of creatine phosphate (CP), adenosine triphosphate (ATP) and glycogen changed the least, whereas the largest decreases in these metabolites occurred in the white gastrocnemius (WG). Lactate (La^-) accumulation and glycogen breakdown were significantly greater in SWUM hindlimb muscles compared to STIM. The high arterial La^-

concentration ($[La^-] = 20 \pm 1 \text{ mmol.L}^{-1}$) in SWUM may contribute to elevated muscle $[La^-]_i$, whereas one-pass perfusion kept arterial $[La^-]$ below 2 mM STIM. In SWUM, intracellular $[Na^+]_i$ increased significantly in the plantaris (PL), red gastrocnemius (RG) and WG, but not in SL; $[Cl^-]_i$ increased and $[K^+]_i$, $[Ca^{++}]_i$, and $[Mg^{++}]_i$ decreased in all muscles. In STIM, there were significant decreases $[K^+]_i$, $[Mg^{++}]_i$ and $[Ca^{++}]_i$, while $[Na^+]_i$ and $[Cl^-]_i$ increased in all muscles. Differences in the magnitude of ion and fluid fluxes between groups can be explained by the different methods of hindlimb perfusion. In conclusion, electrical stimulation of the isolated perfused rat hindlimb is a useful model of in vivo energy metabolism and permits mechanisms of trans-sarcolemmal ion movements to be studied.

INTRODUCTION

Electrical stimulation of the isolated perfused rat hindlimb preparation has been used as a model to study skeletal muscle metabolism during exercise (Berger et al. 1975; Spriet et al. 1985). This preparation enables quantitation of muscle force generation, fatigue and muscle energy expenditure in a small group of hindlimb muscles. The stimulation protocol used generally produces a 45% reduction in tension development over a 5 min period of stimulation (Spriet et al. 1985; 1986). This response has been assumed to be representative high intensity exercise in vivo. The preparation has been criticized on the grounds that the intense repeated tetanic stimulation protocol may result in non-metabolic pre-contractile

fatigue (Bigland-Ritchie and Woods 1984) and thereby invalidate any associations between tension decline, metabolism, and ion regulation during the development of muscle fatigue. One of the purposes of this study, therefore, was to compare the metabolic responses of skeletal muscle to electrical stimulation in vitro with those occurring in high intensity swimming exercise in unanaesthetized animals.

A second purpose of the study was to quantify the magnitude and direction of fluid shifts and strong ions fluxes (those ions which are fully dissociated in physiologic solutions (Stewart 1981): Na^+ , Cl^- , K^+ , Mg^{++} , and La^-) resulting from intense exercise in vivo and in vitro. Differences between the two exercise protocols (STIM vs SWUM) were expected because the former utilizes a one-pass perfusion system in which composition of the arterial perfusion medium is kept constant (Lindinger et al. 1986), compared to the variable arterial composition of the intact circulation in vivo. The one-pass system, therefore, should facilitate the efflux, from working muscle, of substances which are rapidly accumulating, while maintaining arterial composition constant.

Muscle fatigue resulting from heavy exercise is associated with changes in fluid and electrolyte balance (Fenn and Cobb 1936; Sreter 1963; Hnik et al. 1976; Tibes et al. 1977; Hürche et al. 1980; Sjogaard et al. 1985; Juel 1986) of the working muscles. There is an increase in intracellular fluid volume (ICFV) of working muscle, accompanied by an increase in the intracellular concentrations of Na^+ and Cl^- and a reduction in K^+ and La^- (Fenn and Cobb 1936; Sreter 1963; Sjogaard et al. 1985; Juel 1986). These

intracellular disturbances are accompanied by increases in extracellular fluid volume (ECFV), reductions in Na^+ and Cl^- concentrations, and increases in K^+ and La^- concentrations (Hnik et al. 1976; Tibes et al. 1977; Hirsche et al. 1980; Juel 1986).

The present study showed there was little difference in the metabolic response of the muscles in the two exercise protocols. While the magnitude, but not direction, of fluid and ion fluxes differed between groups, these differences will facilitate an investigation of the relationships between ion regulation and metabolism in skeletal muscle. These studies further support the usefulness of the isolated stimulated rat hindlimb preparation as a model for in vivo muscle metabolism during exercise.

METHODS

Animals

Male Sprague-Dawley rats weighing 396 ± 7 g ($n=36$) were used. The animals were fed Purina laboratory chow ad libitum and housed in a controlled environment with 12 h of day and night. The animals were divided into two groups: the in vivo swimming group (SWUM); and the in vitro stimulated perfused hindlimb group (STIM). Each group was subdivided into resting controls ($n = 10$ for SWUM; and $n = 7$ for STIM) and exercised animals ($n = 8$ for SWUM; and $n = 11$ for STIM).

Three to 5 hours prior to tissue sampling the rats were injected via a tail vein with 0.5 ml 0.9% saline solution containing 25 μCi of ^3H -mannitol (New England Nuclear) for determination of muscle extracellular and intracellular fluid volumes (ECFV and ICFV

respectively) as described previously (Appendix B).

Experimental Protocol

(a) STIM. The rats were anaesthetized with an intraperitoneal injection of sodium pentobarbital (6 mg/100g body wt) and the left hindlimb surgically prepared for perfusion and electrical stimulation of the gastrocnemius-plantaris-soleus (GPS) muscle group of the left hindlimb as described by Spriet et al. (1986). The lower trunk of the sciatic nerve was severed and connected to a shielded bipolar platinum electrode using a snug-fitting rubber collar. The left knee and ankle were stabilized with brackets and the GPS tendon attached to a force transducer (Statham No. 10713). The femoral artery and vein were exposed above the knee and occlusively cannulated with 22 and 18 gauge teflon catheters (Deseret Medical Inc.) respectively. The arterial catheter was advanced as far as possible toward the popliteal space in order to restrict perfusion to the lower portion of the limb. The limb was flushed with 1 ml of sterile, heparinized (100 U/ml) 0.9% saline and the animal sacrificed by intracardiac injection of sodium pentobarbital (20 mg). The rat was placed in a 37°C perfusion chamber and the lower hindlimb perfused with an oxygenated bovine erythrocyte perfusion medium (Spriet et al. 1985a; Lindinger et al. 1986), with the characteristics shown in Table C-1.

The resting hindlimbs of the STIM group were perfused for 20 min at a flow rate of $2.0 \text{ ml} \cdot \text{min}^{-1}$. Samples of the SL, RG, PL and WG muscles were immediately removed, freeze-clamped and stored in liquid nitrogen. The stimulated hindlimbs were perfused for 20 min at resting flow rates ($2.0 \text{ ml} \cdot \text{min}^{-1}$), and then for 5 min at a flow

TABLE C-1

Characteristics of the bovine erythrocyte
perfusion medium.

[hemoglobin]	140	g.l^{-1}
hematocrit	39	%
[albumin]	50 ± 1	g.l^{-1}
[glucose]	5.6 ± 0.2	mEq.l^{-1}
[lactate]	1.0 ± 0.1	mEq.l^{-1}
[Na ⁺]	140.0 ± 0.4	mEq.l^{-1}
[Cl ⁻]	119.0 ± 0.6	mEq.l^{-1}
[K ⁺]	5.7 ± 0.3	mEq.l^{-1}
[Ca ⁺⁺] (ionized)	2.6 ± 0.1	mEq.l^{-1}
[SID]	38.6 ± 0.4	mEq.l^{-1}
PCO ₂	40.5 ± 0.9	Torr
HCO ₃ ⁻	22.3 ± 0.8	mEq.l^{-1}
pH	7.41 ± 0.01	
[³ H-mannitol]	160	$\mu\text{Ci.l}^{-1}$

rate of $7-8 \text{ ml} \cdot \text{min}^{-1}$ while being electrically stimulated. At these perfusate flows, tissue oxygen consumption was independent of flow rate. The sciatic nerve was electrically stimulated (Grass Instruments S48) for 5 min to produce muscular contraction. The stimulation was intermittent, consisting of trains lasting 100 msec at a train frequency of 0.5 Hz. Each train contained 10 pulses of 0.2 msec duration at a supramaximal 5 volt intensity at a frequency of 100 Hz. At the end of stimulation, the muscles were immediately sampled, freeze-clamped and stored in liquid nitrogen. The time required for removal of the four muscles was about 90 s; stimulation and perfusate flow to the hindlimb was maintained until the muscles were removed. Arterial and venous perfusates were sampled via syringe at 5 min intervals during rest and at 1 min intervals during stimulation.

The mass of perfused hindlimb muscle was determined on a separate group of 12 rats (300-450 g). Femoral vessels were cannulated as described above and perfused for 5 min with dye (0.1 g toluidine blue in 1.0 liter 0.9% saline). Hindlimb muscles were subsequently removed, blotted lightly to remove excess fluid and wrapped in plastic to prevent dehydration. Muscles were weighed within 10 min of their removal.

(b) SWUM. Control rats of the SWUM group were anaesthetized with sodium pentobarbital (6 mg/100 g body wt ip), the abdomen opened and an arterial blood sample (3-5 ml) obtained via the abdominal aorta using syringes treated with lithium heparin. The hindlimb muscles from both legs were sampled and stored as described above.

Prior to the experiment, a separate group of rats were fitted

with tail weights in order to determine the body mass:tail weight ratio which resulted in exhaustion (defined as the inability to surface for 15 s) after about 5 min of swimming. This ratio was found to be close to 20:1. Thus the rats to be exercised SWUM rats were fitted with tail weights (5% of body weight) and swum singly in a 50 cm deep X 50 cm diameter water bath (37°C) which was aerated to produce vigorous bubbling. The vigorous bubbling ensured that the animals continuously swimming rather than attempting to cling to the side of the container or to passively bob up and down. Rats were swum until exhaustion, quickly removed from the bath and sacrificed by cervical dislocation. Blood and tissues were sampled as described above; total time for sampling was less than 2.5 min.

Analytical Procedures

Perfusate pH, PCO_2 , and PO_2 were measured within 7 min of sampling with a Radiometer BMS 3 blood acid-base analyzer and Radiometer PHM 72 pH meter. Arterial and venous plasma concentrations of Na^+ , K^+ , and ionized Ca^{++} were measured using ion selective electrodes (Radiometer KNA1 sodium/potassium analyzer and Radiometer ICA1 ionized calcium analyzer). Plasma $[\text{Cl}^-]$ was measured using a Buchler-Cotlove chloride titrator.

Muscle samples (100 - 500 mg wet weight) were wrapped in aluminum foil and stored in liquid nitrogen until freeze-dried and analyzed. Each sample was pulverized in liquid nitrogen using a stainless steel mortar and pestle, visible connective tissue removed, and the pulverized sample weighed frozen to determine wet weight. The samples were subsequently freeze-dried and reweighed.

Muscle metabolites (glycogen, lactate — La^- , creatine phosphate — CP and adenosine triphosphate — ATP) were extracted in 25-30 volumes of ice-cold 3 M perchloric acid for 20 min. The solutions were neutralized with an appropriate volume (350-400 μl) of 2.5 M potassium carbonate and the neutralized extract removed after 30 min centrifugation (10,000 rpm) at 4°C (Sorval RC2-B automatic refrigerated centrifuge). These extracts were analyzed for metabolites using standard enzymatic techniques (Bergmeyer, 1965).

Muscle ECFV was determined from the distribution of ^3H -mannitol as described previously (Lindinger and Heigenhauser, submitted). Arterial and venous plasma samples (0.1 ml) and 70-200 mg wet weight muscle samples were digested in 2 ml tissue solubilizer (NCS, Amersham) until a clear solution was obtained (6-9 days). The solution was neutralized with 60 μl glacial acetic acid, and 13 ml fluor (OCS, Amersham) added. Samples were placed in a cool, dark place overnight to reduce chemiluminescence and counted on a Beckman LS-250 scintillation counter. Quench correction was performed using external standards with a series of quench standards prepared from plasma and red and white muscle.

Tissue ECFV for each isotope was calculated from the formula:

$$(C-1) \quad \text{ECFV (ml.g}^{-1} \text{ wet wt.)} = \frac{\text{tissue counts}}{(\text{plasma counts} / \text{plasma water content})}$$

$$(C-2) \quad \text{ECFV (ml.g}^{-1} \text{ dry wt.)} = \text{ECFV (ml.g}^{-1} \text{ WW)} \times (\text{WW} / \text{DW})$$

ICFV was calculated as the difference between TTW and ECFV.

Intracellular muscle ion contents ($\mu\text{Eq/g}$ dry weight) were measured by instrumental neutron activation analysis as described by Lindinger and Heigenhauser (submitted). Briefly, 10-50 mg of freeze-dried muscle powder within a small (8 x 20 mm) polyethylene vial was irradiated with thermal neutrons for 3-10 min near the reactor core (McMaster Nuclear Reactor, Hamilton, Canada). The irradiated sample was analyzed for total content of Na^+ , K^+ , Ca^{++} , Mg^{++} and Cl^- using the isotopic gamma emission energy spectra of the various elements. The gamma energy spectra emitted by a sample were detected by a hyper-pure germanium detector, and collected and analyzed using a multichannel analyzer (Canberra Series 40 or Series 90). Muscle intracellular ion concentrations (mEq/l intracellular fluid — ICF) were calculated as the difference between total elemental content and the ion content of the extracellular fluids, then converted to concentration in mEq/l ICF (Lindinger and Heigenhauser, submitted).

Statistics

All values are presented as mean + standard error. The effects of each treatment on measured muscle variables was assessed by one-way ANOVA. When a significant F ratio was obtained the treatment means were compared using Student's two-tailed t test, unpaired design. Statistical significance was accepted at $p < 0.05$.

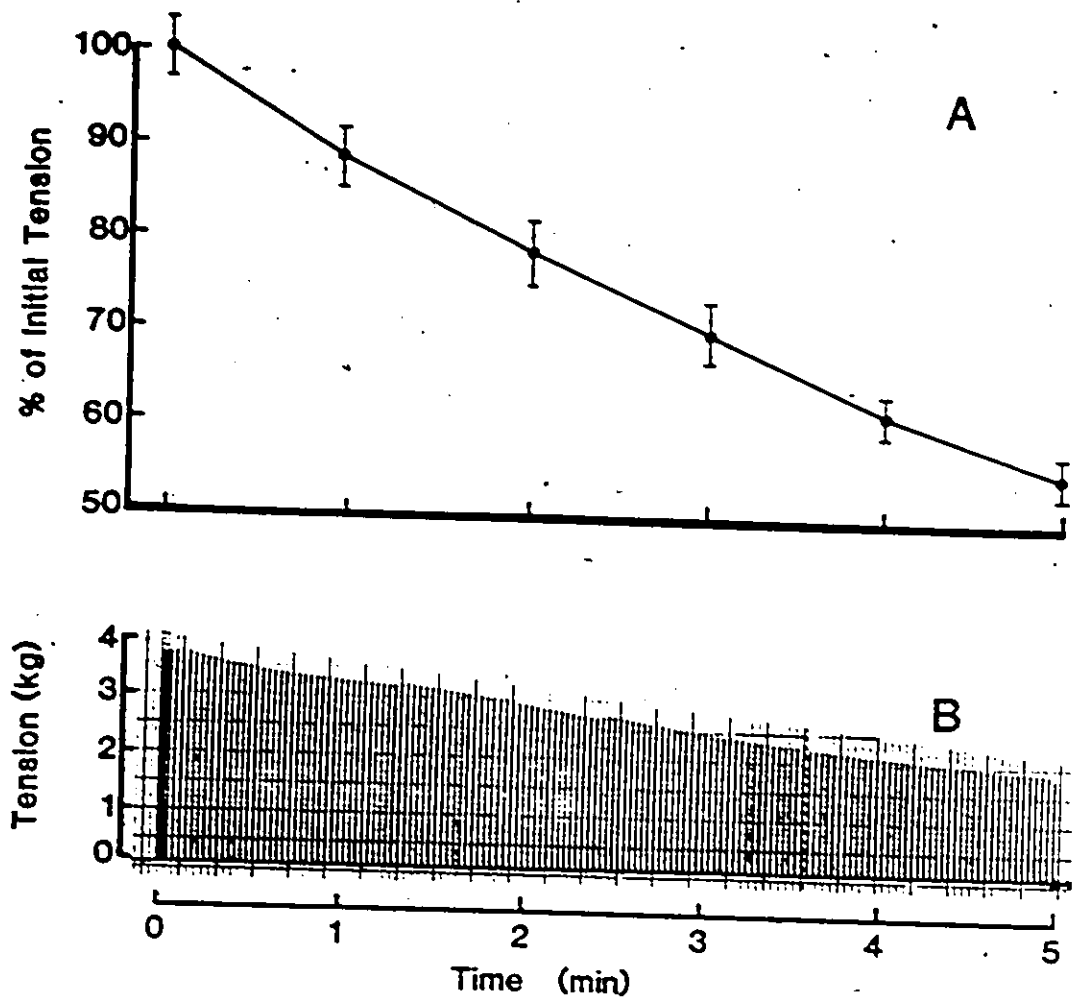


Fig. C-1. (A) Isometric tetanic tension generated (STIM group) by the gastrocnemius-plantaris-soleus muscle group ($n = 11$) during 5 min of electrical stimulation; peak tension = $100\% = 3367 \pm 105$ g (mean \pm SE); (B) typical fatigue curve.

TABLE C-2

Contributions of the soleus, plantaris, red and white gastrocnemius muscles to the total perfused and stimulated hindlimb masses.

Muscle	Relative Mass (mg/100 g body mass)		% of perfused muscle	% of stimulated muscle
	This Study	Reference		
Soleus	43.7 \pm 2.4	43.0 \pm 4.6	2.83	3.44
Red gastrocnemius	(35.7)*	34.5 \pm 8.6	2.31	2.81
Plantaris	103 \pm 4	98.5 \pm 9.3	6.67	8.10
White gastrocnemius		32.3 \pm 3.8		
Mixed gastrocnemius	(496)*	450 \pm 29	32.1	39.0
Entire gastrocnemius	532 \pm 15	514 \pm 44	34.5	41.9
Entire GPS	679 \pm 19	656 \pm 53	44.0	53.4

* Assumes, in the present study, that the fiber type composition of mixed gastrocnemius and white gastrocnemius are sufficiently similar (Armstrong and Phelps 1984) to pool their contributions. The mass of red gastrocnemius used in the present study was 6.7% of the entire gastrocnemius, or 35.7 mg/100 g body mass, leaving 496 mg of "white" gastrocnemius per 100 g body mass. Reference values were calculated from Armstrong and Phelps (1984).

TABLE C-3

Metabolite contents in biopsies taken from resting and exercised muscles from perfused hindlimbs and from swimming group hindlimbs.

Muscle/ Condition	CP	(μmol.g ⁻¹ dry wt)		
		ATP	Glycogen	Lactate
Soleus				
CONTROL	57.7 ± 5.8	19.6 ± 1.4	105 ± 9	3.8 ± 0.7
STIM-rest	56.9 ± 5.5	18.9 ± 1.0	108 ± 13	3.3 ± 0.8
STIM	30.8 ± 3.3	17.8 ± 0.9	106 ± 5	6.5 ± 1.6
SWUM	19.1 ± 5.0	15.0 ± 0.8	87.9 ± 6.2	54.7 ± 5.8
STIM	26.1*	1.1	2.0	-3.2*
SWUM	38.6*	4.6	17.1 [#]	-50.9* [#]
Red Gastrocnemius				
CONTROL	80.9 ± 6.4	27.2 ± 1.6	130 ± 7	3.2 ± 0.5
STIM-rest	82.8 ± 4.3	28.3 ± 0.9	124 ± 8	4.7 ± 0.8
STIM	21.2 ± 6.4	21.3 ± 1.2	65.3 ± 7.9	59.2 ± 8.8
SWUM	17.2 ± 5.4	19.4 ± 2.2	28.1 ± 5.2	104 ± 9
STIM	61.6*	7.0*	65*	-55*
SWUM	63.7*	7.8*	102 [#]	-101* [#]

(cont'd)

TABLE C-3 (cont'd)

Muscle/ Condition	CP	(μmol.g ⁻¹ dry wt)		
		ATP	Glycogen	Lactate
Plantaris				
CONTROL	77.0 ± 4.1	25.1 ± 2.3	122 ± 7	4.1 ± 0.5
STIM-rest	79.9 ± 3.4	29.4 ± 1.2	118 ± 6	7.3 ± 1.0
STIM	25.3 ± 4.8	18.9 ± 1.0	62.1 ± 7.6	76.7 ± 10.8
SWUM	19.4 ± 9.5	18.1 ± 1.6	41.8 ± 6.9	113 ± 9
STIM	54.6 [*]	10.5 [*]	56 [*]	-69 [*]
SWUM	57.6 [*]	7.0 [*]	80 [*]	-109 ^{**}
White Gastrocnemius				
CONTROL	89.9 ± 5.3	30.7 ± 1.1	121 ± 5	4.5 ± 0.6
STIM-rest	93.4 ± 5.8	33.9 ± 0.8	128 ± 8	5.3 ± 0.8
STIM	20.4 ± 6.0	18.4 ± 1.9	32.7 ± 4.2	106 ± 9
SWUM	17.3 ± 8.4	18.2 ± 2.3	48.2 ± 7.7	138 ± 14
STIM	73.0 [*]	15.5 [*]	95 [*]	-101 [*]
SWUM	72.6 [*]	12.5 [*]	73 [*]	-133 ^{**}

CONTROL are means ± SE from 16 right hindlimbs. STIM-rest are from 7 perfused but not stimulated left hindlimbs. STIM are from 7 perfused and stimulated (5 min) left hindlimbs. SWUM are from 4 left and 4 right (n=8) hindlimbs from swim group rats. * indicates significant difference between CONTROL and SWUM, and between REST and STIM values. # indicates significant difference in change between STIM and SWUM groups.

RESULTS

Performance

The peak isometric tension generated by the STIM group was 3367 ± 107 g. Maximal force generation occurred immediately at the start of stimulation, then decreased by 22% and 45% after 2 and 5 min of stimulation (Fig. C-1A). The rate of tension decline during the 5 min appeared to be linear (Fig. C-1B). In comparison, SWUM rats swam for 263 ± 33 s (mean \pm SE), a 12% shorter duration of exercise than the STIM group.

The average mass of perfused muscle tissue in the dye-perfused hindlimb muscles ($n = 12$ hindlimbs) was measured to be 1.54 ± 0.06 g per 100 g rat body mass. The electrically stimulated muscle mass averaged 1.27 ± 0.03 g per 100 g body mass, or 82% of perfused muscle mass. The relative contributions of the gastrocnemius-plantaris-soleus (GPS) muscles as a percentage of perfused and stimulated muscle masses are given in Table C-2. The respective masses of the SL, RG, PL and WG muscle in the present study averaged 185, 151, 436 and 2,098 mg per hindlimb. The entire GPS complex formed 44% of the total perfused muscle mass, and 53.4% of the total stimulated muscle mass.

The flow rates used in the present study were calculated on the basis of perfused muscle mass (see Table C-2) and found to be $0.3 \text{ ml} \cdot \text{min}^{-1} \cdot \text{g}^{-1}$ at rest, and $1.5 \pm 0.1 \text{ ml} \cdot \text{min}^{-1} \cdot \text{g}^{-1}$ during stimulation. Arterial perfusion pressures increased from 80-120 mmHg at rest to 110-150 mmHg during stimulation.

Metabolites

Hindlimb oxygen uptake increased from 2.9 ± 0.2 $\mu\text{mole}\cdot\text{min}^{-1}$ at rest to 15 ± 1 $\mu\text{mole}\cdot\text{min}^{-1}$ during stimulation.

Glucose uptake by the hindlimbs increased from an average of 0.35 $\mu\text{mole}\cdot\text{min}^{-1}$ at rest to 0.52 $\mu\text{mole}\cdot\text{min}^{-1}$ during stimulation.

Hindlimb La^- release increased from 0.55 $\mu\text{mole}\cdot\text{min}^{-1}$ at rest to 11 ± 1 $\mu\text{mole}\cdot\text{min}^{-1}$ averaged over the 5 min of stimulation.

Muscle metabolites are shown in Table C-3. There were no differences between Control and STIM resting values for all metabolites examined, indicating that resting perfusion had no significant effects on muscle metabolism. In SWUM and STIM groups, exercise resulted in significant, and similar, decreases in CP contents of all hindlimb muscles examined. In STIM, SL showed no changes in ATP and glycogen contents and only a small increase in La^- ; however, progressively larger proportions of ATP and glycogen stores were utilized, and La^- produced and accumulated, by RG, PL and WG muscles. Similar changes occurred in the SWUM group, but glycogen utilization and lactate accumulation in all muscles except WG was significantly greater in SWUM than in STIM (Table C-3). In SWUM, the La^- content of SL was 18-fold greater than in STIM. There were no differences in the final contents of ATP between the two exercise groups.

Muscle Fluid Volumes

The TTW of all STIM resting muscles was 2-4% greater than that of Control muscles (Table C-4). The increase in TTW during perfusion of resting muscle was partitioned between a 2-4% increase in ICFV and

a 2-20% increase in ECFV. Exercise resulted in a significant increase in TTW in all muscles from both groups of animals. In STIM, ECFV increased significantly in all muscles except WG, and ICFV also increased significantly in RG and WG. In SWUM, ECFV and ICFV were increased above resting values at the end of exercise, but the differences were not significant. In STIM, the increases in ECFV and ICFV of the SL and RG muscles were greater than in SWUM. There were no differences ECFV and ICFV of PL and WG muscles between groups, at the end of exercise.

Muscle Ions

Total muscle ion contents measured using instrumental neutron activation analysis were corrected for the quantity of ion in the muscle ECFV as described previously to obtain the intracellular ion contents ($\mu\text{Eq/g}$ dry wt.) shown in Table C-5. These values are presented to facilitate comparisons to previous studies of muscle ions. The intracellular ion concentrations calculated from TTW and ICFV measurements (see Appendix B) are presented in Table C-6, together with the calculated intracellular strong ion difference ($[\text{SID}]_i$); these values have greater physiological significance.

In STIM resting muscle, $[\text{K}^+]_i$ was significantly lower than that of Controls in RG and PLT (Table C-6). In all muscles except WG, $[\text{Na}^+]_i$ and $[\text{Cl}^-]_i$ were significantly higher than in Controls. These results indicate that the perfusate and muscles were not, at least initially, in a steady state.

Despite the difference in initial ion concentrations in Control and STIM resting muscles (Table C-6), the intense

TABLE C-4

Total tissue water (TTW), extracellular fluid volume (ECFV) and intracellular fluid volume (ICFV) in biopsies taken from resting and exercised muscles from stimulated group hindlimbs and swim group hindlimbs.

Muscle	Condition	TTW	(ml.g ⁻¹ wet wt) ECFV	ICFV
Soleus				
	CONTROL	.766 ± .004	.079 ± .008	.688 ± .007
	STIM-rest	.798 ± .011	.090 ± .007	.709 ± .006
	STIM	.847 ± .019	.121 ± .015	.726 ± .014
	SWUM	.777 ± .006	.080 ± .014	.698 ± .014
	STIM	.049*	.031*	.017
	SWUM	.011*#	.001#	.010
Red Gastrocnemius				
	CONTROL	.760 ± .003	.058 ± .006	.703 ± .007
	STIM-rest	.778 ± .003	.071 ± .005	.710 ± .009
	STIM	.816 ± .011	.085 ± .010	.729 ± .008
	SWUM	.778 ± .005	.063 ± .010	.717 ± .014
	STIM	.038*	.014*	.019*
	SWUM	.018*#	.005	.014

(cont'd)

TABLE C-4 (cont'd)

Muscle	Condition	TTW	ECFV	ICFV
Plantaris				
	CONTROL	.761 \pm .002	.057 \pm .008	.703 \pm .008
	STIM-rest	.788 \pm .009	.069 \pm .003	.716 \pm .008
	STIM	.802 \pm .009	.082 \pm .009	.716 \pm .013
	SWUM	.778 \pm .005	.073 \pm .012	.707 \pm .010
	STIM	.014*	.013*	0
	SWUM	.017*	.016*	.004
White Gastrocnemius				
	CONTROL	.758 \pm .003	.064 \pm .010	.701 \pm .013
	STIM-rest	.785 \pm .008	.065 \pm .006	.721 \pm .003
	STIM	.830 \pm .023	.072 \pm .022	.755 \pm .005
	SWUM	.776 \pm .005	.071 \pm .014	.714 \pm .010
	STIM	.045*	.007	.034*
	SWUM	.018* [#]	.007	.013

See Table C-3 for definitions and legend.

TABLE C-5

Intracellular strong ion contents in biopsies taken from resting exercised muscles from stimulated group hindlimbs and swim group hindlimbs.

Muscle/ Condition	(pEq.g ⁻¹ dry wt.)				
	K ⁺	Na ⁺	Cl	Mg	Ca
Soleus					
CONTROL	346 ± 14	78 ± 9	30.9 ± 8.8	72.5 ± 2.9	8.6 ± 1.3
STIM-rest	315 ± 20	100 ± 12 [#]	85.3 ± 16.7 [#]	74.6 ± 4.5	11.9 ± 1.5
STIM	306 ± 12	130 ± 20	108 ± 17	57.6 ± 2.2 [*]	5.8 ± 1.1 [*]
SWUM	350 ± 34	104 ± 18	40.0 ± 12.7	67.1 ± 9.6	6.5 ± 0.8
Red Gastrocnemius					
CONTROL	431 ± 11	28.6 ± 2.1	18.7 ± 3.9	95.4 ± 3.5	8.6 ± 0.7
STIM-rest	365 ± 25 [#]	73.0 ± 9.2 [#]	47.5 ± 4.6 [#]	90.9 ± 3.9	12.8 ± 1.2
STIM	343 ± 9	115 ± 24 [*]	91.1 ± 10.0 [*]	70.3 ± 2.9 [*]	5.4 ± 1.1 [*]
SWUM	414 ± 21	43.2 ± 9.1	30.5 ± 7.2	92.5 ± 4.9	8.2 ± 0.6

(cont'd)

TABLE C-5 (cont'd)

Muscle/						
Condition	K ⁺	Na ⁺	Cl	Mg	Ca	
Plantaris						
CONTROL	413 ± 14	32.0 ± 2.0	20.2 ± 3.2	86.4 ± 3.2	8.1 ± 0.8	
STIM-rest	367 ± 18 [#]	80.5 ± 9.8 [#]	56.5 ± 13.6 [#]	90.3 ± 3.5	11.7 ± 0.7	
STIM	336 ± 10	96.1 ± 13.0 [*]	93.7 ± 10.7 [*]	69.3 ± 2.9 [*]	4.5 ± 0.8 [*]	
SWUM	389 ± 16	44.0 ± 7.9	28.9 ± 5.9	89.2 ± 5.0	7.8 ± 0.8	
White Gastrocnemius						
CONTROL	414 ± 9	39.9 ± 2.4	26.0 ± 2.6	90.3 ± 2.8	10.4 ± 1.3	
STIM-rest	419 ± 16	39.2 ± 10.7	37.7 ± 11.4	94.9 ± 3.0	11.4 ± 0.5	
STIM	380 ± 11 [*]	68.9 ± 13.8	47.7 ± 8.8	74.4 ± 2.6 [*]	5.1 ± 1.3 [*]	
SWUM	408 ± 14	49.5 ± 9.5 [*]	34.4 ± 7.3	82.3 ± 8.3	7.6 ± 0.7	

See legend of Table C-3 for definitions and parameters. See also Fig. 2.

TABLE C-6

Intracellular strong ion concentrations in biopsies taken from resting
exercised muscles from stimulated group hindlimbs and swim group hindlimbs.

Muscle & Condition	(μEq.l ⁻¹ ICF)					
	[K]	[Na]	[Cl]	[Mg]	[La]	[SID]
<u>Soleus</u>						
CONTROL	118 ± 5	26 ± 3	11 ± 3	25 ± 1	1.3 ± 0.2	144 ± 3
STIM-rest	90 ± 6	28 ± 3	24 ± 5	21 ± 1	0.9 ± 0.2	104 ± 4
STIM	64 ± 3	27 ± 4	23 ± 4	12 ± 1	1.4 ± 0.3	73 ± 4
SWUM	112 ± 11	33 ± 6	13 ± 4	21 ± 3	17 ± 1.9	126 ± 6
<u>Red Gastrocnemius</u>						
CONTROL	147 ± 4	10 ± 1	6.4 ± 1.3	33 ± 1	1.1 ± 0.2	166 ± 2
STIM-rest	114 ± 8	23 ± 3	15 ± 1.4	28 ± 1	1.5 ± 0.3	135 ± 3
STIM	87 ± 2	29 ± 6	23 ± 2.5	18 ± 1	15 ± 2	92 ± 3
SWUM	128 ± 7	13 ± 3	9.5 ± 2.2	29 ± 2	32 ± 3	114 ± 3

(cont'd)

TABLE C-6 (cont'd)

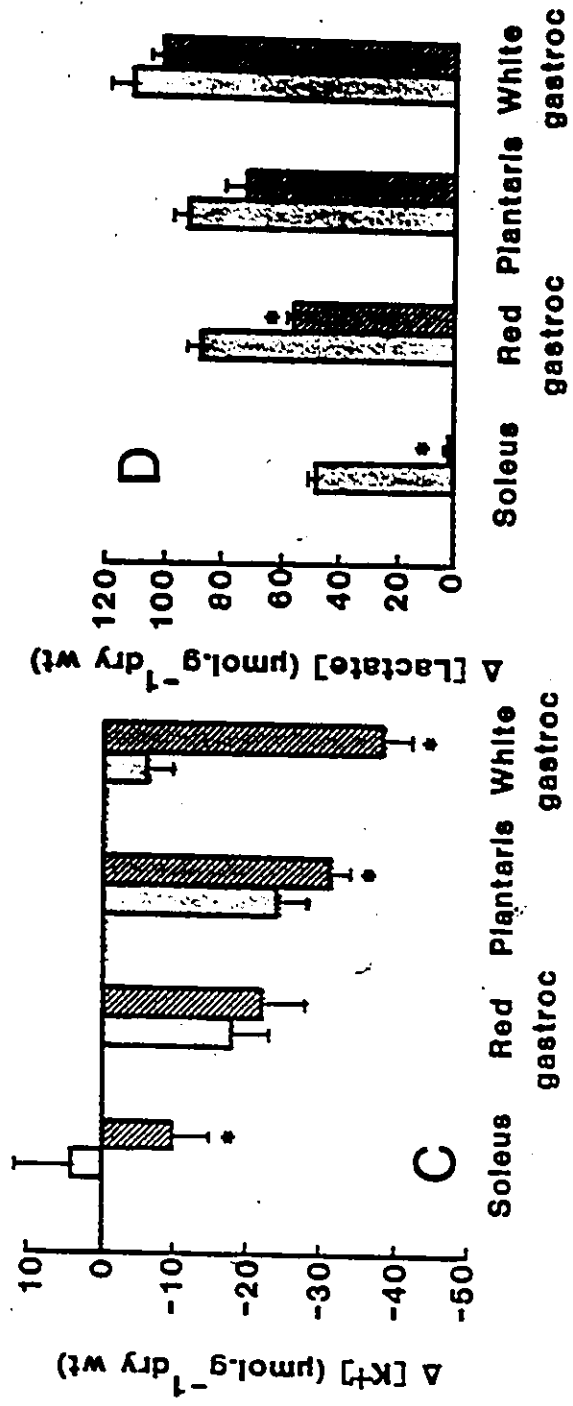
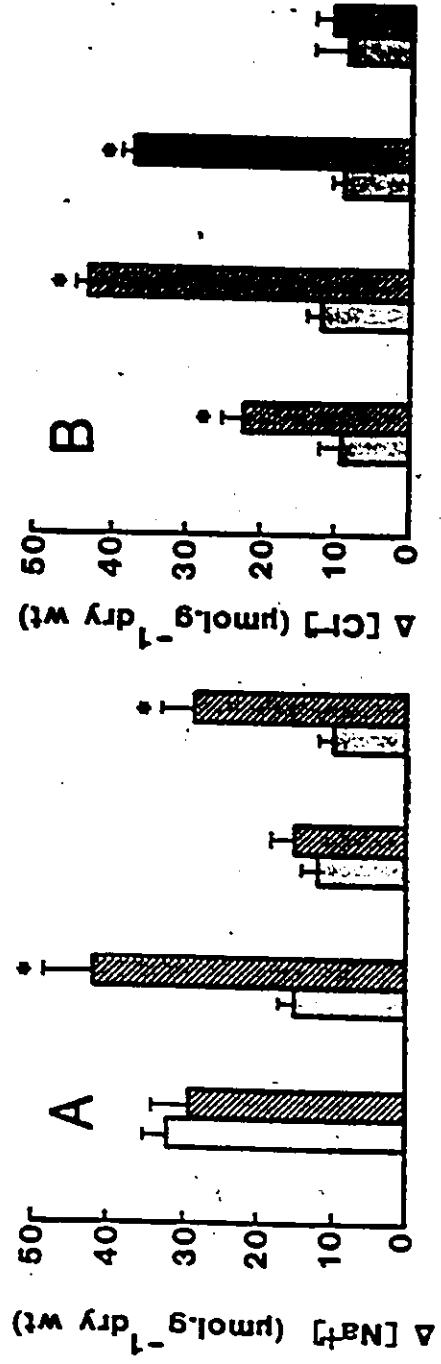
Muscle & Condition	(μEq.l ⁻¹ ICF)					
	[K]	[Na]	[Cl]	[Mg]	[La]	[SID]
<u>Plantaris</u>						
CONTROL	141 ± 5	11 ± 1	6.9 ± 1.1	29 ± 1	1.4 ± 0.2	158 ± 2
STIM-rest	109 ± 5	24 ± 3	17 ± 4	27 ± 1	2.2 ± 0.3	127 ± 3
STIM	93 ± 3	27 ± 4	26 ± 3	19 ± 1	21 ± 3	88 ± 4
SWUM	122 ± 5	14 ± 2	9.1 ± 1.9	28 ± 2	36 ± 3	105 ± 4
<u>White Gastrocnemius</u>						
CONTROL	143 ± 3	14 ± 1	9.0 ± 0.9	31 ± 1	1.6 ± 0.2	162 ± 2
STIM-rest	125 ± 5	12 ± 3	11 ± 3	28 ± 1	1.6 ± 0.2	138 ± 3
STIM	86 ± 2	16 ± 3	11 ± 2	17 ± 1	24 ± 2	81 ± 3
SWUM	130 ± 4	16 ± 3	11 ± 2	26 ± 3	43 ± 4	105 ± 4

Definitions and parameters as in Table C-3. Strong ion difference ([SID]) calculated as the sum of the strong base cations minus the sum of the strong acid anions (Stewart 1981; 1983):

$$[SID] = ([Na^+] + [K^+] + [Mg^{++}]/2) - ([Cl^-] + [La^-]),$$

where the total $[Mg^{++}]$ is halved since about 50% is non-diffusible (Maughan and Rechia 1985).

Fig. C-2. The mean changes in intracellular contents (mEq.g^{-1} dry wt) of (A) Na^+ , (B) Cl^- , (C) K^+ and (D) lactate after 4.5 min exhaustive swimming (SWUM, light shading) and 5 min of electrical stimulation (STIM, dark shading). Asterisks indicate significant differences between groups.



exercise-induced changes in intracellular ion contents between the 2 groups are comparable (Fig. C-2). The obvious difference between the two protocols is that the fluxes of the major strong ions are exaggerated in the hindlimb muscles of the STIM group compared to the SWUM group. In STIM, exercise resulted in significant ($p < 0.05$) decreases in $[K^+]_i$, $[Mg^{++}]$, while $[Na^+]_i$ and $[Cl^-]_i$ increased significantly (Table C-6, Fig. C-2). In SWUM, these changes were significant only at the $p < 0.10$ level (Fig. C-2).

DISCUSSION

The primary purpose of the present study was to compare the metabolic and ionic responses of stimulated perfused skeletal muscle in vitro to that of high intensity exercise in vivo. The exercise-induced changes in metabolites, and fluids and electrolytes were similar in both exercise groups. The single-pass perfusion system resulted in enhanced movements of fluids, ions and metabolites between extra- and intracellular fluids. This is an asset to the investigation of trans-sarcolemmal mechanisms of ion regulation which may otherwise be masked in recirculating perfusion systems.

The parameters used for in vitro perfusion of rat hindlimb muscles were within the physiological range for these tissues with respect to arterial pressure, perfusate flow rate (Mackie and Terjung 1983; Armstrong and Laughlin 1984; Gorski et al. 1986) and oxygen extraction (Folkow and Halicka 1968; Hood et al. 1986).

The appropriate controls for the SWUM group are those values obtained from rats anaesthetized with sodium pentobarbital; the values

of measured parameters obtained in this may appear to closely represent the condition of the resting animal (Lindinger and Heigenhauser, unpublished; Fregosi and Dempsey 1986). A group of resting rats sacrificed by cervical dislocation showed a significant lowering of intramuscular CP and glycogen and increased La^- , similar to that reported by Fregosi and Dempsey (1986) using decapitation. Fregosi and Dempsey (1986) concluded that traumatic procedures for sacrificing animals result in a masking of exercise effects, and should be avoided in controls. Following exercise, however, decapitation was an appropriate method for sacrificing the animals, yielding results similar to other methods.

One major physiological difference between the two groups is the nature of muscle fiber recruitment. With STIM, intermittent supramaximal electrical stimulation was employed so that, at least initially, all motor units within the stimulated muscle groups were fully activated with each stimulus. The SWUM group, on the other hand, used volitional swimming movements and therefore the pattern of motor unit recruitment is expected to change with time from the selective activation of those motor units used for initial burst performance, towards greater involvement of motor units used for sustained propulsion. Such a mechanism has been indicated for running rats (Sullivan and Armstrong 1978).

In both groups, there were similar decrements in the contents of CP, ATP and glycogen in the bulk to the sample muscle mass (primarily WG, Table C-2) with exercise, despite the differences in muscle stimulation. This suggests that the intermittent electrical

stimulation protocol employed in the present study did not result in an impairment of glycolytic metabolism of skeletal muscle due to fatigue occurring at sites prior to excitation-contraction coupling. This is also supported by the linear decrement in force production of the electrically stimulated hindlimb shown in Fig. 1B.

Exercise-induced changes in muscle metabolites (Table C-3) were similar to those previously reported in treadmill exercised rats (Sullivan and Armstrong 1978; Fregosi and Dempsey 1986) or in electrically stimulated perfused rat hindlimb muscles in vitro (Spriet et al. 1985b; Spriet et al. 1986) and in situ (Kushmerick and Meyer 1985).

The significantly higher intracellular $[La^-]$ in hindlimb muscles from the SWUM group, compared to STIM, may be due to three separate effects acting on muscles of different fiber type population. In SL, in which very little glycolysis occurred (Table C-3), the accumulated La^- appears to be partially due to the movement of La^- from plasma into the muscle. For example, of the 55 $\mu\text{mol/g}$ dry wt of La^- accumulated in SL (Table C-3), only 70% can be accounted for by glycogenolysis (17 μmol glucosyl units/g dry wt). In SWUM rats, arterial $[La^-]$ was equal to intracellular SL $[La^-]$ ($20 \pm 1 \text{ mmol}\cdot\text{L}^{-1}$, Table C-6) at the end of exercise. The high blood flows to SL during rest and exercise (Armstrong and Laughlin 1984; Hood et al. 1986) maintains a relatively high ECF to ICF gradient for La^- when plasma $[La^-]$ is high, therefore, a passive movement of La^- from the ECF into the SL intracellular compartment could occur.

The increased $[La^-]_i$ in SWUM group muscles may also have resulted from an increased rate of uptake of exogenous glucose, providing additional substrate for La^- production. Also, the elevated plasma $[La^-]$ in the SWUM group reduces the concentration difference for La^- across the sarcolemma and may thus impede La^- removal from the ICF. In contrast, in the STIM group, the one-pass perfusion system kept arterial plasma $[La^-]$ low (Table 1), potentially enhancing La^- removal in the STIM muscles.

The quantity of K^+ loss, [SID] reduction (Table C-6; Fig. C-2C) and fluid uptake (Table C-4) was proportional to the muscle's glycolytic activity and La^- accumulation (Tables C-3 & C-6). Thus La^- accumulation (and release) is greatest in the fast-twitch glycolytic WG, where the largest net K^+ efflux, fluid influx and [SID] reduction is observed. It is evident that the magnitude of the fluid movement to ECF or ICF depends on the relative ion concentration differences between plasma and interstitial fluids and between interstitial fluids and ICF (Tibes et al. 1977). The changes in intracellular concentrations of La^- and other strong ions are quantitatively greater in WG than SL (Table C-6) and, accordingly, muscle fluid volumes increased to a greater extent in WG than in SL.

The increase in muscle TTW during exercise in both groups of animals was partitioned into both the ECF and ICF compartments (Table C-4). The magnitude of the increases in muscle fluid volumes during exercise tended to be greater in STIM than in the SWUM group. With the single-pass perfusion system the arterial blood does not become concentrated during intense exercise as occurs in vivo (Harrison

1985); this may account for the higher fluid volumes in STIM than SWUM muscles. The exercise-induced increase in TTW was similar to that found in previous studies in rat (Sreter 1963), rabbit (Tibes et al. 1977) and human muscle (Sjogaard et al. 1985). Most of the increase in muscle water was partitioned into the ICFV, however the percentage increase in ICFV was always less than that of the ECFV (Table C-4). In agreement with the present study, Sreter (1963) also found that the ECFV increased to a greater extent than the ICFV, and that the largest increase in ICFV occurred in the WG.

Muscle contraction results in an increase in venous plasma $[K^+]$ and a decrease in venous plasma $[Na^+]$ and $[Cl^-]$ in man (Sjogaard et al. 1985; Bergstrom et al. 1973; Hermansen et al. 1984) and in isolated or in situ stimulated muscle preparations (Fenn and Cobb 1936; Sreter 1963; Hnik et al. 1976; Tibes et al. 1977; Hirsche et al. 1980). Accordingly, intracellular $[K^+]$ of working muscle decreases while intracellular $[Na^+]$ and $[Cl^-]$ increases (Fig. C-2). These changes have been attributed to incomplete re-uptake of K^+ and higher $[Na^+]$ and $[Cl^-]$ during muscle contractions (Hnik et al. 1976; Tibes et al. 1977; Hirsche et al. 1980; Sjogaard 1983; Juel 1986). The altered extra- and intracellular Na^+ and K^+ concentrations during muscle activity are associated with a decrease in the resting membrane potential and may depolarize the muscle cells (Juel 1986) according to the relationships described by Jakobsson (1980) and Beauge and Sjodin (1976). This depolarization may reduce the magnitudes of the action potential and Ca^{++} release (Ashley and Ridgway 1979), decrease the free

intracellular $[Ca^{++}]$ (Holmberg and Waldeck 1980), and thus contribute to force decline during muscle activity (Juel 1986). Also, the increased interstitial $[K^+]$ in contracting muscle (Hnik et al. 1976; Tibes et al. 1977) may aid muscle function via local regulation of exercise hyperemia (Dawes 1941; Hnik et al. 1976; Tibes et al. 1977; Birche et al. 1980; Sjogaard et al. 1985).

The disadvantages of the isolated perfused stimulated rat hindlimb are associated with assessing the relative contributions of working versus inactive muscle (Table C-2), to the changes in arterial-to-venous perfusate characteristics. The wide variety of muscle fiber types in the rat hindlimb (Armstrong and Phelps 1984) also hampers accurate quantitation of fluid, ion and metabolite fluxes between active and inactive muscles and blood. The ideal preparation would utilize a single muscle composed of a single muscle fiber type so that intramuscular changes in response to a given set of stimuli can be directly correlated to changes in the arterial to venous perfusate composition.

The single-pass perfusion system provides an effectively infinite sink for the removal of metabolic endproducts, and maintains a constant supply of substances having a higher arterial concentration than interstitial or intracellular fluids. This results in enhanced movements of fluid, ions and metabolites between ICF and ECF, i.e. in STIM compared to SWUM (Tables C-4 and C-6), a finding which should prove advantageous when investigating trans-sarcolemmal mechanisms of ion regulation which might otherwise be masked in recirculating perfusion systems. The further advantage of a constant arterial

perfusate is that it permits the study of the muscles' responses to a single set of defined parameters and thus simplifies the investigation of the mechanisms involved. Mechanisms of trans-sarcolemmal ion movements may be studied by applying ion flux inhibitors and radiotracers to the arterial perfusate or by prior preparation of the intact animal with various drugs. The preparation can be used to quantify a wide spectrum of physiological responses to a variety of acute and chronic perturbations to intact animals.

In conclusion, the isolated stimulated perfused rat hindlimb has been shown to provide a useful model of muscle metabolism and ion regulation. The single-pass perfusion system accentuates the fluxes of ions and metabolites between muscle and perfusate, permitting quantification of the fluxes over time with a controlled arterial perfusate composition. The magnitude of metabolic and ionic changes in vivo and in vitro are similar in the rat hindlimb muscles: the greatest changes occurred in the fast twitch glycolytic muscles (WG and PL) while the smallest changes were seen in the slow oxidative SL muscle.

ACKNOWLEDGEMENTS

The authors gratefully acknowledge the technical assistance of M. Ganagarajah, Sandra Peters, and Dr. S. Landsberger and staff of the McMaster University Nuclear Reactor. We also thank Dr. P.A. Stewart for his review of the manuscript. This work was supported by a grant from the Medical Research Council of Canada.

APPENDIX D

Published in Med. Sci. Sports Exer., April 1987

ION CHANGES IN ARTERIAL RED BLOOD CELLS IN MAXIMAL EXERCISE.

R.S. McKelvie*, M.I. Lindinger* and G.J.F. Heigenhauser, FACSM.
Dept. of Medicine, McMaster University, Hamilton, Ontario, Canada.
L8N 3Z5.

Five healthy males performed four 30-s bouts of maximal isokinetic cycling with 4-min rests between bouts. Muscle biopsies were taken from the vastus lateralis and arterial and femoral venous blood was sampled during exercise and 90 min of recovery. During exercise, arterial plasma $[K^+]$ rose by 1.9 mM, and RBC $[K^+]$ rose by 10.9 mM intracellular fluid; the RBC carried 90% of the total increase in whole blood $[K^+]$. In recovery, arterial RBC $[K^+]$ fell by 15 mM from peak values (149 mM) as plasma $[K^+]$ was reduced and muscle $[K^+]$ increased. Arterial plasma and RBC [lactate] ($[La^-]$) rose by 20 mM and 9.4 mM respectively; the RBC's carried 32% of the total increase in whole blood $[La^-]$. Arterial RBC $[Cl^-]$ rose during exercise to 91 mM and returned to resting values (78 mM) by 25 min recovery. The arterio-venous RBC $[Cl^-]$ difference showed a net flux of Cl^- into the RBC during exercise and early recovery, probably by Cl^-/HCO_3^- exchange. We conclude that RBC's are important in the regulation of plasma ion concentrations during maximal exercise.

Supported by the Ontario Heart and Stroke Foundation and the Medical Research Council of Canada.

THE ROLE OF THE RED BLOOD CELL IN BUFFERING ION CHANGES ACROSS INACTIVE ARM MUSCLE DURING HIGH-INTENSITY EXERCISE.

G.J.F. Heigenhauser, FACSM, M.I. Lindinger* and R.S. McKelvie*.
Dept. of Medicine, McMaster University, Hamilton, Ontario, Canada.
L8N 3Z5.

Eight males performed four 30-s bouts (EB) of maximal isokinetic cycling with 4-min rests between bouts. Arterial and arm vein blood samples were taken after each EB and for 90 min into recovery. Resting arterial (a) RBC $[Na^+]_a$, $[K^+]_a$, $[Cl^-]_a$ and lactate ($[La^-]_a$) were 46.6, 140.9, 77.5 and 0.52 mM intracellular fluid. Resting RBC arterio-venous difference (A-V) $[Na^+]$, $[K^+]$, $[Cl^-]$ and $[La^-]$ were 1.9, 3.9, 1.5 and -0.58 mM. RBC $[Na^+]_a$ rose to 54.8 mM during exercise. RBC $[Na^+]_a$ A-V fell to -15.6 mM by 15 min recovery. RBC $[K^+]_a$ rose to 150.3 mM at the end of the second EB. RBC $[K^+]_a$ A-V peaked at 11.1 mM after the second EB; K^+ efflux from RBC's continued until 15 min of recovery. RBC $[Cl^-]_a$ rose to 88.9 mM at the end of the third EB. RBC $[Cl^-]_a$ A-V fell during exercise to -4.9 mM. RBC $[La^-]_a$ rose to 14.9 mM at the end of the fourth EB. The plasma $[La^-]_a$ at the end of the fourth EB was 24.9 mM. Plasma $[La^-]_a$ was always greater than RBC $[La^-]_a$. The RBC $[La^-]_a$ A-V rose to 5.6 mM at the end of the fourth EB. La^- efflux from RBC's continued until 40 min of recovery. We conclude that RBC's are important in transporting and releasing K^+ into the plasma during transit through inactive muscle. La^- uptake by inactive muscle occurs during exercise and early recovery, but at a slower rate than the loss of La^- from RBC's.

Supported by the Ontario Heart & Stroke Foundation and the MRC of Canada.

BIBLIOGRAPHY

- Abdel-Aziz, M., W. Manning, K.M. Ward and A.C. Wareham. 1985.
³H-ouabain binding in normal and dystrophic mouse skeletal muscles
and the effect of age. J. Neurol. Sci. 70: 47-53.
- Ackerman, J.J.H., T.H. Grove, G.G. Wong, D.G. Gadian and G.K. Radda.
1980. Mapping of metabolites in whole animals by ³¹P NMR using
surface coils. Nature 283: 167-170.
- Adrian, R.H. and L.D. Peachy. 1974. Reconstruction of the action
potential of frog sartorius muscle. J. Physiol. Lond. 235: 103-131.
- Adrian, R.H. and C.L. Slayman. 1966. Membrane potential and
conductance during transport of sodium, potassium and rubidium in frog
muscle. J. Physiol. Lond. 184: 970-1014.
- Aickin, C.C. and R.C. Thomas. 1977. An investigation of the ionic
mechanism of intracellular pH regulation in mouse soleus muscle
fibers. J. Physiol. Lond. 273: 295-316.
- Akaike, N. 1975. Contribution of an eletrogenic sodium pump to
membrane potential in mammalian skeletal muscle fibers. J. Physiol.
Lond. 245: 499-520.

- Albritton, E.C. 1952. Standard values in blood. Philadelphia: Saunders, pp. 423.
- Altman, P.L. and D.S. Dittmer. 1971. Respiration and Circulation. In: Biological Handbooks. Washington, American Physiological Society. pp.159-190.
- Andersen, P. 1975. Capillary density in skeletal muscle of man. Acta Physiol. Scand. 95: 203-205.
- Antonini, E. and M. Brunori. 1971. Hemoglobin and myoglobin in their reactions with ligands. New York: American Elsevier, pp. 166.
- Armstrong, R.B. and M.H. Laughlin. 1984. Exercise blood flow patterns within and among rat muscles after training. Am. J. Physiol. 246: H59-H68.
- Armstrong, R.B. and R.O. Phelps. 1984. Muscle fiber type composition of the rat hindlimb. Am. J. Anat. 171: 259-272.
- Ashley, C.C. and E.B. Ridgway. 1979. On the relationships between membrane potential, calcium transient and tension in single barnacle muscle fibers. J. Physiol. Lond. 209: 105-130.
- Astrand, P.-O., E. Hultman, A. Juhlin-Dannfelt and G. Reynolds. 1986. Disposal of lactate during and after strenuous exercise in humans. J. Appl. Physiol. 61: 338-343.

- Avison, M.J., H.P. Hetherington and R.G. Shulman. 1986. Applications of NMR to studies of tissue metabolism. *Ann. Rev. Biophys. Biophys. Chem.* 15: 377-402.
- Bailey, K. 1942. Myosin and adenosinetriphosphatase. *Biochem. J.* 36: 121-139.
- Bartels, H. and H. Harms. 1959. Sauerstoffdissoziationskurven des Blutes von Saugetieren. *Pfluegers Arch.* 268: 334-365.
- Bartels, H., P. Hilpert, K. Barbey, K. Betke, K. Riegel, E.M. Lang and J. Metcalfe. 1963. Respiratory functions of blood of the yak, llama, camel, Dybowski deer, and African elephant. *Am. J. Physiol.* 205: 331-336.
- Beauge, L.A. and R.A. Sjodin. 1976. Analysis of the influence of membrane potential and metabolic poisoning with azide on the sodium pump in skeletal muscle. *J. Physiol. Lond.* 263: 383-403.
- Benade, A.J.S. and N. Heisler. 1978. Comparison of efflux rates of hydrogen and lactate ions from isolated muscles in vitro. *Resp. Physiol.* 32: 369-380.
- Berger, M., S. Hagg and N.B. Ruderman. 1975. Glucose metabolism in perfused skeletal muscle: interaction of insulin and exercise on glucose uptake. *Biochem. J.* 146: 231-238.

Bergmeyer, H.U. 1965. Methods of Enzymatic Analysis. New York: Academic Press.

Bergstrom, J. 1962. Muscle electrolytes in man. Determined by neutron activation analysis on needle biopsy specimens. A study on normal subjects, kidney patients, and patients with chronic diarrhoea. Scand. J. Clin. Lab. Invest. 14, (Suppl. 68): 1-110.

Bernard, C. 1859. De la matiere glycogene consideree comme condition de developpement de certain tissus, chez le foetus, avant l'apparition de la fonction glycogenique du foie. Compt. rend. des seances de l'Acad. des Sci. 48.


Bernstein, J. 1902. Untersuchungen zur Thermodynamik der bioelektrischen Strome. Arch. f. ges. Physiol. 92: 521-533.

Bernstein, J. 1912. Elektrobiologie. Braunschweig: Vieweg & Sohn.

Berzelius, J.J. 1840. Lehrbuch der Chemie, Vol. 9: 567.

Bianchi, C.P. and S. Narayan. 1982. Muscle fatigue and the role of transverse tubules. Science 215: 295-296.

Bigland-Ritchie, B. and J.J. Woods. 1984. Changes in muscle contractile properties and neural control during human muscular fatigue. Muscle & Nerve 7: 691-699.



- Boron, W.F. 1977. Intracellular pH transients in giant barnacle muscle fibers. *Am. J. Physiol.* 233: C61-C73.
- Boron, W.F. and A. Roos. 1976. Comparison of microelectrode, DMO, and methylamine methods for measuring intracellular pH. *Am. J. Physiol.* 231: 799-809.
- Boyer, P.D., H.A. Lardy and P.H. Phillips. 1943. Further studies on the role of potassium and other ions in the phosphorylation of the adenylic system. *J. Biol. Chem.* 149: 529-541.
- Boyle, P.J. and E.J. Conway. 1941. Potassium accumulation in muscle and associated changes. *J. Physiol. Lond.* 100: 1-63.
- Brodie, D.A. and D.M. Woodbury. 1958. Acid-base changes in brain and blood of rats exposed to high concentrations of carbon dioxide. *Am. J. Physiol.* 192: 91-94.
- Brooke, M.H. and K.K. Kaiser. 1970. Muscle fibre types: How many and what kind? *Arch. Neurol.* 23: 369-379.
- Bullard, R.W., C. Broumand and F.W. Meyer. 1966. Blood characteristics and volume in two rodents native to high altitude. *J. Appl. Physiol.* 21: 994-998.
- Burnell, J.M. 1968. In vivo response of muscle to changes in CO₂

- tension or extracellular bicarbonate. *Am. J. Physiol.* 215: 1376-1383.
- Caille, J., M. Ildefonse and O. Rougier. 1985.
Excitation-contraction coupling in skeletal muscle. *Prog. Biophys. Mol. Biol.* 46: 185-239.
- Caldwell, P.C. 1954. An investigation of the intracellular pH of crab muscle fibres by means of micro-glass band micro-tungsten electrodes. *J. Physiol. Lond.* 128: 169-180.
- Campion, D.S. 1974. Resting membrane potential and ionic distribution in fast- and slow-twitch mammalian muscle. *J. Clin. Invest.* 54: 514-518.
- Carlson, F.D. and A. Siger. 1960. The mechanochemistry of muscular contraction. I. The isometric twitch. *J. Gen. Physiol.* 44: 33-60.
- Carlstrom, A.B., R. Ege und V. Henriques. 1928. Untersuchungen uber die Reaktion der Gewebe. *Biochem. Z.* 198: 442-462.
- Carter, N.W., F.C. Rector, R.T. Champion and D.W. Seldin. 1967.
Measurement of intracellular pH of skeletal muscle with pH-sensitive glass microelectrodes. *J. Clin. Invest.* 46: 920-933.
- Challiss, R.A.J., J.R.S. Arch and E.A. Newsholme. 1984. The rate of substrate cycling between fructose-6-phosphate and fructose-1,6-bisphosphate in skeletal muscle. *Biochem. J.* 221:

153-161.

Chalovich, J.M. and E. Eisenberg. 1982. Inhibition of actomyosin ATPase activity by troponin-tropomyosin without blocking the binding of myosin to actin. *J. Biol. Chem.* 257: 2432-2437.

Chasiotis, D. 1983. The regulation of glycogen phosphorylase and glycogen breakdown in human skeletal muscle. *Acta Physiol. Scand.* Suppl. 518: 1-68.

Chasiotis, D., K. Sahlin and E. Hultman. 1983. Acidotic depression of cyclic AMP accumulation and phosphorylase b to a transformation in skeletal muscle of man. *J. Physiol. Lond.* 335: 197-204.

Chi, M.M.-Y., C.S. Hintz, J. Henriksson, S. Salmons, R.P. Hellendahl, J.L. Park, P.M. Nemeth and O.H. Lowry. 1986. Chronic stimulation of mammalian muscle: enzyme changes in individual fibers. *Am. J. Physiol.* 251: C633-C642.

Chutkow, J.G. 1973. Magnesium, potassium, and sodium in "red" and "white" skeletal muscle in the rat. *Proc. Soc. Exp. Biol. Med.* 143: 430-432.

Clausen, T. 1986. Regulation of active Na^+/K^+ transport in skeletal muscle. *Physiol. Rev.* 66: 542-580.

Clausen, T. and O. Hansen. 1982. The Na^+/K^+ -pump, energy metabolism,

and obesity. *Biochem. Biophys. Res. Commun.* 104: 357-362.

Close, R.I. 1972. Dynamic properties of mammalian skeletal muscles. *Physiol. Rev.* 52: 129-197.

Cohen, P. 1981. The role of calmodulin, troponin, and cyclic AMP in the regulation of glycogen metabolism in mammalian skeletal muscle. *Adv. Cycl. Nucl. Res.* 14: 345-359.

Cohen, S.M. and C.T. Burt. 1977. ^{31}P nuclear magnetic relaxation studies of phosphocreatine in intact muscle: Determination of intracellular free magnesium. *Proc. Natl. Acad. Sci. USA* 74: 4271-4275.

Conway, E.J. and F. Kane. 1934. Diffusion rates of anions and urea through tissues. *Biochem. J.* 28: 1769-1783.

Cooke, R. and E. Pate. 1985. The effects of ADP and phosphate on the contraction of muscle fibers. *Biophys. J.* 48: 789-798.

Cori, G.T., S.P. Colowick and C.F. Cori. 1938. The enzymatic conversion of glucose-1-phosphoric ester to 6-ester in tissue extracts. *J. Biol. Chem.* 124: 543-555.

Costill, D.L., F. Verstappen, H. Kuipers, E. Janssen and W. Fink. 1984. Acid-base balance during repeated bouts of exercise: Influence of HCO_3^- . *Int. J. Sports Med.* 5: 228-231.

- Cotlove, E. 1954. Mechanism and extent of distribution of inulin and sucrose in chloride space of tissues. *Am. J. Physiol.* 176: 396-410.
- Cotlove, E., M.A. Holliday, R. Schwartz and W.M. Wallace. 1951. Effects of electrolyte depletion and acid-base disturbance on muscle cations. *Am. J. Physiol.* 167: 665-675.
- Danforth, W.R. 1965. Activation of glycolytic pathway in muscle. In: Control of Energy Metabolism, edited by B. Chance, R.W. Estabrook and J.R. Williamson. London, Academic Press, pp. 287-297.
- Davies, S.F., C. Iber, S. A. Keene, C.D. McArthur and M.J. Path. 1986. Effect of respiratory alkalosis during exercise on blood lactate. *J. Appl. Physiol.* 61: 948-952.
- Dawes, G. S. 1941. The vasodilator action of potassium. *J. Physiol. Lond.* 99: 224-238.
- DeSote, D., R. Gijbels and J. Hoste. 1972. Growth and decay of radioactivity during and after irradiation. In: Neutron Activation Analysis, Vol. 34 of Chemical Analysis. Wiley-Interscience, Toronto. pp. 123-159.
- Dill, D.B., J.H. Talbott and H.T. Edwards. 1930. Studies in muscular activity. VI. Response of several individuals to a fixed task. *J. Physiol.* 69: 267-305.

- Dixon, E.C. and E.C. Webb. 1979. Enzymes, third edition. New York: Academic Press, pp. 138-164.
- Dobson, G.F., E. Yamamoto and P.W. Hochachka. 1986. Phosphofructokinase control in muscle: nature and reversal of pH-dependent ATP inhibition. *Am. J. Physiol.* 250: R71-R76.
- Donaldson, P.J. and J.P. Leader. 1984. Intracellular ionic activities in the EDL muscle of the mouse. *Pflugers Arch.* 400: 166-170.
- Donaldson, S.K.B. 1983. Effect of acidosis on maximum force generation of peeled mammalian skeletal muscle fibers. In: Biochemistry of Exercise, Vol. 13. Edited by H.G. Knuttgen, J.A. Vogel and J. Poortmans. Champaign, IL: Human Kinetics, pp. 126-133.
- Donaldson, S. and W. Kerrick. 1975. Characterization of the effects of Mg^{2+} on Ca^{2+} - and Sr^{2+} -activated tension generation of skinned skeletal muscle fibers. *J. Gen. Physiol.* 66: 427-444.
- Drahota, Z. 1961. The ionic composition of various types of striated muscles. *Physiol. Bohemoslov.* 10: 160-165.
- Dubuisson, M. 1939. Studies on the chemical processes which occur in muscle before, during and after contraction. *J. Physiol. Lond.* 94: 461-482.
- Dulhunty, A. 1978. The dependence of membrane potential on

extracellular chloride concentrations in mammalian skeletal muscle fibres. J. Physiol. Lond. 276: 67-82.

Dulhunty, A. 1982. Effects of membrane potential on mechanical activation in skeletal muscle. J. Gen. Physiol. 79: 233-251.

Ebashi, S. 1976. Excitation-contraction coupling. A. Rev. Physiol. 38: 293-313.

Ebashi, S. and M. Endo. 1968. Calcium ion and muscle contraction. Prog. Biophys. Mol. Biol. 18: 125-183.

Edsall, J.T. and J. Wyman. 1958. Biophysical Chemistry, Vol. 1. New York: Academic, pp. 578-587.

Edstrom, L., E. Hultman, K. Sahlin and H. Sjoholm. 1982. The contents of high-energy phosphates in different fibre types in skeletal muscles from rat, guinea-pig and man. J. Physiol. Lond. 332: 47-57.

Edwards, R.H.T. 1981. Human muscle function and fatigue. In: Human Muscle Fatigue: Physiological Mechanisms, edited by R. Porter and J. Whelan. Ciba Foundation Symposium 82. London: Pitman Medical, pp. 1-18.

Edwards, R.H.T., M.J. Dawson, D.R. Wilkie, R.E. Gordon and D. Shaw. 1982. Clinical use of nuclear magnetic resonance in the investigation of myopathy. Lancet 1: 725-731.

- Eggleton, P. and G.P. Eggleton. 1927. The inorganic phosphate and a labile form of organic phosphate in the gastrocnemius of the frog. *Biochem. J.* 21: 190.
- Emden, G., W. Griesbach and E. Schmitz. 1914. Über Milchsäurebildung und Phosphorsäurebildung im Muskelpresssaft. *Z. f. Physiol. Chem.* 93: 1-9.
- Ernst, E. and L. Csucs. 1929. Untersuchungen über Muskelkontraktion. IX. Mitteilung. Permeabilität und Tätigkeit. *Pflügers Arch* 223: 663-670.
- Fabiato, A. and F. Fabiato. 1978. The effects of pH on the myofilaments and the sarcoplasmic reticulum of skinned cells from cardiac and skeletal muscles. *J. Physiol.* 276: 233-255.
- Favier, R.H., S.H. Constable, M. Chen and J.O. Holloszy. 1986. Endurance exercise training reduces lactate productions. *J. Appl. Physiol.* 61: 885-889.
- Fenn, W.O. 1936. Electrolytes in muscle. *Physiol. Rev.* 16: 450-487.
- Fenn, W.O. 1938. Factors affecting the loss of potassium from stimulated muscles. *Am. J. Physiol.* 124: 213-229.
- Fenn, W.O. 1939. The deposition of potassium and phosphate with

- glycogen in rat livers. J. Biol.Chem. 128: 297-307.
- Fenn, W.O. and D.M. Cobb. 1934. The potassium equilibrium in muscle. J. Gen. Physiol. 17: 629-656.
- Fenn, W.O. and D.M. Cobb. 1936. Electrolyte changes in muscle during activity. Am. J. Physiol. 115: 345-356.
- Fenn, W.O., D.M. Cobb and B.S. Marsh. 1934. Sodium and chloride in frog muscle. Am. J. Physiol. 110: 261-272.
- Fenn, W.O., D.M. Cobb, J.F. Manery and W.R. Bloor. 1938. Electrolyte changes in cat muscle during stimulation. Am. J. Physiol. 121: 595-608.
- Fenn, W.O., R.H. Koenemann and E.T. Sheridan. 1940. The potassium exchange of perfused frog muscle during asphyxia. J. Cell. Comp. Physiol. 16: 255-264.
- Fenn, W.O. and F.W. Maurer. 1935. The pH of muscle. Protoplasma 24: 337-345.
- Fink, R., S. Hase, H. Ch. Luttgau and E. Wettwer. 1983. The effect of cellular energy reserves and internal calcium ions on the potassium conductance in skeletal muscle of the frog. J. Physiol. Lond. 336: 211-228.

- Fischer, E., J.W. Moore, H.V. Skowlund, K.W. Ryland and N.J. Copenhaver. 1950. The potassium permeability and the capacity for potassium storage of normal and atrophied muscle, investigated with the radioactive isotope K^{42} . Arch. Phys. Med. 31: 429-441.
- Fiske, C.H. and Y. Subbarow. 1928. The isolation and function of phosphocreatine. Science 67: 169.
- Fitts, R.H., J.B. Courtright, D.H. Kim and F.A. Witzmann. 1982. Muscle fatigue with prolonged exercise: contractile and biochemical alterations. Am. J. Physiol. 242: C65-C73.
- Fitts, R.H. and J.O. Holloszy. 1976. Lactate and contractile force in frog muscle during development of fatigue and recovery. Am. J. Physiol. 231: 430-433.
- Fletcher, W.M. 1904. The osmotic properties of muscle, and their modifications in fatigue and rigor. J. Physiol. Lond. 30: 414-438.
- Flock, E., J.L. Ballman, F.C. Mann and E.C. Kendall. 1938. The effect of the intravenous injection of glucose and other substances on the concentration of potassium in the serum of the dog. J. Biol. Chem. 125: 57-64.
- Folkow, B. and H.D. Halicka. 1968. Comparison between "red" and "white" muscle with respect to blood supply, capillary surface area and oxygen uptake. Microvas. Res. 1: 1-14.

- Fregosi, R.F. and J.A. Dempsey. 1986. Anesthetic effects on $[H^+]_a$ and muscle metabolites at rest and following exercise. *Resp. Physiol.* 65: 85-98.
- Frumento, A.S. 1965. Sodium pump: its electrical effects in muscle. *Science* 147: 1442-1443.
- Fuchs, F. 1974. Chemical properties of the calcium receptor site of troponin as determined from binding studies. In: Calcium Binding Proteins, edited by W. Drabikowski, H. Strzelecka-Golaszewska and E. Carafoli. Amsterdam: Elsevier, pp. 1-27.
- Furusawa, K. and P.M.T. Kerridge. 1927. The hydrogen ion concentration of the muscles of the cat. *J. Physiol. Lond.* 63: 33-41.
- Gahlenbeck, H., A.M. Rathsclag and H. Bartels. 1968. Triiodothyronine induced changes of oxygen affinity of blood. *Resp. Physiol.* 6: 16-22.
- Galler, S. and H. Moser. 1986. The ionic mechanism of intracellular pH regulation in crayfish muscle fibres. *J. Physiol. Lond.* 374: 137-151.
- Gevers, E.W. and E. Dowdle. 1963. The effect of pH on glycolysis in vitro. *Clin. Sci.* 25: 343-349.

Glasby, M.A. 1985. Mannitol penetration of liver cells in estimations of extracellular fluid volume. *Quart.J. Exp. Physiol.* 70: 585-589.

Gleiss, W. 1887. Ein betrag zur Muskelchemie. *Arch. f. ges. Physiol.* 41: 69.

Gonzalez, N.C. and R.L. Clancy. 1986. Intracellular pH regulation during prolonged hypoxia in rats. *Resp. Physiol.* 65: 331-339.

Gonzalez-Serratos, H., A.V. Somlyo, G. McClellan, H. Shuman, L.M. Borrero and A.P. Somlyo. 1978. Composition of vacuoles and sarcoplasmic reticulum in fatigued muscle: electron probe analysis. *Proc. Natl. Acad. Sci. USA* 75: 1329-1333.

Goodman, M.N., S.M. Druz, M.A. McElaney, E. Belur and N.B. Ruderman. 1983. Glucose uptake and insulin sensitivity in rat muscle: changes during 3-96 weeks of age. *Am. J. Physiol.* 244: E93-E100.

Goodman, M.N., M.A. McElaney and N.B. Ruderman. 1981. Adaptation to prolonged starvation in the rat: curtailment of skeletal muscle proteolysis. *Am. J. Physiol.* 241: E321-E327.

Gorski, J., D.A. Hood and R.L. Terjung. 1986. Blood flow distribution in tissues of perfused rat hindlimb preparations. *Am. J. Physiol.* 250: E441-E448.

Graham, J.A., J.F. Lamb and A.L. Linton. 1967. Measurement of body

water and intracellular electrolytes by means of muscle biopsy. *Lancet* 1967 II: 1172-1176.

Gray, L.H. and J.M. Steadman. 1964. Determination of the oxyhaemoglobin dissociation curves for mouse and rat blood. *J. Physiol. Lond.* 175: 161-171.

Gray, W.D. and C.E. Rauh. 1958. The anticonvulsant action of carbon dioxide: interaction with reserpine and inhibitors of carbonic anhydrase. *J. Pharmacol. Exp. Ther.* 163: 431-438.

Greenstein, J.P. and J.T. Edsall. 1940. Effect of denaturing agents on myosin. *J. Biol. Chem.* 133: 397-408.

Gupta, B.L., and T.A. Hall. 1981. Ions and water in cells and tissues studied by microprobe analysis of frozen hydrated sections in the SEM. In: 39th Ann. Proc. Electron Microscopy Soc. Amer., edited by G.W. Bailey. Atlanta, pp. 654-657.

Gupta, R.K., P. Gupta and R.D. Moore. 1984. NMR studies of intracellular metal ions in intact cells and tissues. *Ann. Rev. Biophys. Bioeng.* 13: 221-246.

Hall, F.G. 1966. Minimal utilizable oxygen and the oxygen dissociation curve of blood of rodents. *J. Appl. Physiol.* 21: 375-378.

Harms, S.J. and R.C. Hickson. 1983. Skeletal muscle mitochondria and

myoglobin, endurance, and intensity of training. J. Appl. Physiol. 54: 279
798-802.

Harned, H.S. and B.O. Owen. 1958. The Physical Chemistry of Electrolyte Solutions, 3rd. ed. New York: Van Nostrand-Reinhold.

Harris, E.J. 1950. The transfer of sodium and potassium between muscle and the surrounding medium. Trans. Farad. Soc. 46: 872-882.

Hazeyama, Y. and H.V. Sparks. 1979. A model of potassium ion efflux during exercise of skeletal muscle. Am. J. Physiol. 236: R83-R90.

Hebisch, S., H. Sies and S. Soboll. 1986. Function dependent changes in the subcellular distribution of high energy phosphates in fast and slow rat skeletal muscles. Pflugers Arch. 406: 20-24.

Heigenhauser, G.J.F., M.I. Lindinger and L.L. Spriet. 1986. Lactate, proton and ion fluxes in the stimulated perfused rat hindlimb. In: Biochemistry of Exercise VI, edited by B. Saltin. Champaign, IL: Human Kinetics, pp. 396-399.

Heisler, N. 1975. Intracellular pH of isolated rat diaphragm muscle with metabolic and respiratory changes of extracellular pH. Resp. Physiol. 23: 243-355.

Henderson, L.J., A.V. Bock, H. Field, Jr. and J.L. Stoddard. 1924. Blood as a physicochemical system. J. Biol. Chem. 59: 379-431.

- Herbst, M. and P. Piontek. 1972. Über den Verlauf des intracellularen pH-Wertes des Skelettmuskels während der Kontraktion. Pflugers Arch. 335: 213-223.
- Hermansen, L., A. Orheim and O.M. Sejersted. 1984. Metabolic acidosis and changes in water and electrolyte balance in relation to fatigue during maximal exercise of short duration. Int. J. Sport Med. Supple. 5: 110-115.
- Hermansen, L. and J.B. Osnes. 1972. Blood and muscle pH after maximal exercise in men. J. Appl. Physiol. 32: 304-308.
- Hermansen, L. and O. Vaage. 1977. Lactate disappearance and glycogen synthesis in human muscle after maximal exercise. Am. J. Physiol. 233: E422-E429.
- de Hevesy, G., and H. Levi. 1936. The action of neutrons on the rare earth elements. Kgl. Danske Videnskab. Selskab. Math.-fys. Medd. 14, No. 5.
- Hess, P. and R. Weingart. 1981. Free magnesium in cardiac and skeletal muscle measured with ion-selective micro-electrodes. J. Physiol. Lond. 318: 14P-15P.
- Heydorn, K. 1984. Neutron Activation Analysis for Clinical Trace Element Research. Two volumes. Baton Rouge: CRC Press.

- Hibberd, M.G., J.A. Dantzig, D.R. Trentham and Y.E. Goldman. 1985. Phosphate release and force generation in skeletal muscle fibers. *Science* 228: 1317-1319.
- Hibberd, M.G. and D.R. Trentham. 1986. Relationships between chemical and mechanical events during muscular contraction. *Ann. Rev. Biophys. Biophys. Chem.* 15: 119-161.
- Hill, A.V. and P.S. Kupalov. 1930. The vapour pressure of muscle. *Proc. Roy. Soc. Lond. Ser. B* 106: 445-477.
- Hilpert, P., R.G. Fleischmann, D. Kempe and H. Bartels. 1963. The Bohr effect related to blood and erythrocyte pH. *Am. J. Physiol.* 205: 337-340.
- Hinke, J.A.M. 1959. Glass micro-electrodes for measuring intracellular activities of sodium and potassium. *Nature* 184: 1257-1258.
- Hinke, J.A.M. and D.C. Gayton. 1971. Transmembrane K⁺ and Cl⁻ activity gradients for the muscle fiber of the giant barnacle. *Can. J. Physiol. Pharmacol.* 49: 312-322.
- Hinke, J.A.M. and S.G.A. McLaughlin. 1967. Release of bound sodium in single muscle fibers. *Can. J. Physiol. Pharm.* 45: 655-667.

Hinke, J.A.M. and M.R. Menard. 1976. Intracellular pH of single crustacean muscle fibers by the DMO and electrode methods during acid and alkaline conditions. J. Physiol. Lond. 262: 533-552.

Hironaka, T. and S. Morimoto. 1980. Intracellular chloride concentration and evidence for the existence of a chloride pump in frog skeletal muscle. Jpn. J. Physiol. 30: 257-263.

Hirche, H., E. Schumacher and H. Hagemann. 1980. Extracellular K^+ concentration and K^+ balance of the gastrocnemius of the dog during exercise. Pflugers Arch. 387: 231-237.

Hirche, H., V. Hombach, H.D. Langohr, U. Wacker and J. Busse. 1975. Lactic acid permeation rate in working gastrocnemii of dogs during metabolic alkalosis and acidosis. Pflugers Arch. 356: 209-222.

Hironaka, T. and S. Morimoto. 1980. Intracellular chloride concentration and evidence for the existence of a chloride pump in frog skeletal muscle. Jpn. J. Physiol. 30: 257-263.

Hnik, P., M. Holas, I. Krekule, N. Kriz, J. Mejstnar, V. Smiesko, E. Ujec and F. Vyskocil. 1976. Work-induced potassium changes in skeletal muscle and effluent blood assessed by liquid ion-exchanger microelectrodes. Pflugers Arch. 362: 85-94.

Hober, R. 1906. Physikalische Chemie der Zelle und der Gewebe. Leipzig: Englemann.

- Hodgkin, A.L. and P. Horowicz. 1959a. The influence of potassium and chloride ions on the membrane potential of single muscle fibres. *J. Physiol. Lond.* 148: 127-160.
- Hodgkin, A.L. and P. Horowicz. 1959b. Movements of Na and K in single muscle fibres. *J. Physiol. Lond.* 145: 405-432.
- Hogg, R.J., L.R. Pucacco, N.W. Carter, A.R. Laptook and J.P. Kokko. 1984. In situ PCO_2 in the renal cortex, liver, muscle, and brain of the New Zealand White rabbit. *Am. J. Physiol.* 247: F491-F498.
- Holmberg, E. and B. Waldeck. 1980. On the possible role of potassium ions in the action of terbutaline on skeletal muscle contraction. *Acta Pharmacol. Toxicol.* 46: 141-149.
- Hood, D.A., J. Gorski and R. L. Terjung. 1986. Oxygen cost of twitch and tetanic isometric contractions of rat skeletal muscle. *Am. J. Physiol.* 250: E449-E456.
- Hoppeler, H., H. Howald, K. Conley, S.L. Lindstedt, H. Claassen, P. Vock and E.R. Weibel. 1985. Endurance training in humans: aerobic capacity and structure of skeletal muscle. *J. Appl. Physiol.* 59: 320-327.
- Horowicz, P. and C.J. Gerber. 1965. Effects of sodium azide on sodium fluxes in frog striated muscle. *J. Gen. Physiol.* 48: 515-525.

- Hubert, E., J. Villaneuva, A.M. Gonzalez and F. Marcus. 1970. Univalent cation activation of fructose 1,6-diphosphatase. Arch. Biochem. Biophys. 138: 590-597.
- Huisman, T.H.J. and J. Kitchens. 1968. Oxygen equilibria studies of the hemoglobins from normal and anemic sheep and goats. Am. J. Physiol. 215: 140-149.
- Hultman, E. 1967. Studies on muscle metabolism of glycogen and active phosphate in man with special reference to exercise and diet. Scand. J. Clin. Lab. Invest. 19, suppl 94:1-63.
- Hultman, E., S. Del Canale and H. Sjöholm. 1985. Effect of induced metabolic acidosis on intracellular pH, buffer capacity and contraction force of human skeletal muscle. Clin. Sci. 69: 505-510.
- Hultman, E. and K. Sahlin. 1980. Acid-base balance during exercise. Exer. Sport Sci. Rev. 8: 41-128.
- Hultman, E. and J. Sjöholm. 1986. Biochemical causes of fatigue. In: Human Muscle Power, edited by N.L. Jones, N. McCartney and A.J. McComas. Champaign, IL: Human Kinetics, pp. 215-238.
- Huxley, H.E. 1969. The mechanism of muscular contraction. Science 164: 1356-1366.
- Idstrom, J.-P., V.H. Subramanian, B. Chance, T. Schersten and A.-C.

- Bylund-Fellenius. 1985. Oxygen dependence of energy metabolism in contracting and recovering rat skeletal muscle. *Am. J. Physiol.* 248: H40-H48.
- Itoh, T., Y. Kamura and H. Kuriyama. 1986. Inorganic phosphate regulates the contraction-relaxation cycle in skinned muscles of the rabbit mesenteric artery. *J. Physiol. Lond.* 376: 231-252.
- Jakobsson, E. 1980. Interactions of cell volume, membrane potential, and membrane transport parameters. *Am. J. Physiol.* 238: C196-C206.
- James, D.E., K.M. Burleigh, L.H. Storlien, S.P. Bennett and E.W. Kraegen. 1986. Heterogeneity of insulin action in muscle: influence of blood flow. *Am. J. Physiol.* 251: E422-E430.
- Jaweed, M.M., R.C. DeGroof, G.J. Herbison, J.F. Ditunno, and C.P. Bianchi. 1982. Muscle electrolyte changes in young exercised rats. In: Biochemistry of Exercise. International Series on Sport Sciences, Vol. 13. Edited by H.G. Knuttgen, J.A. Vogel, and J. Poortmans. Champaign, IL: Human Kinetics. pp. 557-563.
- Jones, N.L., J.R. Sutton, R. Taylor and C.J. Toews. 1977. Effect of pH on cardiorespiratory and metabolic responses to exercise. *J. Appl. Physiol.* 43: 959-964.
- Juel, C. 1986. Potassium and sodium shifts during in vitro isometric muscle contraction, and the time course of the ion-gradient recovery.

Kachmar, J.F. and P.D. Boyer. 1953. Kinetic analysis of enzyme reactions II. The potassium activation and calcium inhibition of pyruvic phosphoferase. J. Biol. Chem. 200: 669-682.

Kalckar, H.M. 1943. The role of myokinase in transphosphorylations. II. The enzymatic action of myokinase on adenine nucleotides. J. Biol. Chem. 148: 127-137.

Kamminga. C.E., A.F. Willebrands, J. Groen and J.R. Blickman. 1950. Effect of insulin on the potassium and inorganic phosphate content of the medium in experiments with isolated rat diaphragm. Science 111: 30-31

Katz, A., D.L. Costill, D.S. King, M. Hargreaves and W.J. Fink. 1984. Maximal exercise tolerance after induced alkalosis. Int. J. Sports Med. 5: 107-110.

Katz, A., K. Sahlin and J. Henriksson. 1986. Muscle ammonia metabolism during isometric contraction in humans. Am. J. Physiol. 250: C834-840.

Katz, J. 1896. Die mineralischen Bestandteile des Muskelfleisches. Pflugers Arch. ges. Physiol. 63: 1.

Kayer, S.R., H. Claasen, H. Hoppeler and E.R. Weibel. 1986.

Mitochondrial distribution in relation to changes in muscle metabolism in rat soleus. *Resp. Physiol.* 64: 1-11.

Kennedy, B.G. and P. DeWeer. 1977. Relationships between Na:K and Na:Na exchange by the sodium pump of skeletal muscle. *Nature* 268: 165-167.

Kernan, R.P. 1962. Membrane potential changes during sodium transport in frog sartorius muscle. *Nature* 193: 986-987.

Kernan, R.P., M. MacDermott and W. Westphal. 1974. Measurement of chloride activity within frog sartorius muscle fibres by means of chloride sensitive micro-electrodes. *J. Physiol. Lond.* 241: 60P-61P.

Kerut, C., P.A. MacLennan, and P.W. Watt. 1986. Characteristics of L(+)lactate transport in rat skeletal muscle. *J. Physiol. (Lond)* 372: 55P.

Khuri, R.N., K.K. Bogharian and S.K. Agulian. 1974. Intracellular bicarbonate in single skeletal muscle fibers. *Pflugers Arch.* 349: 285-299.

Kilmartin, J.V. and L. Rossi-Bernardi. 1973. Interaction of hemoglobin with hydrogen ions, carbon dioxide, and organic phosphates. *Physiol. Rev.* 53: 836-890.

Kindermann, W., J. Keul and G. Hunter. 1977. Physical exercise after

induced alkalosis (bicarbonate or Tris-buffer). Eur. J. Appl. Physiol. 37: 197-204.

Kirkwood, S.P., E.A. Munn and G.A. Brooks. 1986. Mitochondrial reticulum in limb skeletal muscle. Am. J. Physiol. 251: C395-C402.

Kjeldsen, K., A. Norgaard and T. Clausen. 1984. The age-dependent changes in the number of ^3H -ouabain binding sites in mammalian skeletal muscle. Pflugers Arch. 402: 100-108.

Kobayashi, N. and K. Yonemura. 1967. The extracellular space in red and white muscles of the rat. Jpn. J. Physiol. 17: 698-707.

Kostyuk, P.G. and Z.A. Sorokina. 1961. On the mechanism of hydrogen ion distribution between cell protoplasm and the medium. In: Membrane Transport Metabolism, edited by A. Kleinzeller and A. Kotyk. New York: Academic, pp. 193-203.

Kostyuk, P.G., Z.A. Sorokina and Y.D. Kholodova. 1969. Measurement of activity of hydrogen, potassium and sodium ions in striated muscle fibers and nerve cells. In: Glass Microelectrodes, edited by M. Lavalley, O.F. Schanne and N.C. Hebert. New York: Wiley, pp. 322-348.

Kowalchuck, J.M., G.J.F. Heigenhauser and N.L. Jones. 1984. Effect of pH on metabolic and cardiorespiratory responses during progressive exercise. J. Appl. Physiol. 57: 1558-1563.

- Krebs, E.G., D.J. Graves and E.H. Fisher. 1959. Factors affecting the ²⁸⁹ activity of muscle phosphorylase b kinase. J. Biol. Chem. 234: 2867-2873.
- Krogh, A. 1946. The active and passive exchange of inorganic ions through the surface of living cells and through living membranes generally. Proc. Roy. Soc. Lond. B 133: 140-200.
- Krebs, H.A. and K. Henseleit. 1932. Untersuchungen uber die Harnstoffbildung im Tierkorper. Hoppe-Seyler's Z. Physiol. Chem. 210: 33-66.
- Kuret, C., P.A. MacLennan and P.W. Watt. 1986. Characteristics of L(+) lactate transport in rat skeletal muscle. J. Physiol. (Lond) 372: 55P.
- Kushmerick, M.J. Energetics of muscle contraction. 1983. In: Handbook of Physiology, Skeletal Muscle, edited by L.D. Peachey, R.H. Adrian and S.R. Geiger. Bethesda, MD: American Physiological Society, pp. 189-235.
- Kushmerick, M.J. and R.A. Meyer. 1985. Chemical changes in rat leg muscle by phosphorus nuclear magnetic resonance. Am. J. Physiol. 248: C542-C549.
- Lahiri, S. 1975. Blood oxygen affinity and alveolar ventilation in relation to body weight in mammals. Am. J. Physiol. 229: 529-536.

- Lardy, H.A. 1951. The influence of inorganic ions on phosphorylation reactions. In: Phosphorus Metabolism, edited by W.D. McElroy and B. Glass. Baltimore: Johns Hopkins Press, pp. 477-499.
- Laughlin, M.H. and R.B. Armstrong. 1982. Muscular blood flow distribution patterns as a function of running speed in rats. *Am. J. Physiol.* 243: H296-H306.
- Law, R.O. and C.F. Phelps. 1966. The size of the sucrose, raffinose, and inulin spaces in the gastrocnemius muscle of the rat. *J. Physiol. (London)* 186: 547-557.
- Leader, J.P., J.J. Bray, A.D.C. Macknight, D.R. Mason, D. McCaig and R.G. Mills. 1984. Cellular ions in intact and denervated muscles of the rat. *J. Membr. Biol.* 81: 19-27.
- Lechner, A.J. 1976. Respiratory adaptations in burrowing pocket gophers from sea level and high altitude. *J. Appl. Physiol.* 41: 168-173.
- Lee, C.O. and W.M. Armstrong. 1974. State and distribution of potassium and sodium ions in frog skeletal muscle. *J. Membr. Biol.* 15: 331-362.
- Lehninger, A.L. and E.P. Kennedy. 1948. The requirements of the fatty acid oxidase complex of rat liver. *J. Biol. Chem.* 173: 753-771.

- Lenfant, C. 1973. High altitude adaptation in mammals. *Am. Zool.* 13: 447-456.
- Lewis, M.S. and H.A. Saroff. 1957. The binding of ions to the muscle proteins. Measurements on the binding of potassium and sodium ions to myosin A, myosin B and actin. *J. Am. Chem. Soc.* 79: 2112-2117.
- Liebig, J. 1847. Über die Bestandtheile der flüssigkeit des Fleisches. *Ann. Chem. Pharmac.* 62: 257.
- Lindinger, M.I., and G.J.F. Heigenhauser. 1987. Intracellular ion content of skeletal muscle measured by instrumental neutron activation analysis. *J. Appl. Physiol.* (submitted).
- Lindinger, M.I., G.J.F. Heigenhauser and N.L. Jones. 1986. Acid-base and respiratory properties of a buffered bovine erythrocyte perfusion medium. *Can. J. Physiol. Pharmacol.* 64: 550-555.
- Ling, G. and R.W. Gerard. 1949. The membrane potential and metabolism of muscle fibers. *J. Cell. Comp. Physiol.* 34: 413-438.
- Lipmann, F. and O. Meyerhof. 1930. Über die Reaktionsänderung des tatigen Muskels. *Biochem. Z.* 227: 84-109.
- Lohmann, K. and O. Meyerhof. 1934. Über die enzymatische Umwandlung von Phosphoglycerinsäure in Brenztraubensäure und Phosphorsäure.

Biochem. Z. 273: 60-72.

Lundsgaard, E. 1934. Phosphagen- und Pyrophosphatumsatz in jodessigsauerevergifteten Muskeln. Biochem. Z. 269: 308-328.

Lundsgaard, E. 1938. The biochemistry of muscle. Ann. Rev. Biochem. 7: 377-398.

Macchia, D.D., M.J. Didelot and W.M. Anderson. 1984. Anion permeability of toad skeletal muscle incubated in plasma and Ringer solution. Muscle & Nerve 7: 415-423.

Mackie, B.G. and R.L. Terjung. 1983a. Blood flow to different skeletal muscle fiber types during contraction. Am. J. Physiol. 245: H265-H275.

Mackie, B.G. and R.L. Terjung. 1983b. Influence of training on blood flow to different skeletal muscle fiber types. J. Appl. Physiol. 55: 1072-1078.

Madias, N.E. and J.J. Cohen. 1982. Acid-base chemistry and buffering. In: Acid-base, Chapter 1, edited by J.J. Cohen and J.P. Kassirer. Boston: Little, Brown and Co., pp. 8.

Mainwood, G.W. and G.E. Lucier. 1972. Fatigue and recovery in isolated frog sartorius muscles: the effects of bicarbonate concentration and associated potassium loss. Can. J. Physiol.

Mainwood, G.W. and P. Worsley-Brown. 1975. The effects of extracellular pH and buffer concentration on the efflux of lactate from frog sartorius muscle. J. Physiol. Lond. 250: 1-22.

Mainwood, G.W., P. Worsley-Brown and R.A. Paterson. 1972. The metabolic changes in frog sartorius muscle during recovery from fatigue at different external bicarbonate concentrations. Can. J. Physiol. Pharmacol. 50: 143-155.

Mainwood, G.W. and J. Zepetnek. 1985. Post-tetanic responses in creatine-depleted rat EDL muscle. Muscle & Nerve 8: 774-782.

Maison, G.L., O.S. Orth and K.E. Lemmer. 1938. pH changes in rabbit and human striated muscle after contraction. Am. J. Physiol. 121: 311-324.

Malan, A., T.L. Wilson and R.B. Reeves. 1976. Intracellular pH in col-blooded vertebrates as a function of body temperature. Resp. Physiol. 28: 29-47.

Manery, J.F. 1954. Water and electrolyte metabolism. Physiol. Rev. 34: 334-417.

Margaria, R. 1976. Biomechanics and Energetics of Muscular Exercise. Oxford: Clarendon.

- Mason, M.J., G.W. Mainwood and J.S. Thoden. 1986. The influence of extracellular buffer concentration and proprionate on lactate efflux from frog muscle. *Pflugers Arch.* 406: 472-479.
- Maughan, D. and C. Recchia. 1985. Diffusible sodium, potassium, magnesium, calcium and phosphorus in frog skeletal muscle. *J. Physiol. Lond.* 368: 545-563.
- McCaig, D. and J.P. Leader. 1984. Intracellular chloride activity in the extensor digitorum longus (EDL) muscle of the rat. *J. Membrane Biol.* 81: 9-17.
- McCartney, N., G.J.F. Heigenhauser and N.L. Jones. 1983. Effects of pH on maximal power output and fatigue during short-term dynamic exercise. *J. Appl. Physiol.* 55: 225-229.
- McCartney, N., L.L. Spriet, G.J.F. Heigenhauser, J.M. Kowalchuk, J.R. Sutton and N.L. Jones. 1986. Muscle power and metabolism in maximal intermittent exercise. *J. Appl. Physiol.* 60: 1164-1169.
- McIver, D.J.L. and A.D.C. Macknight. 1974. Extracellular space in some isolated tissues. *J. Physiol. Lond.* 239: 31-49.
- McLaughlin, S.G.A. and J.A.M. Rinke. 1968. Optical density changes of single muscle fibers in sodium-free solutions. *Can. J. Physiol. Pharmacol.* 46: 247-260.

- McKelvie, R.S., M.I. Lindinger and G.J.F. Heigenhauser. 1986. Effects of maximal isokinetic cycling exercise (MICE) on blood metabolites and acid-base state in man. *Med. Sci. Sports Exer.* 18 (Suppl): 377.
- Meyer, R.A., T.R. Brown and M.J. Kushmerick. 1985. Phosphorus nuclear magnetic resonance of fast- and slow-twitch muscle. *Am. J. Physiol.* 248: C297-C287.
- Meyerhof, O. 1927. Über die enzymatische Milchsäurebildung im Muskelextrakt. III. Mitteilung: Die Milchsäure aus den garfähige Hexosen. *Biochem. Z.* 183: 176.
- Meyerhof, O. 1930. Über die Änderung des osmotischen Drucks des Muskels bei Ermüdung und Starre. *Biochem. Z.* 226:1-15.
- Michaelis, L. c and A. Kramsztyk. 1914. Die Wasserstoffionenkonzentration der Gewebssäfte. *Biochem. Z.* 62: 180-185.
- Mildvan, A.S. 1974. Mechanism of enzyme action. *Ann. Rev. Biochem.* 43: 357-399.
- Milligan, C.L. and C.M. Wood. 1985. Intracellular pH transients in rainbow trout tissues measured by DMO distribution. *Am. J. Physiol.* 248: R668-R673.

Milner-Brown, H.S. and R.G. Miller. 1986. Muscle membrane excitation²⁹⁶
and impulse propagation velocity are reduced during muscle fatigue.
Muscle & Nerve 9: 367-374.

Mitchell, P.H. and J.W. Wilson. 1921. The selective absorption of
potassium by animal cells. J. Gen. Physiol. 4: 45-56.

Moller, J.V., J.P. Andersen and M. Lemaire. 1982. The sarcoplasmic
reticulum Ca^{2+} -ATPase. Mol. Cell. Biochem. 42: 83-107.

Mond, R. and H. Netter. 1930. Andert sich die Ionen Permeabilitat des
Muskels wahrend seiner tatigkeit? Pflugers Arch. 224: 702-709.

Nakamaru, Y. and A. Schwartz. 1972. The influence of hydrogen ion
concentration on calcium binding and release by skeletal muscle
sarcoplasmic reticulum. J. Gen. Physiol. 59: 22-32.

Nakashimi, K. and S. Tuboi. 1976. Size-dependent allosteric effects
of monovalent cations on rabbit liver fructose-1,6-bisphosphate. J.
Biol. Chem. 251: 4315-4321.

Najjar, V.A. 1948. The isolation and properties of
phosphoglucomutase. J. Biol. Chem. 175: 281-290.

Nasse, O. 1869. Beitrage zur Physiologie der contractilen Substanz.
Arch. f. Ges. Physiol. 2: 97.

Needham, D.M. 1971. Machina Carnis. Cambridge University Press.

Neely, J.R., J.T. Whitmer and M.J. Rovetto. 1975. Effect of coronary blood flow on glycolytic flux and intracellular pH in isolated rat hearts. *Circ. Res.* 37: 733-741.

Newsholme, E.A. 1986. Application of principles of metabolic control to the problem of metabolic limitations in sprinting, middle distance, and marathon running. In: Human Muscle Power, edited by N.L. Jones, N. McCartney and A.J. McComas. Champaign, IL: Human Kinetics, pp. 169-182.

Newsholme, E.A. and C. Start. 1973. Regulation in Metabolism. Toronto: John Wiley & Sons.

Nichols, G. Jr. 1958. Serial changes in tissue carbon dioxide content during acute respiratory acidosis. *J. Clin. Invest.* 37: 1111-1122.

Nunn, J.F. 1959. The accuracy of the determination of blood P_{CO_2} by interpolation methods. In: A Symposium on pH and Blood Gas Measurement. Edited by A. Woolmer. Churchill Press, London.

Overton, E. 1902. Beitrage zur allgemeinen Muskel-und, Nervenphysiologie II. Uber die Unenbehrlichkeit von Natrium - (oder Lithium-) Ionen fur den Contractionsact des Muskels. *Arch. f. Ges. Physiol.* 92: 346.

Owen, J.D., H.M. Brown and J.P. Pemberton. 1976. Ca^{++} in the Aplysia giant cell and the Balanus eburneus muscle fiber. Biophys. J. 16: 34a.

Paetkau, V. and H.A. Lardy. 1967. Phosphofructokinase. Correlation of physical and enzymatic properties. J. Biol. Chem. 242: 2035-2042.

Page, E. 1962. Cat heart muscle in vitro III. The extracellular space. J. Gen. Physiol. 46: 201-213.

Palade, P.T. and R.L. Barchi. 1977. Characteristics of the chloride conductance in muscle fibers of the rat diaphragm. J. Gen. Physiol. 69: 325-342.

Parnas, J.K. 1929. Über die Ammoniakbildung im Muskel und ihren Zusammensetzung mit Funktion und Zustandsänderung. VI. Mitteilung: Der Zusammensetzung der Ammoniakbildung mit der Umwandlung des Adeninnucleotids zu Inosinsäure. Biochem. Z. 206: 16-38.

Piontek, P. and M. Herbst. 1971. Probleme der photometrischen Messung mit Farbindicatoren an Skelettmuskeln. Pflügers Arch. 328: 356-362.

Portzehl, H., P. Zaoralek and J. Gaudin. 1969. The activation by Ca^{2+} of the ATPase of extracted muscle fibrils with variation of ionic strength, pH and concentration of MgATP. Biochim. Biophys. Acta 189: 440-448.

- Ranke, J. 1865. Tetanus. Leipzig: Engelmann.
- Ranvier, M.L. 1873. Des muscles rouge et des muscles blanc chez les rongeurs. Compt. rend. Acad. Sci. 77: 1030.
- Ray, W.J. and G.A. Roscelli. 1966. Activation and inhibition in the phosphoglucomutase system. J. Biol. Chem. 241: 2596-2602.
- Reeves, R.B. and T.L. Wilson. 1970. Intracellular pH in bullfrog striated and cardiac muscle as a function of body temperature. Fed. Proc. 28: 782.
- Reeves, R.B. and A. Malan. 1976. Model studies of intracellular acid-base temperature responses in ectotherms. Resp. Physiol. 28: 49-63.
- Rippe, B. and B. Haraldsson. 1986. Capillary permeability in rat hindquarters as determined by estimations of capillary reflection coefficients. Acta Physiol. Scand. 127: 289-303.
- Robinson, R.A. and R.H. Stokes. 1970. Electrolyte Solutions. 2nd ed. revised. London: Butterworth.
- Roos, A. and W.F. Boron. 1981. Intracellular pH. Physiol. Rev. 61: 296-434.
- Root, W.S. 1933. The carbon dioxide dissociation curve of frog's

skeletal muscle with special reference to the time of exposure to carbon dioxide. *J. Cell. Comp. Physiol.* 3: 101-112.

Ruderman, N.B., C.R.S. Houghton and R. Hems. 1971. Evaluation of the isolated perfused rat hindquarter for the study of muscle metabolism. *Biochem. J.* 124: 639-651.

Ruderman, N.B., F.W. Kemmer, M.N. Goodman and M. Berger. 1980. Oxygen consumption in perfused skeletal muscle. Effect of perfusion with aged, fresh and age-rejuvenated erythrocytes on oxygen consumption, tissue metabolites and inhibition of glucose utilization by acetoacetate. *Biochem. J.* 190: 57-64.

Saborowski, F., D. Lang and C. Albers. 1973. Intracellular pH and buffering curves of cardiac muscle in rats as affected by temperature. *Resp. Physiol.* 18: 161-170.

Sahlin, K. 1978. Intracellular pH and energy metabolism in skeletal muscle of man. *Acta Physiol. Scand. Suppl.* 455: 1-56.

Sahlin, K., A. Alvestrand, J. Bergstrom and E. Hultman. 1977. Intracellular pH and bicarbonate concentration as determined in biopsy samples from the quadriceps muscle of man. *Clin. Sci. Mol. Med.* 53: 459-466.

Sahlin, K., A. Alvestrand, R. Brandt and E. Hultman. 1978. Intracellular pH and bicarbonate concentration in human muscle during

recovery from exercise. J. Appl. Physiol. 45: 474-480.

Sahlin, K., L. Edstrom and H. Sjöholm. 1983. Fatigue and phosphocreatine depletion during carbon dioxide-induced acidosis in rat muscle. Am. J. Physiol. 245: C15-C20.

Sahlin, K., L. Edstrom, H. Sjöholm and E. Hultman. 1981. Effects of lactic acid accumulation and ATP decrease on muscle tension and relaxation. Am. J. Physiol. 240: C121-C126.

Sahlin, K., R.C. Harris, B. Nylinde and E. Hultman. 1976. Lactate content and pH in muscle samples obtained after dynamic exercise. Pflugers Arch. 367: 143-149.

Saltin, B. and P.D. Gollnick. 1983. Skeletal muscle adaptability: significance for metabolism and performance. In: Handbook of Physiology, Section 10: Skeletal Muscle, edited by L.D. Peachey, R.H. Adrian and S.R. Geiger. Bethesda: American Physiological Society, pp. 555-631.

Sandow, A. 1965. Excitation-contraction coupling in skeletal muscle. Pharm. Rev. 17: 265.

Scales, D.J. and R.A. Sabbadini. 1979. Microsomal T system. A stereological analysis of purified microsomes derived from normal and dystrophic skeletal muscle. J. Cell Biol. 83: 33-46.

- 302
- Schwartz, A., G.E. Lindenmayer and J.C. Allen. 1972. The Na⁺,K⁺-ATPase membrane transport system: importance in cellular function. *Curr. Top. Membr. Transp.* 3: 1-82.
- Schloerb, P.R., G.L. Blackburn and J.J. Grantham. 1967. Carbon dioxide dissociation curve in potassium depletion. *Am. J. Physiol.* 212: 953-956.
- Scott-Emuakpor, D., A.H.J. Maas, T.T.C. Ruigroch and A.E. Zimmerman. 1976. Acid-base curve nomogram for dog blood. *Pflugers Arch.* 363: 141-147.
- Segal, S.S., J.A. Faulkner and T.P. White. 1986. Skeletal muscle fatigue in vitro is temperature dependent. *J. Appl. Physiol.* 61: 660-665.
- Sembrowich, W.L., D. Johnson, E. Wang and T.E. Hutchinson. 1982. Electron microprobe analysis of fatigued fast- and slow-twitch muscle. In: Biochemistry of Exercise, Vol. 13, edited by H.G. Knuttgen, J.A. Vogel, and J. Poortmans. Champaign, IL: Human Kinetics, pp. 571-576.
- Seo, Y. 1984. Effects of extracellular pH on lactate efflux from frog sartorius muscle. *Am. J. Physiol.* 247: C175-C181.
- Seo, Y., K. Yoshizaki and T. Morimoto. 1983. A ¹H-nuclear magnetic resonance study on lactate and intracellular pH in frog muscle. *Jpn. J. Physiol.* 33: 721-731.

- Severinghaus, J.W. 1965. Blood gas concentrations. In: Handbook of Physiology, Respiration, Vol. II. Edited by W.O. Fenn and H. Rahn. Washington, Am. Physiol. Soc. pp. 1475-1487.
- Shetty, R.P.M., D.J. Krishna and D.D. Macchia. 1985. Effects of albumin on resting membrane potential of toad semitendinosus muscles. *Pflugers Arch.* 404: 83-85.
- Siēsjo, B.K., and G. Thews. 1962. Ein verfahren zur Bestimmung der CO_2 -Leitfähigkeit der CO_2 -Diffusionskoeffizienten und des scheinbaren CO_2 -Löslichkeitkoeffizienten in Gehirngewebe. *Pfluegers Arch.* 276: 192-210.
- Siggaard-Andersen, O. 1963. Blood acid-base alignment nomogram. Scales for pH, P_{CO_2} , base excess of whole blood of different hemoglobin concentrations, plasma bicarbonate, and plasma total- CO_2 . *Scand. J. Clin. Invest.* 15: 211-217.
- Sillau, A.H. 1986. Capillarity, oxidative capacity, and fibre composition of the soleus and gastrocnemius muscles of rats in hypothyroidism. *J. Physiol. Lond.* 361: 281-295.
- Shiota, M. and T. Sugano. 1986. Characteristics of rat hindlimbs perfused with erythrocyte- and albumin-free medium. *Am. J. Physiol.* 251: C78-C84.

- Sjodin, R.A. 1971. The kinetics of sodium extrusion in striated muscle as functions of the external sodium and potassium concentrations. *J. Gen. Physiol.* 57: 164-187.
- Sjodin, R.A. 1982. Transport of electrolytes in muscle. *J. Membr. Biol.* 68: 161-178.
- Sjogaard, G. 1983. Electrolytes in slow and fast muscle fibers of human at rest and with dynamic exercise. *Am. J. Physiol.* 245: R25-R31.
- Sjogaard, G., R.P. Adams and B. Saltin. 1985. Water and ion shifts in skeletal muscle of humans with intense dynamic knee extension. *Am. J. Physiol.* 248: R190-R196.
- Sjogaard, G. and B. Saltin. 1982. Extra- and intracellular water spaces in muscles of man at rest and with dynamic exercise. *Am. J. Physiol.* 243: R271-R280.
- Smiley, K.L. and C.H. Suelter. 1967. Univalent cations as allosteric activators of muscle adenosine 5'-phosphate deaminase. *J. Biol. Chem.* 242: 1980-1981.
- Snugden, P.R. and E. Newsholme. 1975. The effects of ammonium, inorganic phosphate and potassium ions on the activity of phosphofructokinases from muscle and nervous tissues of vertebrates and invertebrates. *Biochem. J.* 150: 113-122.

- Sommerkamp, H., K. Riegel, P. Hilpert, and K. Brecht. 1961. Über den Einfluss der Kationenkonzentration im Erythrocyten auf die Lage der Sauerstoffdissociationskurve des Blutes. *Pflugers Arch. ges. Physiol.* 272: 591-602.
- Spriet, L.L., C.G. Matsos, S.J. Peters, G.J.F. Heigenhauser and N.L. Jones. 1985a. Muscle metabolism and performance in perfused rat hindquarter during heavy exercise. *Am. J. Physiol.* 248: C109-C118.
- Spriet, L.L., C.G. Matsos, S.J. Peters, G.J.F. Heigenhauser, and N.L. Jones. 1985b. Effects of acidosis on rat muscle metabolism and performance during heavy exercise. *Am. J. Physiol.* 248: C337-C347.
- Spriet, L.L., M.I. Lindinger, G.J.F. Heigenhauser and N.L. Jones. 1986. Effects of alkalosis on skeletal muscle metabolism and performance during exercise. *Am. J. Physiol.* 251: R833-R839.
- Spriet, L.L., K. Soderlund, J.A. Thomson and E. Hultman. 1986. pH measurement in human skeletal muscle samples: effect of phosphagen hydrolysis. *J. Appl. Physiol.* 61: 1949-1954.
- Sreter, F.A. 1963. Distribution of water, sodium, and potassium in resting and stimulated mammalian muscle. *Can. J. Biochem. Physiol.* 41: 1035-1045.
- Sreter, F.A. 1963. Cell water, sodium, and potassium in stimulated red and white mammalian muscles. *Am. J. Physiol.* 205: 1295-1298.

- Sreter, F.A. and G. Woo. 1963. Cell water, sodium, and potassium in red and white mammalian muscles. *Am. J. Physiol.* 205: 1290-1294.
- Stadtman, E.R. 1970. Mechanisms of enzyme regulation in metabolism. In: The Enzymes, Vol. 1, edited by P.D. Boyer. New York: Academic Press, pp. 397-459.
- Staudte, H.W., G.U. Exner and D. Pette. 1973. Effects of short-term, high intensity (sprint) training on some contractile and metabolic characteristics of fast and slow muscle of the rat. *Pflugers Arch.* 344: 159-169.
- Steinbach, H.B. 1951. Permeability. *Ann. Rev. Physiol.* 13:21-40.
- Steinhagen, C., H.J. Hirche, H.W. Nestle, U. Bovenkamp and I. Hosselmann. 1976. The interstitial pH of the working gastrocnemius muscle of the dog. *Pfluegers Arch.* 367: 151-156.
- Stella, G. 1929. The combination of carbon dioxide with muscle: its heat of neutralization and its dissociation curve. *J. Physiol. Lond.* 68: 49-66.
- Stewart, P.A. 1978. Independent and dependent variables of acid-base control. *Resp. Physiol.* 33: 9-26.
- Stewart, P.A. 1981. How to Understand Acid-Base: A Quantitative

Primer for Biology and Medicine. New York: Elsevier North Holland.

Stewart, P.A. 1983. Modern quantitative acid-base chemistry. Can. J. Physiol. Pharmacol. 61: 1444-1461.

Stonnington, H.H. and A.G. Engel. 1973. Normal and dystrophic muscle. A morphometric study of fine structure. Neurology 23: 714-724.

Sullivan, T.E. and R.B. Armstrong. 1978. Rat locomotory muscle fiber activity during trotting and galloping. J. Appl. Physiol. 44: 358-363.

Sutton, J.R., N.L. Jones and C.J. Toews. 1981. Effect of pH on muscle glycolysis during exercise. Clin. Sci. 61: 331-338.

Tabor, H. and A.B. Hastings. 1943. The ionization constant of secondary magnesium phosphate. J. Biol. Chem. 148: 627-632.

Thomason, D.B., K.M. Baldwin and R.E. Herrick. 1986. Myosin isozyme distribution in rodent hindlimb skeletal muscle. J. Appl. Physiol. 60: 1923-1931.

Tibes, U., E. Haberkorn-Butendeich and F. Hammersen. 1977. Effect of contraction on lymphatic, venous, and tissue electrolytes and metabolites in rabbit skeletal muscle. Pflugers Arch. 368: 195-202.

Trivedi, B. and W.H. Danforth. 1966. Effect of pH on the kinetics of frog muscle phosphofructokinase. J. Biol. Chem. 241: 4110-4112.

- Troup, J.P., J.M. Metzger and R.H. Fitts. 1986. Effect of high-intensity exercise training on functional capacity of limb skeletal muscle. *J. Appl. Physiol.* 60: 1743-1751.
- Tyuma, I. 1984. The Bohr effect and the Haldane effect in human hemoglobin. *Jap. J. Physiol.* 34: 205-216.
- Ussing, H.H. 1947. Interpretation of the exchange of radio-sodium in isolated muscle. *Nature* 160: 262-263.
- Van Slyke, D.D., A.B. Hastings, A. Hiller and J. Sendroy. 1928. Studies of gas and electrolyte equilibria in blood. XIV. The amounts of alkali bound by serum albumin and globulin. *J. Biol. Chem.* 79: 769-780.
- Veloso, D., R.W. Gynn, M. Oskarsson and R.L. Veech. 1973. The concentration of free and bound magnesium in rat tissues. *J. Biol. Chem.* 369: 4811-4819.
- Vernadakis, A. and D.M. Woodbury. 1964. Electrolyte and nitrogen changes in skeletal muscle of developing rats. *Am. J. Physiol.* 206: 1365-1368.
- Waddel, W.J. and T.C. Butler. 1959. Calculation of intracellular pH from the distribution of 5,5-dimethyl-2,4-oxazolidinedione (DMO). Application to skeletal muscle of the dog. *J. Clin. Invest.* 38:

- Wallace, W.M. and A.B. Hastings. 1942. The distribution of bicarbonate ion in mammalian muscle. J. Biol. Chem. 144: 637-649.
- Walsh, K.X., D.M. Millikan, K.K. Schlender and E.M. Reimann. 1970. Calcium-dependent phosphorylation of glycogen synthase by phosphorylase kinase. J. Biol. Chem. 254: 6611-6616.
- Walsh, P.J., D.G. McDonald and C.E. Booth. 1984. Acid-base balance in the sea mussel, Mytilus edulis. II. Effects of hypoxia and air-exposure on intracellular acid-base status. Marine. Biol. Lett. 5: 359-369.
- Wareham, A.C. 1978. Effect of denervation and ouabain on the response of the resting membrane potential of rat skeletal muscle to potassium. Pflugers Arch. 373: 225-228.
- Watson, P.D. 1983. Effects of blood-free perfusion on CFC in the isolated cat hindlimb. Am. J. Physiol. 245: H911-H919.
- Weiskopf, R.B., M.I. Townsley, K.K. Riordan, D. Harris and K. Chadwick. 1983. Acid-base curve and alignment nomograms for swine blood. J. Appl. Physiol. 54: 978-983.
- White, H.L. and D. Rolf. 1957. Whole body and tissue inulin and sucrose spaces in the rat. Am. J. Physiol. 188: 151-155.

- Wilkie, D.R. 1981. Shortage of chemical fuel as a cause of fatigue: studies by nuclear magnetic resonance and bicycle ergometry. In: Human Muscle Fatigue: Physiological Mechanisms, edited by R. Porter and J. Whelan. Ciba Foundation Symposium 82. London: Pitman Medical, pp. 102-119.
- Wilkes, D., N. Gledhill and R. Smyth. 1983. Effect of acute induced metabolic alkalosis on 800 m racing time. *Med. Sci. Sports Exer.* 15: 277-280.
- Wilkie, D.R. 1986. Muscular fatigue: effects of hydrogen ions and inorganic phosphate. *Fed. Proc.* 45: 2921-2923.
- Williams, G.J., S. Collins, J.R. Muir and M.R. Stephens. 1975. Observations on the interaction of calcium and hydrogen ions on ATP hydrolysis by the contractile elements of cardiac muscle. In: Recent Advances in Studies on Cardiac Structure and Metabolism, Vol. 5, Basic Functions of Cations in Myocardial Activity, edited by A. Fleckenstein and N.S. Dhalla. Baltimore: University Park, pp. 273-280.
- Witzmann, F.A., D.H. Kim and R.H. Fitts. 1983. Effect of hindlimb immobilization on the fatiguability of skeletal muscle. *J. Appl. Physiol.* 54: 1242-1248.
- Woittiez, R.D., G.C. Bain, P.A. Huijing and R.H. Rozendal. 1985. Functional characteristics of the calf muscles of the rat. *J. Morphol.*

184: 375-387.

Woodbury, W.J. 1974. Body acid-base state and its regulation. In: Physiology and Biophysics II. Circulation, Respiration and Fluid Balance, twentieth edition, edited by T.C. Ruch and H.D. Patton. Toronto: Saunders, pp. 480-524.

Yonemura, K. 1967. Resting and action potentials in red and white muscle of the rat. Jpn. J. Physiol. 17: 708-719.